Aspects of D-brane inflation

Dariush Kaviani

A Thesis presented for the degree of
Doctor of Philosophy

Institute for Particle Physics Phenomenology
Department of Physics
University of Durham
England

February 2013

Dedicated to

Bahi

Aspects of D-brane inflation

Dariush Kaviani

Submitted for the degree of Doctor of Philosophy
February 2013

Abstract

Inflation has been suggested as a solution to cosmological problems but it ultimately needs to be derived from a fundamental theory such as string theory. In this thesis we study the embedding of inflation into string theory using the D-brane inflation scenario as case study. We first review the relevant aspects of string compactifications and D-branes and construct the effective action of the inflationary D3-brane. We then study multifield D-brane inflation including compactification corrections to the inflaton action that arise from UV deformations of a warped throat geometry emerging from the ISD supergravity solution. One particular issue here is to investigate in detail the cosmological consequences of realistic angular dependent potentials in the D-brane inflation scenario in a fully UV/IR consistent way. Embedding a warped throat into a compact Calabi-Yau space with all moduli stabilized breaks the no-scale structure and induces angular dependence in the potential of the probe D3-brane. We solve the D3-brane equations of motion from the DBI action in the warped deformed conifold including linearized as well as non-linear perturbations around the ISD supergravity solution. Our numerical solutions show that angular dependence is a next to leading order correction to the dominant radial motion of the brane, however, just as angular motion typically increases the amount of inflation (spinflation), having additional angular dependence from linearized perturbations also increases the amount of inflation.

Declaration

The work in this thesis is based on research carried out at the Institute for Particle Physics Phenomenology, Department of Physics, Durham University, England. No part of this thesis has been submitted here or elsewhere for any other degree or qualification and is all my own work unless referenced to the contrary in the text. Chapter 2 of this thesis is a review on the necessary geometric background used in subsequent chapters. Chapter 3 includes the necessary review and background material for the study of D-brane inflation in the later chapters. Chapter 4 is based on original work done in collaboration with my supervisor Prof. Ruth Gregory [1]. This chapter contains corrections which were noted after the paper was published. Apart from section 5.1 which contains some review, all the rest of Chapter 5 is based on my own original work [2]. This chapter includes further analytical discussions and numerical illustrations not contained in the paper. These are also my own work.

Acknowledgements

I am very grateful to my supervisor, Professor Ruth Gregory, for her competent supervision of my PhD study at Durham University. I also would like to thank my parents for supporting me in the whole duration of my study. I am particularly grateful to my mother for her invaluable support and sacrifices without which this thesis could have never been written. Thank you Bahi! Not lastly, I would like to thank my wife, Magdalena, for patience and love in the all duration of my study.

Contents

Abstract **iii**

Declaration **iv**

Acknowledgements **v**

1 Introduction **1**

1.1 Cosmological problems 2

1.1.1 The flatness problem 2

1.1.2 The horizon problem 5

1.1.3 The monopole problem 6

1.2 The period of inflation 7

1.2.1 A brief history of inflation 7

1.2.2 Slow-roll formalism 11

1.2.3 Solving the flatness and horizon problems 14

1.2.4 Solving the monopole problem 16

1.2.5 Shortcomings of inflation 16

1.3 Inflation in string theory 17

1.3.1 Motivation 17

1.3.2 Moduli and inflatons 18

1.3.3 Moduli stabilization obstacles to inflation 21

1.3.4 Classification of string inflationary models 23

1.3.5 Case study: D-brane inflation 23

2 The supergravity model **29**

2.1 Calabi-Yau flux compactification of type IIB superstring theory . . . 29

2.1.1 Type IIB superstring spectrum . . . 30

2.1.2 Type IIB action and equations of motion . . . 32

2.1.3 Type IIB theory on Calabi-Yau manifolds . . . 37

2.1.4 Moduli and effective actions . . . 40

2.1.5 The warped deformed conifold . . . 42

2.1.6 Large hierarchy and complex structure moduli fixing . . . 49

2.2 Kähler moduli stabilization . . . 51

2.2.1 General Perturbations around the ISD solution . . . 51

2.2.2 The KKLT scenario . . . 57

3 Review of D-brane inflation **65**

3.1 D-branes . . . 65

3.1.1 D-brane action . . . 66

3.1.2 D-brane tension . . . 69

3.2 The effective multifield D3-brane action . . . 70

3.2.1 DBI action . . . 72

3.2.2 WZ action . . . 73

3.2.3 The full action and equations of motion . . . 75

3.3 The field range bound . . . 76

3.4 Spinflation . . . 77

3.4.1 Equations of motion . . . 78

3.4.2 Numerical analysis . . . 80

4 Spinflation with angular potentials **83**

4.1 Brane inflation with an angular potential . . . 83

4.2 Inflationary analysis . . . 87

4.3 Summary and conclusions . . . 95

5 Spinflation with backreaction **99**

5.1 Review of D3/D7-brane inflation . . . 100

5.2 Multifield D-brane inflation . . . 107
5.3 Inflationary solutions . . . 114
5.4 Summary and conclusions . . . 119

6 Summary and conclusions **125**

Appendix **128**

A Rudiments of Calabi-Yau spaces **128**
A.1 The nonlinear sigma-model . . . 128
A.2 Kähler manifolds . . . 129
A.3 Calabi-Yau manifolds . . . 135
A.3.1 Motivation . . . 135
A.3.2 Calabi-Yau three-folds . . . 137
A.3.3 Complete intersection Calabi-Yau 3-folds . . . 139
A.4 Nodes and smoothings . . . 142
A.4.1 Smoothings in general . . . 142
A.4.2 Nodes and small resolution . . . 143
A.5 Moduli spaces . . . 146
A.5.1 The conifold . . . 146
A.5.2 The deformed and resolved conifold . . . 147
A.5.3 L^2 and intersection cohomology . . . 149
A.5.4 Cycles in conifolds . . . 150
A.5.5 Fluxes in conifolds . . . 151
A.5.6 Complex structure moduli . . . 154
A.5.7 Kähler class moduli . . . 154
A.5.8 The metric on moduli space . . . 156
A.5.9 The complex structure moduli space . . . 157
A.5.10 The Kähler class moduli space . . . 161
A.6 Metrics on Calabi-Yau cones . . . 163
A.6.1 Finiteness of distances between manifolds . . . 163
A.6.2 Metrics on conifolds . . . 166

B The supergravity F-term potential 170

B.1 Coordinates and trajectories 170

B.2 The F-tem potential 172

C DBI equations of motion 179

Bibliography 184

List of Figures

1.1 The False vacuum state (left), almost all of which has decayed into the true vacuum state (right) forming an inflationary bubble, but small regions were left behind. 8

1.2 The small regions of false vacuum state that were left behind continued to inflate while the bubble stopped to inflate (left). After a certain period of time, other inflationary bubbles formed (right) and our universe is supposed to take place in one of such bubbles (which are not all the same). 8

1.3 A mobile D3-brane moving towards an anti-D3-brane fixed at IR location at the bottom of the warped throat region of a flux compactification. The throat is smoothly glued to a Calabi-Yau three-fold in the UV region where moduli stabilizing D7-branes enter the throat. In principle, our universe may exist in various parts of compactification, including other warped throats not shown in the diagram. This figure is from [54]. 24

2.1 A plot of the metric functions C_i , which shows how the deformation of the conifold increases as the tip is approached. The metric asymptotes the $T^{1,1}$ cone, but near the origin, rC_1 and rC_3 remain finite leaving the nonsingular S^3 metric at the tip of the 'cone'. The axis is labeled both in terms of the original η coordinate, as well as the normalized proper distance up the throat, $\hat{r} = \epsilon^{-2/3} r$. 46

3.1 The behavior of the scale factor with (light purple) and without (blue) angular momentum l_θ. This figure is from [71]. 82

3.2 The behaviour of the gamma-factor. This figure is from [71]. 82

4.1 Planck mass constraint: The numerical integral of $I(\eta)\sinh^2\eta$ with the large η behaviour factored out. 88

4.2 Some sample inflationary trajectories with a flux parameter of $g_sM = 100$, inflaton mass $m_0 = 20$, and a saturated Planck mass from $\eta_{\rm UV} = 10$. The values of ϵ and $\mathcal{C} = c_2\epsilon^{-4/3}$, are indicated. 89

4.3 The amount of inflation along a trajectory with $m_0 = 20$, $g_sM = 100$, $\epsilon = 0.001$ with (grey dashed, $c_2 = \epsilon^{4/3}/2$) and without (solid black) angular terms in the potential. 93

4.4 The number of e-foldings as a function of the deformation parameter ϵ for $m_0 = 10$ (blue circles) and $m_0 = 20$ (red squares) with $c_2 = \epsilon^{4/3}/2$ and $g_sM = 100$. The analytic dependence is shown for comparison. . 94

5.1 The behaviour of σ_F obtained from the root of Eq. (5.2.47) for choice of compactification parameters (4.1), and the behaviour of σ_m for choice of parameters (4.1) with $\theta = 0$ (solid), $\pi/2$ (tiny-dashed) and π (large-dashed).115

5.2 The behaviour of the function F and $\delta\sigma$ for the choice of parameters (4.1) and $\theta = \pi$. 115

5.3 The Hubble rate, $H^2 \simeq V/3M_{\rm pl}^2$, and the σ mass squared, M_σ^2 for the choice of parameters (4.1) and $\theta = \pi$. 115

5.4 The behaviour of the function F and $\delta\sigma$ with $\mu = 0.005$ and the rest of parameters as (4.1) and $\theta = \pi$. 116

5.5 The Hubble rate, $H^2 \simeq V/3M_{\rm pl}^2$, and the σ mass squared, M_σ^2 with $\mu = 0.005$ and the rest of parameters as (4.1) and $\theta = \pi$. 116

5.6 The Kähler modulus, σ_*, on the entire supergravity background with the choice of compactification parameters (4.1). 120

5.7 The derivatives of the Kähler modulus, $\partial_\eta\sigma_*$ and $\partial_\theta\sigma_*$, on the entire supergravity background with the choice of compactification parameters (4.1). 121

5.8 The number of e-foldings, $\mathcal{N}$, and the γ-factor, $\gamma_{\rm DBI}$, with (gray-dashed) and without (black-solid) non-linear harmonic dependent corrections for the choice of compactification parameters (4.1). 122

A.1 The deformation and small resolution of the singular conifold near the singularity at the tip of the cone. This figure is from [111]. 147

Chapter 1

Introduction

The standard big bang theory is a widely accepted theory that describes the structure and evolution of the universe following an initial singularity or "a bang". The underlying assumption of this theory is the possibility to jump from nothingness, i.e., no space, no radiation, no matter and energy, into somethingness followed by the successive periods of radiation, matter, and vacuum energy dominance. This immediately poses a problem: When the universe begins from such a violent rapid event, we might expect it to be initially be very inhomogeneous, nonuniform, and highly curved, and the present universe would still have some trace of a very inhomogeneous and highly curved universe that it began with. But as we shall discuss in Section 1.1, following the standard text books [3–6] and also some of their original references [7–17], the universe that we see today is remarkably flat, homogeneous, and isotropic, in contradiction with the very inhomogeneous and highly curved universe that we expect to see after the big bang. In order to solve this problem another assumption is added to the standard big bang theory, which is the assumption of inflation discussed in Section 1.2, following again [3–6] and some of their original references [18–24]. The assumption is that before the radiation era, the universe was dominated by a period of slowly varying vacuum energy, called inflation, during which the universe underwent a nearly exponential expansion. This exponential inflation would have smoothed any curvature and inhomogenity of space, so that the universe we see today would make sense. Despite its success in solving the problems of the standard big bang theory, inflation ultimately needs to be derived from a

fundamental theory such as string theory, which we briefly discuss in Section 1.3 and analyse in more technical detail in the subsequent chapters.

1.1 Cosmological problems

1.1.1 The flatness problem

The homogenity and isotropy of the universe requires its spacetime metric to be the Friedman-Robertson-Walker (FRW) metric given by[1] [3, 4, 6–9]

$$ds^2 = dt^2 - a(t)^2\left[\frac{dr^2}{1-Kr^2} + r^2(d\theta^2 + \sin\theta^2 d\phi^2)\right], \tag{1.1.1}$$

where K denotes the curvature of the universe and $a(t)$ is the scale factor, which feeds into the proper distance.

The proper distance between any two co-moving objects in the universe is [3]:

$$\mathscr{D}(r,t) = a(t)\int_0^r \frac{dr}{\sqrt{1-Kr^2}} = a(t)\times\begin{cases}\sin^{-1} r & K=+1\\ r & K=0\\ \sinh^{-1} r & K=-1\end{cases} \tag{1.1.2}$$

with r being the relative time-independent radial coordinate of co-moving objects. For a ray of light we have $ds^2 = 0$, and hence the maximum radial distance $r_m(t_0)$ from which an observer at time t_0 will be able to receive light signals at $t = 0$ is constrained and therefore puts a limit on distances at which past events can be observed. These are called particle horizons. The proper distance of the horizon size is given as

$$\mathscr{D}_{\rm m}(t_0) = a(t_0)\int_0^{r_{\rm m}(t_0)} \frac{dr}{\sqrt{1-Kr^2}} = a(t_0)\int_0^{t_0}\frac{dt}{a(t)}. \tag{1.1.3}$$

The Einstein equations for the FRW ansatz give the fundamental Friedmann equation [3, 4, 6]

[1] Throughout this thesis we take the flat spacetime metric to be exactly the FRW metric and thereby consider the fields to be homogeneous.

$$\dot{a}^2 + K = \frac{8\pi\, G\rho\, a^2}{3}, \tag{1.1.4}$$

and the conservation law

$$\dot{\rho} = -\frac{3\dot{a}}{a}(\rho + p). \tag{1.1.5}$$

For any value of the Hubble constant[2] $H_0 = \dot{a}(t_0)/a(t_0)$, we may define a critical present density

$$\rho_{0,\mathrm{crit}} = \frac{3H_0^2}{8\pi G} = 1.878 \times 10^{-29} h^2\, \mathrm{g/cm^3}, \tag{1.1.6}$$

for which $K = 0$ in Eq. (1.1.4) and hence the universe is flat. Given p as a function of ρ, we can solve Eq. (1.1.5) to find ρ as a function of a, and then use this in Eq. (1.1.4) to find a as a function of t. Making the ansatz $p = w\rho$, we obtain [3]:

$$\rho \propto a^{-3-3w}. \tag{1.1.7}$$

• **Matter dominated expansion**: Here $p = 0$, giving $\rho = \rho_0(a/a_0)^{-3}$, and therefore Eq. (1.1.4) reduces to $\dot{a}^2 + K \simeq a^{-1}$. In the very early universe $a \to 0$, so that we may neglect K in Eq. (1.1.4) and obtain:

$$a(t) \propto t^{2/3}. \tag{1.1.8}$$

In this case a simple relation between the age of the universe and the Hubble constant is given as $t_0 = 2/3H_0 = 6.52 \times 10^9 h^{-1}\,\mathrm{yr}$. According to Eq. (1.1.8), Eq. (1.1.4) and Eq. (1.1.5) the energy density at time t is $\rho = 1/6\pi G t^2$.

• **Radiation dominated expansion**: Here $p = \rho/3$, giving $\rho = \rho_0(a/a_0)^{-4}$, and therefore Eq. (1.1.4) reduces to $\dot{a}^2 + K \simeq a^{-2}$. Again, in the very early times we may neglect K in Eq. (1.1.4) and obtain:

$$a(t) \propto t^{1/2}. \tag{1.1.9}$$

[2]The current best direct measurement of the Hubble constant is 73.8km/sec/Mpc, corresponding to a 3 percent uncertainty; the Hubble constant with uncertainty is denoted h.

The relation between the age of the universe and the Hubble constant is given by $t_0 = 1/2H_0$. The energy density at time t is $\rho = 3/32\pi G t^2$.

• **Vacuum dominated expansion**: According to Lorenz invariance, for the energy-momentum tensor in a general coordinate system we must have $T_V^{\mu\nu} \propto g^{\mu\nu}$. Comparing this with the energy-momentum tensor of a perfect fluid

$$T^{\mu\nu} = pg^{\mu\nu} + (\rho + p)u^\mu u^\nu, \qquad g_{\mu\nu}u^\mu u^\nu = -1 \tag{1.1.10}$$

shows that the vacuum has $p_V = -\rho_V$, so that $T_V^{\mu\nu} = -\rho_V g^{\mu\nu}$. In the absence of any other form of energy this would satisfy the conservation law $T_V^{\mu\nu}{}_{;\mu} = g^{\mu\nu}\partial\rho_V/\partial x^\mu = 0$, so that ρ_V would be constant, independence of spacetime position, known as cosmological constant or vacuum energy. For $K = 0$, Eq. (1.1.4) requires that $\rho_V > 0$, and has the solution

$$a(t) \propto \exp(Ht), \tag{1.1.11}$$

where H is the Hubble constant given by

$$H = \sqrt{\frac{8\pi\, G\, \rho_V}{3}}. \tag{1.1.12}$$

The above solutions have a puzzling property: for a matter and radiation dominated universe at very early times we could neglect the the curvature constant K and obtain the solutions of the Friedmann equation (1.1.4) in the form of Eq. (1.1.8) and Eq. (1.1.9) consistent with a flat universe. But as we mentioned at the beginning of this chapter, at sufficiently early times we expect the universe to be highly warped and curved, in contradiction with a flat universe described by the above solutions. This therefore poses a problem known as the flatness problem [3]. As we shall see in Section 1.2, this problem can be solved if the radiation dominated era was preceded by a sufficient period of inflation, which can explain why the curvature was so small in the early universe.

1.1.2 The horizon problem

We can obtain important information about the structure and evolution of the universe from the radiation that was left after the big bang. This radiation is called the cosmic microwave background radiation and its origin can be understood as follows. Thus, at some early time, the temperature will have been high enough that atoms would have been ionized, and matter and radiation would have been in thermal equilibrium. Then, as the universe expanded and temperature dropped, the electrons would combine with nuclei, the photons decouple, and radiation began a free expansion.

In 1965 Arno Penzias and Robert Wilson discovered this radiation in a study of noise backgrounds in a radio telescope [10]. Subsequent studies confirmed that this radiation has the form of black-body radiation, and contains very small nonuniformities that provide us with important information about the structure and evolution of the universe. The original observation of the nonuniformities in the cosmic microwave radiation background was made by the COBE satellite in 1992 [11], and subsequently in 1996 [12–16], using the same instruments. The accuracy of the results were then greatly improved by the observations of the Wilkinson Microwave Anisotropy Probe (WMAP) satellite launched in 2001, which confirmed a nonuniformity in the microwave background at a relative magnitude of 10^{-5} [17]. This high degree of isotropy of the cosmic microwave radiation background poses a problem. We can see this by comparing the angular diameter distance[3] at the time of last scattering with the acoustic horizon distance[4] which, respectively, read as [3, 4]

[3]Inspection of the FRW metric (1.1.1) shows that a source of co-moving radial coordinate r_1 that emits light at the time t_1 and is observed at present to subtend a small angle θ will extend over a proper distance s (normal to the line of sight) equal to $a(t_1)r_1\theta$. The angular diameter distance is $\mathscr{D}_A$ is defined such that θ is given by the familiar relation of Euclidean geometry $\theta = s/\mathscr{D}_A$ and one can see that $\mathscr{D}_A = a(t_1)r_1$. By computing r_1 one can obtain the full relation for $\mathscr{D}_A$.

[4]The dominant perturbations to the plasma of nucleons, electrons and photons that are relevant to the nonuniformities of the cosmic microwave background are sound waves. The full acoustic horizon distance can be obtained from Eq. (2.2.142) taking into account the speed of sound.

$$\mathscr{D}_H \approx \mathcal{O}(H_0^{-1}\mathscr{R}_L^{-3/2}), \quad \mathscr{D}_A \approx \mathcal{O}(H_0^{-1}\mathscr{R}_L^{-1}), \tag{1.1.13}$$

where $\mathscr{R}_L = 1 + z_L$. Thus the horizon at the time of last scattering now subtends an angle

$$\mathscr{D}_H/\mathscr{D}_A \approx \mathcal{O}(\mathscr{R}_L^{-1/2}). \tag{1.1.14}$$

According to this, for the redshift $z_L \simeq 1100$, points of the same temperature subtend an angle of about 1.6 degrees. This reveals an appreciable anisotropy, in contradiction with the nearly perfect isotropy observed in the cosmic microwave radiation background. This is called the horizon problem [3, 4].

1.1.3 The monopole problem

In the early times after the big bang when the temperature dropped, the universe went through a phase transition in which the putative grand unified symmetry broke down spontaneously to the gauge symmetry $SU(3) \times SU(2) \times U(1)$ of the standard model. As a consequence of this symmetry breaking, extended spacetime-dependent field configurations such as monopoles were produced [3, 5]. This gives rise to another problem: before the phase transition occurred, the scalar fields which account for the symmetry breaking would have inevitably been unrelated at distances larger than the horizon distance corresponding to the maximum distance that light could have travelled since the very beginning of the big bang. During the early times when the universe was presumably radiation dominated, the scale factor grew according to Eq. (1.1.9), and by Eq. (1.1.3), $\mathscr{D}_m(t) = 2t = 1/H$. During the radiation dominated era the expansion rate is $H \approx (G(k_BT)^4)^{1/2}$, which gives the horizon distance of order $t \approx (G(k_BT)^4)^{-1/2}$. Thus the number density of monopoles produced when the temperature drops to M/k_B would have been of order $t^{-3} \approx (GM^4)^{3/2}$. Compared to the number density of photons which is roughly M^3 at $T \approx M/k_B$, the number density of monopoles is suppressed by a factor $(GM^2)^{3/2}$. If the grand unified symmetry is broken at an energy $M \approx 10^{16}$ GeV, then for the Newton constant $G \simeq (10^{19}\,\mathrm{GeV})^{-2}$ the number density of monopoles is suppressed by a factor 10^{-9}

compared to the number density of photons M^3 at $T \approx M/k_B$. But natural sources show that the number density of monopoles is 10^{-39} times less than the number density of photons, a discrepancy by a factor 10^{-30}. This is known as the monopole problem [3, 5]. As we shall see in the next section, inflation can explain this discrepancy provided that the era of radiation dominance proceeded by the period of inflation before as well as after the production of monopoles.

1.2 The period of inflation

In the previous sections we saw that at sufficiently early times the curvature of space is negligible or vanishing, in contradiction with a highly curved universe that we expect to see after the big bang. In 1980 Alan Guth realized that this flatness problem could be solved if another assumption is put in the standard big bang theory, which is the assumption of inflation [18]. The assumption is that before the radiation dominated era, during which the scale factor $a(t)$ grew according to Eq. (1.1.9), the universe was dominated by a period of slowly rolling vacuum energy called inflation, so that $a(t)$ evolved exponentially as in Eq. (1.1.11). As we shall show below, this inflation not only solves the flatness problem but also the horizon and monopole problems. Before going into technical details showing how inflation solves these problems, we discuss the history of inflation and make clear how inflation really works.

1.2.1 A brief history of inflation

"Old inflation"

In order to have inflation, we have to assume that there is a form of energy (other than matter and radiation) that causes the universe to inflate. This form of energy is unstable and has to decay, so that we can end inflation and turn this inflationary energy into something that produces matter and radiation that composes the galaxies and stars and ourselves. The form of energy that has this property is called "false vacuum" state [5]. For this energy, the scalar field expectation values are at a local minimum that is higher than the true minimum of the effective potential.

Figure 1.1: The False vacuum state (left), almost all of which has decayed into the true vacuum state (right) forming an inflationary bubble, but small regions were left behind.

Figure 1.2: The small regions of false vacuum state that were left behind continued to inflate while the bubble stopped to inflate (left). After a certain period of time, other inflationary bubbles formed (right) and our universe is supposed to take place in one of such bubbles (which are not all the same).

This "false vacuum" state corresponding to a local minimum is not a permanent state of being and will decay into the "true vacuum" state corresponding to the true minimum [5]. This decay occurs by quantum mechanical barrier penetration. It is very likely, though not observed, that this process took place several times in the history of the universe since various symmetries have become spontaneously broken. Because the decay happens through a quantum process, and that a quantum process is by nature random, the decay does not occur by a change in the scalar field simultaneously everywhere in space, but by the formation of bubbles of true vacuum in false vacuum background. When quantum mechanical barrier penetration ends, the bubbles of true vacuum will enlarge at the speed of light and at last collide with other bubbles until the entire space is in the state of lowest energy [5].

In his original work [18], Guth considered a model of Grand unification and

noted that in such models scalar fields could get trapped in a local minimum of some potential corresponding to an unbroken grand unified symmetry. When a scalar field gets trapped in a local minimum, the energy of empty space would stay constant for a certain period of time during which the universe continues to expand. This would then result a constant rate of expansion requiring the scale factor to evolve exponentially. This exponential inflation would be ended by quantum-mechanical barrier penetration, after which the scalar field would start rolling down the potential toward a global minimum, corresponding to the present universe. The flatness of the universe was then explained by Guth as a result of a very large exponential expansion which makes the curvature parameter $\Omega_K = |K|/a^2H^2$ very small.

Despite its success in solving the problems of the standard big bang theory, it became clear to Guth and others that his model of inflation had a fatal problem because of the way it ends: the graceful exit problem. To see how this problem comes about, note that in Guth's original work the exponential inflation occurs as a result of a delayed first-order phase transition where a scalar field was first trapped in a local minimum of some potential, and then penetrated through the potential barrier and rolled toward a true minimum of the potential. Because the transition from the initial supercooled false vacuum phase to the lowest energy true vacuum phase (corresponding to the present universe) occurs through a quantum process, and that a quantum process is inherently unpredictable and has some degree of randomness, the transition could not take place everywhere at the same time. It could have occurred here and there in some bubble of true vacuum state which formed when *almost* all of the inflationary energy decayed (see Fig. 1.1 (right)). The smaller fractions of energy that were left behind as false vacuum state continued to inflate while the bubble being true vacuum state stopped to inflate (see Fig. 1.2 (left)). In this way the background of false vacuum would in the end dominate the volume of the universe, and the scalar field would have been still trapped in its local minimum. As the time passed, more and more bubbles formed (see Fig. 1.2 (right)) and the universe would be reheated by collisions between bubble walls. But if inflation lasted long enough (as a result of a high tunneling amplitude), collisions between bubble walls would be exceedingly rare, resulting in no radiation, and therefore not

reheating the universe properly.

"New inflation"

Guth's model of "old inflation" was then replaced by "new inflation" due to the work of Linde [19, 20], Albrecht and Steinhardt [21]. New inflation was originally introduced in a model of grand unification in which the grand unified symmetry is no longer restored. In this model, the grand unified symmetry is broken down by applying the Coleman-Weinberg symmetry breaking mechanism [22]. The potential for the scalar field ϕ obtained within this formalism takes the form

$$V(\phi) \equiv \phi^4 \ln\left(\frac{\phi}{\lambda}\right) + T^2\phi^2. \tag{1.2.15}$$

The first term in this potential comes from one-loop radiative corrections to $V_{T=0}$ which is assumed to have vanishing second derivative at $\phi = 0$. This term has an unstable stationary point at $\phi = 0$ and a minimum at $\phi_0 = \lambda/e^{1/4}$, where λ is a constant.. The second quadratic term includes finite temperature contributions and takes the stationary point $\phi = 0$ into a local minimum. Like in old inflation, in this set up phase the transition takes place by the formation of bubbles, but the difference is that for low temperature the potential barrier is very small and hence the field inside the bubble starts with ϕ close to zero. The field then rolls slowly down the potential whereas the universe experiences exponential inflation. Finally, the scalar field undergoes damped oscillations about the minimum of its potential and the scalar field energy gets converted into ordinary particles that fill the bubble, reheating the universe.

The basic element of new inflation was a more-or-less exponential expansion during the slow-roll of one or more scalar fields with the effects depending on the slow-roll of the scalar field after bubble formation and not on the process of bubble formation itself. In fact all that really matters does not depend on grand unification or the Coleman-Weinberg mechanism but instead on the existence of a scalar field ϕ called the inflaton which at some early times has a value at which the potential $V(\phi)$ is large but quite flat. The flatness of the potential guarantees the slow-roll of the scalar field during which the Hubble constant decreases only slowly making the

universe expand nearly exponentially. In this scenario reheating occurs not because of bubble wall collisions but due to damped oscillations of the scalar field about the minimum of the potential where the potential steepens and inflation ends.

1.2.2 Slow-roll formalism

To see how new inflation works qualitatively, we may start with simplest scalar field theory Lagrangian [3]

$$\mathscr{L}(\phi) = -\sqrt{-\det g}\left[\frac{1}{2}g^{\mu\nu}\partial_\mu\phi\partial_\nu\phi - V(\phi)\right]. \tag{1.2.16}$$

Using this Lagrangian, the equation of motion for a spatial homogeneous field, $\phi \equiv \phi(t)$, in the FRW coordinate system takes the form

$$\ddot{\phi} + 3H\dot{\phi} + V'(\phi) = 0, \tag{1.2.17}$$

where as before $H = \dot{a}/a$ is the expansion rate. The field energy density and pressure take the form

$$\rho = \frac{1}{2}\dot{\phi}^2 + V(\phi), \tag{1.2.18}$$

$$p = \frac{1}{2}\dot{\phi}^2 - V(\phi). \tag{1.2.19}$$

During the period of scalar field energy dominance the expansion rate is

$$H = \sqrt{\frac{8\pi\, G\rho}{3}} = \sqrt{\frac{8\pi\, G}{3}\left(\frac{1}{2}\dot{\phi}^2 + V(\phi)\right)}. \tag{1.2.20}$$

The time derivative of this together with Eq. (1.2.17) gives

$$2H\dot{H} = \frac{8\pi\, G}{3}(\dot{\phi}\ddot{\phi} + V'(\phi)\dot{\phi}) = -8\pi G H\dot{\phi}^2, \tag{1.2.21}$$

and hence

$$\dot{H} = -4\pi G\dot{\phi}^2. \tag{1.2.22}$$

According to $\dot{H} + H^2 = \ddot{a}/a$, a evolves like $\exp(Ht)$ if we have

$$|\dot{H}| \ll H^2. \tag{1.2.23}$$

From Eq. (1.2.20) and Eq. (1.2.22), we have $\dot{H}/H^2 \simeq \dot{\phi}^2/V(\phi)$, so the condition (1.2.23) requires

$$\dot{\phi}^2 \ll |V(\phi)|. \tag{1.2.24}$$

From Eq. (1.2.19) and (1.2.24) we can see that the effective pressure of the material driving the expansion has to be negative, $p \simeq -\rho$. The scalar fields that have this property are called inflatons. Thus, according to Eq. (1.1.4) and Eq. (1.1.5), during inflation we have

$$\ddot{a} > 0. \tag{1.2.25}$$

This relation tells us what inflation is: It describes a period of accelerated expansion. The condition (1.2.24) also reduces Eq. (1.2.20) to

$$H = \sqrt{\frac{8\pi G V(\phi)}{3}}. \tag{1.2.26}$$

In addition to the condition, we may also assume that

$$|\ddot{\phi}| \ll H|\dot{\phi}|. \tag{1.2.27}$$

According to this, from Eq. (1.2.17) we obtain the following relation

$$\dot{\phi} = -\frac{V'(\phi)}{3H} = \frac{V'(\phi)}{\sqrt{24\pi G V(\phi)}}. \tag{1.2.28}$$

Thus the condition for having prolonged exponential inflation is

$$\varepsilon = \frac{|\dot{H}|}{H^2} = \frac{1}{2}\sqrt{\frac{3}{8\pi G}}\left|\frac{V'(\phi)\dot{\phi}}{V^{3/2}(\phi)}\right| = \frac{1}{16\pi G}\left(\frac{V'(\phi)}{V(\phi)}\right)^2 \ll 1. \tag{1.2.29}$$

Taking the derivatives of both sides of Eq. (1.2.28) with respect to time gives

$$\ddot{\phi} = -\frac{V''(\phi)\dot{\phi}}{3H} + \frac{V'(\phi)\dot{H}}{3H^2} = \frac{V''(\phi)V'(\phi)}{9H^2} - \frac{1}{16\pi G}\left(\frac{V'(\phi)}{V(\phi)}\right)^2 \frac{V'(\phi)}{3}. \tag{1.2.30}$$

By $\varepsilon \ll 1$ the last term of (1.2.30) is much less than $V'(\phi)$, so in order to have $|\ddot{\phi}|$ much less than $V'(\phi)$, according to Eq. (1.2.27), we have to have $V''(\phi) \ll 9H^2$, or equivalently

$$\eta = \frac{1}{24\pi G}\left|\frac{V''(\phi)}{V(\phi)}\right| \ll 1. \tag{1.2.31}$$

The parameters η and ε are know as slow-roll parameters and the conditions (1.2.29) and (1.2.31) are called slow-roll conditions[5]. Potentials that satisfy these conditions are classified as flat potentials and produce a large number of e-foldings. To see this, consider the scale factor

$$\frac{a(t_2)}{a(t_1)} = \exp\left[\int_{t_1}^{t_2} H dt\right] = \exp\left[\int_{\phi_1}^{\phi_2} \frac{H d\phi}{\dot{\phi}}\right], \tag{1.2.32}$$

and note that the number of e-foldings is defined by

$$\mathcal{N} = \int_{t_1}^{t_2} H dt = \int_{\phi_1}^{\phi_2} \frac{H d\phi}{\dot{\phi}}. \tag{1.2.33}$$

By inserting H and $\dot{\phi}$ by their values given by Eq. (1.2.26) and Eq. (1.2.28), we can rewrite (1.2.32) in the form

$$\exp\left[-\int_{\phi_1}^{\phi_2}\left(\frac{8\pi G V(\phi)}{V'(\phi)}\right)d\phi\right] = \exp\left[-\int_{\phi_1}^{\phi_2}\sqrt{4\pi G}\left(\frac{1}{\sqrt{16\pi G}}\frac{V'(\phi)}{V(\phi)}\right)^{-1} d\phi\right]. \tag{1.2.34}$$

According to the slow-roll condition (1.2.29), the absolute value of the term in the square brackets of Eq. (1.2.34) is much less than unity. This means that the argument of the exponential in Eq. (1.2.34) is much greater than $\sqrt{4\pi G}|\phi_1 - \phi_2|$. Thus when the slow-roll condition is satisfied, a large number of e-foldings can be produced in any time interval during which $|\phi_1 - \phi_2|$ has the minimum amount of $1/\sqrt{4\pi G} = 3.4 \times 10^{18}$ GeV.

[5] As we shall see below, meeting these conditions in string theory is highly non-trivial because corrections from moduli stabilization generically ruin the flatness of the potential. Slow-roll inflation is then possible only if, there exists a fine-tuned cancellation by additional corrections that can flatten the potential. However, as we shall see below, in string theory it is possible to drive inflation even when the potential remains steep.

1.2.3 Solving the flatness and horizon problems

According to the above discussion, inflation is a period of slowly rolling vacuum energy during which the scale factor evolves exponentially, $a \simeq \exp(N)$. This means that if inflation started with the curvature density parameter $\Omega_K = |K|/a^2H^2$ of order unity, then inflation ended with $\Omega_K = |K|/a_I^2H_I^2$ of order $\exp(-2N)$. This implies Ω_K for the present time to be

$$|\Omega_K| = \frac{|K|}{a_0^2H_0^2} = \exp(-2N)\left(\frac{a_IH_I}{a_0H_0}\right)^2. \tag{1.2.35}$$

In order to explain why the curvature of space was so small in the early universe, we have to have the condition

$$\exp(N) > \frac{a_IH_I}{a_0H_0}. \tag{1.2.36}$$

Thus the flatness problem can be solved if the above condition is satisfied [3]. The above condition also solves the horizon problem. To see this, recall that the proper horizon distance at the time of last scattering is

$$\mathscr{D}_H(t) = a(t)\int_{t_*}^{t_L}\frac{dt}{a(t)}, \tag{1.2.37}$$

where t_* is the time when inflation starts and t_I is the time when inflation ends, as before. As already mentioned, during inflation $a(t)$ evolves exponentially and we may take

$$a(t) = a(t_*)\exp\Big(H_I(t-t_*)\Big) = a_I\exp\Big(-H_I(t_I-t)\Big). \tag{1.2.38}$$

By taking $N = H(t_I - t_*)$ to be the number of e-foldings we obtain

$$\mathscr{D}_H(t_L) = \frac{a(t_L)}{a_IH_I}\big[\exp(N)-1\big]. \tag{1.2.39}$$

In the above relation we may only consider the first term since a sufficient amount of inflation requires $\exp(N) \gg 1$. The angular diameter distance at the time of last scattering is

$$\mathscr{D}_A(t_L) \approx \frac{a(t_L)}{H_0a_0}. \tag{1.2.40}$$

The high degree of isotropy in the cosmic microwave background requires $\mathscr{D}_H > \mathscr{D}_A$, and this can accounted followed by having the (same) condition

$$\exp(N) > \frac{a_I H_I}{a_0 H_0}. \tag{1.2.41}$$

Thus the horizon problem can be solved if the above condition holds [3]. In order to estimate the number of e-foldings required to solve the flatness and horizon problems, we need to evaluate this bound. To do so, recall that the period of inflation is succeeded by the radiation dominated era, so for the transition between these eras we may assume

$$a_I H_I \simeq a_1 H_1, \tag{1.2.42}$$

where a_1 and H_1 denote the scale factor and the expansion rate of the radiation dominated era, respectively. The expansion rate over the whole periods of radiation and matter dominance takes the form

$$H = \frac{H_{\rm EQ}}{\sqrt{2}} \sqrt{\left(\frac{a_{\rm EQ}}{a}\right)^3 + \left(\frac{a_{\rm EQ}}{a}\right)^4}, \tag{1.2.43}$$

where $a_{\rm EQ} = a_0 \Omega_R / \Omega_M$ and $H_{\rm EQ} = \sqrt{2\Omega_M} H_0 (a_0/a_{\rm EQ})^{3/2}$ are the scale factor and expansion rate at matter-radiation equality. By putting $a = a_1 \ll a_{\rm EQ}$ we obtain

$$H_1 = \frac{H_{\rm EQ}}{\sqrt{2}} \left(\frac{a_{\rm EQ}}{a_1}\right)^2. \tag{1.2.44}$$

We can use this relation to get eliminate a_1 and obtain the bound (1.2.36) as

$$\exp(N) > \left(\frac{\Omega_M a_{\rm EQ}}{a_0}\right)^{1/4} \sqrt{\frac{H_1}{H_0}} = \Omega_R^{1/4} \sqrt{\frac{H_1}{H_0}} = \left(\Omega_R \frac{\rho_1}{\rho_{0,\rm crit}}\right)^{1/4} = \frac{[\rho_1]^{1/4}}{0.037\ h\ \text{eV}}, \tag{1.2.45}$$

where $\rho_{0,\rm Crit} = [3 \times 10^{-3} \text{eV}]^4 h^2$ and ρ_1 denote the critical density (1.1.6) and the energy density at the beginning of the radiation-dominated era, respectively. From this relation we can estimate the number of e-foldings by noting that ρ_1 should not be greater than Planck energy density $G^{-2} = [1.22 \times 10^{29}\ \text{GeV}]^4$, so that for $h = 0.7$ we obtain 5×10^5, or about 60 e-foldings. Thus in order to solve the flatness and horizon problems about 60 e-foldings need to be produced during the period of

inflation[6] [3].

1.2.4 Solving the monopole problem

As discussed in the previous section, the number density of monopoles is 10^{-39} times less than the number density of photons, a discrepancy by a factor 10^{-30}. Inflation can explain this discrepancy: if the era of radiation dominance proceeded by the period of inflation before as well as after the production of monopoles, then the exponential expansion before the production of monopoles would have increased the horizon distance, and the exponential expansion after the production of monopoles would have decreased the photon to monopole ratio [3] . To solve the monopole problem, the photon to monopole ratio has to be reduced by inflation by a factor 10^{-30}. This requires an exponential inflation that increases the horizon distance by a factor 10^{10}, which means that the horizon distance after inflation $\exp(N)/H_1$ must be 10^{10} times greater than the estimated horizon distance $(GM^4)^{-1/2}$. The expansion rate during the radiation dominated era is $H_1 \approx (G(k_BT)^4)^{1/2}$, which for $T \approx M/k_B$ gives $H_1 \approx (GM^4)^{1/2}$. According to this, the number of e-foldings needed to solve the monopole problem has to be greater than $\ln 10^{10} = 23$ [3]. Thus if inflation can solve the flatness and horizon problems, for which the number of e-foldings has to be about 60, then it can also solve the monopole problem[7].

1.2.5 Shortcomings of inflation

In the inflationary picture discussed in the previous sections, we had to make a number of assumptions. We had to assume a big bang, and we had to assume a special form of energy that decays in certain way. In principle, the idea was that once we have inflation we can set up the large scale structure of the universe and explain everything else that happens in the universe from that point onwards without making any further assumptions. But this does not work quite that way.

[6] As we shall see in Chapter 4, this amount of e-foldings can be produced in D-brane inflation.

[7] This is probably the reason why in the literature one mostly talks about inflation as the solution to the flatness and horizon problems.

In 1998, two research groups, the Supernova Cosmology Project [23] and the High-z Supernova Search [24] groups, measured the luminosity distances versus redshift of various Type Ia supernovae. They found that their curve of measured luminosity distances versus redshift is consistent with an accelerating universe whose large part of energy density is of the form unlike ordinary matter or radiation, called dark energy, that was unexpected and not predicted by the inflationary picture.

Although the inflationary picture agrees with the data, it agrees at a certain price. Firstly, it is definitely finely tuned. To get inflation to give really the right statistical distribution of anisotropies that we see in the cosmic microwave background radiation in the WMAP satellite, the energy has to have very specific properties; it has to have a very specific amount, strength, concentration and it has to decay in a very specific way, otherwise we get the wrong pattern. When we add dark energy it also works but we have to add that by hand by the cost of fine tuning. Secondly, it is a kind of patchwork of disconnected elements, including ordinary matter, dark matter and dark energy that have been added one by one to fit the observations. To match the universe as it is seen today, all three components must exist in a particular precise combination. Thirdly, as we saw in Section 1.2, inflation amplifies rare quantum events which amplify randomness, so instead of having a very ordered universe we will have a disordered universe. In this way the formed pockets in one of which our universe is supposed to take place are not all the same. An infinite number of them will have the physical laws like our universe and an infinite number of them will not. The question that arises is that which case is more probable, which cannot be answered when the distribution is so uneven. Fourthly, inflation has to be derived from a fundamental theory such as string theory which can verify the origin of the inflaton field and its potential.

1.3 Inflation in string theory

1.3.1 Motivation

In the previous section we saw that the very early universe underwent a period of rapid expansion, known as inflation, resulting in a very nearly flat, homogeneous

and isotropic initial state. While a simple scalar field model of inflation with a suitable potential satisfies many of the cosmological requirements, such models are rather ad hoc from the high energy particle theory point of view. The challenge is to find a theory which has a clear derivation from a fundamental high energy theory incorporating gravity at the quantum level. String theory as a finite theory of quantum gravity naturally is the prime candidate for such a fundamental theory. In particular, string theory can tell us which field plays the role of the inflaton (e.g. the field parameterizing the distance between two branes as described below), where does its potential come from (e.g. from supersymmetry breaking between two branes as described below) and how does it couple to the Standard Model sector. Furthermore, as we saw in the previous section, the flatness of the inflaton potential in Planck units is guaranteed by two nontrivial constraints, the slow-roll conditions (1.2.29) and (1.2.31). In effective field theories, four-dimensional Planck-suppressed operators with vacuum expectation values comparable to the inflationary energy density produce mass terms in the inflaton potential, which violate the slow-roll conditions (see Subsection 1.3.3.). In order to determine whether despite such corrections inflation can still take place, one has to have detailed information about Planck-suppressed corrections to the inflaton potential. This requires microphysical knowledge about physics at Planck-scale, which can be obtained from string theory. In string theory, such corrections can be computed from first principles and the complete shape of the inflaton potential including all degrees of freedom can be determined (see Subsection 1.3.5). These provide enough motivation for embedding inflation into string theory.

1.3.2 Moduli and inflatons

It is well known that in string theory the dimension of spacetime is ten, and four-dimensional physics related to our universe emerges upon compactification. In particular, one is interested in string vacua for which only four dimensions are non-compact and the other six extra dimensions are compact. The four non-compact dimensions span our universe and the other six extra dimensions form a compact internal space. The relevant metric is the sum of the four-dimensional (Minkowski)

and the six-dimensional metric

$$ds^2 = g_{\mu\nu}dx^\mu dx^\nu + g_{mn}dy^n dy^m. \tag{1.3.46}$$

If these solutions preserve at least one supersymmetry, then g_{mn} is Ricci-flat, Kähler, and the internal space is a compact Calabi-Yau manifold [25] (see Appendix A). There is generically a many-parameter family of the metrics of these manifolds, which all share the same topology. This means that upon small variations in the metric on the internal manifold

$$g_{mn} \to g_{mn} + \delta g_{mn} \tag{1.3.47}$$

the new background still satisfies the Calabi-Yau conditions given by

$$R_{mn}(g_{..}) = 0, \qquad R_{mn}(g_{..} + \delta g_{..}) = 0. \tag{1.3.48}$$

There are metric deformations which only account for coordinate changes and are uninteresting. In order to eliminate them, one fixes the gauge [26]

$$\nabla^m \delta g_{mn} - \frac{1}{2}\nabla_n \delta g^m_m = 0, \tag{1.3.49}$$

where $\delta g^m_m = g^{mp}\delta g_{mp}$. Expanding the second equation in (1.3.48) to linear order in δg and using the Ricci-flatness of g leads to the Lichnerowicz equation given as [26]

$$\nabla^k \nabla_k \delta g_{mn} + 2R^{p\,q}_{mn}\delta g_{pq} = 0. \tag{1.3.50}$$

The latter equation in (1.3.48) introduces the differential equations for δg whose number of solutions counts the number of ways the background metric can be deformed while preserving supersymmetry and topology. The coefficients of these independent solutions are moduli. They are the expectation values of massless scalar fields, called the moduli fields. These moduli parameterize changes of the size and shape of the internal Calabi-Yau manifold but not its topology. Due to the special properties of Kähler manifolds (see Appendix A) the zero modes of Eq. (1.3.50) of mixed type, $\delta g_{\mu\bar{\nu}}$, and those of pure type, $\delta g_{\mu\nu}$, $\delta g_{\bar{\mu}\bar{\nu}}$, satisfy Eq. (1.3.50), respectively [26]. These two types of variations imply that the moduli space of Calabi-Yau

manifolds decomposes, at least locally, into a product with the space of parameters of the complex structure as one factor and a complex extension of the parameter space of the Kähler class as the other [26] (see Appendix A). The moduli space of a (topological class of a) Calabi-Yau three-fold is smooth at its generic points but there exist special regions, called "boundary", where the moduli spaces of topologically distinct Calabi-Yau spaces meet. These 'interface' regions correspond to certain singular limits of the respective Calabi-Yau three-folds, called conifolds [27] (see Appendix A). By including these limit points the moduli spaces of a large number of Calabi-Yau spaces piece together into a "connected web". It has been shown that the distances between two topologically distinct Calabi-Yau three-folds in this web is finite [28] (see Appendix A) and the explicit form of the unique Ricci-flat Kähler metric on conifolds is known [27] (see Appendix A) :

$$g_{mn}dy^m dy^n = dr^2 + r^2 ds^2_{X_5}, \tag{1.3.51}$$

which describes the geometry of a cone, the base of which is a five-dimensional Einstein manifold parameterized by five angular directions.

For embedding inflation into string theory, one has to specify a string compactification whose low-energy effective theory contains a suitable inflaton, so that the relating potential satisfies slow-roll conditions (1.2.29) and (1.2.31). The many moduli fields that arise from Calabi-Yau compactifications as the solutions of Eq. (1.3.48) can provide a large number of candidate scalar fields in the four dimensional theory and any of these scalar fields may play the role of the inflaton field. However, moduli fields have non-universal couplings to matter and make different types of matter get different acceleration, which leads to the violation of the equivalence principle of general relativity. Moreover, these moduli fields are generically either massless, or have a potential with runaway behavior, which makes their interpretation as inflatons rather difficult. In addition to this, the computation of the effective potential in terms of all these scalar fields and degrees of freedom is a highly nontrivial task. Nevertheless, by considering the systematics of flux compactifications [29] and non-perturbative effects [30] in string theory (see Chapter 2), it is possible to reduce the degrees of freedom and stabilize all the moduli fields, as required for constructing

a successful cosmology from string theory[8]. In the presence of fluxes a much richer Calabi-Yau geometry is produced and the background gets modified by warping through the gravitational fields created by fluxes. The metric (1.3.46) is modified to a warped metric of the form [29, 30]

$$ds^2 = e^{2A(y)} g_{\mu\nu} dx^\mu dx^\nu + e^{-2A(y)} g_{mn} dy^n dy^m, \tag{1.3.52}$$

where e^{4A} is the warp factor depending on the internal coordinates, y, of the warped background. The resulting geometry corresponds to a configuration containing warped throats that (according to gauge/gravity duality) smoothly close off at the infrared (IR) and attached to the compact Calabi-Yau space in the ultraviolet (UV) (e.g. see Fig 1.3). In the UV the six-dimensional metric in Eq. (1.3.52) is (asymptotically) the same as the metric given by Eq. (1.3.51) but in general it has a more complicated form due to differential wrapping (see Chapter 2). In Calabi-Yau flux compactifications many vacua and various such throat solutions are produced since fluxes can take many different discrete values. Currently, there is no known criterion for choosing among these vacua.

1.3.3 Moduli stabilization obstacles to inflation

The most severe problem that arises in embedding inflation into string theory (according to the above set up) is that moduli stabilization generically induces an inflaton mass term that spoils the flatness of the inflaton potential (see the reviews [34–40]). To see this, note that in $N = 1$ supergravity a key term in the scalar potential is the F-term potential [30] (see also Chapters 2 and 5),

$$V_F = e^{K/M_{\rm pl}^2} \left[K^{\varphi\bar{\varphi}} D_\varphi W \overline{D_\varphi W} - \frac{3}{M_{\rm pl}} |W|^2 \right]. \tag{1.3.53}$$

Here $K(\varphi, \bar{\varphi})$ and $W(\varphi)$ are the Kähler potential and the superpotential, respectively; φ is a complex scalar field which is taken to be the inflaton; and we have

[8] As an aside, we would like to remark that the inclusion of nonperturbative effects in quantum field theories alleviate the problems of perturbative field theories, which arise from the masslessness of gauge modes [31–33].

defined $D_\varphi W \equiv \partial_\varphi W + M_{\rm pl}^{-2}(\partial_\varphi K)W$.

The Kähler potential determines the inflaton kinetic term, $K_{,\varphi\bar{\varphi}}\partial\varphi\partial\bar{\varphi}$, while the superpotential determines the interactions. To derive the inflaton mass, we expand K around some chosen origin, which is denoted here by $\varphi \equiv 0$ without loss of generality, i.e., $K(\varphi,\bar{\varphi}) = K_0 + K_{,\varphi\bar{\varphi}}|_0\varphi\bar{\varphi} + \cdots$. This yields the inflationary Lagrangian of the form

$$\begin{aligned} \mathscr{L} &\approx -K_{\varphi\bar{\varphi}}\partial\varphi\partial\bar{\varphi}\left(1 + K_{,\varphi\bar{\varphi}}|_0\frac{\varphi\bar{\varphi}}{M_{\rm pl}^2} + \cdots\right) \\ &\equiv -\partial\phi\partial\bar{\phi} - V_0\left(1 + \frac{\phi\bar{\phi}}{M_{\rm pl}^2}\right) + \cdots \end{aligned} \tag{1.3.54}$$

where we have defined the canonical inflaton field $\phi\bar{\phi} \approx K_{\varphi\bar{\varphi}}|_0\varphi\bar{\varphi}$ and $V_0 \equiv V_F|_{\varphi=0}$. We have retained the leading correction to the potential originating in the expansion of $e^{K/M_{\rm pl}^2}$ in Eq. (1.3.53), which could plausibly be called a universal correction in F-term scenarios. The omitted terms, some of which can be of the same order as the terms we keep, arise from expanding the term inside the square brackets of Eq. (1.3.53) and clearly depend on the model-dependent structure of the Kähler potential and the superpotential. According to Eq. (1.2.31), the potential term on the RHS of Eq. (1.3.54) contributes to the slow-roll parameter by (see also Eqs.(1.3.56) - (1.3.57))

$$\Delta\eta = 1. \tag{1.3.55}$$

This makes slow-roll inflation impossible. To evade this problem, one of the major challenges has been to show that in a non-vanishing fraction of the vast number of string vacua the inclusion of various compactification effects in the effective field theory induce correction terms in the inflaton potential that can cancel to high precision with the inflaton mass term, so that a suitable inflationary model can be obtained [38, 40] (see also Subsection 1.3.5.).

1.3.4 Classification of string inflationary models

To construct inflationary models in string theory (see the reviews [34–40]), it is natural to identify the inflaton either with closed string moduli or with open string moduli, as in string theory strings are either closed or open. Since open strings end on hypersurfaces called D-branes [41] (see Chapter 3), the string inflationary scenario in which the inflaton is identified with open string moduli is called (warped) D-brane inflation. As the moduli are the most promising closed string modes, the inflationary scenario in which the inflaton is identified with closed string moduli is called moduli inflation. Apart from these string inflationary scenarios, there is also a string inflationary scenario called landscape inflation which is based on the general properties of the 'string landscape' (e.g. high dimensionality) instead of direct specification of the inflaton. In the string theory landscape, flux compactifications typically give very many possible vacua, since the fluxes can take many different discrete values, and there is no known criterion for choosing among them. The number of solutions from fluxes comes about 10^{500} and these vacua can be regarded as extrema of some potential, which describes the string theory landscape. The large number of solutions would indicate that a few of these universes will have the properties of our observable inflationary universe, and we happen to live in one of those (in the same way that there are many galaxies and planets in the universe and we just happen to live in one).

In the last decade there has been a great progress towards the embedding of inflation into string theory using these classifications. In this thesis we focus on a particular model called warped D-brane inflation, which is both natural and testable.

1.3.5 Case study: D-brane inflation

In D-brane inflation our universe is identified with a spacetime filling mobile D3-brane whose location in the compactification is given by the inflaton field. The D3-brane is pointlike in the extra dimensions and inflation is supposed to take place due to the existence of a flat inflaton potential corresponding to a weak force between the D3-brane brane and a distant anti-D3-brane fixed in the Calabi-Yau compact-

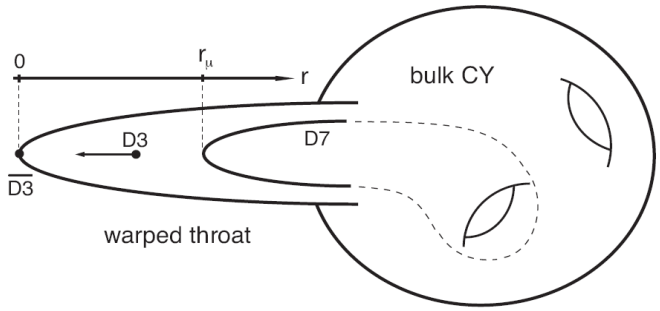

Figure 1.3: A mobile D3-brane moving towards an anti-D3-brane fixed at IR location at the bottom of the warped throat region of a flux compactification. The throat is smoothly glued to a Calabi-Yau three-fold in the UV region where moduli stabilizing D7-branes enter the throat. In principle, our universe may exist in various parts of compactification, including other warped throats not shown in the diagram. This figure is from [54].

ification [42–45]. In this set up inflation ends as the branes collide and annihilate each other by which the inflationary energy density ultimately gets transformed to heat for the later hot big bang. The problem that arises is that in Calabi-Yau compactifications the size of the internal manifold is a modulus making the potential too steep for inflation. One of the major challenges has been to stabilize all the moduli and show that in a non-vanishing fraction of the vast number of string vacua the inclusion of various compactification effects in the effective field theory leaves a suitable inflationary model.

In recent years there has been significant progress within the 'KKLT' framework, [30], in which the older idea of brane inflation [42–45] is realised via the motion of a brane in internal, hidden, extra dimensions [46] (see also [47–61] and the reviews [34–40]). In these scenarios volume modulus stabilization obstacles to inflation (see subsection 1.3.3), but the inflaton potential (of the position of a probe D3-brane) is flattened by fine-tuned cancellation of correction terms from further moduli stabilization from wrapped branes and bulk effects so that inflation can occur (see Fig 1.3). In more detail, the most general inflaton potential and its relating contribution to the slow-roll parameter take the form [55]

$$V(\phi) = V_0(\phi) + H_0^2\phi^2 + \Delta V(\phi) \tag{1.3.56}$$

$$\eta(\phi) = \eta_0(\phi) + \frac{2}{3} + \Delta\eta(\phi) = ? \tag{1.3.57}$$

In Eq. (1.3.56), the first term on the RHS defines terms in the potential that have negligible contributions to η, $\eta_0 \ll 1$, the second term is the inflaton mass term that has a large (order unity) contribution to η given by 2/3, which spoils the flatness of the inflaton potential, and the last term contains all other corrections to the inflaton potential whose associated contribution to η is given by $\Delta\eta$. In order to flatten the inflaton potential, one has to compute ΔV and show that under fine tuning its associated $\Delta\eta$ compensates against the problematic (order unity) term 2/3, so that the inflaton potential becomes flat (see below). However, whether or not the potential can be made flat to meet the slow-roll conditions, DBI inflation, [62, 63], is also possible, even when the potential is steep. In this case, while the motion of the brane can be strongly relativistic (in the sense of a large γ-factor) strong warping of the local throat region renders their contribution to the local energy density subdominant to that of the inflaton potential terms. To see this, note that in the (type IIB) supergravity background with metric ansatz (1.3.52) the effective action takes the form [62, 63] (see Chapter 3)

$$\begin{aligned} S &= \frac{M_{\rm pl}}{2}\int d^4x\sqrt{-g}\mathcal{R} \\ &\quad -g_s^{-1}\int d^4x\sqrt{-g}\Big[T_3e^{-4A}(\gamma_{\rm DBI}^{-1}-1)+V(\phi^m)\Big], \\ \gamma_{\rm DBI} &= \sqrt{1-e^{4A}g_{mn}g^{\mu\nu}\partial_m\phi^m\partial_n\phi^n/T_3}. \end{aligned} \tag{1.3.58}$$

Here T_3 is the D3-brane tension, g_s is the string coupling, and $M_{\rm pl}$ is the Planck mass. The first term in this action is the ordinary four-dimensional Einstein-Hilbert action, which arises from dimensional reduction of the closed string sector of the ten dimensional action. The second part contains the action that controls the dynamics of the fields, parameterizing the position of the brane along the internal coordinates, ϕ^m. In a strongly warped region, $e^{4A} \gg 1$, the kinetic energy's pre-factor of e^{-4A} in Eq. (1.3.58) suppresses it relative to $V(\phi^m)$ even when the motion is relativistic.

In either case (whether slow-roll or DBI), the approach taken is to consider a D3-brane moving in a warped throat region of a Calabi-Yau flux compactification of type IIB theory with ISD conditions [29]. However, when the UV end of the warped throat is attached to the compact Calabi-Yau space with all moduli stabilized, violations of ISD conditions with important implications for the action of the brane are expected. The perturbations around the ISD solution satisfy the supergravity equation of motion [55–57] (see Chapter 2)

$$\Delta_{(0)}\Phi_- = \frac{g_s}{96}|\Lambda|^2 + \mathcal{R}_4. \tag{1.3.59}$$

Here $\mathcal{R}_4$ denotes the Ricci-scalar, Λ is the (IASD) flux, $\Delta_{(0)}$ is the Laplace operator with respect to the leading order Calabi-Yau metric $g^{(0)}_{mn}$, and $\Phi_- = e^{4A} - \alpha$ with e^{4A} being the warp factor in the metric (1.3.52) and α a potential for the five-form on this background given by [29]

$$\tilde{F}_5 = (1 + \star_{10})\Big[d\alpha(y) \wedge dx^0 \wedge dx^1 \wedge dx^2 \wedge dx^3\Big]. \tag{1.3.60}$$

In an ISD background $\alpha = e^{4A}$ and Φ_- is vanishing. In the presence of perturbations around the ISD solution Φ_- is nonvanishing and the potential of the mobile D3-brane in such a background receives corrections in the form [55–57]

$$\Delta V = T_3(e^{4A} - \alpha) \equiv T_3\Phi_-. \tag{1.3.61}$$

Hence the corrections to the D3-brane potential are computed from the solution of Eq. (1.3.59), which takes the form [55–57] (see also Chapter 2)

$$\Phi_-(r, \Psi) = \sum_{LM} \Phi_{LM} f_{LM}(r) Y_{LM}(\Psi), \tag{1.3.62}$$

where Φ_{LM} are constants, $f_{LM}(r)$ and $Y_{LM}(\Psi)$ denote the radial and angular eigenfunctions on the conical geometry that is approximately described by the metric (1.3.51). The solution (1.3.62) implies in particular that the potential of a mobile D3-brane in the compactified throat geometry receives angular dependent corrections, [52–57], which until recently, have been largely neglected (although see [58–60, 64]). In slow roll inflation, it was presumed that the angular directions would

stabilise rapidly, with the radial (slow-roll) direction dominating the inflationary trajectory. In this case the chief motivation of computing supergravity perturbations in the form of Eq. (1.3.62) is to obtain inflaton corrections in the form of Eq. (1.3.61), which (upon minimization of the angular eigenfunction) may lead to a fine tuned cancellation against the inflaton mass term in Eq. (1.3.56), so that slow-roll inflation can occur. However, for generic brane motion the effect of angular motion is less clear, particularly in the presence of angular terms in the potential.

Angular motion of branes was initially explored in the probe limit, i.e. where the brane does not back-react at all on either the internal or external dimensions. Unsurprisingly, the angular motion has a conserved momentum, which can give interesting brane universes (see e.g. [65–69]), however the mirage style, [70], interpretation of the cosmology of these universes leads to a rather unsatisfactory picture. Based on the probe understanding, it was conjectured that angular motion would not affect a more realistic inflationary scenario to any great extent, an expectation largely borne out by the "spinflation" study, [71–74], which found a marginal increase of a couple of e-foldings due to angular motion, coming mainly from the initial stages of inflation before the angular momentum becomes redshifted away. This increase is however parameter sensitive, a point not noted in this original study. In [71–74], a general DBI-inflationary universe was considered near the tip of the warped deformed conifold throat, the Klebanov-Strassler (KS) solution [75], with a simple radial brane potential; with a more realistic potential including angular terms, the spinflationary picture could potentially be rather different.

In this thesis therefore, we investigate the cosmological implications of including angular dependence in the DBI brane inflation scenario. Building on the results of Baumann et al. [52–57], we consider D3-brane motion in the warped throat region of the compact Calabi-Yau subject to UV deformations of the geometry that induce angular dependent corrections in the potential of the probe D3-brane. Taking into account perturbations around the ISD solution, we solve the D3-brane equations of motion from the DBI action with angular dependence induced by the leading correction to the potential allowed by the symmetries of the compactification. Our aim is to consider angular momentum in a fully UV/IR consistent fashion, and to

account for angular momentum in a more general potential. As with the simpler radial spinflation potential, our numerical solutions show that angular dependence tends to increase the inflationary capacity of a trajectory, increasing the number of e-foldings, albeit at a subdominant level. To a large extent, the trajectories are still predominantly radial, however, do exhibit rotational motion due to the angular potential.

An important question is how generic such trajectories are. In general, as the brane arrives in the throat, one expects a range of initial conditions in terms of angular values and velocities. We find that the D brane trajectories and number of e-foldings are dependent more on model parameters than on the initial condition of the brane motion, thus indicating that the results of our investigation are reasonably robust.

The thesis is organized as follows. In Chapter 2, we discuss the supergravity background that we use to study of brane inflation in subsequent chapters. In Chapter 3, we first review some of the relevant aspects of D-branes and construct the multifield D-brane action. We then derive the equations of motion from the action and review a multifield DBI brane inflation model known as Spinflation. In Chapter 4, we study Spinflation in the presence of linearized (first order) perturbations around the ISD supergravity solution, which induce angular dependence in brane motion. In Chapter 5, we extend our study of Chapter 4 by taking into account non-linear (second order) perturbations around the ISD solution including further angular corrections from the effects of backreaction sourced by moduli stabilizing wrapped D7-branes. In Chapter 6, we briefly comment on future directions for further investigations.

Chapter 2

The supergravity model

In this chapter, we discuss the supergravity background used for the study of brane inflation in the subsequent chapters. We first outline the general type IIB supergravity background, following [29, 76], and consider as a specific example the warped deformed conifold with known metric and known background fluxes, following [75, 77, 78]. We then discuss perturbations around such backgrounds from compactification effects sourced by UV deformations of the ten-dimensional supergravity solution including the effects of moduli stabilization, following [30, 57].

2.1 Calabi-Yau flux compactification of type IIB superstring theory

In brane inflation, a mobile D3-brane (or anti-brane) is embedded in the internal manifold, with its four infinite dimensions parallel to the four-dimensional noncompact universe. The position of the brane on the internal manifold then provides an effective four-dimensional scalar field - the inflaton. The ten-dimensional set-up is assumed to be a flux compactification of type IIB string theory on an orientifold of a Calabi-Yau threefold (or an F-theory compactification on a Calabi-Yau fourfold) [29]. We are interested in the situation where fluxes have generated a warped throat in the internal space, and will be examining primarily the deep throat region.

2.1.1 Type IIB superstring spectrum

The most popular approach to superstring theory is to consider $1+1$–dimensional superconformal invariant quantum field theories over the world sheet. The starting point to analyse the spectrum of the superstring is to put superconformal field theory (SCFT) on a circle. The full SCFT action takes the form [76]:

$$S = \frac{1}{4\pi}\int d^2w\left(\frac{2}{\alpha'}\partial X^\mu \bar{\partial} X_\mu + \psi^\mu \partial_{\bar{w}}\psi_\mu + \tilde{\psi}^\mu \partial_w \tilde{\psi}_\mu\right), \tag{2.1.1}$$

where $w = \sigma^1 + i\sigma^2$ is the cylinder coordinate. Here the first part of the action depending on X describes the bosonic degrees of freedom and is known as the Polyakov action. The second part is the matter fermion action with the fields ψ and $\tilde{\psi}$ are holomorphic (left-moving) and antiholomorphic (right-moving). This action must be invariant under periodic identification of the cylinder, $w \simeq w + 2\pi$. This together with Lorentz invariance will allow the following two periodicity conditions:

$$\text{Ramond (R)} : \psi^\mu(w+2\pi) = +\psi^\mu(w), \tag{2.1.2}$$

$$\text{Neveu–Schwarz (NS)} : \psi^\mu(w+2\pi) = -\psi^\mu(w). \tag{2.1.3}$$

Here the sign being the same for all μ. In the same way one has two possible periodicities for $\tilde{\psi}^\mu$. Hence there are four ways to put the theory on a circle and there are four different kinds of closed superstring, which will be denoted by NS–NS, NS–R, R–NS, and R–R.

To analyze the massless particle spectrum, we first note that in D-dimensional spacetime for the massless states there is no rest frame and one chooses the frame $p^\mu = (E, E, 0, ..., 0)$. The $SO(D-2)$ acting on the transverse directions leaves the momenta p^μ invariant and is a subgroup of the Lorentz group called the little group[1]. Thus the massless particle states arising from the lowest string states in $D = 10$ are classified by their behavior under $SO(8)$ rotations that leave the momentum invariant. In the NS sector, the physical state conditions imply that the massless physical

[1]The massive case is different in that one considers the rest frame $p^\mu = (m, 0, 0, 0)$ and the states form then a representation of the spatial rotation group $SO(D-1)$.

states are the eight transverse polarisations forming the vector representation $\mathbf{8}_V$ of $SO(8)$. In the R sector, the physical state conditions for the lowest states lead to the massless Dirac equation by which the massless lowest states form a representation of the Dirac algebra; in ten dimensions this representation has dimension 32. The Dirac representation **32** decomposes into two Weyl representations **16** and **16′**, differing by their chirality. Upon $SO(9,1) \to SO(1,1) \times SO(8)$ each of these two decompose into a sum of $\mathbf{8_s}$ and $\mathbf{8_c}$. Each state of combinations $\mathbf{8_v} \oplus \mathbf{8_{s,c}}$ then describes the massless degrees of freedom on each side of the closed superstring. The consistent chiral closed superstring theory, known as type IIB string theory, has the following massless sector under $SO(8)$ [76]:

$$\text{Type IIB}: \quad (\mathbf{8_v} \oplus \mathbf{8_s}) \otimes (\mathbf{8_v} \oplus \mathbf{8_s}). \tag{2.1.4}$$

The products in the NS–NS and R–R sectors are given as

$$\text{NS–NS}: \quad \mathbf{8_v} \otimes \mathbf{8_v} = \phi \oplus B_{\mu\nu} \oplus G_{\mu\nu} = \mathbf{1} \oplus \mathbf{28} \oplus \mathbf{35} \tag{2.1.5}$$

$$\text{R–R}: \quad \mathbf{8_s} \otimes \mathbf{8_s} = [0] \oplus [2] \oplus [4]_+ = \mathbf{1} \oplus \mathbf{28} \oplus \mathbf{35}_+. \tag{2.1.6}$$

Here $[n]$ denotes an antisymmetric rank n tensor of the representation $SO(8)$, with $[4]_+$ being self-dual. In the NS–R and R–NS sectors the products are

$$\text{NS–R}: \quad \mathbf{8_v} \otimes \mathbf{8_s} = \mathbf{8_c} \oplus \mathbf{56_s}. \tag{2.1.7}$$

The $\mathbf{56_s}$ includes two massless vector–spinor gravitinos of the same chirality. The physical state conditions for the NS–R gravitino state imply local spacetime supersymmetry and associated with it there are two supercharges each transforming under the **16** of the $SO(9,1)$.

To this end, we note that type IIB supergravity has two supercharges of the same chirality, both tranforming under **16**. Its graviton multiplet contains two scalars, the traceless symmetric graviton, two antisymmetric 2-forms, and a 4-form with self-dual field strength giving $2 + 35 + 28 + 28 + 35 = 128$ bosonic states in all.

This is the same as the massless content of the type IIB superstring in NS–NS and R–R sector discussed above. Thus the NS–NS and R–R spectra together form the bosonic components of the type IIB (chiral) supergravity [76].

2.1.2 Type IIB action and equations of motion

In the previous section we saw that the field content of the massless spectrum of type IIB superstring theory consists of the R–R and NS–NS forms. For the R–R fields we may use C_p and F_{p+1} for the potential and field strength, and for the NS–NS fields B_2 and H_3. One can construct an action using these forms. But it should be noted from the previous section that the massless spectrum of type IIB theory also contains a self-dual 5-form field strength, $\tilde{F}_5 = *\tilde{F}_5$. There is no covariant action for such a field but the following action comes close [76]:

$$
\begin{aligned}
S_{\rm IIB} &= S_{\rm NS} + S_{\rm R} + S_{\rm CS}, && (2.1.8)\\
S_{\rm NS} &= \frac{1}{2\kappa_{10}^2}\int d^{10}x(-g)^{1/2}e^{-2\Phi}\Big(\mathcal{R} + 4\partial_\mu\Phi\partial^\mu\Phi - \frac{1}{2}|H_3|^2\Big), && (2.1.9)\\
S_{\rm R} &= -\frac{1}{4\kappa_{10}^2}\int d^{10}x(-g)^{1/2}\Big(|F_1|^2 + |\tilde{F}_3|^2 + \frac{1}{2}|\tilde{F}_5|^2\Big), && (2.1.10)\\
S_{\rm CS} &= -\frac{1}{4\kappa_{10}^2}\int C_4 \wedge H_3 \wedge F_3, && (2.1.11)
\end{aligned}
$$

where

$$
\begin{aligned}
\tilde{F}_3 &= F_3 - C_0 \wedge H_3, && (2.1.12)\\
\tilde{F}_5 &= F_5 - \frac{1}{2}C_2 \wedge H_3 + \frac{1}{2}B_2 \wedge F_3. && (2.1.13)
\end{aligned}
$$

Also, κ_{10}^2 is the ten-dimensional gravitational coupling given by

$$\kappa_{10}^2 = \frac{(2\pi)^7\alpha'^4 g_s^2}{2}. \qquad (2.1.14)$$

The equations of motion and Bianchi identity for $\tilde{F}_5$ are:

$$d * \tilde{F}_5 = d\tilde{F}_5 = H_3 \wedge F_3. \qquad (2.1.15)$$

The spectrum of the type IIB string includes degrees of freedom of a self-dual five-form field strength and the field equations (2.1.8) - (2.1.11) are consistent with:

$$*\tilde{F}_5 = \tilde{F}_5. \tag{2.1.16}$$

The supergravity action can be put in a $SL(2,\mathbf{R})$ symmetric form. Consider

$$g_{\mathrm{E}\mu\nu} = e^{-\Phi/2} g_{\mu\nu}, \qquad \tau = C_0 + i e^{-\Phi}, \tag{2.1.17}$$

$$M_{ij} = \frac{1}{\mathrm{Im}\tau} \begin{bmatrix} |\tau|^2 & -\mathrm{Re}\tau \\ -\mathrm{Re}\tau & 1 \end{bmatrix}, \qquad F_3^i = \begin{bmatrix} H_3 \\ F_3 \end{bmatrix}. \tag{2.1.18}$$

In (2.1.17) we transformed the metric to the Einstein frame. The action then takes the form [76]:

$$\begin{aligned} S_{\mathrm{IIB}} = & -\frac{1}{2\kappa_{10}^2} \int d^{10}x (-g_{\mathrm{E}})^{1/2} \Big(\mathcal{R}_{\mathrm{E}} - \frac{\partial_\mu \bar{\tau} \partial^\mu \tau}{2(\mathrm{Im}\tau)^2} \\ & - \frac{M_{ij}}{2} F_3^i \cdot F_3^i - \frac{1}{4} |\tilde{F}_5|^2 \Big) - \frac{\epsilon_{ij}}{8\kappa_{10}^2} \int C_4 \wedge F_3^i \wedge F_3^i \end{aligned} \tag{2.1.19}$$

Here τ in (2.1.17) is the axion-dilaton field, and in (2.1.18) $F_3 = dC_2$ and $H_3 = dB_2$ are the R–R and NS–NS three-form fluxes, as before. This action is invariant under $SL(2,\mathbf{R})$ symmetry by:

$$\tau' = \frac{a\tau + b}{c\tau + d}, \tag{2.1.20}$$

$$F_3^{i'} = \Lambda^i_j F_3^j, \quad \Lambda^i_j = \begin{bmatrix} d & c \\ b & a \end{bmatrix}, \tag{2.1.21}$$

$$\tilde{F}_5' = \tilde{F}_5, \quad g'_{\mathrm{E}\mu\nu} = g_{\mathrm{E}\mu\nu} \tag{2.1.22}$$

with a, b, c, $d \in \mathbb{R}$ and $\det \Lambda = 1$. The $SL(2,\mathbf{R})$ invariance of the τ kinetic term is clear, and that of F_3 kinetic term follows from $M' = (\Lambda^{-1})^T M \Lambda^{-1}$. It should be noted that the global $SL(2,\mathbf{R})$ symmetry of type IIB supergravity is not shared by the full type IIB superstring theory. In fact, it is broken by a variety of stringy

and quantum effects to the infinite discrete subgroup $SL(2,\mathbf{Z})$. To see this, consider stable strings in this background. As there are two two-form gauge fields B_2 (NS–NS two-form) and C_2 (R–R two-form) there are two types of charge that a string can carry. The F-string (or fundamental string) has charge $(1,0)$, which means that it has one unit of the charge that couples to B_2 and none of the charge that couples to C_2 . In similar fashion, the D-string couples to C_2 and has charge $(0,1)$. As the two-forms form a doublet of $SL(2,\mathbf{R})$, it follows that these strings also transform as a doublet. Generally, they transform into (p,q) strings, which carry both kinds of charge. The restriction to the $SL(2,\mathbf{Z})$ subgroup is essential to make sure that these charges are integers, as is required by the Dirac quantization conditions. The low-energy IIB supergravity action in the Einstein frame can be put in an $SL(2,\mathbf{Z})$ invariant form as [76]:

$$\begin{aligned} S_{\rm IIB} = \frac{1}{2\kappa_{10}^2}\int d^{10}x\sqrt{|g|}\left[\mathcal{R} - \frac{|\,\partial\tau|^2}{2(\mathrm{Im}\tau)^2} - \frac{|\,G_3|^2}{12\,\mathrm{Im}\tau} - \frac{|\,\tilde{F}_5|^2}{4\cdot 5\,!}\right] \\ + \frac{1}{8i\kappa_{10}^2}\int \frac{C_4\wedge G_3\wedge G_3^*}{\mathrm{Im}(\tau)} + S_{\rm loc}, \end{aligned} \tag{2.1.23}$$

where

$$G_3 = F_3 - \tau H_3. \tag{2.1.24}$$

Here the term $S_{\rm loc}$ is the action of localized sources including contributions from wrapped D7-branes and mobile D3-branes [29]. These are Bogomolnyi–Prasad–Sommerfield (BPS) states, meaning that they are invariant under a nontrivial subalgebra of the full supersymmetry algebra. These states always carry conserved charges, and the supersymmetry algebra determines the mass of the state exactly in terms of its charges and the mass is subject to the BPS bound.

In a flux compactification to four dimensions we are assuming a block diagonal Ansatz for the metric [29]:

$$ds_{10}^2 = \sum_{M,N=0}^{9} g_{MN}dx^M dx^N = e^{2A(y)}g_{\mu\nu}dx^\mu dx^\nu - e^{-2A(y)}g^{(0)}_{mn}dy^m dy^n, \tag{2.1.25}$$

in which the warp factor, $e^{4A(y)}$, depends only on the internal coordinates y^m, the internal metric g_{mn} is independent of the spacetime coordinates (and will be taken to be a known supergravity solution) and the four-dimensional metric, $g_{\mu\nu}$, is taken as Minkowski for the computation of the supergravity flux background, but ultimately will be assumed to have an FRW form once the general cosmological solution is sought.

Following [29], we take the self-dual five-form to be given by

$$\tilde{F}_5 = (1 + \star_{10})\Big[d\alpha(y) \wedge dx^0 \wedge dx^1 \wedge dx^2 \wedge dx^3\Big], \tag{2.1.26}$$

in the Poincare invariant case, where $\alpha(y)$ is a function of the internal coordinates, and $\star_{10}$ is the ten-dimensional Hodge star operator (see appendix A).

The Einstein equations take the form

$$\mathcal{R}_{MN} = \kappa_{10}^2\bigg(T_{MN} - \frac{1}{8}g_{MN}T\bigg), \tag{2.1.27}$$

where

$$T_{MN} = -\frac{-2}{\sqrt{-g}}\frac{\delta S}{\delta g^{MN}} \tag{2.1.28}$$

is the energy-momentum tensor, and T is the trace. The noncompact components take the form

$$\mathcal{R}_{\mu\nu} = -g_{\mu\nu}\bigg(\frac{G_{mnp}\overline{G}^{mnp}}{48\mathrm{Im}\tau} + \frac{e^{-8A}}{4}\partial_m\alpha\partial^m\alpha\bigg) + \kappa_{10}^2\bigg(T^{\mathrm{loc}}_{\mu\nu} - \frac{1}{8}g_{\mu\nu}T^{\mathrm{loc}}\bigg). \tag{2.1.29}$$

According to the metric (2.1.25), the Ricci components can be computed as

$$\mathcal{R}_{\mu\nu} = -g_{\mu\nu}e^{4A}\Delta_{(0)}A = -\frac{1}{4}g_{\mu\nu}(\Delta_{(0)}e^{4A} - e^{-4A}\partial_m e^{4A}\partial^m e^{4A}). \tag{2.1.30}$$

This together with the trace of (2.1.29) gives [29]

$$\Delta_{(0)}e^{4A} = e^{2A}\frac{G_{mnp}\overline{G}^{mnp}}{12\mathrm{Im}\tau} + e^{-6A}[\partial_m\alpha\partial^m\alpha + \partial_m e^{4A}\partial^m e^{4A}] + \frac{\kappa_{10}^2}{2}e^{2A}(T^m_m - T^\mu_\mu)^{\mathrm{loc}}. \tag{2.1.31}$$

The five-form Bianchi identity takes the form [29]

$$d\tilde{F}_5 = H_3 \wedge F_3 + 2\kappa_{10}^2 T_3 \rho_3, \tag{2.1.32}$$

where ρ_3 is the D-brane charge density from localized sources and includes contributions from the D7-branes and mobile D3-branes. Integrating this Bianchi identity over the internal manifold gives the type IIB tadpole-cancellation condition [29]

$$\frac{1}{2\kappa_{10}^2 T_3} \int_M H_3 \wedge F_3 + Q_3^{\rm loc} = 0. \tag{2.1.33}$$

This states that the total D3-brane charge from supergravity backgrounds and localized sources vanishes. In terms of the potential α the Bianchi identity (2.1.32) becomes [29]

$$\Delta_{(0)}\alpha = ie^{2A}\frac{G_{mnp}(\star_6 \overline{G}^{mnp})}{12{\rm Im}\tau} + 2e^{-6A}\partial_m\alpha\partial^m e^{4A} + 2\kappa_{10}^2 e^{2A} T_3 \rho_3^{\rm loc}. \tag{2.1.34}$$

The Einstein equations (2.1.31) and five-form Bianchi identity (2.1.34) imply [29]

$$\Delta_{(0)}\Phi_- = \frac{e^{8A+\Phi}}{24}|\,G_-|^2 + e^{-6A}|\nabla\Phi_-|^2 + 2\kappa^2 e^{2A}\left[\frac{1}{4}(T_m^m - T_\mu^\mu)^{\rm local} - T_3\rho_3^{\rm loc}\right], \tag{2.1.35}$$

where $\Delta_{(0)}$ is the Laplacian with respect to the six-dimensional unperturbed Calabi-Yau metric $g_{mn}^{(0)}$, and we have defined:

$$G_\pm \equiv (i \pm \star_6)G_3, \qquad \Phi_\pm \equiv e^{4A} \pm \alpha. \tag{2.1.36}$$

The equation of motion for the three-form flux is [29]

$$d\Lambda + \frac{i}{2}\frac{d\tau}{{\rm Im}(\tau)} \wedge (\Lambda + \bar{\Lambda}) = 0, \tag{2.1.37}$$

where by definition

$$\Lambda \equiv \Phi_+ G_- + \Phi_- G_+. \tag{2.1.38}$$

The LHS of Eq. (2.1.35) integrates to zero, so the global constrains for the supergravity solution are [29]:

• The three-form flux is imaginary self-dual,

$$\star_6 G_3 = iG_3 \tag{2.1.39}$$

• The warp factor and four-form potential are related,

$$e^{4A} = \alpha. \tag{2.1.40}$$

• The localized sources saturate a 'BPS-like' bound

$$\frac{1}{4}(T^m_m - T^\mu_\mu)^{\text{local}} = T_3 \rho_3^{\text{loc}}. \tag{2.1.41}$$

A compactification satisfying the conditions (2.1.39) - (2.1.41) is called ISD.

2.1.3 Type IIB theory on Calabi-Yau manifolds

In this subsection, we follow closely [76] (and Appendix A) and discuss the moduli fields of Calabi-Yau compactification of type IIB superstring theory that form the massless field content of $N = 2$ spacetime supersymmetry.

The massless fields in four dimensions arise from those modes of the ten-dimensional massless fields that are annihilated by the internal part of the Laplace operator. For the type IIB string on a Calabi-Yau manifold the massless fields come from the NS–NS fluctuations g_{MN}, b_{MN}, ϕ (bosonic supergravity fields) and the R–R fluctuations c, c_{MN} and c_{MNPQ}. Here the ten-dimensional indices separate as $M \to (\mu, i, \bar{i})$. Thus these will include the four-dimensional metric $g_{\mu\nu}$, dilaton ϕ, and axion $b_{\mu\nu} \leftrightarrow a$, and also the scalar c, and a second axion $c_{\mu\nu} \leftrightarrow a'$. These components with all indices noncompact each have a single zero mode (the constant function) giving the corresponding field in four dimensions.

Every Calabi-Yau manifold has exactly one $(3, 0)$-form (see Appendix A) and the relevant Laplace operator is Δ_d (see Appendix A). The zero modes of $c_{\mu ijk}$ satisfy $\Delta_d c_{\mu ijk} = 0$ and therefore define harmonic forms. The space of harmonic forms is isomorphic to the cohomology groups (see Appendix A). Thus according to the

Hodge numbers of Calabi-Yau three-folds (see Appendix A) this gives $h^{3,0} = 1$ zero modes. This is a vector.

The components g_{ij} correspond to changes in the complex structure because a coordinate change would be needed to bring the metric back to Hermitian form. This field is symmetric and therefore not a (p, q)-form. But by using the metric and antisymmetric three-form we can produce $g_{i\bar{l}\bar{m}} = g_{ij}g^{j\bar{k}}\Omega_{\bar{k}\bar{l}\bar{m}}$, which is a $(2, 1)$-form. The relevant Laplace operator is Δ_d and the zero modes or moduli satisfy the operator equation $\Delta_d g_{i\bar{l}\bar{m}} = 0$ and therefore define harmonic $(2, 1)$-forms. Hence according to the Hodge numbers of Calabi-Yau three-folds this gives $h^{2,1}$ zero modes or complex structure moduli. These are complex fields with $g_{\bar{i}\bar{j}}$ being the conjugate. These fields are scalars. The component $c_{\mu i j\bar{k}}$ can also be regarded as a $(2, 1)$-form the zero modes of which give $h^{2,1}$ vectors. It should be noted that there are no additional scalars from $c_{\mu\bar{i}\bar{j}\bar{k}}$ because the five-form field strength of the type IIB background is self-dual meaning that these give the same vector states.

The component $g_{i\bar{j}}$ is a $(1, 1)$-form and the relevant Laplace operator is again Δ_d. The zero modes or moduli satisfy the operator equation $\Delta_d g_{i\bar{j}} = 0$ and therefore define harmonic $(1, 1)$-forms. Thus according to the Hodge numbers of Calabi-Yau three-folds it gives $h^{1,1}$ zero modes or real moduli. The fields $b_{i\bar{j}}$ and $c_{i\bar{j}}$ are also $(1, 1)$-forms and give rise to $h^{1,1}$ zero modes or real moduli. These combine to form $h^{1,1}$ complex fields. These fields are scalars. The component $c_{\mu\nu i\bar{j}}$ can also be regarded as a $(1, 1)$-form the zero mode of which gives $h^{1,1}$ scalars from its Poincare dual. It should be noted that there are no scalars from $c_{ij\bar{k}\bar{l}}$ with $h^{2,2}$ harmonic $(2, 2)$-forms due to the Hodge numbers of Calabi-Yau three-folds since the five-form field strength of the type IIB background is self-dual and in fact these are identical to the states form $c_{\mu\nu i\bar{j}}$.

The components $g_{\mu i}$, $b_{\mu i}$ and $c_{\mu i}$ are $(1, 0)$-forms, and the relevant Laplace operator is Δ_d, giving according to the Hodge numbers of Calabi-Yau three-folds, $h^{1,0} = 0$ zero modes. The components b_{ij} and c_{ij} are $(2, 0)$-forms and the relevant wave operator is Δ_d giving again by the Hodge numbers of Calabi-Yau three-folds $h^{2,0} = 0$ zero modes.

In summary, we have the following fields: for each harmonic $(1, 1)$-form there is

a scalar from $g_{i\bar{j}}$ and one from $b_{i\bar{j}}$, and also one from $c_{i\bar{j}}$ and a fourth one from the Poincare dual of $c_{\mu\nu i\bar{j}}$. For each harmonic $(2,1)$-form there are scalars from g_{ij} and $g_{\bar{i}\bar{j}}$ and a vector from $c_{\mu ij\bar{k}}$.

Now let us see how the above fields fit into multiplets of $N = 2$ spacetime supersymmetry. The metric $g_{\mu\nu}$ plus vector $c_{\mu ijk}$ comprise the bosonic content of the supergravity multiplet. The remaining model independent fields are four real scalars: ϕ, c, a and a'. This is the bosonic content of one hypermultiplet. For each harmonic $(1,1)$-form there are three scalars plus an additional one again forming a hypermultiplet. For each harmonic $(2,1)$-form there are two scalars and a vector, the bosonic content of the vector multiplet. In total, the massless type IIB states form a $N = 2$ supergravity multiplet plus:

$$\text{IIB}: \quad h^{2,1} \text{ vector multiplet}, \quad h^{1,1} + 1 \text{ hypermultiplet}. \tag{2.1.42}$$

In summary, the Calabi-Yau moduli and supersymmetry multiplets in type IIB theory are related as: the Kähler $(1,1)$ moduli are related to hypermultiplets and the complex structure moduli to vector multiplets.

In low energy $N = 2$ supergravity the potential is determined completely by gauge interactions. In Calabi-Yau compactification of type IIB theory the gauge fields all come from the R–R sector. Hence all strings are neutral and so the potential vanishes. It is therefore conclusive that all the scalars found above are moduli. This is a consequence of symmetry and thereby valid in all orders of string perturbation theory, even in the nonperturbative regime. However, as we shall see in the next sections, in $N = 1$ supergravity this is no longer the case and nonperturbative effects can produce a potential (see section 2.2). Since here the potential is vanishing the low energy action is fully determined by supersymmetry in terms of the kinetic terms for the moduli – the metric on moduli space. By supersymmetry the kinetic terms of the hypermultiplet scalars are independent of the vector multiplet scalars and the kinetic terms for the vectors and their scalar partners are independent of the hypermultiplet scalars. This means that the moduli space is a product (see also Appendix A). The vector multiplet space is a special Kähler manifold and the hypermultiplet moduli space a quaternionic manifold.

2.1.4 Moduli and effective actions

The global constraints of warped compactification discussed in the previous section are invariant under $g^{(0)}_{mn} \to \lambda^2 g^{(0)}_{mn}$. Thus a warped compactification has a radial modulus, but there is no dilaton modulus as the dilaton couples to the NS–NS and R–R fluxes differently giving a nontrivial potential, and, as discussed below, fluxes also stabilize the complex structure moduli [29].

Let us now consider the effective four-dimensional action. To be concrete, consider a Calabi-Yau manifold with a single Kähler modulus characterizing its size. In the absence of fluxes, there are massless fields describing the complex-structure moduli z^α, for $\alpha = 1, ..., h^{2,1}$, the axion-dilaton τ and the superfield ρ containing the Kähler modulus.

The Kähler potential for the complex structure moduli takes the form [26] (see Appendix A)

$$\mathcal{K}^{2,1} = -\log\left(i\int_M \Omega\wedge\bar{\Omega}\right). \tag{2.1.43}$$

In addition to this, we need to compute the Kähler potential for the radial modulus and for the axion-dilaton modulus. In order to do so, we consider dimensional reduction of the ten-dimensional type IIB action by taking the Calabi-Yau manifold large. We consider the action on a background of the form [29]

$$ds^2 = c^{-6u(x)} g_{\mu\nu} dx^\mu dx^\nu - e^{2u(x)} g_{mn} dy^m dy^n, \tag{2.1.44}$$

where $u(x)$ parameterizes the volume of the Calabi-Yau three-fold. The power of $e^{u(x)}$ in the first term has been chosen to give a canonically normalized Einstein term in four-dimensions.

The supersymmetric partner of the radial modulus is another axion $\hat{b}$, which descends from the four-form according to

$$C_{\mu\nu pq} = \hat{a}_{\mu\nu} J_{pq}, \tag{2.1.45}$$

where J is the Kähler form [29] (see Appendix A). In four dimensions the two-form $\hat{a}$ can be dualized to a scalar $\hat{b}$ according to [29]

$$d\hat{a} = c^{-8u(x)} * d\hat{b}. \tag{2.1.46}$$

Setting

$$\rho = \frac{\hat{b}}{\sqrt{2}} + ie^{4u}, \tag{2.1.47}$$

the resulting low-energy effective action is [29]

$$S = \frac{1}{2\kappa_4^2}\int d^4x\sqrt{-g}\left(R - \frac{1}{2}\frac{\partial_\mu\tau\partial^\mu\bar{\tau}}{(\mathrm{Im}\tau)^2} - \frac{3}{2}\frac{\partial_\mu\rho\partial^\mu\bar{\rho}}{(\mathrm{Im}\rho)^2}\right). \tag{2.1.48}$$

Here the four-dimensional gravitational coupling constant is given by $\kappa_4^2 = \kappa_{10}^2/\nu$, where ν is the volume of the Calabi-Yau three-fold computed using the metric g_{mn}. The kinetic terms for τ and ρ correspond to the first two terms in the Kähler potential

$$\mathcal{K} = -3\log[-i(\rho - \bar{\rho})] - \log[-i(\tau - \bar{\tau})]. \tag{2.1.49}$$

Thus the complete Kähler potential takes the form [29]

$$\mathcal{K} = -3\log[-i(\rho - \bar{\rho})] - \log[-i(\tau - \bar{\tau})] - \log\left(i\int_M \Omega\wedge\bar{\Omega}\right). \tag{2.1.50}$$

The presence of fluxes generate a superpotential of the form [79]

$$W_0 = \int \Omega\wedge G_3, \tag{2.1.51}$$

where Ω is the holomorphic three-form of the Calabi-Yau three-fold. This superpotential is independent of ρ. The ISD constraint $\star_6 G_3 = iG_3$ can be derived from this superpotential. Note that a solution to the ISD condition is a harmonic form of type $(2,1)+(0,3)$, but in supersymmetric solutions only the primitive part of the $(2,1)$ component is allowed, meaning that the index structure is $\bar{i}jk$ and the contraction with the Kähler form $J^{\bar{i}j}$ vanishes.

The condition for unbroken supersymmetry is [29]

$$\mathcal{D}_a W = \partial_a W + \partial_a \mathcal{K} W = 0. \tag{2.1.52}$$

Here $a = \rho, \tau, \alpha$ label all the supermoduli fields and hence the following three conditions follow

$$\mathcal{D}_\rho W = \partial_\rho \mathcal{K} W = -\left(\frac{3}{\rho - \bar{\rho}}\right) W = 0, \tag{2.1.53}$$

$$\mathcal{D}_r W = \frac{1}{\tau - \bar{\tau}} \int \Omega \wedge \bar{G}_3 = 0, \tag{2.1.54}$$

$$\mathcal{D}_\alpha W = \int \varphi_\alpha \wedge G_3 = 0, \tag{2.1.55}$$

where φ_α is a basis of harmonic $(2,1)$-forms (see Appendix A). The first condition is derived from observing the fact that the superpotential (2.1.51) is independent of the radial modulus. This condition implies that for a supersymmetric solution $W = 0$, so that the $(0,3)$ component of G_3 has to vanish. The second condition implies that the $(3,0)$ component of G_3 also has to vanish. The third condition is satisfied by all harmonic $(2,1)$-forms and so supersymmetry is unbroken if [29]

$$G_3 \in H^{(2,1)}(M). \tag{2.1.56}$$

We should remark that for compact Calabi-Yau manifolds $h^{1,0} = 0$ (see Appendix A). In such a case any harmonic $(2,1)$-form is primitive, again meaning that the index structure is $\bar{i}jk$ and the contraction with the Kähler form $J^{\bar{i}j}$ vanishes, and so we have [29]

$$G_3 \in H^{(2,1)}_{\text{primitive}}(M). \tag{2.1.57}$$

We also note that in addition to being primitive, the φ_α are also ISD. Then Eq. (2.1.56) is in agreement with the condition that G_3 is ISD, in correspondence with the ten-dimensional ISD conditions [29].

2.1.5 The warped deformed conifold

The particular concrete example we will be interested in is where the background is the warped deformed conifold, or Klebanov-Strassler (KS), solution [75]. The

deformed conifold is a noncompact and nonsingular Calabi-Yau three-fold in $\mathbb{C}^4$ defined by the following constraint equation [27] (see Appendix A):

$$\sum_{\alpha=1}^{4}(z_\alpha)^2 = \epsilon^2, \tag{2.1.58}$$

where $\{z_\alpha, \alpha = 1,2,3,4\}$ represent the local complex coordinates in $\mathbb{C}^4$, and ϵ is the deformation parameter which can be made real by phase rotation. For vanishing ϵ, Eq. (2.1.58) gives the singular conifold and describes a cone over a five-dimensional Einstein manifold X_5. For us the nonsingular limit is relevant in which X_5 is the $\big[SU(2)\times SU(2)\big]/U(1)$ coset space $T^{1,1}$ of topology $S^2\times S^3$ parametrised by a set of five Euler angles $\Psi = \{\theta_i, \varphi_i, \psi\}$ with $0 \le \theta_i \le \pi$, $0 \le \varphi_i \le 2\pi$, $0 \le \psi \le 4\pi$ $(i = 1,2)$, and the would-be singularity at the tip, $r = 0$, is replaced by a blown-up S^3 of $T^{1,1}$ amounting to the deformation measured by ϵ. The base of the cone can be parametrised by the coordinates y_i in a standard way [27]

$$\begin{aligned}
y_1 &= \frac{1}{\sqrt{2}}\bigg(\cos\frac{\theta_1}{2}\cos\frac{\theta_2}{2}e^{\frac{i}{2}(\varphi_1+\varphi_2+\psi)} - \sin\frac{\theta_1}{2}\sin\frac{\theta_2}{2}e^{-\frac{i}{2}(\varphi_1+\varphi_2-\psi)}\bigg), && (2.1.59)\\
y_2 &= \frac{i}{\sqrt{2}}\bigg(\cos\frac{\theta_1}{2}\cos\frac{\theta_2}{2}e^{\frac{i}{2}(\varphi_1+\varphi_2+\psi)} + \sin\frac{\theta_1}{2}\sin\frac{\theta_2}{2}e^{-\frac{i}{2}(\varphi_1+\varphi_2-\psi)}\bigg), && (2.1.60)\\
y_3 &= -\frac{1}{\sqrt{2}}\bigg(\cos\frac{\theta_1}{2}\sin\frac{\theta_2}{2}e^{\frac{i}{2}(\varphi_1-\varphi_2+\psi)} + \sin\frac{\theta_1}{2}\cos\frac{\theta_2}{2}e^{\frac{i}{2}(\varphi_2-\varphi_1+\psi)}\bigg), && (2.1.61)\\
y_4 &= \frac{i}{\sqrt{2}}\bigg(\cos\frac{\theta_1}{2}\sin\frac{\theta_2}{2}e^{\frac{i}{2}(\varphi_1-\varphi_2+\psi)} - \sin\frac{\theta_1}{2}\cos\frac{\theta_2}{2}e^{\frac{i}{2}(\varphi_2-\varphi_1+\psi)}\bigg). && (2.1.62)
\end{aligned}$$

In tems of these, the coordinates of the deformed conifold in (2.1.58) read as

$$\begin{aligned}
z_1 &= \frac{\epsilon}{\sqrt{2}}(e^{\frac{\eta}{2}}y_1 + e^{-\frac{\eta}{2}}\overline{y}_1), \qquad z_2 = \frac{\epsilon}{\sqrt{2}}(e^{\frac{\eta}{2}}y_2 + e^{-\frac{\eta}{2}}\overline{y}_2),\\
z_3 &= \frac{\epsilon}{\sqrt{2}}(e^{\frac{\eta}{2}}y_3 + e^{-\frac{\eta}{2}}\overline{y}_3), \qquad z_4 = \frac{\epsilon}{\sqrt{2}}(e^{\frac{\eta}{2}}y_4 + e^{-\frac{\eta}{2}}\overline{y}_4),
\end{aligned} \tag{2.1.63}$$

where η is the 'radial coordinate'. The six-dimensional Calabi-Yau metric, $ds_6^2 = g^{(0)}_{mn}dy^m dy^n$, on the deformed conifold can be obtained from the Kähler potential given as [27]

$$k(\eta) = \frac{\epsilon^{4/3}}{2^{1/3}}\int_0^\eta d\eta'[\sinh(2\eta') - 2\eta']^{1/3}. \tag{2.1.64}$$

Here we note that this Kähler potential is derived from the relation [27]

$$r^3 = \sum_{\alpha=1}^{4} |z_\alpha|^2 = \epsilon^2 \cosh\eta, \tag{2.1.65}$$

and the metric for the deformed conifold reads as [27] (see Appendix A and also [80])

$$ds_6^2 = g^{(0)}_{mn} dy^m dy^n = \frac{1}{2}\epsilon^{4/3} K(\eta) \Bigg[\frac{1}{3K(\eta)^3} \{d\eta^2 + (g^5)^2\} + \cosh^2\frac{\eta}{2}\{(g^3)^2 + (g^4)^2\} + \sinh^2\frac{\eta}{2}\{(g^1)^2 + (g^2)^2\} \Bigg]. \tag{2.1.66}$$

This internal metric is a strongly warped and deformed throat, which interpolates between a regular $\mathbb{R} \times S^3$ tip, and an $\mathbb{R} \times T^{1,1}$ cone in the UV. The deformation of the conifold is measured by ϵ, as before; it is a dimensionful parameter ($[\epsilon^{2/3}] = L$), and sets a scale for the throat as we will see presently. The 'radial' coordinate, η, is chosen so that the function K is expressible explicitly in analytic form:

$$K(\eta) = \frac{(\sinh(2\eta) - 2\eta)^{1/3}}{2^{1/3}\sinh\eta}, \tag{2.1.67}$$

and the g^i's are forms representing the angular directions, given explicitly by

$$g^{1,3} = \frac{e^1 \mp e^3}{\sqrt{2}}, \quad g^{2,4} = \frac{e^2 \mp e^4}{\sqrt{2}}, \quad g^5 = e^5 \tag{2.1.68}$$

with

$$\begin{aligned} e^1 &= -\sin\theta_1 d\varphi_1, \qquad e^2 = d\theta_1, \qquad e^3 = \cos\psi\sin\theta_2 d\varphi_2 - \sin\psi d\theta_2, \\ e^4 &= \sin\psi\sin\theta_2 d\varphi_2 + \cos\psi d\theta_2, \qquad e^5 = d\psi + \cos\theta_1 d\varphi_1 + \cos\theta_2 d\varphi_2. \end{aligned} \tag{2.1.69}$$

It is also useful to visualise this metric in terms of a proper radial coordinate

$$r(\eta) = \frac{\epsilon^{2/3}}{\sqrt{6}} \int_0^\eta \frac{dx}{K(x)} \tag{2.1.70}$$

which measures the actual distance up the throat in the six-dimensional metric $g^{(0)}_{mn}$. The metric can now be written as:

$$ds_6^2 = dr^2 + r^2\left[\frac{C_3^2(r)}{9}(g^5)^2 + \frac{C_1^2(r)}{6}\{(g^3)^2+(g^4)^2\} + \frac{C_2^2(r)}{6}\{(g^1)^2+(g^2)^2\}\right], \quad (2.1.71)$$

where the functions $C_i(r)$ are given implicitly from (2.1.66), and are shown in Fig. 2.1.5. At small r

$$r \sim \frac{\epsilon^{2/3}}{3^{1/6}2^{5/6}}\eta, \qquad K \simeq \left(\frac{2}{3}\right)^{1/3}, \quad (2.1.72)$$

and the metric (2.1.66) smoothly closes off at $r = 0$ with a finite S^3 of radius $\epsilon^{2/3}/12^{1/6}$. At large r, or for $\eta \sim 10 - 15$, the C_i's âs become unity, and the throat explicitly takes the form of a cone: $\mathbb{R} \times T^{1,1}$. Thus $\epsilon^{2/3}$ gives the radius of a nonsingular S^3 at the base of the throat, and the scale at which the throat asymptotes the $T^{1,1}$ cone: it sets the IR scale of the geometry. In the UV region the Kähler potential becomes [27]

$$k = \frac{3}{2}\left(\sum_{\alpha=1}^{4}|z_\alpha|^2\right)^{2/3} = \frac{3}{2}r^2, \quad (2.1.73)$$

and the metric reduces to that of the singular conifold given by Eq. (1.3.51) with $ds^2_{X_5}$ given by [27] (see Appendix A, and also [80])

$$ds^2_{T^{1,1}} = \frac{1}{9}\left(d\psi + \sum_{i=1}^{2}\cos\theta_i d\varphi_i\right)^2 + \frac{1}{6}\sum_{i=1}^{2}(d\theta_i^2 + \sin^2\theta_i d\varphi_i^2). \quad (2.1.74)$$

The warping in this background is induced by the presence of type IIB background fluxes including M units of F_3 flux through the cycle A and $-K$ units of H_3 flux through the cycle B. Due to the presence of three-form fluxes the above background emerges as a solution to Einstein's equations and the resulting supergravity background is described by a throat with its tip being located at a finite radial coordinate $r_{\rm IR}$ while at $r_{\rm UV}$ the throat is glued into an unwarped bulk geometry. For small η, the background fields are given by [75, 77]

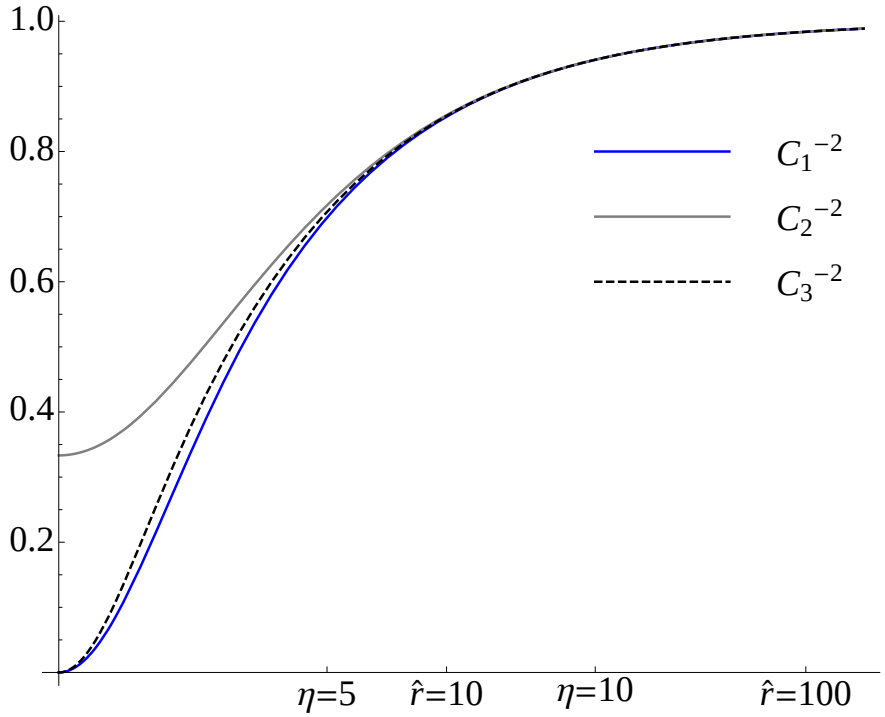

Figure 2.1: A plot of the metric functions C_i , which shows how the deformation of the conifold increases as the tip is approached. The metric asymptotes the $T^{1,1}$ cone, but near the origin, rC_1 and rC_3 remain finite leaving the nonsingular S^3 metric at the tip of the 'cone'. The axis is labeled both in terms of the original η coordinate, as well as the normalized proper distance up the throat, $\hat{r} = \epsilon^{-2/3} r$.

$$B_2 = \frac{g_s M \alpha'}{2}\big[f(\eta) g^1 \wedge g^2 + k(\eta) g^3 \wedge g^4\big], \tag{2.1.75}$$

$$H_3 = \frac{g_s M \alpha'}{2}\big[d\eta \wedge (f' g^1 \wedge g^2 + k' g^3 \wedge g^4) + \frac{1}{2}(k - f) g^5 \wedge (g^1 \wedge g^3 + g^2 \wedge g^4)\big], \tag{2.1.76}$$

$$F_3 = \frac{M \alpha'}{2}\big[g^5 \wedge g^3 \wedge g^4 (1 - F) + g^5 \wedge g^1 \wedge g^2 F + F' d\eta \wedge (g^1 \wedge g^3 + g^2 \wedge g^4)\big], \tag{2.1.77}$$

$$\tilde{F}_5 = \mathcal{F}_5 + \star \mathcal{F}_5 = B_2 \wedge F_3 + dC_4, \tag{2.1.78}$$

$$\mathcal{F}_5 = B_2 \wedge F_3 = \frac{g_s M^2 (\alpha')^2}{4} l(\eta) g^1 \wedge g^2 \wedge g^3 \wedge g^4 \wedge g^5, \tag{2.1.79}$$

$$\star \mathcal{F}_5 = 4 g_s M^2 (\alpha')^2 \epsilon^{-8/3} dx^0 \wedge dx^1 \wedge dx^2 \wedge dx^3 \wedge d\eta \frac{l(\eta)}{K^2 e^{-8A} \sinh^2 \eta}. \tag{2.1.80}$$

Here $l(\eta) = f(1-F) + kF$; the R–R zero-form vanishes since $F_{3\mu\nu\lambda}H_3^{\mu\nu\lambda} = 0$; the dilaton is constant on the deformed conifold: $g_s^2 F_3^2 = H_3^2$; and a system of first-order equations consistent with type IIB equations satisfied by three-form fluxes is

$$\begin{aligned} f' &= (1-F)\tanh^2(\eta/2), \\ k' &= F\coth^2(\eta/2), \\ F' &= \frac{1}{2}(k-f), \end{aligned} \tag{2.1.81}$$

and

$$\frac{d(e^{-4A})}{d\eta} = -\alpha\frac{f(1-F)+kF}{K(\eta)\sinh^2\eta}, \tag{2.1.82}$$

where

$$\alpha = 4(g_s M\alpha')^2\epsilon^{8/3}. \tag{2.1.83}$$

The set of equations (2.1.81) form a closed system and imply the self-duality of the three-form with respect to the metric of the deformed conifold: $*_6 G_3 = iG_3$, where G_3 is a harmonic $(2,1)$ form on the deformed conifold. Combining (2.1.81) and using the boundary conditions for small and large η, one can obtain a second order differential equation for F whose solution yields:

$$F(\eta) = \frac{\sinh\eta - \eta}{2\sinh\eta}, \tag{2.1.84}$$

$$f(\eta) = \frac{\eta\cosh\eta - 1}{2\sinh\eta}(\cosh\eta - 1), \tag{2.1.85}$$

$$k(\eta) = \frac{\eta\cosh\eta - 1}{2\sinh\eta}(\cosh\eta + 1). \tag{2.1.86}$$

For large η, the other background fields take the form [77, 78]

$$B_2 = \frac{3g_sM\alpha'}{4}\left[\ln\frac{r}{r_0}\right](g^1\wedge g^2+g^3\wedge g^4), \tag{2.1.87}$$

$$H_3 = \frac{3g_sM\alpha'}{4r}dr\wedge(g^1\wedge g^2+g^3\wedge g^4), \tag{2.1.88}$$

$$F_3 = \frac{M\alpha'}{4}g^5\wedge(g^1\wedge g^2+g^3\wedge g^4), \tag{2.1.89}$$

$$\tilde{F}_5 = \mathcal{F}_5+\star\mathcal{F}_5, \tag{2.1.90}$$

$$\mathcal{F}_5 = B_2\wedge F_3 = 27\pi(\alpha')^2\left[N+\frac{3(g_sM)^2}{2\pi}\ln\frac{r}{r_0}\right]\mathrm{Vol}(T^{1,1}), \tag{2.1.91}$$

$$\star\mathcal{F}_5 = dC_4 = g_s^{-1}d(e^{4A})\wedge dx^0\wedge dx^1\wedge dx^2\wedge dx^3. \tag{2.1.92}$$

Here we note that the two- and three-forms on RHSs including only wedge products of g^is are closed. We also note that

$$g_s *_6 F_3 = -H_3, \qquad g_sF_3 = *_6H_3. \tag{2.1.93}$$

Hence the complex three-form G_3 satisfies the self-duality condition

$$*_6G_3 = iG_3, \qquad G_3 = F_3+\frac{i}{g_s}H_3. \tag{2.1.94}$$

We also note from (2.1.93) that

$$g_s^2F_3^2 = H_3^2, \tag{2.1.95}$$

which implies that the dilaton is constant, $\Phi = 0$. Since $F_{3\mu\nu\lambda}H_3^{\mu\nu\lambda} = 0$, the R–R scalar vanishes as well.

Now having solved for the three-forms on the deformed conifold, the warp factor can be determined by integrating (2.1.82), which gives in terms of η [75, 77]

$$e^{-4A} = 2(g_sM\alpha')^2\epsilon^{-8/3}I(\eta), \tag{2.1.96}$$

where[2]

$$I(\eta)\equiv\int_\eta^\infty dx\frac{x\cosh x-1}{\sinh^2 x}(\sinh(2x)-2x)^{1/3}. \tag{2.1.97}$$

[2]Note that this definition of I relocates a factor of $2^{1/3}$ relative to the KS expression [75].

Thus for small η

$$\begin{aligned} e^{-4A} &\sim 2(g_s M\alpha')^2\epsilon^{-8/3}\left[I(0) - \frac{\eta^2}{12}\left(\frac{2}{3}\right)^{1/3}\right] \\ &= (2g_s\alpha')^2\epsilon^{-8/3}\left[0.5699 - \epsilon^{-4/3}\frac{r^2}{3}\right] \end{aligned} \tag{2.1.98}$$

and for large η:

$$\begin{aligned} e^{-4A} &\sim 3\cdot 2^{1/3}(g_s M\alpha')^2\epsilon^{-8/3}(\eta - 1/4)e^{-4\eta/3} \\ &= \frac{27}{8}\frac{(g_s M\alpha')^2}{r^4}\left(\ln\frac{r^3}{\epsilon^2} + \ln\frac{4\sqrt{2}}{3\sqrt{3}} - \frac{1}{4}\right), \end{aligned} \tag{2.1.99}$$

which shows how the warp factor interpolates between the Klebanov-Tseytlin (KT) form [77, 78], for large r, to a smooth cap for $r\epsilon^{2/3} \lesssim 1$. In addition, for sufficiently small ϵ, there is an intermediate adS region for $|\ln r| \ll |\ln \epsilon^{2/3}|$, in which the logarithmic dependence on r is subdominant to the deformation term.

2.1.6 Large hierarchy and complex structure moduli fixing

We now consider the explicit supergravity background discussed in the previous subsection and show that the NS–NS and R–R fluxes generate a large hierarchy and stabilize all the moduli up to the Kähler modulus [29]. We first consider a compact manifold with moduli z, ρ, τ, where z is a complex structure modulus. We then explain how additional complex structure moduli can be included in the same way.

In the warped deformed conifold, the tensor fields $F_3 = dC_2$ and $H_3 = dB_2$ are nonvanishing, so that the associated fluxes thread cycles in the internal manifold (see Appendix). There are M units of F_3 flux through an A-cycle and -K units of H_3 flux through a B-cycle [29]:

$$\frac{1}{2\pi\alpha'}\int_A F_3 = 2\pi M \quad \text{and} \quad \frac{1}{2\pi\alpha'}\int_B H_3 = -2\pi K. \tag{2.1.100}$$

We can also understand this by requiring D3-brane charge conservation like in (2.1.33)

$$\frac{1}{2\kappa_{10}^2 T_3}\int_{\mathcal{M}} H_3 \wedge F_3 = M\,K. \tag{2.1.101}$$

Hence in the sense of Poincare duality we have

$$F_3 = (2\pi)^2\alpha' M[B], \qquad H_3 = (2\pi)^2\alpha' K[A]. \tag{2.1.102}$$

From this the superpotential (2.1.51) can be written in the from [29]

$$W = \int G_3 \wedge \Omega = (2\pi)^2\alpha'\bigg(M\int_B \Omega - K\tau\int_A \Omega\bigg). \tag{2.1.103}$$

The integrals appearing on the RHS of Eq. (2.1.103) are the periods defining the complex structure of the conifold [29] (see also Appendix A). One particular A-cycle which vanishes at the tip of the conifold is an S^3. This A-cycle can be described by the coordinate [29] (see also Appendix A)

$$z = \int_A \Omega. \tag{2.1.104}$$

The dual cycle of this is described by (see Appendix A)

$$\mathscr{G}(z) = \int_B \Omega = \frac{z}{2\pi i}\log z + \text{holomorphic} \tag{2.1.105}$$

The superpotential then takes the form [29]

$$W = (2\pi)^2\alpha'(M\mathscr{G}(z) - K\tau z). \tag{2.1.106}$$

The vanishing of Kähler covariant derivative of the superpotential gives

$$0 = \mathcal{D}_z W \propto M\partial_z\mathscr{G} - K\tau + \partial_z\mathcal{K}(M\mathcal{G} - K\tau z). \tag{2.1.107}$$

To obtain a large hierarchy, one will consider K/g_s to be large, which will imply an exponentially small z. Accordingly, the dominant terms in $\mathcal{D}_z W$ are [29]

$$\mathcal{D}_z W \propto \frac{M}{2\pi i}\log z - i\frac{K}{g_s} + \mathcal{O}(1), \tag{2.1.108}$$

For $K/Mg_s \gg 1$, it follows

$$z \simeq e^{-2\pi K/Mg_s}, \tag{2.1.109}$$

which is exponentially small [29]. Thus we obtain a large hierarchy of scales if, say, $M = 1$ and $K/g_s = 5$, assuming that the dilaton is frozen in this solution [29].

In the vicinity of N coincident D3-branes the spacetime metric takes the form

$$ds^2 = \left(\frac{r}{R}\right)^2 |d\vec{x}|^2 + \left(\frac{R}{r}\right)^2 (dr^2 + r^2 d\Omega_5^2) \quad \text{with} \quad R^4 = 4\pi g_s N(\alpha')^2, \tag{2.1.110}$$

where r is the distance from the D3-brane located at $r \approx 0$. On the deformed conifold the minimum value of r is given by the deformation parameter z as [29]

$$r_{\min} \simeq \rho_{\min}^{2/3} = z^{1/3} \simeq e^{-2\pi K/3Mg_s}. \tag{2.1.111}$$

This relation shows that the warp factor approaches a nonzero, small and positive value close to the D3-brane.

In our discussion so far we assumed that there is a single complex structure parameter z. We may suppose there are further complex structure deformations, controlled by moduli v_i. In this way the v_i enter in the regular terms in the periods and $\mathscr{G}(z)$ becomes $\mathscr{G}(z, v_i)$. Under the assumption that z has been successfully stabilized in the vicinity of the conifold point in moduli space like above, we may solve the equations [29]

$$\mathcal{D}_{v_i} W\big|_{z=0} = 0, \tag{2.1.112}$$

and obtain fixed values for the other moduli v_i. Thus in the flux compactification of type IIB theory the presence of the NS–NS and R–R fluxes fix all of the complex structure moduli and dilaton, but leave the Kähler modulus ρ unfixed.

2.2 Kähler moduli stabilization

2.2.1 General Perturbations around the ISD solution

As we saw at the end of the previous section, in an ISD compactification such as the warped deformed conifold, only the complex-structure moduli are stabilized but not

the Kähler moduli (that characterize the size of the internal Calabi-Yau). When the no-scale structure is broken to stabilize the Kähler moduli, perturbations around the ISD solution are expected. In supergravity, these perturbations are sourced by attaching the UV end of the throat to a fully stabilised Calabi-Yau sector, and one can treat these perturbations by considering a full perturbative expansion including perturbations in all fields [57]

$$X = X_0 + X_1 + X_2 + \cdots, \quad X \equiv \{\Phi_-, \Phi_+, G_-, G_+, \phi, g_{mn}\}, \tag{2.2.113}$$

where X_0 is the background, X_1 is the first-order perturbation, X_2 is the second-order perturbation and so on. Recall from the previous section that in an ISD background we have

$$\Phi_-^{(0)} = G_-^{(0)} = 0. \tag{2.2.114}$$

In the absence of local sources and curvature Eq. (2.1.35) is

$$\Delta\Phi_- = \frac{e^{8A+\phi}}{24}|\,G_-|^2 + e^{-4A}|\Delta\Phi_-|^2. \tag{2.2.115}$$

The Laplacian depends on the metric, so in terms of metric perturbations the Laplacian is

$$\Delta = \Delta_{(0)} + \Delta_{(1)} + \cdots \tag{2.2.116}$$

At first order in all perturbations we get the Laplace equation [57]

$$\Delta_{(0)}\Phi_-^{(1)} = 0, \tag{2.2.117}$$

and at second order we have [57]

$$\Delta_{(1)}\Phi_-^{(1)} + \Delta_{(0)}\Phi_-^{(2)} = \frac{g_s}{96}\big(\Phi_+^{(0)}\big)^2|\,G_-^{(1)}|^2 + 2|\,\Delta_0\Phi_-^{(1)}|^2/\Phi_+^{(0)}. \tag{2.2.118}$$

For $\Phi_-^{(1)} \neq 0$, the linearized equation (2.2.117) determines the leading solution. For $\Phi_-^{(1)} = 0$, the second order terms become important, and the first order equation (2.2.117) is identically satisfied. Eq. (2.2.118) then simplifies to

$$\Delta_{(0)}\Phi_-^{(2)} = \frac{g_s}{96}\big(\Phi_+^{(0)}\big)^2 |\, G_-^{(1)}|^2. \tag{2.2.119}$$

To identify the the source term in the above equation, consider Eq. (2.1.37). Because the Φ_- Eq. (2.2.119) is second order in fluxes, it is sufficient to solve Eq. (2.1.37) at first order. We have [57]

$$d\Lambda_{(1)} = 0, \tag{2.2.120}$$

where

$$\Lambda_{(1)} = \Phi_+^{(0)} G_-^{(0)} + \Phi_-^{(1)} G_+^{(0)}. \tag{2.2.121}$$

Since the flux induced contributions to Φ_- are only important when $\Phi_-^{(1)} = 0$, we may consider

$$\Lambda_{(1)} \approx \phi_+^{(0)} G_-^{(1)}. \tag{2.2.122}$$

This is exactly the source term in Eq. (2.2.119). Thus we have [57]

$$\Delta_{(0)}\Phi_-^{(2)} = \frac{g_s}{96}|\Lambda_{(1)}|^2. \tag{2.2.123}$$

By perturbing the Hodge star operator, metric perturbations induce changes in the definition of of IASD fluxes. But because of $\Lambda_{(0)} = 0$, the relevant IASD condition at first order is [57]

$$\star_6^{(0)} \Lambda_{(1)} = -i\Lambda_{(1)}. \tag{2.2.124}$$

Eq. (2.2.124) tells us that $\Lambda_{(1)}$ is IASD with respect to the background metric. Thus, as in Eq. (2.2.117), one does not need the explicit form of the perturbed metric in order to find the leading IASD flux solution.

In summary, the perturbations around the ISD supergravity solution with $\Phi_- = G_- = 0$ satisfy at leading order[3] the supergravity equation of motion [57]

[3] In addition to fluxes, coupling to the Ricci-scalar also induces a source term in the supergravity equation of motion (2.2.124), but at leading order fluxes provide the dominant source.

$$\Delta_{(0)}\Phi_- = \frac{g_s}{96}|\Lambda|^2, \tag{2.2.125}$$

where

$$d\Lambda = 0, \qquad \star_6\Lambda = -i\Lambda. \tag{2.2.126}$$

• Linearized perturbations

To determine linearized (first order) perturbations, it suffices to solve the Laplace equation (2.2.117)

$$\Delta_{(0)}\Phi_- = 0. \tag{2.2.127}$$

In a noncompact throat geometry, we can solve the Laplace equation and obtain the structure of Φ_-, which then feeds in to a potential for the D3-brane motion. (See [52–57] for a detailed explanation and computation of potentials away from the tip of the throat.)

In most of the literature (and hence in most inflationary models), the potential is computed away from the tip of the throat, and the geometry is approximated by $AdS_5 \times T^{1,1}$. In this case, the angular part of the Laplace equation, (2.2.127) is relatively straightforward, and solutions take a particularly clean form [55, 57]:

$$\Phi_-(r,\theta) = \sum_M \Phi_{LM} Y_{LM}(\Psi)\left(\frac{r}{r_{\rm UV}}\right)^{\Delta(L)}, \tag{2.2.128}$$

where r is the proper radial distance in the metric $g^{(0)}_{mn}$, (5.1.10), and

$$\Delta(L) \equiv -2 + \sqrt{6[l_1(l_1+1) + l_2(l_2+1) + R^2/8] + 4} \tag{2.2.129}$$

is the radial eigenfunction weight, coming from the eigenvalues of the angular eigenfunctions, $Y_{LM}(\Psi)$, of the Laplacian on $T^{1,1}$, [81, 82]. $L \equiv (l_1, l_2, R)$, $M \equiv (m_1, m_2)$ label $SU(2) \times SU(2) \times U(1)_R$ quantum numbers under the corresponding isometries of $T^{1,1}$, and Φ_{LM} are constant coefficients. The leading order terms of interest have

the lowest $\Delta(L)$, the smallest eigenvalues corresponding to non-trivial perturbations being

$$\Delta = \frac{3}{2} \text{ for } (l_1, l_2, R) = (1/2, 1/2, 1),\ Y_{LM}(\Psi) \sim \cos\frac{\theta_1}{2}\cos\frac{\theta_2}{2}e^{i(\phi_1+\phi_2+\psi)} \quad (2.2.130)$$

$$\Delta = 2 \text{ for } (l_1, l_2, R) = (1, 0, 0), (0, 1, 0),\ \ Y_{LM}(\Psi) \sim \cos\theta_i. \quad (2.2.131)$$

In [52–57] , the first mode, (2.2.130), was used to construct an inflection potential for the inflationary universe, however, this mode is not allowed in the warped deformed conifold, as the $U(1)_R$ isometry is broken to a discrete $\mathbb{Z}_2$ and therefore (2.2.130) is forbidden. In Chapter 4, we present an exact analytic solution of the Laplace equation on the deformed conifold allowed by this symmetry.

• Non-linear perturbations

To obtain non-linear perturbations, we confine ourselves to the leading order case including only fluxes as source term. In this case, one needs to solve Eq. (2.2.125) with RHS nonvanishing,

$$\Delta_{(0)}\Phi_- = \frac{g_s}{96}|\Lambda|^2. \quad (2.2.132)$$

The solution of this equation can always be put in the form [57]

$$\Phi_-(y) = \frac{g_s}{96}\int d^6y'\mathcal{G}(y;y')|\Lambda|^2(y') + \Phi_{\mathcal{H}}(y), \quad (2.2.133)$$

where

$$\Delta_{(0)}\mathcal{G}(y;y') = \delta(y-y'), \quad (2.2.134)$$

and

$$\Delta_{(0)}\Phi_{\mathcal{H}}(y) = 0, \quad (2.2.135)$$

which gives the homogeneous solution obtained above. Here and in what follows y denotes a collective internal coordinate consisting of the radial and six angular directions, where the latter will always be denoted by Ψ. On a general Calabi-Yau

cone with Kähler form J and holomorphic (3,0)-form Ω, we may turn on (1,2) flux, Λ_1, and a non-primitive (2,1) flux, Λ_2 [56, 57] (see Appendix A subsection A.5.5):

$$\Lambda_1 = \partial\partial f_1 \bar{\Omega}, \qquad \Lambda_2 = \partial f_2 \wedge J, \tag{2.2.136}$$

with f_1 and f_2 being holomorphic functions. The solution (2.2.133) takes the form [56, 57]:

$$\Phi_-^{(2)}(y) = \frac{g_s}{32}\left[\mathcal{K}^{\Sigma\bar{\Xi}}\partial_\Sigma f_1 \overline{\partial_\Xi f_1} + 2|f_2|^2\right], \tag{2.2.137}$$

where $\mathcal{K}^{\Sigma\bar{\Omega}}$ is the Kähler metric. For a specific choice of the f_i's, Eq. (2.2.137) determines the explicit solution of Eq. (2.2.132) up to harmonic terms. In the $AdS_5 \times T^{1,1}$ limit, the harmonic terms take the form [57]

$$\Phi_- = \sum_{\delta_i,\delta_j} r^{\Delta(\delta_i,\delta_j)} h_{(\delta_i,\delta_j)}(\Psi), \tag{2.2.138}$$

where $h_{(\delta_i,\delta_j)}(\Psi)$ are harmonic functions from the overlapping of different flux modes, and $\Delta(\delta_i,\delta_j) \equiv \delta_i + \delta_j - 4$ with Δ_i and Δ_j being the supergravity modes of the individual fluxes. The relating supergravity modes are [57]

$$\Delta_\Lambda = 1,\, 2,\, \frac{5}{2},\, \sqrt{28} - \frac{5}{2}, ... \tag{2.2.139}$$

In the IR region of the throat where η is small, the Green's function is that of the deformed conifold and takes the form [83, 84]

$$\mathcal{G}(y;y') = \mathcal{G}(\eta, y_4; \mathbf{e_0}) = -\frac{3^{2/3}}{2^{8/3}\pi^3\epsilon^{8/3}} \sum_{j=0,\frac{1}{2},1,...} \sum_{m=-j}^{j} \frac{\sqrt{2j+1}}{\eta} \mathcal{F}_{jm}(y_4, \overline{y}_4), \tag{2.2.140}$$

where $\mathbf{e_0}$ parametrizes the blown up S^3 at $\eta = 0$ and $\mathcal{F}_{jm}$ stand for the hypergeometric functions on the deformed conifold given by

$$\begin{aligned}
&\mathcal{F}_{0,0} = 1, \qquad \mathcal{F}_{\frac{1}{2},\frac{1}{2}} = 2y_4, \qquad \mathcal{F}_{\frac{1}{2},-\frac{1}{2}} = 2\overline{y}_4, \qquad \mathcal{F}_{1,1} = 2\sqrt{3}y_4^2,\\
&\mathcal{F}_{1,0} = -\sqrt{3}(1 - 4y_4\overline{y}_4), \qquad \mathcal{F}_{1,-1} = 2\sqrt{3}\overline{y}_4^2, \quad \mathcal{F}_{\frac{3}{2},\frac{3}{2}} = 4\sqrt{2}y_4^3,\\
&\mathcal{F}_{\frac{3}{2},\frac{1}{2}} = -4\sqrt{2}y_4(1 - 3y_4\overline{y}_4), \quad \mathcal{F}_{\frac{3}{2},-\frac{1}{2}} = -4\sqrt{2}\overline{y}_4(1 - 3y_4\overline{y}_4),\\
&\mathcal{F}_{\frac{3}{2},\frac{3}{2}} = 4\sqrt{2}\overline{y}_4^3.
\end{aligned} \tag{2.2.141}$$

In the UV region of the throat where η is large, we may introduce another radial coordinate r through $r^3 \sim \epsilon^2 e^{\eta}$ (see Eq. (2.1.65)) and the Green's function is that of the singular conifold given by [52]

$$\mathcal{G}(y;y') = \sum_L \frac{Y_L^*(\Psi')Y_L(\Psi)}{2\sqrt{\Lambda_L+4}} \times \begin{cases} \frac{1}{r'^4}\left(\frac{r}{r'}\right)^{c_L^+} & r \le r' \\ \frac{1}{r^4}\left(\frac{r'}{r}\right)^{c_L^+} & r \ge r' \end{cases} \tag{2.2.142}$$

with the harmonic eigenfunctions

$$Y_L(\Psi) = Z_{j_1,m_1,R}(\theta_1) Z_{j_2,m_2,R}(\theta_2) e^{im_1\varphi_1 + im_2\varphi_2} e^{\frac{i}{2}R\psi}, \tag{2.2.143}$$

$$\begin{aligned} Z^{\rm I}_{j_i,m_i,R}(\theta_i) &= N_L^{\rm I}(\sin\theta_i)^{m_i}\left(\cot\frac{\theta_i}{2}\right)^{R/2} \times \\ &\quad {}_2F_1\left(-j_i+m_i, 1+j_i+m_i, 1+m_i-\frac{R}{2}; \sin^2\frac{\theta_i}{2}\right), \qquad (2.2.144) \\ Z^{\rm II}_{j_i,m_i,R}(\theta_i) &= N_L^{\rm II}(\sin\theta_i)^{R/2}\left(\cot\frac{\theta_i}{2}\right)^{m_i} \times \\ &\quad {}_2F_1\left(-j_i+\frac{R}{2}, 1+j_i+\frac{R}{2}, 1-m_i+\frac{R}{2}; \sin^2\frac{\theta_i}{2}\right). \qquad (2.2.145) \end{aligned}$$

Here the normalization factors $N_L^{\rm I/II}$ relation is given by

$$V_{T^{1,1}} \int_0^1 dx [Z_{j_1,m_1,R}(x)]^2 \int_0^1 dy [Z_{j_2,m_2,R}(y)]^2 = 1. \tag{2.2.146}$$

In the above relations ${}_2F_1(a,b,c;d)$ stands for hypergeometric functions; L is a multi-index with the data $L \equiv (j_1,j_2),(m_1,m_2),R$, where j_1 and j_2 are both integers or half-integers with $m_1 \in \{-j_1,\cdots,j_1\}$ and $m_2 \in \{-j_2,\cdots,j_2\}$; $\Lambda_L = 6(j_1(j_1+1)+l_2(j_2+1)-R^2/8)$ denotes the spectrum of the full wave function and the eigenfunctions transform under $SU(2)_1 \times SU(2)_2$ as the spin (j_1,j_2) representation and under the $U(1)_R$ with charge R; $c_L^+ \equiv -2 \pm \sqrt{\Lambda_L+4}$.

2.2.2 The KKLT scenario

In this final section we first discuss the four-dimensional $N=1$ supergravity Lagrangian, following closely [76], and show that nonperturbative corrections to the

superpotential break the no-scale structure of the Lagrangian and lead to supersymmetry preserving AdS vacua in which the Kähler modulus is fixed [30]. We then add extra effects that break supersymmetry and lift the minimum of the potential to a positive value, yielding dS space [30]. As we shall see in chapter 5, the flux induced potential from the holomorphic solution of the noncompact ten-dimensional supergravity equation of motion (2.2.132) equals the the scalar potential of four-dimensional $N = 1$ supergravity discussed below [57].

The massless irreducible multiplets from the $N = 1$ supersymmetry algebra consist of the chiral, vector, and graviton multiplets. In general, there will be a number of massless chiral and vector multiplets. The particle content of the former corresponds to a complex scalar field ϕ and a Majorana spinor ψ. The particle content of the latter corresponds to a gauge field A_μ and a Majorana spinor λ. There is also an auxiliary complex field F in the chiral multiplet and an auxiliary real field D in the vector multiplet. Putting these together gives the following superfields [76]:

$$\Phi^i \;:\; \phi^i\,,\, \psi^i,\, F^i, \tag{2.2.147}$$

$$V^a \;:\; A^a_\mu\,,\, \lambda^a,\, D^a. \tag{2.2.148}$$

We now would like to write down the supergravity Lagrangian. We note from the previous section the occurrence of moduli in type IIB string theory on Calabi-Yau manifolds. These moduli are scalar fields with flat potentials and can have large classical values. In order to write down the effective Lagrangian one needs to consider moduli space power counting. Such a power counting assigns scalars the scaling l^0 with l being length. Supersymmetry then assigns the fermionic partners of these scalar fields scaling $l^{-1/2}$. Keeping all terms of the same order as the kinetic terms for these fields requires all terms in the Lagrangian density to have dimension l^m with $m \geq -2$. In order to keep the kinetic terms for the gauge multiplet, assign A_μ scaling l^0 and λ scaling $l^{-1/2}$. Lastly, assign the metric scaling l^0 as it has a classical expectation value.

The low energy effective action within this approximation depends on three func-

tions: the holomorphic superpotential $W(\Phi)$, the holomorphic function $f_{ab}(\Phi)$ corresponding to the gauge coupling, and the Kähler potential $\mathcal{K}(\Phi, \Phi^*)$ which is a general function of the superfields. The bosonic part of the Lagrangian density takes the form [76]:

$$\begin{aligned}\frac{\mathscr{L}_{\rm bos}}{(-G)^{1/2}} &= \frac{R}{2\kappa^2} - \mathcal{K}_{,\bar{i}j}\mathcal{D}_\mu\phi^{i*}\mathcal{D}^\mu\phi^j - \frac{1}{4}\mathrm{Re}(f_{ab}(\phi))F^a_{\mu\nu}F^{b\mu\nu} \\ &\quad -\frac{1}{8}\mathrm{Im}f_{ab}\epsilon^{\mu\nu\sigma\rho}F^a_{\mu\nu}F^b_{\sigma\rho} - V(\phi,\phi^*), \end{aligned} \tag{2.2.149}$$

where

$$V(\phi,\phi^*) = \exp(\kappa^2\mathcal{K})(\mathcal{K}^{\bar{i}j}W^*_{,i}W_{,j} - 3\kappa^2 W^*W) + \frac{1}{2}f_{ab}D^aD^b, \tag{2.2.150}$$

$$W_{,i} = \partial_i W + \kappa^2\partial_i\mathcal{K}W, \tag{2.2.151}$$

$$\mathrm{Re}(f_{ab}(\phi))D^b = -2\xi_a - \mathcal{K}_{,i}t^a_{ij}\phi^j. \tag{2.2.152}$$

Here the t_{ij} are the gauge group representation matrices, ξ_a is the additional parameter for each gauge group $U(1)$, and $\mathcal{K}^{\bar{i}j}$ is the inverse matrix to $\partial_j\partial_{\bar{k}}\mathcal{K}$. The negative term in (2.2.150) proportional to κ^2 is a supergravity effect. The first part of the potential is known as the F-term potential, form the superpotential, and the last term of the potential is known as the D-term, from gauge interactions.

We note that the kinetic term for the scalars is field-dependent and the metric for the space of scalar fields is given by (see Appendix A)

$$\mathcal{K}_{,\bar{i}j} = \frac{\partial^2\mathcal{K}(\phi,\phi^*)}{\partial\phi^{i*}\partial\phi^j}. \tag{2.2.153}$$

A metric of this form is known as Kähler metric and is invariant under Kähler transformations (see Appendix A)

$$\mathcal{K}(\phi,\phi^*) \to \mathcal{K}(\phi,\phi^*) + f(\phi) + f(\phi)^*. \tag{2.2.154}$$

Thus the moduli space is Kähler which means that the $2n$ real moduli can be grouped into n complex fields ϕ^i with the metric $G_{\bar{i}j} = \mathcal{K}_{,\bar{i}j}$. The invariance under Kähler

transformations is the invariance of the whole action if the superpotential also transforms as:

$$W(\phi) \to \exp[-\kappa^2 f(\phi)] W(\phi). \tag{2.2.155}$$

The supersymmetry transformations of the fermion fields take the form [76]:

$$\begin{aligned} \delta P_+ \psi^i / 2^{1/2} &= -K^{i\bar{j}} W^*_{,j} P_+ \zeta + \Gamma^\mu P_- \zeta \mathcal{D}_\mu \phi^i & (2.2.156) \\ \delta \lambda^a &= \frac{1}{2} \Gamma^{\mu\nu} \zeta F^a_{\mu\nu} + i \Gamma \zeta D^a, & (2.2.157) \\ \delta \psi_\mu &= \mathcal{D}_\mu \zeta + \frac{1}{2} \Gamma_\mu \zeta \exp(\kappa^2 \mathcal{K}/2) W. & (2.2.158) \end{aligned}$$

Here ζ is the supersymmetry parameter, Γ_μ are the matrices forming the Dirac representation, $\mathcal{D}_\mu$ is the covariant derivative, ψ is the gravitino and $P_\pm$ are parity operators. The variations (2.2.156) - (2.2.158) all vanish if the metric is flat, the gauge field is zero, the scalars and ζ are constant, and $\partial_i W = D^a = W = 0$.

A simple calculation shows that this potential does not depend on the radial modulus. Using the result for the Kähler potential for ρ derived in (2.1.50), we obtain [29, 30]

$$\mathcal{K}^{\rho\bar{\rho}} \mathcal{D}_\rho W \mathcal{D}_{\bar{\rho}} \bar{W} - 3\kappa^2 |W|^2 = 0 \tag{2.2.159}$$

According to this, the scalar potential is of the no-scale type [29, 30]

$$V = e^{\mathcal{K}} \sum_{i,j \neq \rho} \mathcal{K}^{i\bar{j}} \mathcal{D}_i W \mathcal{D}_{\bar{j}} \bar{W}. \tag{2.2.160}$$

At the minimum of the potential $\mathcal{D}_i W = 0$ which gives $V = 0$ although supersymmetry is broken in general because $\mathcal{D}_\rho W \neq 0$.

An important nonrenormalization theorem states that the tree-level superpotential (2.1.51) contained in the F-term potential does not receive perturbative corrections [76], but it can receive nonperturbative corrections [76] depending on ρ [30]. This will break the no-scale structure and stabilize all moduli of type IIB compactification. Generally, nonperturbative corrections can include multiple exponentials,

but for simplicity we assume that there is only one exponential correction to the superpotential [30]:

$$W_{\rm np} = Ae^{ia\rho}, \tag{2.2.161}$$

where ρ is the radial modulus, A is the one-loop determinant[4] and the coefficient $a = 2\pi/n$ is a constant that depends on the specific source of the nonperturbative effects; $n = 1$ corresponds to nonperturbative effects such as instantons arising from Euclidean D3-branes wrapping four-cycles, and $n > 1$ corresponds to strong gauge dynamics of D7-branes, which might be present and wrapped around internal four-cycles. We may also assume that the volume of the internal manifold is large, so that the relating Kähler potential receives no corrections and is therefore given by its tree-level result. By the assumption that all other modes are stable, we are left with an effective theory for the radial modulus. In what follows, we assume that the Kähler modulus characterizes the size of the internal Calabi-Yau, and according to the previous section, the dilaton and the complex structure moduli are stabilized by ISD fluxes. The full superpotential is then [30]

$$W = W_0 + W_{\rm np}. \tag{2.2.162}$$

By letting ρ be the volume of a given four-cycle that admits a nonperturbative effect, the nonperturbative effects depend then exponentially on the warped volume of the associated four-cycle. This means that the warped volume governs the instanton action in the case of Euclidean D3-branes, and the gauge coupling in the case of strong gauge dynamics on D7-branes. To see this, consider a warped background with the line element (2.1.25). The Yang-Mills coupling g_7 of the 7+1 dimensional theory living on a stack of D7-branes is given by [52]

$$g_7^2 \equiv 2(2\pi)^5 g_s(\alpha')^2. \tag{2.2.163}$$

[4] As we shall discuss in Chapter 5, the presence of a mobile D3-brane in this supergravity background makes A depend on radial as well as angular directions of the internal Calabi-Yau space.

The action for gauge fields on D7-branes that wrap a four-cycle is [52]

$$S_{D7} = \int_{\Sigma_4} d^4\zeta \sqrt{g^{ind}} e^{4A(y)} . \int d^4x \sqrt{g} g^{\mu\alpha} g^{\nu\beta} \mathrm{Tr} F_{\mu\nu} F_{\alpha\beta}, \tag{2.2.164}$$

where ζ are coordinates on the four-cycle and g^{ind} is the metric induced on the four-cycle from g_{ij}. A key point in the appearance of a single power of $e^{4A(y)}$. Defining the warped volume as

$$V_{\Sigma_4}^{\omega} \equiv \int_{\Sigma_4} d^4\zeta \sqrt{g^{ind}} e^{4A(y)}, \tag{2.2.165}$$

and the D3-brane tension (see chapter 3)

$$T_3 = ((2\pi)^3 g_s (\alpha')^2)^{-1}, \tag{2.2.166}$$

we can read off the gauge coupling of the four-dimensional theory from (2.2.164):

$$\frac{1}{g^2} = \frac{V_4}{g_7^2} = \frac{T_3 V_4}{8\pi^2}. \tag{2.2.167}$$

The modulus of the gaugino condensate superpotential in $SU(N_{D7})$ is [52]

$$|W_{np}| = 16\pi^2 M_{UV}^3 \exp\left(-\frac{1}{N_{D7}} \frac{8\pi^2}{g^2}\right) \propto \exp\left(-\frac{T_3 V_4}{N_{D7}}\right), \tag{2.2.168}$$

where M_{UV} is the UV cutoff.

In the cases that the nonperturbative effect comes from a Euclidean D3-brane, the instanton action is [52]

$$S = T_3 \int_{\Sigma_4} d^4\zeta \sqrt{G^{ind}} = T_3 \int_{\Sigma_4} d^4\zeta \sqrt{g^{ind}} e^{4A(y)} \equiv T_3 V_4, \tag{2.2.169}$$

so that, just as in (2.2.164), the action depends on a single power of $e^{4A(y)}$. The modulus of the nonperturbative superpotential is then [52]

$$|W_{np}| \propto \exp(-T_3 V_4). \tag{2.2.170}$$

The superpotentials (2.2.170) and (2.2.168) can be written in a unified way as [52]

$$|W_{np}| \propto \exp(-T_3 V_4/n), \tag{2.2.171}$$

where for D7-branes $n = N_{D7}$, and for Euclidean D3-branes $n = 1$.

We now turn to the effective F-term potential containing such nonperturbative effects in its superpotential (2.2.162). Consider the condition (2.1.53)

$$\mathcal{D}_\rho W = \partial_\rho W + \partial_\rho \mathcal{K} W = 0 \quad \text{with} \quad \mathcal{K} = -3\log[-i(\rho - \bar{\rho})]. \tag{2.2.172}$$

This condition implies [30]

$$W_0 = -A\left(\frac{2}{3}a\sigma_0 + 1\right)e^{-a\sigma_0}, \tag{2.2.173}$$

or

$$W_0 = -\frac{2}{3}Aa\sigma_0 e^{-a\sigma_0}. \tag{2.2.174}$$

Thus the minimum of the potential

$$V(\phi, \phi^*) = \exp(\kappa^2\mathcal{K})(\mathcal{K}^{\rho\bar{\rho}}\mathcal{D}_\rho W \mathcal{D}_{\bar{\rho}}\overline{W} - 3\kappa^2|W|^2), \tag{2.2.175}$$

is given by [30]

$$V_0 = -\frac{a^2A^2}{6\sigma_0}e^{-2a\sigma_0}, \tag{2.2.176}$$

where σ_0 is the value of σ in the radial modulus $\rho = i\sigma$ at the minimum of the potential. Clearly this potential is negative, and the only maximally symmetric space-time solution allowed by such a supersymmetric compactification is AdS space-time [30].

By adding anti-D3-branes it is possible to break supersymmetry, so that the compactification becomes a dS space [30]. This gives an additional term in the scalar potential of the form

$$\delta V = \frac{D}{\sigma^2} \tag{2.2.177}$$

with D being proportional to the number of anti-D3-branes, which can be chosen so that the vacuum energy density becomes positive giving a dS space [30]. The inclusion of anti-D3-brane gives the scalar potential [30]

$$V(\sigma) = \frac{aAe^{-a\sigma}}{2\sigma^2}\left(\frac{1}{3}\sigma aAe^{-a\sigma} + W_0 + Ae^{-a\sigma}\right) + \frac{D}{\sigma^2}. \tag{2.2.178}$$

The vacua obtained in this way are only metastable as all of the sources of energy vanish as $\sigma \to \infty$, but the lifetime could be extremely long.

Chapter 3

Review of D-brane inflation

We are now ready to study D-brane inflation. We first review some relevant aspects of D-branes, following [76], and construct the full effective action for a mobile D3-brane emdedded in the supergravity background discussed in the previous chapter, following [85–88]. We then discuss an interesting example of a multifield D-brane inflation scenario known as Spinflation [71] in which the inflationary D3-brane has radial as well as angular motion in the warped deformed conifold[1].

3.1 D-branes

The emergence of D-branes in string theory follows from toroidal compactification [76]. In the simplest toroidal compactification one dimension is periodic at some radius R while the rest of the dimensions are noncompact. Underlying toroidal compactification is a symmetry knows as T-duality by which the physics taking the $R \to 0$ limit is isomorphic to the physics taking the opposite $R \to \infty$ limit. When an open string theory with Neumann boundary conditions is toroidally compactified taking $R \to 0$, the physics is described by compactification with $R \to \infty$ but with open string endpoints restricted to lie on hyperplanes with Dirichlet conditions

[1] In this chapter, we review spinflation in the warped deformed conifold as an exact ISD supergravity solution discussed in section 2.1. In the next two chapters, we study spinflation in the warped deformed conifold subject to perturbations around the ISD solution including the effects of Kähler moduli stabilization discussed in section 2.2.

called Dirichlet membranes or D-branes for short [76]. In particular, taking the $R \to 0$ limit of the open and unoriented type I superstring theory leads to D-branes and orientifold planes. The most remarkable property of D-branes is that they spontaneously break 16 of the 32 spacetime supersymmetries [41, 76]. The fact that D-branes leave half of the supersymmetries unbroken classifies them as BPS states [41, 76]. It is well known that BPS states must carry conserved charges. The most natural set of charges with correct Lorentz properties are the antisymmetric R–R charges [41, 76]. The world-volume of a p-brane naturally couples to a $p+1$-form potential

$$\int C_{p+1}. \tag{3.1.1}$$

Here the integral runs over the D-brane world-volume. Considering type I superstring theory and taking T-duality on any even number of dimensions we can reach type IIB superstring theory with a Dp-brane of any odd p. Thus in type IIB theory has D_1-,D_3-,D_5-D_7- and D_9-branes one needs 2-, 4-, 6-, 8-, and 10-form potentials. The last 10-form arises from the type I divergences whereas the first four arise in either electric or magnetic descriptin of the propagating R–R states, the coupling of which to D-branes is dicussed below.

3.1.1 D-brane action

The massless fields on the world-volume of a Dp-brane consist of a $U(1)$ vector and $9-p$ world-brane scalars describing fluctuations. The world-brane fields interact with massless closed string fields, whose type IIB action has been discussed in the previous chapter. We first consider the coupling of a D-brane to NS–NS closed string fields. For this we may introduce coordinates ξ^a with $a = 0, ..., p$ on the brane. The fields on the brane consist of the embedding $X^\mu(\xi)$ and the gauge field $A_a(\xi)$. The D-brane action takes the form [76]:

$$S_{\rm DBI} = -T_p \int d^{p+1}\xi \, e^{-\Phi} \sqrt{-\det\left(G_{ab} + B_{ab} + 2\pi\alpha' F_{ab}\right)}. \tag{3.1.2}$$

Here T_p is the D-brane tension discussed in the next subsection, F_{ab} is the gauge field living on the brane, G_{ab} and B_{ab} are the components of the spacetime NS–NS fields parallel to the brane being the induced metric and antisymmetric tensor on the brane. These are given by:

$$G_{ab}(\xi) = \frac{\partial X^\mu}{\partial \xi^a}\frac{\partial X^\nu}{\partial \xi^b} G_{\mu\nu}(X(\xi)), \quad B_{ab}(\xi) = \frac{\partial X^\mu}{\partial \xi^a}\frac{\partial X^\nu}{\partial \xi^b} B_{\mu\nu}(X(\xi)). \tag{3.1.3}$$

The above action is called the Dirac–Born–Infeld (DBI) action. The argument leading to this form of action is as follows. Taking only into account the spacetime metric and the embedding, the simplest and lowest-derivative coordinate-invariant action in the world-volume given by the integral of $(-\det G_{ab})^{1/2}$. According to (3.1.3), this term depends on the embedding $X^\mu(\xi)$ and expanded about a flat D-brane implies the action for the fluctuations.

The dilaton dependence from $e^{-\Phi} \propto g_c^{-1}$ is due to the fact that (3.1.2) is an open string tree-level action.

The F_{ab} dependence follows from T-duality. Take a D-brane spanned by the X^1- and X^2-directions with no other dimensions spacified, and let F_{12} be a constant gauge field on this brane. T-duality operation on the 2-direction replaces Neumann boundary condition with Dirichlet boundary condition, therefore reducing a dimension of the D-brane. But under T-duality along the 2-direction X^2 is replaced by X'^2 of the from

$$X'^2 = -2\pi\alpha' A_2 = -2\pi\alpha' X^1 F_{12}. \tag{3.1.4}$$

This produces a geometric factor

$$\int dX^1 \left[1 + (\partial_1 X'^2)^2\right]^{1/2} = \int dX^1 \left[1 + (2\pi\alpha' F_{12})^2\right]^{1/2}. \tag{3.1.5}$$

Now consider a combination of boost and rotation for any D-brane. Boosting alignes the brane with the coordinate axes and rotation takes F_{ab} into block-diagonal form. This reduces the action to a product of factors (3.1.5) and produces an equivalent form of the term F_{ab} term in the determinant (3.1.2).

The B_{ab} dependence follows from the string world-sheet action which is given by the sum of the bulk action and a boundary term as:

$$\frac{i}{4\pi\alpha'}\int_M d^2\sigma\, g^{1/2}\,\partial_a X^\mu \partial_b X^\nu B_{\mu\nu} + i\int_{\partial M} dX^\mu A_\mu, \tag{3.1.6}$$

where $B_{\mu\nu}$ is the closed string field and A_μ is the open string field. This action is invariant under gauge transformations of these fields given by:

$$\delta A_\mu = \partial_\mu \lambda, \qquad \delta B_{\mu\nu} = \partial_\mu \xi_\nu - \partial_\nu \xi_\mu. \tag{3.1.7}$$

The first of these changes the boundary term in (3.1.6) by an integral of a total derivative, and the second one changes the bulk action in (3.1.6) by a total derivative. On a noncompact world-sheet though the latter transformation produces a surface term which can only be canceled out if the open string field too transforms under the tensor gauge symmetry. This means that:

$$\delta A_\mu = -\xi_\mu/2\pi\alpha'. \tag{3.1.8}$$

But invariance under both symmetries requires the following combination to appear in the action:

$$B_{\mu\nu} + 2\pi\alpha' F_{\mu\nu} \equiv 2\pi\alpha' \mathcal{F}_{\mu\nu} \qquad \text{with} \qquad F_{\mu\nu} = \partial_\mu A_\mu - \partial_\nu A_\mu. \tag{3.1.9}$$

Finally, consider the coupling of the D-brane to the R–R fields. The action takes the form [76]:

$$S_{\rm WZ} = iT_3 \int_{p+1} \mathrm{Tr}\left[\exp[2\pi\alpha' F_2 + B_2]\right] \wedge \sum_q C_q. \tag{3.1.10}$$

This action is called the Wess–Zumino action. To see how this comes about, take a 1-brane in the $(1,2)$ plane, and again use T-duality. The action for this is:

$$\int C_2 = \int dx^0 (dx^1 C_{01} + dx^2 C_{02}) = \int dx^0 dx^1 (C_{01} + \partial_1 X^2 C_{02}). \tag{3.1.11}$$

T-duality along the 2-direction gives:

$$\int dx^0 dx^1 (C_{012} + 2\pi\alpha' F_{12} C_0). \tag{3.1.12}$$

Generalizing this to an arbitrary configuration produces the action (3.1.10).

Thus the total D-brane action is [76]:

$$\begin{aligned} S_{\text{Dp-brane}} &= S_{\text{DBI}} + S_{\text{WZ}} \\ &= -T_p \int d^{p+1}\xi\, e^{-\Phi} \sqrt{-\det\left(G_{ab} + B_{ab} + 2\pi\alpha' F_{ab}\right)} \\ &\quad iT_p \int_{p+1} \text{Tr}\left[\exp[2\pi\alpha' F_2 + B_2]\right] \wedge \sum_q C_q. \end{aligned} \tag{3.1.13}$$

3.1.2 D-brane tension

In our discussions above, we argued that D-branes are extended BPS objects carrying R–R charges. We now use this property to briefly discuss the tension of the D-brane that was left undetermined in the action (3.1.13). We note that there is no force between static BPS objects. The vanishing of the force is due to a cancellation between attraction from the graviton and dilaton and repulsion from the R–R tensor. These forces can be computed as follows. Take two parallel D-branes fixed at different positions in the background. The branes interact with each other by exchanging closed strings. The string amplitude is the cylinder vacuum amplitude with one end on each D-brane. For the exchange of light NS–NS closed strings, the cylinder vacuum amplitude is [76]:

$$\begin{aligned} \mathscr{A}_{\text{NS–NS}} &\approx \frac{iV_{p+1} 4 \times 16}{8\pi(8\pi^2\alpha')^5} \int_0^\infty \frac{\pi dt}{t^2} (8\pi^2\alpha' t)^{(9-p)/2} \exp\left(\frac{ty^2}{2\pi\alpha'}\right) \\ &= iV_{p+1} 2\pi (4\pi^2\alpha')^{3-p} \mathcal{G}_{9-y}(y). \end{aligned} \tag{3.1.14}$$

Here $\mathcal{G}(y)$ is the scalar Green's function with y specifying the separation of the stretched string, and V_{p+1} is the volume. By supersymmetric cancellation in the trace, the R–R exchange amplitude is:

$$\mathscr{A}_{\text{R–R}} = -\mathscr{A}_{\text{NS–NS}}. \tag{3.1.15}$$

This means that the total force is vanishing, as expected from BPS states.

The field theory amplitude for the dilaton-graviton potential is [76]:

$$2iV_{p+1}\kappa^2\tau_p^2\mathcal{G}_{9-p}(y) \tag{3.1.16}$$

Comparing this with $\mathscr{A}_{\text{NS–NS}}$ gives:

$$\tau_p^2 = \frac{\pi}{\kappa^2}(4\pi^2\alpha')^{3-p}. \tag{3.1.17}$$

For the R–R exchange, the low-energy action is

$$-\frac{1}{4\kappa_{10}^2}\int d^{10}x(-G)^{1/2}|F_{p+1}|^2 + \mu_p\int C_{p+1}. \tag{3.1.18}$$

For the canonically normalized kinetic term the propagator is $2\kappa_{10}^2 i/k^2$ and the field theory amplitude is:

$$-2\kappa_{10}^2 i\mu_p^2\mathcal{G}_{9-p}(y). \tag{3.1.19}$$

Thus we obtain [76]:

$$\mu_p^2 = \frac{\pi}{\kappa_{10}^2}(4\pi^2\alpha')^{3-p} = e^{2\Phi_0}\tau_p^2 = T_p^2. \tag{3.1.20}$$

For future reference, we note that relation (3.1.20) for $p = 3$ and κ_{10}^2 given by (2.1.14) gives the tension of a D3-brane as:

$$T_3 = ((2\pi)^3\alpha'^2)^{-1}. \tag{3.1.21}$$

3.2 The effective multifield D3-brane action

To derive the effective action of a probe D3-brane in type IIB supergravity, we denote the coordinates of the compact space by y^m $(m = 1, \cdots, 6)$ whereas for coordinates of the noncompact spacetime we consider x^μ $(\mu = 0, 1, 2, 3)$. In terms of these coordinates, the ten-dimensional metric (2.1.25) reads as [88]

$$\begin{aligned} ds^2 &= h^{-1/2}(y^k)g_{\mu\nu}(x^\lambda)dx^\mu dx^\nu - h^{1/2}(y^k)g^{(0)}_{mn}(y^k)dy^m dy^n \\ &\equiv \gamma_{AB}dY^A dY^B, \end{aligned} \tag{3.2.22}$$

where $Y^A = \{x^\mu, y^m\}$. In order to restore four-dimensional local Lorentz invariance, the three-fluxes F_3 and H_3 have only compact components and the axion C_0 and dilaton Φ can only vary along the compact manifold. Consequently, we fix the gauge so that C_2 and B_2 have nontrivial components only along the compact directions, whereas C_4 has components only along the noncompact spacetime dimensions. Hence we have [88]

$$B_{ml} \neq 0 \quad B_{\mu l} = B_{\mu\nu} = 0, \tag{3.2.23}$$

$$C_{\mu m} \neq 0 \quad C_{ml} = C_{\mu\nu} = 0$$

$$C_{\mu\nu\rho\sigma} \neq 0, \quad \text{with all other components vanishing.} \tag{3.2.24}$$

The action of the D3-brane in this supergravity background takes the form:

$$S_{\rm D3} = S_{\rm DBI} + S_{\rm WZ}, \tag{3.2.25}$$

$$S_{\rm DBI} = -T_3 \int d^4x e^{-\Phi} \sqrt{-\det\left(\hat{\gamma}_{\mu\nu} + \hat{B}_{\mu\nu} + 2\pi\alpha' F_{\mu\nu}\right)} \tag{3.2.26}$$

$$S_{\rm WZ} = -T_3 \int_{\rm brane} \sum_{n=0,2,4} \hat{C}_n \wedge e^{(\hat{B}_2 + 2\pi\alpha' F_2)}\Big|_{\text{4-form}}. \tag{3.2.27}$$

In these actions and in what follows, a hat denotes a pull-back onto the brane so that $\hat{\gamma}_{\mu\nu}$, for instance, is the induced metric on the brane. In the Wess-Zumino term, we keep only the 4-forms resulting from the wedge product, and F_2 is the field strength of the $U(1)$ worldvolume gauge field, i.e., $F_{\mu\nu} = \partial_\mu A_\nu - \partial_\nu A_\mu$. This enters the brane's action only through the combination $\mathcal{F}_{\mu\nu} = \hat{B}_{\mu\nu} + 2\pi\alpha' F_{\mu\nu}$, as before. Finally, for the brane embedding we define functions

$$Y_b^A(x^\mu) = (x^\mu, \varphi^m(x^\mu)), \tag{3.2.28}$$

where the brane spacetime coordinates x^μ are taken to to coincide with the first four bulk coordinates.

3.2.1 DBI action

According to (3.2.22) - (3.2.23), the metric and two-form induced on the brane take the following forms [88]

$$\hat{\gamma}_{\mu\nu} = \gamma_{AB}\partial_\mu Y_b^A \partial_\nu Y_b^B = h^{-1/2}(g_{\mu\nu} - h g^{(0)}_{mn}\partial_\mu\varphi^m\partial_\nu\varphi^n), \tag{3.2.29}$$

$$\hat{B}_{\mu\nu} = B_{AB}\partial_\mu Y_b^A \partial_\nu Y_b^B = B_{mn}\partial_\mu\varphi^m\partial_\nu\varphi^n. \tag{3.2.30}$$

We consider the following rescalings:

$$\phi^m = \sqrt{T_3}\varphi^m, \qquad G_{mn} = e^{-\Phi} g^{(0)}_{mn}, \qquad b_{mn} = \frac{h^{1/2}}{T_3} B_{mn}. \tag{3.2.31}$$

We may also define the functions:

$$f(\phi^k) \equiv e^{\Phi}\frac{h}{T_3}, \qquad \lambda(\phi^k) = 2\pi\alpha' h^{1/2}. \tag{3.2.32}$$

Hence we can write the DBI action in the form [88]:

$$S_{\rm DBI} = \int d^4x\sqrt{-g}\Big(- \frac{1}{f}\sqrt{\rm Det}\Big) \tag{3.2.33}$$

with the determinant is given by

$$\rm Det \equiv \det(\delta^\mu_\nu + f G_{mn}\partial_\mu\phi^m\partial_\nu\phi^n + b_{mn}\partial^\mu\phi^m\partial_\nu\phi^n + \lambda F^\mu_\nu). \tag{3.2.34}$$

Here the Greek indices are raised and lowered with the 'spacetime' metric $g_{\mu\nu}$. We may rewrite the determinant in the form

$$\rm Det = \det(\mathbf{I} + \mathbf{S} + \mathbf{B}), \tag{3.2.35}$$

where $\mathbf{I}$ denotes the four-dimensional identity matrix, and from Eq. (3.2.34) the matrices $\mathbf{S}$ and $\mathbf{B}$ can be defined in terms of their components as

$$S^\mu_\nu = f G_{mn}\partial^\mu\phi^m\partial_\nu\phi^n \qquad (S_{\mu\nu} = S_{\nu\mu}), \tag{3.2.36}$$

$$B^\mu_\nu = f G_{mn}\partial^\mu\phi^m\partial_\nu\phi^n + \lambda F^\mu_\nu = \frac{\lambda}{2\pi\alpha'} g^{\mu\lambda}\mathcal{F}_{\lambda\nu} \quad (B^{\mu\nu} = -B^{\nu\mu}). \tag{3.2.37}$$

We can compute the determinant in Eq. (3.2.35) and obtain [88]

$$\begin{aligned}\mathrm{Det} &= \mathrm{Det}_S - \frac{1}{2}\mathrm{Tr}(\mathcal{B}^2)(1+\mathrm{Tr}\mathbf{S}) + \mathrm{Tr}(\mathbf{S}\mathcal{B}^2)(1+\mathrm{Tr}\mathbf{S}) - \mathrm{Tr}(\mathbf{S}^2\mathcal{B}^2) \\ &\quad -\frac{1}{4}\mathrm{Tr}(\mathcal{B}^2)[(\mathrm{Tr}(\mathbf{S})^2 - \mathrm{Tr}(\mathbf{S}^2)] - \frac{1}{2}\mathrm{Tr}(\mathbf{S}\mathcal{B}\mathbf{S}\mathcal{B}) \\ &\quad +\frac{1}{8}\big[(\mathrm{Tr}(\mathcal{B}^2))^2 - 2\mathrm{Tr}(\mathcal{B}^4)\big], \end{aligned} \tag{3.2.38}$$

$$\mathrm{Det}_S \equiv 1 + \mathrm{Tr}\mathbf{S} + \frac{1}{2}[(\mathrm{Tr}\mathbf{S}) - \mathrm{Tr}(\mathbf{S}^2)] + S^{[\alpha}_{\alpha} S^{\beta}_{\beta} S^{\gamma]}_{\gamma} + S^{[\alpha}_{\alpha} S^{\beta}_{\beta} S^{\gamma}_{\gamma} S^{\delta]}_{\delta}. \tag{3.2.39}$$

For vanishing $\mathbf{S}$, Det reduces to the determinant of standard Born-Infeld theory [87]. On the other hand, when the brane and bulk fields are ignored Det reduces Det_S, which depends only on the scalar fields. It can be written in the form [88]

$$\mathrm{Det}_S = 1 - 2fG_{mn}X^{mn} + 4f^2 X^{[m}_{m} X^{n]}_{n} - 8f^3 X^{[m}_{m} X^{n}_{n} X^{l]}_{l} + 16 f^4 X^{[m}_{m} X^{n}_{n} X^{l}_{l} X^{k]}_{k}, \tag{3.2.40}$$

where we have defined

$$X^{mn} \equiv -\frac{1}{2}\partial^{\mu}\phi^{m}\partial^{\nu}\phi^{n} \qquad X^{n}_{m} = G_{ml}X^{ln}. \tag{3.2.41}$$

Here the brackets denote antisymmetrisation of the field indices and the field indices are raised and lowered with the field space metric G_{mn} defined in (3.2.32).

3.2.2 WZ action

We now come to the Wess-Zumino part. According to Eq. (**??**), the explicit expression is by [88]

$$\begin{aligned} S_{\mathrm{WS}} &= -T_3\Big[\int_{\mathrm{brane}} \hat{C}_4 + \int_{\mathrm{brane}} \hat{C}_2 \wedge \big(\hat{B}_2 + 2\pi\alpha' F_2\big) \\ &\quad +\frac{1}{2}\int_{\mathrm{brane}} B_2 \wedge B_2 + 4\pi\alpha' \hat{B}_2 \wedge F_2 + (2\pi\alpha')^2 F_2 \wedge F_2\Big] \\ &\equiv S^{[4]}_{\mathrm{WS}} + S^{[2]}_{\mathrm{WS}}, \end{aligned} \tag{3.2.42}$$

where $S^{[4]}_{\rm WS}$ comes from the 4-form $\hat{C}_4$ and $S^{[2]}_{\rm WS}$ contains two-forms $\hat{C}_2$, $\hat{B}_2$ and F_2. The four-form $\hat{C}_4$ is given by

$$\hat{C}_4 = \mathcal{V}\epsilon_4 \tag{3.2.43}$$

where ϵ_4 is the fully antisymmetric tensor associated with the four-dimensional metric $g_{\mu\nu}$ (so that $\sqrt{-g}$) and the coefficient $\mathcal{V}$ depends only on the compact coordinates. Thus the first term on the RHS of Eq. (3.2.42) gives a potential term depending on the scalar fields ϕ^m parameterizing the brane position in the compact space [88]:

$$S^{[4]}_{\rm WZ} = -T_3 \int_{\rm brane} \hat{C}_4 = -\int d^4x\sqrt{-g}T_3\mathcal{V}(\phi^m). \tag{3.2.44}$$

We now consider the different terms in $S^{[2]}_{\rm WS}$. The first term includes $\hat{C}_2$ and is proportional to [88]

$$\begin{aligned}\int_{\rm brane} \hat{C}_2 \wedge \hat{B}_2 &= -\frac{1}{4}\int d^4x\sqrt{-g}\epsilon^{\mu\nu\rho\sigma}C_{AB}\frac{\partial Y_b^A}{\partial x^\mu}\frac{\partial Y_b^B}{\partial x^\nu}B_{CD}\frac{\partial Y_b^C}{\partial x^\rho}\frac{\partial Y_b^D}{\partial x^\sigma} \\ &= -\frac{1}{4T_3^2}\int d^4x\sqrt{-g}\epsilon^{\mu\nu\rho\sigma}C_{mn}B_{kl}\partial_\mu\phi^m\partial_\nu\phi^n\partial_\rho\phi^l\partial_\sigma\phi^k.\end{aligned} \tag{3.2.45}$$

In writing this expression we noted that the brane embedding function is given by Eq. (3.2.28) and that $\hat{C}_2$ has only compact indices. The next term is proportional to [88]

$$\int_{\rm brane} \hat{C}_2 \wedge F_2 = -\frac{1}{4T_3}\int d^4x\sqrt{-g}C_{mn}\epsilon^{\mu\nu\rho\sigma}\partial_\mu\phi^m\partial_\nu\phi^n F_{\rho\sigma}. \tag{3.2.46}$$

The two terms involving $\hat{B}_2 \wedge \hat{B}_2$ and $\hat{B}_2 \wedge F_2$ are similar to (3.2.45) and (3.2.46), respectively, and therefore are not written down here. The last term contains C_0 and takes the form [88]

$$\int_{\rm brane} C_0 F_2 \wedge F_2 = -\frac{1}{4}\int d^4x\sqrt{-g}C_0\epsilon^{\mu\nu\rho\sigma}F_{\mu\nu}F_{\rho\sigma} = -\frac{1}{2}\int d^4x\sqrt{-g}C_0 F_{\mu\nu}\tilde{F}^{\mu\nu}. \tag{3.2.47}$$

Here we have considered the dual of the field strength $\tilde{F}^{\mu\nu} = \frac{1}{2}\epsilon^{\mu\nu\rho\sigma}F_{\rho\sigma}$.

3.2.3 The full action and equations of motion

The full four-dimensional effective action takes the form [88]

$$\begin{aligned} S &= \frac{M_{Pl}}{2}\int d^4x\sqrt{-g}R^{(4)} + S_{\text{brane}} \\ S_{\text{brane}} &= \int d^4x\sqrt{-g}\Big[-\frac{1}{f(\phi^m)}(\sqrt{\text{Det}}-1) - V\Big] + S^{[2]}_{\text{WZ}}. \end{aligned} \tag{3.2.48}$$

Recall from Chapter 1 that we consider the four-dimensional (flat) metric to be the FWR metric, i.e., $\text{diag}(1, -a(t)^2, -a(t)^2, -a(t)^2)$, so that the fields can be taken to be homogeneous $\phi^m = \phi^m(t)$. In this way the field strength on the brane must vanish, $F_{\mu\nu} = 0$. By virtue of this the tensor B^μ_ν defined by Eq. (3.2.37) vanishes (since $b_{mn}\dot{\phi}^m\dot{\phi}^n = 0$ by antisymmetry of b_{mn}) and that the only nonzero component of the matrix $\mathbf{S}$ is S^0_0. Hence there are only two nonzero terms in the determinant Det of Eq. (3.2.34) and they are the first two terms of Det_S. Since all terms involving $F_{\mu\nu}$, $\hat{C}_2 \wedge \hat{B}_2$ and $\hat{B}_2 \wedge \hat{B}_2$ vanish $S^{[2]}_{\text{WZ}}$ vanishes on the background. Also, note from Chapter 2 that in our supergravity set up, the dilaton (together with the axion and the complex structure moduli) is stabilized by the fluxes and therefore we identify G_{mn} with $g^{(0)}_{mn}$ since the argument in the exponential appearing in the middle term of (3.2.31) is fixed. In summary, the four-dimensional effective action for the brane takes the explicit form

$$S_{\text{brane}} = -\int d^4x\sqrt{-g}\big[f(\phi)^{-1}\left(\gamma^{-1}_{\text{DBI}} - 1\right) + V(\phi^m)\big], \tag{3.2.49}$$

$$\gamma^{-1}_{\text{DBI}} = \sqrt{1 + f(\phi)g^{(0)}_{mn}g^{\mu\nu}\partial_\mu\phi^m\partial_\nu\phi^n}. \tag{3.2.50}$$

Here γ_{DBI} is a generalization of the usual relativistic Lorentz factor to the warped background. The variation of this action with respect to the metric gives the energy-momentum tensor. This has the form of a perfect fluid, with energy density and pressure:

$$E = \frac{1}{f}[\gamma_{\text{DBI}} - q] + V, \qquad P = \frac{1}{f}[q - \gamma^{-1}_{\text{DBI}}] - V \tag{3.2.51}$$

By varying the action we obtain the $(n+1)$-equations of motion for the scale factor $a(t)$, and the scalar fields ϕ^n, in the form [71] (see Appendix C)

$$\frac{\ddot{a}}{a} = -\frac{1}{6M_{pl}^2 g_s}(E+3P), \tag{3.2.52}$$

$$\frac{1}{a^3}\frac{d}{dt}[a^3 \tilde{g}_{mn}\gamma\dot{\phi}^n] = \left[\frac{\gamma\partial_m f}{2f^2}(\gamma^{-1}-q)^2 + \frac{\gamma}{2}\frac{\partial\tilde{g}_{mn}}{\partial\phi^m}\dot{\phi}^m\dot{\phi}^n - \partial_m V\right]. \tag{3.2.53}$$

These equations come with the Friedmann constraint

$$H^2 = \frac{1}{3g_s M_{Pl}^2}E, \tag{3.2.54}$$

and the equation of conservation of energy

$$\dot{E} + 3H(E+P) = 0. \tag{3.2.55}$$

3.3 The field range bound

Before analysing the D3-brane equations of motion, we discuss an important microscopic bound on the field range of the inflationary D3-brane inside the throat[2].

A crucial consistency requirement is that the inflationary region should fit well inside the throat, where the metric is known. The length of the throat is measured by $\Delta r = r_{\rm IR} - r_{\rm UV}$, and the location of the inflationary D3-brane inside the throat is given by the canonical inflaton field, $\phi = \sqrt{T_3}r$. Accordingly, there is an upper limit on the inflaton variation [89]

$$\Delta\phi^2 < T_3 r_{\rm UV}^2. \tag{3.3.56}$$

This may give the indication that the inflaton variation can be made arbitrary large by just increasing the length of the throat. But this changes the volume of the compact space, which affects the four-dimensional Planck-mass, the unit in which the inflaton variation should be measured. In order to take this effect into account, one notes that the effective four-dimensional Planck mass is obtained from a reduction of the ten-dimensional supergravity action

[2]The bound also applies to the field range of wrapped D7-branes involved moduli stabilization, which we will consider in our inflationary analysis in Chapter 5.

$$\frac{1}{\kappa_{10}^2}\int d^{10}X R_{10} \;=\; \frac{1}{\kappa_{10}^2}\int d^4x d^6y\sqrt{\det g_{\mu\nu}}y\sqrt{\det g_{mn}}e^{2A}\{e^{2A}R(g_{\mu\nu})+\cdots\}. \tag{3.3.57}$$

Thus the Planck scale is given by

$$M_{Pl}^2=\frac{V_6}{\kappa_{10}^2}. \tag{3.3.58}$$

Here the (warped) volume of the internal space is given by:

$$V_6\equiv\int d^6y\sqrt{g}e^{2A(y)} \tag{3.3.59}$$

Because one is interested in the upper limit on $\Delta\phi/M_{Pl}$ one bounds V_6 from below by the volume of the throat region (including an estimate of the bulk volume would only strengthen the conclusions) [89]

$$V_6>(V_6)_{\rm throat}={\rm Vol}(X_5)\int_0^{r_{\rm UV}}dr\,r^5e^{2A(y)}=2\pi^4g_sN(\alpha')^2r_{\rm UV}^2, \tag{3.3.60}$$

where $N\equiv MK$ denotes the flux. For the supergravity approximation to be valid, one requires $N\gg 1$. The combination of the above results yields [89]

$$\frac{\Delta\phi}{M_{Pl}}<\frac{2}{\sqrt{N}}. \tag{3.3.61}$$

The requirement $N\gg 1$ implies the inflaton variation to be sub-Planckian, $\Delta\phi\ll 1$, and this puts a strong constraint on inflation.

3.4 Spinflation

We now consider the D3-brane equations of motion (3.2.52) - (3.2.53) for the case in which the brane is allowed to have radial as well as spiral motion in the throat [71]. The conserved angular momentum in brane motion turns out to slow down the radial speed and to increase the amount of acceleration. In order to demonstrate this, we derive the relating brane equations of motion and discuss their numerical solutions.

3.4.1 Equations of motion

To derive the explicit form of the brane equations of motion in an ISD compactification recall from the previous chapter that for an ISD compactification we have:

$$\Delta_{(0)}\Phi_- = 0 \quad \text{with} \quad \Phi_- = 0. \tag{3.4.62}$$

Thus for the potential of a mobile D3-brane moving on this unperturbed ISD background the only possible correction comes from a mass term generated for the canonical inflaton

$$\phi = \sqrt{T_3}r. \tag{3.4.63}$$

The simplest and most generic inflaton potential associated with a mass term generated for the canonical inflation (3.4.63) takes the form [71]:

$$V(\phi) = m^2\phi^2 = m^2 T_3 r^2. \tag{3.4.64}$$

Hence the equations of motion following form Eq. (3.2.53) read as [71]:

$$\frac{1}{a^3}\frac{d}{dt}\left[a^3\dot{\phi}\gamma_{\rm DBI}\right] = \gamma_{\rm DBI}(\gamma_{\rm DBI}^{-1}-1)\frac{\partial_\phi f}{2f^2} + \frac{\gamma_{\rm DBI}}{2}\partial_\phi g_{\alpha\beta}\dot{\theta}^\alpha\dot{\theta}^\beta - \partial_\phi V, \tag{3.4.65}$$

$$\frac{1}{a^3}\frac{d}{dt}\left[a^3 g_{\alpha\beta}\dot{\theta}^\beta\gamma_{\rm DBI}\right] = 0. \tag{3.4.66}$$

Here we note that $\gamma_{\rm DBI}$ is given by

$$\gamma_{\rm DBI} = \frac{1}{\sqrt{1 - f(\dot{\phi}^2 + g_{\alpha\beta}\dot{\theta}^\alpha\dot{\theta}^\beta)}}. \tag{3.4.67}$$

By inserting this into Eq. (3.4.65) and Eq. (3.4.66) we can disentangle $\ddot{\phi}$ and $\ddot{\theta}$ upon cross elimination and obtain the second order brane equations of motion. However, instead of doing this we note that Eq. (3.4.65) and Eq. (3.4.66) describe brane motion with conserved angular momentum and therefore we may define the quantity in the square brackets in Eq. (3.4.66) as the conserved angular momentum, i.e., $l_\alpha \equiv a^3 g_{\alpha\beta}\dot{\theta}^\beta\gamma_{\rm DBI}$. It is straightforward to show that [71]

$$\gamma = \sqrt{\frac{1 + f\, l^2(\phi)/a^6}{1 - f\, \dot{\phi}^2}} \qquad \text{with} \qquad l^2(\phi) = T_3 g^{\alpha\beta} l_\alpha l_\beta. \tag{3.4.68}$$

First, note that the DBI action puts a bound on radial velocity, forcing $1 - f\, v^2 > 0$. This translates into the requirement $f\, \dot{\phi}^2 < 1$, independent of the value of the angular momentum l [71]. Second, by using Eq. (3.4.68) and Eq. (3.2.51) we can write down the alternative first order form of the Eq. (3.2.52) - (3.2.53) in the warped deformed conifold. To do this, first note that for an S^3 round on the deformed conifold we have:

$$\begin{aligned} ds^2 &= \mathcal{A}(\eta) d\eta^2 + \mathcal{B}(\eta) d\theta^2, && (3.4.69)\\ \mathcal{A}(\eta) &= \frac{\epsilon^{4/3}}{6K(\eta)^2}, && (3.4.70)\\ \mathcal{B}(\eta) &= \frac{\epsilon^{4/3} K(\eta)}{4}\big(\cosh^2\eta + \sinh^2\eta\big). && (3.4.71) \end{aligned}$$

We also note that for the canonical inflaton we have:

$$\phi = \epsilon^{2/3}\sqrt{\frac{T_3}{6}} \int_0^\eta \frac{dx}{K(x)}, \qquad \dot{\phi} = \sqrt{T_3 \mathcal{A}(\eta)}\dot{\eta}. \tag{3.4.72}$$

According to this, the alternative first order form of the Eqs. (3.2.52) - (3.2.53) in the warped deformed conifold read as [71]:

$$\begin{aligned} \dot{a} &= Ha, && (3.4.73)\\ \dot{\eta} &= \sqrt{\left[1 - \left(1 + \frac{(2\pi)^3 h(\eta) l(\phi)^2}{a^6}\right)\right] \cdot (\mathcal{A}(\eta) h(\eta))^{-1}} && (3.4.74)\\ &\quad \times \left(1 + h(\eta)\left(\frac{H^2}{\beta} - V(\eta)\right)\right)^{-1}, && (3.4.75)\\ \dot{H} &= -\frac{3\beta}{2}\left[2\left(\frac{H^2}{\beta} - V(\eta)\right) + h(\eta)\left(\frac{H^2}{\beta} - V(\eta)\right)^2\right] \\ &\quad \times \left(1 + h(\eta)\left(\frac{H^2}{\beta} - V(\eta)\right)\right)^{-1}. && (3.4.76) \end{aligned}$$

From equation (3.4.74) we can immediately see that angular momentum decreases the speed and this increases the degree of exponential expansion. To see this, we may rewrite Eq. (3.4.76) as [71]:

$$|\dot{H}| = \frac{3\beta}{2}\left[1+h(\eta)\left(\frac{3H^2}{\beta}-V\right)\right] \times\left\{\dot{\eta}^2+\frac{(2\pi)^3 l(\phi)^2}{a^6}\left[1+h(\eta)\left(\frac{3H^2}{\beta}-V\right)\right]^{-2}\right\}. \quad (3.4.77)$$

It is clear that the decrease in speed due to angular momentum decreases the value of the first term inside {...} [71]. We can also see this from Eq. (1.2.32), according to which the exponential expansion increases as the speed decreases (by angular momentum). Equivalently, we can see from (1.2.33) that when the speed decreases the number of e-foldings increases. In the limit of vanishing speed the amount of inflation is effectively reduced by the angular momentum. This is called *spinflation* [71].

So far we analysed brane motion with conserved angular momentum qualitatively. In order to have a quantitative analysis, we need to look at numerical solutions of the brane equations of motion, which we turn to discuss now.

3.4.2 Numerical analysis

In order to integrate the D3-brane equations of motion, one needs to consider a consistent choice of parameters. In the previous section we saw that the Planck-mass (3.3.58) depends of the warped volume of the throat given by (3.3.59). For the warp deformed conifold with $\eta_{\rm UV} \sim \mathcal{O}(1-10)$, we have [71]:

$$V_6 \simeq \frac{\epsilon^4\pi^3}{3}(g_s M\alpha')^2\eta_{\rm UV}^3. \quad (3.4.78)$$

For the supergravity approximation to be valid, g_sM has to be large, i.e., $g_sM \gg 1$. Thus the Planck-mass attains a large value. However, the Planck-mass cannot be too large because otherwise it reduces the gravitational coupling, β, which strongly decreases the inflationary effect. Thus in order to have control over the volume of the throat, on which the Planck-mass and hence the gravitational coupling depends, ϵ has to be small. One reasonable choice of parameters considered in [71] is:

$$\epsilon = 0.05, \quad g_s = 0.1, \quad g_S M = 300, \quad M_{\rm pl} = 100, \quad \eta_{\rm UV} = 15, \quad l_\theta = 5.8 \times 10^6. \tag{3.4.79}$$

The brane equations are integrated for the choice of parameters in (3.4.79), and the numerical solutions are displayed in Fig. 3.1 - 3.2 [71]. The solution describes brane motion from the UV end (where the throat is attached to the compact Calabi-Yau space) to the IR region (where the throat smoothly closes off), where the brane probes the supergravity background. As the brane falls down the the throat from the UV it accelerates, and reaches the bottom of the throat in the IR location with nonzero velocity and continues its motion smoothly back up the throat until it reaches a turning point, where it is pulled down again due to the attractive potential. The scale factor stops accelerating before the brane reaches the tip of the throat and inflation ends naturally as a result of a geometric constraint – the (KS) warp factor approaches a constant value at the IR location. The bouncing motion of the brane continues, with the brane oscillating for a few more cycles, causing the universe to expand and accelerate briefly near the turning points. The inflationary solution has two main features, which are summarised as follows.

• When the angular momentum is switched on, it provides the brane with an extra kick of acceleration (spinflation). This increases the number of e-foldings compared to the case with no angular dependence, though the dominant number of e-foldings is due to radial motion (see Fig. 3.1).

• In order to have enough inflation, $g_s M$ has to be large, in agreement with the supergravity approximation. This causes a problem. In such strongly warped throats the relativistic $\gamma_{\rm DBI}$-factor is unacceptably huge (see Fig. 3.2) and this amounts a very large nongaussianity. It could be the case that certain corrections to the inflaton action may evade this problem, but we defer the further analysis of this to the following up chapters.

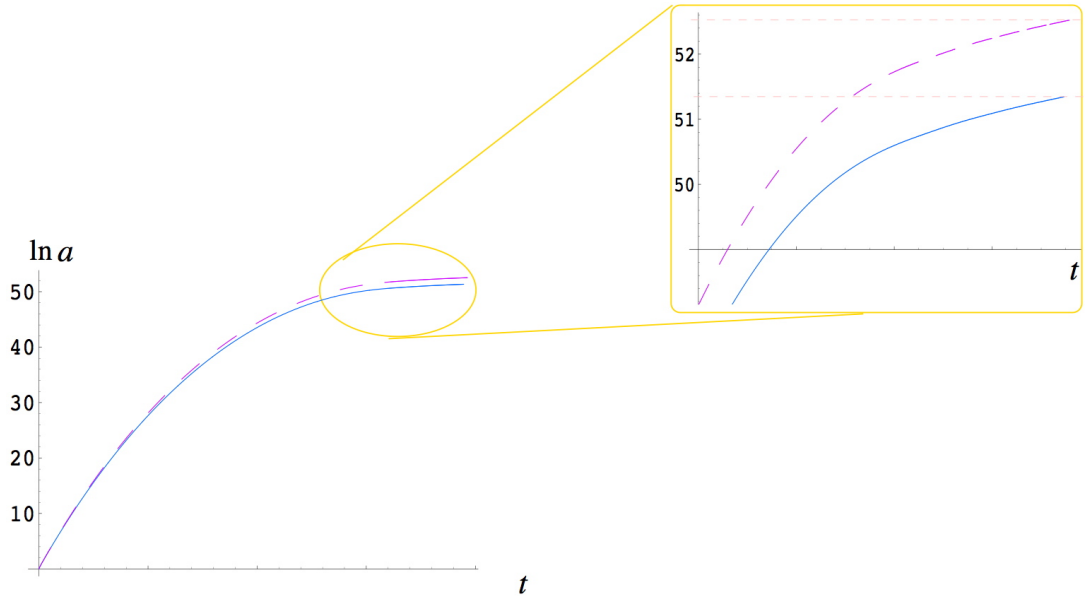

Figure 3.1: The behavior of the scale factor with (light purple) and without (blue) angular momentum l_θ. This figure is from [71].

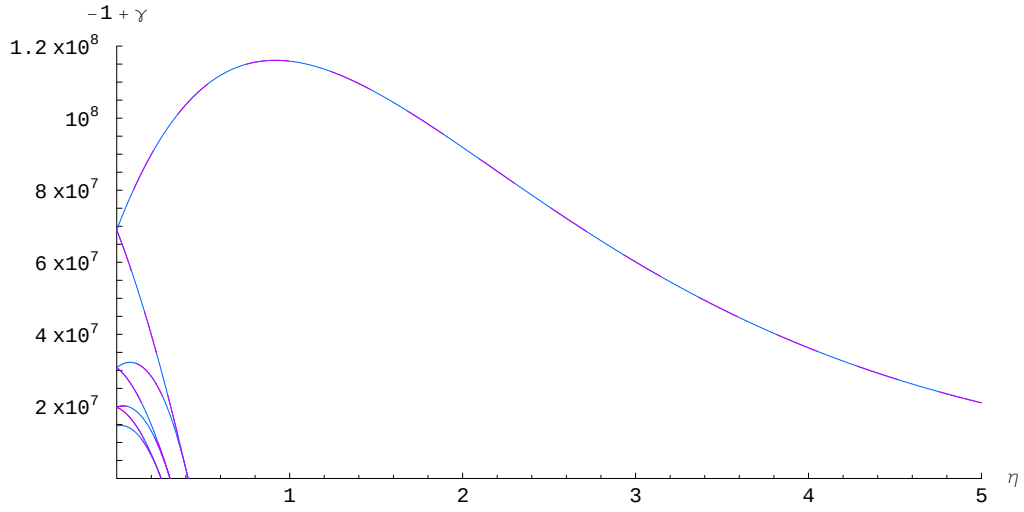

Figure 3.2: The behaviour of the gamma-factor. This figure is from [71].

Chapter 4

Spinflation with angular potentials

In this chapter based on [1] we extend the brane inflation scenario reviewed in the previous chapter. At the end of the previous chapter we reviewed an interesting example of a multifield DBI brane inflationary scenario in the KS background and saw that a handful of extra e-foldings can be produced provided that the D3-brane is allowed to move along the radial as well as angular directions. Although the dominant number of e-folding were produced by the radial motion of the brane, we saw that the effect of angular motion could increase the total number of e-foldings. However, the example that we considered (Spinflation) did not include the effects of moduli stabilization corresponding to perturbations around the ISD supergravity solution. In this chapter we study Spinflation including linearized preturbations around the ISD solution, which induce angular dependence in brane motion. As we shall see, as angular motion typically increases the number of e-foldings (Spinflation), having additional angular dependence also increases the number of e-foldings.

4.1 Brane inflation with an angular potential

The premise of brane inflation is that a D3-brane, extended in the non-compact dimensions, can move around on the internal manifold in such a way that the 'scalar' field y^m, representing the location of the brane on the internal manifold, plays the role of the inflaton. For a mobile D3-brane moving on a supergravity background, the effective action is given by combining the DBI effective action for the world-

brane coordinates, and the Wess-Zumino coupling to the RR-background. Choosing a gauge which aligns with the coordinate system ($X^a_{D3} = (x^\mu, y^m(x^\mu))$, gives the explicit form (See Chapter 3):

$$\begin{aligned} S_{DBI} + S_{WZ} &= -T_3 \int d^4\xi \, \sqrt{-\det(\gamma_{ab} + \mathcal{F}_{ab})} + T_3 \int_{\mathcal{W}} C_4 \,, \\ &= -T_3 \int d^4x \sqrt{-g} \left[e^{4A} \sqrt{\det(\delta^\mu_\nu - e^{-4A} y^{m,\mu} y^n_{,\nu} \tilde{g}_{mn})} - \alpha \right] \,, \end{aligned} \tag{4.1.1}$$

where $T_3 = 1/(2\pi)^3 g_s \alpha'^2$ is the D3-brane tension. The energy momentum from this action,

$$T_{\mu\nu} = T_3 \left\{ e^{4A} \sqrt{\det(\delta^\mu_\nu - e^{-4A} y^{m,\mu} y^n_{,\nu} \tilde{g}_{mn})} \left(g_{\mu\nu} - e^{-4A} y^m_{,\mu} y^n_{,\nu} \tilde{g}_{mn} \right) - \alpha g_{\mu\nu} \right\} \tag{4.1.2}$$

can then drive gravitational physics in the noncompact dimensions. In general, there will also be additional terms coming from corrections to the supergravity background which will appear as effective potential terms for the internal coordinates.

The four-dimensional effective gravitational action can be obtained by integrating out (2.1.23) for the background (2.1.25):

$$S = -\frac{1}{2\kappa_{10}^2} \int d^{10}x \sqrt{g_{10}} \, \mathcal{R} \to -\frac{1}{2\kappa_{10}^2} \left(\int d^6y \, e^{-4A} \sqrt{\tilde{g}} \right) \int d^4x \sqrt{g} R(g) \ , \tag{4.1.3}$$

which gives the 4D Planck mass as

$$M_p^2 = \frac{1}{\kappa_{10}^2} \int e^{-4A} \sqrt{\tilde{g}} \, d^6y \geq \frac{1}{6 g_s^2 \alpha'^4} \left(\frac{\epsilon}{2\pi} \right)^4 \int_0^{\eta_{UV}} e^{-4A} \sinh^2 \eta \, d\eta \ , \tag{4.1.4}$$

and provides a constraint on the parameters of the solution, [89].

For an inflationary solution, we will take the position of the D3 brane to be homogeneous, i.e. $y^m = y^m(t)$, and we will assume a four-dimensional FRW metric:

$$g_{\mu\nu} dx^\mu dx^\nu = dt^2 - a^2(t) d\mathbf{x}^2 \,. \tag{4.1.5}$$

Defining the relativistic $\gamma-$factor as

$$\gamma = 1/\sqrt{1 - e^{-4A} \dot{y}^m \dot{y}^n \tilde{g}_{mn}} \,, \tag{4.1.6}$$

the energy-momentum tensor of the brane is:

$$T^\mu_\nu = T_3 \, \mathrm{diag} \left(e^{4A}\gamma - \alpha, e^{4A}\gamma^{-1} - \alpha, e^{4A}\gamma^{-1} - \alpha, e^{4A}\gamma^{-1} - \alpha \right) \,. \tag{4.1.7}$$

To leading order, $e^{4A}-\alpha = \Phi_- = 0$, but we will allow for leading order corrections of the form (4.1.10) coming from the perturbation of Φ_-. Recall from Chapter 2 that in an ISD compactification such as the warped deformed conifold, only the complex-structure moduli are stabilized but not the Kähler moduli (that characterize the size of the internal Calabi-Yau). When the no-scale structure is broken to stabilize the Kähler moduli, a perturbations around the ISD solution are expected. In supergravity, these perturbations are sourced by attaching the UV end of the throat to a fully stabilised Calabi-Yau sector. Recall that in an ISD solution, we have $G_- = 0$ and $\alpha = e^{4A}$, so that $\Phi_- = 0$. In a perturbed solution, Φ_- is nonvanishing and its value is determined by the solution of the supergravity equation of motion (2.2.125). The dominant source for Φ_- is the IASD flux, G_-, however this flux sources only second order perturbations, and the perturbations of Φ_- around ISD conditions satisfy, at linear level, the six-dimensional Laplace equation with respect to the unperturbed metric (see Section 2.2)

$$\Delta_{(0)}\Phi_- = 0. \tag{4.1.8}$$

The Laplacian on a general warped deformed conifold was computed in [83, 84], although the radial eigenfunctions were not computed explicitly. Fortunately, since we are only interested in the low lying states dependent on only one angle, θ_i , the Laplacian reduces to

$$\frac{1}{\sinh^2\eta}\left[6\frac{\partial}{\partial\eta}K(\eta)^2\sinh^2\eta\frac{\partial}{\partial\eta} + \frac{2}{K(\eta)}\frac{\cosh\eta}{\sin\theta_i}\frac{\partial}{\partial\theta_i}\sin\theta_i\frac{\partial}{\partial\theta_i}\right]\Phi_- = 0, \tag{4.1.9}$$

which for $l = 1$ can be solved analytically to obtain the eigenfunction:

$$\Phi_-(\eta,\theta) \propto (\cosh\eta\sinh\eta - \eta)^{1/3}\cos\theta, \tag{4.1.10}$$

where θ stands for either θ_1 or θ_2 . Since $r \propto e^{\eta/3}$ for large η, it is easy to see that this corresponds to the second eigenfunction, (2.2.131), of the mid-throat region. Note however that there is no clean expression of this eigenfunction in terms of the radial coordinate.

We will thus use this leading order correction to the background near the tip of the throat to investigate the effect of angular perturbations on the brane motion in inflation. In addition, we expect other corrections to the D3 brane potential, in particular, a mass term for the canonically normalised radial scalar inflaton, given to leading order by

$$\phi = \sqrt{T_3}\, r(\eta)\,. \tag{4.1.11}$$

Note that the normalisation is strictly dependent on the position of the brane, which affects the volume modulus (see e.g. [52–57], and also on the trajectory of the brane, even in the slow roll approximation, due to the inflaton, $\phi \leftrightarrow y^m$, being a sigma model field, [90–92]. Putting these together, we can write the overall potential for the D3 brane as:

$$T_3 V = T_3\Phi_- + \frac{1}{2}m_0^2\phi^2 = T_3\left(\frac{1}{2}m_0^2\left[r(\eta)^2 + c_2 K(\eta)\sinh\eta\cos\vartheta\right] + V_0\right)\,, \tag{4.1.12}$$

where the constant V_0 is chosen so that the global minimum of V is $V = 0$, and c_2 is an arbitrary constant. Because c_2 multiplies a solution to a free Laplace equation, it is not fixed per se, but to keep within a self-consistent expansion, one would expect c_2 to be smaller, or of a similar magnitude to other terms in the potential. Indeed, it is natural for the profile of the throat to set the scale for any corrections to the potential, which would mean that c_2 would be set by the deformation parameter: $c_2 \sim \epsilon^{4/3}$. Thus the energy and pressure of the brane are

$$E = T_3\left(e^{4A}\left[\gamma - 1\right] + V\right), \tag{4.1.13}$$

$$P = T_3\left(e^{4A}\left[1 - \gamma^{-1}\right] - V\right). \tag{4.1.14}$$

The full equations of motion (in terms of the coordinates) are:

$$H^2 = \frac{E}{3M_p^2}, \tag{4.1.15}$$

$$\dot{H} = -\frac{(E+P)}{2\,M_p^2}, \tag{4.1.16}$$

$$\frac{1}{a^3}\frac{d}{dt}\left[a^3\gamma\,\tilde{g}_{mn}\,\dot{y}^n\right] = -2\gamma\,\left(\gamma^{-1}-1\right)^2\,e^{4A}\,\partial_m A + \frac{\gamma}{2}\,\frac{\partial\tilde{g}_{ln}}{\partial y^m}\,\dot{y}^l\dot{y}^n - \partial_m V. \tag{4.1.17}$$

The first step is to disentangle the radial and angular equations from (4.1.17), by a process of cross elimination. For simplicity, we will consider motion in a single angular direction only, writing the relevant part of the internal metric in the general form

$$ds^2 = \epsilon^{4/3}\left[\frac{d\eta^2}{6K(\eta)^2}, +B(\eta)d\vartheta^2\right]. \tag{4.1.18}$$

This gives the η and ϑ equations as (see Appendix C):

$$\begin{aligned}\ddot{\eta} &= -\frac{3H}{\gamma^2}\dot{\eta} - 4A'(\gamma^{-1}-1)\dot{\eta}^2 - 12\epsilon^{-4/3}K^2A'e^{4A}(\gamma^{-1}-1)^2 \\ &\quad + \frac{K'}{K}\dot{\eta}^2 + 3K^2B'\dot{\vartheta}^2 + e^{-4A}\dot{\vartheta}\dot{\eta}\frac{V_\vartheta}{\gamma} - (6K^2\epsilon^{-4/3} - e^{-4A}\dot{\eta}^2)\frac{V_\eta}{\gamma}, \qquad (4.1.19)\\ \ddot{\vartheta} &= -\frac{3H}{\gamma^2}\dot{\vartheta} - 4A'(\gamma^{-1}-1)\dot{\eta}\dot{\vartheta} - \frac{B'}{B}\dot{\eta}\dot{\vartheta} + e^{-4A}\dot{\eta}\dot{\vartheta}\frac{V_\eta}{\gamma} - \left(\frac{\epsilon^{-4/3}}{B} - e^{-4A}\dot{\vartheta}^2\right)\frac{V_\vartheta}{\gamma}. \qquad (4.1.20)\end{aligned}$$

These can then be solved numerically, along with the cosmological evolution, for the relevant potential. Generally, potentials can have complicated angular dependence, but we confine ourselves here to the most simple case including only the lowest nontrivial eigenmode with one angular direction. This should be sufficient for estimating the inflationary implications of brane angular dependence.

4.2 Inflationary analysis

In order to explore the effect of angular terms in the potential, we use the leading order potential (4.1.12). Because we are neither slow-rolling, nor restricting ourselves to a specific conical region, we have to keep the full richness of the structure of the internal space and the nonlinear kinetic terms of the brane motion. Although the canonical inflaton field, ϕ, is conventionally used in expositions of slow roll inflation, it proves more useful here to remain with the coordinate label, η, as many of the metric functions have analytic forms in terms of η. We focus on motion which takes place in the angular direction, ϑ, appearing in this potential, thus from (2.1.66), (2.1.67) and (2.1.68) we can read off the function $B = \frac{1}{2}K\cosh\eta$, that appears in the ϑ equation of motion, (4.1.20).

Before presenting the results of the numerical analysis, a few remarks about the various parameters are in order. First of all, the supergravity approximation

is only valid if the curvature radius remains large compared to the string scale, which clearly requires the flux $g_s M \gg 1$. Secondly, as noted by Baumann and McAllister (see Section 3.2), [89], the Planck mass is constrained by the volume of the compactification, which in turn is bounded from the UV cut-off of the throat. Rewriting (4.1.4) shows that

$$M_p^2 > \frac{\epsilon^{4/3} g_s M^2 T_3}{6\pi} J(\eta_{UV}) \tag{4.2.21}$$

where $J(\eta) = \int I(\eta) \sinh^2 \eta$ is the integral in (4.1.4), which is exponentially growing in η - see Fig. 4.1.

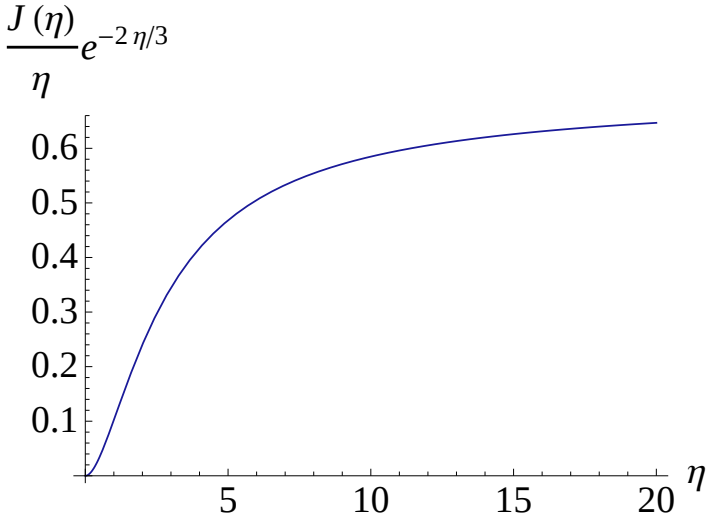

Figure 4.1: Planck mass constraint: The numerical integral of $I(\eta) \sinh^2 \eta$ with the large η behaviour factored out.

Apart from $J_{UV} = J(\eta_{UV})$, the other parameters in this relation are set by the compactification data: $g_s M^2$ is large, ϵ is generally 'small', and T_3 is determined by the string coupling. The hierarchy between the string scale and the Planck scale is therefore strongly dependent on the UV cutoff as J_{UV} grows very quickly with η_{UV}. Generally, as the Planck mass rises, the effective scale of inflation is lowered, and thus the amount of inflation will drop unless the parameter choices allow it to persist for a correspondingly increased time (see the discussion after (4.2.27)). In these models, as in slow-roll inflation, [89], this bound on the Planck mass proves to be a strong constraint.

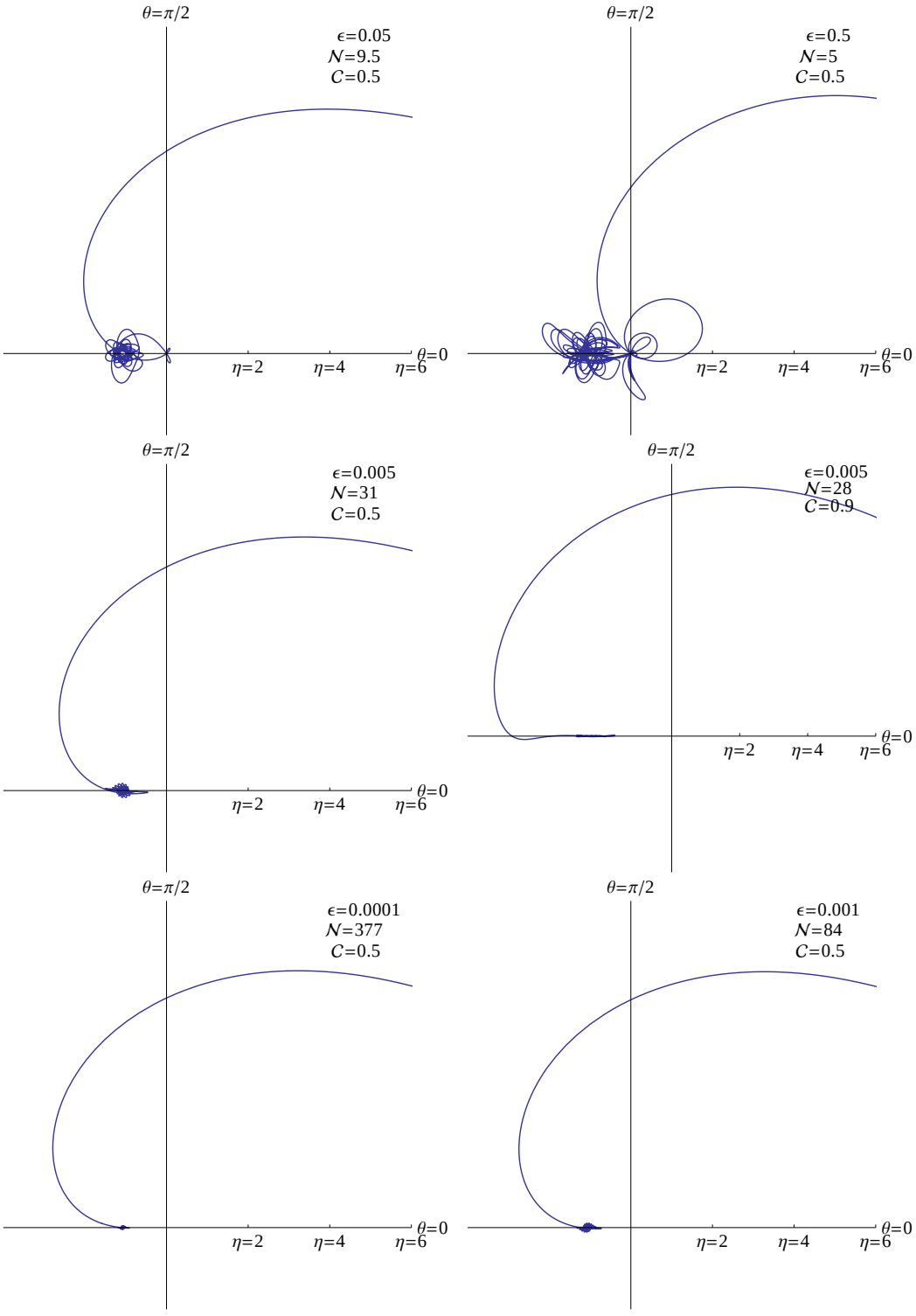

Figure 4.2: Some sample inflationary trajectories with a flux parameter of $g_s M = 100$, inflaton mass $m_0 = 20$, and a saturated Planck mass from $\eta_{\rm UV} = 10$. The values of ϵ and $\mathcal{C} = c_2 \epsilon^{-4/3}$, are indicated.

To solve the full cosmological and brane equations, a numerical analysis is required. In order to deal with the dependence of the system on large (or small) parameters, we can rescale the equations of motion by setting $\tau = \epsilon^{2/3}t/(g_sM\alpha')$, and rewriting the metric functions as:

$$\hat{h} = \frac{\epsilon^{8/3}}{(g_sM\alpha')^2}e^{-4A} \quad , \qquad \hat{V} = \epsilon^{-4/3}V, \tag{4.2.22}$$

so that $\hat{h}$ and $\hat{V}$ now have no explicit ϵ or M dependence. Note also that

$$\gamma^{-2} = 1 - \hat{h}\left[\frac{\dot{\eta}^2}{6K^2} + B\dot{\vartheta}^2\right], \tag{4.2.23}$$

where a dot now denotes $d/d\tau$, also has no ϵ or M dependence.

Writing $\hat{H} = a^{-1}\frac{da}{d\tau}$, and setting $\alpha' = 1$, the full equations of motion of the system now read:

$$\hat{H}^2 = \frac{T_3}{3M_p^2}\left[(g_sM)^2\hat{V} + \frac{\epsilon^{4/3}}{\hat{h}}(\gamma - 1)\right] \longrightarrow \frac{2\pi g_s}{J_{UV}}\left[\epsilon^{-4/3}\hat{V} + \frac{\gamma - 1}{(g_sM)^2\hat{h}}\right], \tag{4.2.24}$$

$$\dot{\hat{H}} = -\frac{\epsilon^{4/3}T_3}{2M_p^2\hat{h}}(\gamma - \gamma^{-1}) \longrightarrow -\frac{3\pi g_s(\gamma - \gamma^{-1})}{(g_sM)^2J_{UV}\hat{h}}, \tag{4.2.25}$$

$$\begin{aligned}\ddot{\eta} = &-\frac{3\hat{H}}{\gamma^2}\dot{\eta} + \frac{\hat{h}'}{\hat{h}}(\gamma^{-1} - 1)\dot{\eta}^2 + 3K^2\frac{\hat{h}'}{\hat{h}^2}(\gamma^{-1} - 1)^2 \\ &+\frac{K'}{K}\dot{\eta}^2 + 3K^2B'\dot{\vartheta}^2 + \frac{(g_sM)^2}{\epsilon^{4/3}\gamma}\left[\hat{h}\dot{\vartheta}\dot{\eta}\hat{V}_\vartheta - (6K^2 - \hat{h}\dot{\eta}^2)\hat{V}_\eta\right],\end{aligned} \tag{4.2.26}$$

$$\begin{aligned}\ddot{\vartheta} = &-\frac{3\hat{H}}{\gamma^2}\dot{\vartheta} + \frac{(g_sM)^2}{\epsilon^{4/3}\gamma}\left[\hat{h}\dot{\eta}\dot{\vartheta}\hat{V}_\eta - (1 - \hat{h}B\dot{\vartheta}^2)\frac{\hat{V}_\vartheta}{B}\right] \\ &+\left[\frac{\hat{h}'}{\hat{h}}(\gamma^{-1} - 1) - \frac{B'}{B}\right]\dot{\eta}\dot{\vartheta},\end{aligned} \tag{4.2.27}$$

where we have shown the effect of saturating the Planck mass bound in (4.2.24) and (4.2.25). We can now see the impact of the various compactification parameters. The effect of the flux and deformation parameter is to increase the importance of the potential term in the brane motion, however, with the Planck mass bound saturated, during an inflationary period with $\dot{\hat{H}} \ll \hat{H}^2$, the inflationary scale is relatively independent of the flux, but strongly dependent on the deformation parameter, ϵ, as well as the UV cutoff via J_{UV}. Crudely therefore, we can see how increasing m_0 or decreasing ϵ will directly increase the number of e-foldings, whereas increasing the UV cutoff will correspondingly reduce the e-foldings if all other parameters are kept

equal. Varying the parameter M however, would appear to have a subdominant effect, although it will alter the timescale of the motion via the parameter τ.

For our integrations, we chose $\eta_{UV} = 10$, so that the metric functions are showing evidence of both the throat tip deformation, as well as the asymptotic $T^{1,1}$ structure commonly used in the slow-roll models. We also set $2\pi g_s = 1$ for convenience. For the compactification data, we set the Planck mass at its minimum allowed value, as determined by (4.2.21), and varied ϵ, M and m_0, following the motion of the mobile brane with and without the angular term in the potential. For initial conditions, the initial radial brane velocity was taken to vanish, and the angular brane velocity was taken to be highly relativistic. The initial value of the angular coordinate, $\vartheta_0 = \pi/6$ was chosen to maximize the impact of the angular term, when present. For each trajectory, we followed the brane motion until it settled into oscillations around the minimum of the potential, counting the number of e-foldings of the associated cosmology, to see how this varied with the model parameters. Fig. 4.2 shows representative trajectories for the brane as it nears the tip of the throat.

Our findings can be summarized in the following:

• In terms of the trajectory of the mobile brane, one feature that all the brane trajectories share is that, independent of any angular dependence or initial momentum, the brane rapidly becomes highly relativistic, picking up strong angular features near the tip of the throat as inflation per se ends.

• In agreement with the rescaled equations (4.2.24) - (4.2.27), varying the flux parameter slows down the brane, but makes very little difference to the overall number of e-foldings (for the saturated Planck mass). Increasing m_0, and decreasing ϵ, as expected, increases the overall amount of inflation.

• Increasing the angular perturbation (c_2) has the effect of shifting the minimum of the potential, and thus changing the endpoint of the brane motion, but the effect on the inflationary capacity of the trajectory is sub-dominant.

In selecting a range of sample trajectories for Fig. 4.2, we have focussed on varying the parameters ϵ and $\mathcal{C} = c_2\epsilon^{-4/3}$. The equations of motion (4.2.24) - (4.2.27) show that varying the flux parameter slows down the brane in a similar way to decreasing ϵ, thus higher flux trajectories will look similar to smaller deformation

parameter trajectories, but with a lower number of e-foldings. Increasing the inflaton mass however, will increase the amount of inflation, but will not change the trajectory so dramatically. Thus, the main kinematical differences in the trajectories are well illustrated by fixing the flux and inflaton mass, and varying the deformation parameter and angular dependence. All of the sample trajectories in Fig. 4.2 show the brane trajectory for a flux parameter of $g_s M = 100$, an inflaton mass $m_0 = 20$, and a saturated Planck mass.

The first two plots in Fig. 4.2 show brane motion for relatively large values of deformation parameter: $\epsilon = 0.5, 0.05$. These show clearly how the brane moves around quite freely near the tip of the throat, making large oscillations before settling at the minimum of the potential. The brane motion is less relativistic, however the amount of expansion can be seen to be very low ($\mathcal{N} \sim 5$ and 9.5 respectively), and is not a viable inflationary scenario.

The middle pair of plots of Fig. 4.2 are more interesting. These show the effect of changing the angular dependence of the potential, $\mathcal{C} = 0.5, 0.9$. Here, the shift of the minimum of the potential is quite clear. It is perhaps worth emphasizing that although at large η, the solution of the Laplace equation has the same approximate radial dependence as the inflaton mass term ($(\cosh\eta \sinh\eta - \eta)^{1/3} \sim r^2$), at small η, this eigenfunction has quite a different dependence, $(\cosh\eta \sinh\eta - \eta)^{1/3} \propto \eta \propto r$, and in fact dominates over the mass term near the tip. Although from the kinematical perspective increasing angular dependence shifts the trajectories more significantly, the inflationary impact of the angular terms is subdominant, as can be seen by looking at the number of e-foldings which only changes a little. Fig. 4.3 shows this in more detail by plotting the number of e-foldings as a function of time along an inflationary trajectory with $m_0 = 20$, $g_s M = 100$, $\epsilon = 0.001$, comparing the amount of inflation with and without angular dependence in the potential. This clearly shows the subdominance of angular terms, illustrating that the bulk of inflation occurs along the initial, radial, sweep.

Finally, the last two plots of Fig. 4.2 show how for very small deformation parameters the strong warping of the throat provides a very strong 'brake' on the coordinate speeds of the brane, giving a very slow sweep of the brane down the

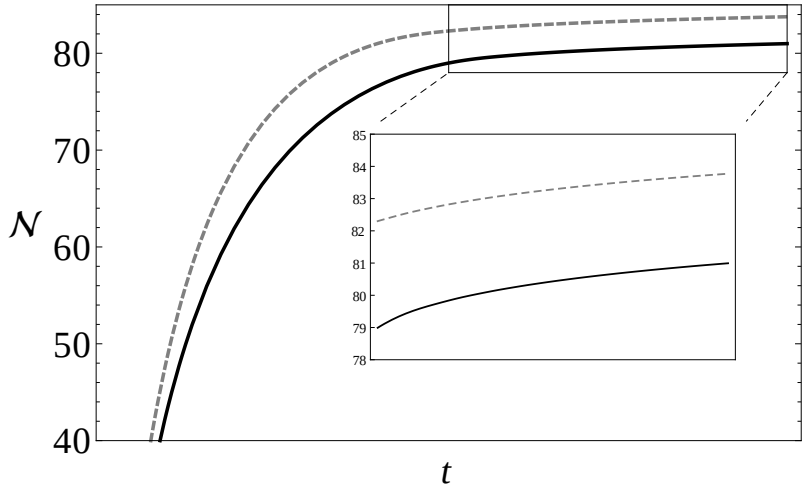

Figure 4.3: The amount of inflation along a trajectory with $m_0 = 20$, $g_s M = 100$, $\epsilon = 0.001$ with (grey dashed, $c_2 = \epsilon^{4/3}/2$) and without (solid black) angular terms in the potential.

throat with a large number of e-foldings.

Although these equations must be solved numerically to extract the actual cosmological impact, an estimate for the number of e-foldings can be approximated analytically, which highlights some of the dependences we have found numerically. Essentially, we use the observation from the numerics that the bulk of cosmological expansion occurs on the first sweep down the throat of the brane. This then allows an approximate Hamilton-Jacobi analysis of the motion in a similar manner to that of the original Silverstein-Tong calculation [62, 63]. Approximating this motion as precisely radial, the number of e-foldings of the universe, $\mathcal{N}$, can be written as

$$\mathcal{N} = \int H dt = \int \frac{H}{\dot{\eta}} d\eta \tag{4.2.28}$$

and we can approximate

$$H^2 \sim \frac{T_3 V}{3M_p^2} \quad , \quad \frac{\epsilon^{4/3} e^{-4A} \dot{\eta}^2}{6K^2} \sim 1 \tag{4.2.29}$$

giving

$$\mathcal{N} \sim \sqrt{\frac{T_3}{3M_p^2}} \int \sqrt{\frac{V}{6}} e^{-2A} \frac{d\eta}{K} \leq \frac{\epsilon^{-2/3} m_0 \sqrt{4\pi g_s}}{6 J_{UV}} \int_{\eta_f}^{\eta_i} \frac{I(\eta) \epsilon^{-2/3} r(\eta)}{6K} d\eta \tag{4.2.30}$$

The ratio of the integral to J_{UV} is explicitly independent of the various parameters, and only depends on η_{UV}.

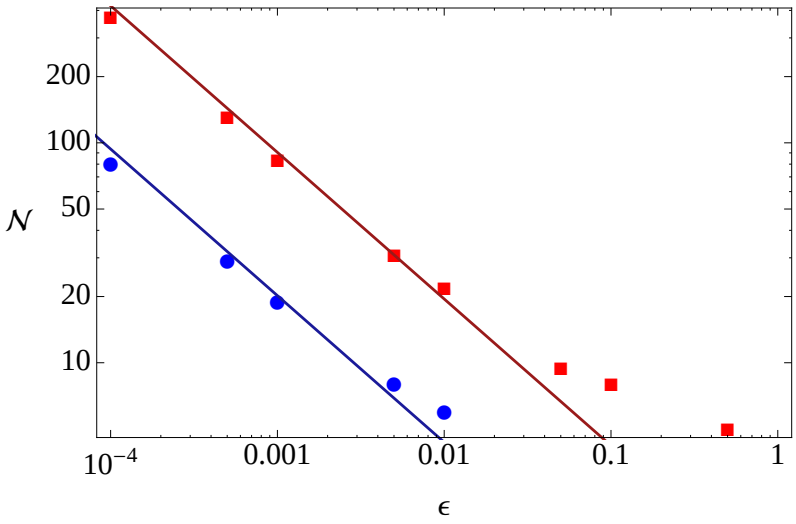

Figure 4.4: The number of e-foldings as a function of the deformation parameter ϵ for $m_0 = 10$ (blue circles) and $m_0 = 20$ (red squares) with $c_2 = \epsilon^{4/3}/2$ and $g_s M = 100$. The analytic dependence is shown for comparison.

This argument is somewhat flawed in that it uses a large γ factor to estimate the coordinate velocity, yet assumes that the γ terms are negligible compared to the potential, nonetheless, it gives a good guide as to the general dependence of the e-foldings from brane motion near the tip, which is reasonably accurate for small ϵ as can be seen by comparing the numerical and analytical results in Fig. 4.4. Thus for small ϵ the numerical and analytical results are in good agreement.

In this plot we see clearly that for $\epsilon \leq 0.01$, the estimate gives a very good approximation to the dependence of $\mathcal{N}$ on ϵ. For strongly deformed throats ($\epsilon \geq 0.1$) the estimate does not work so well, but since these have much more varied angular motion and very few e-foldings, this is not at all surprising. Unlike the small ϵ trajectories, which spend a very long time on the initial radial sweep, exiting inflation very close to the minimum of the potential, these trajectories fall reasonably quickly to the tip, and cosmological expansion takes place equally from the initial sweep as from the following large angular oscillations. Finally, it also explains qualitatively the incremental increase in e-foldings from the angular term. Given a change in $\mathcal{C}$, the percentage increase of e-foldings is given at most by $100(\sqrt{\frac{1+\mathcal{C}_2}{1+\mathcal{C}_1}} - 1)$, which can

be seen to be in the ten percent range provided $\mathcal{C} < 1$.

4.3 Summary and conclusions

In this chapter we studied generic brane motion in a warped deformed throat incorporating full angular dependence of both the brane potential and brane motion. This is the first such study of D3-brane inflation which samples the many features of a warped throat, including both UV and IR features of the geometry, as well as IR consistent supergravity corrections. We considered a generic mass term for the D3 brane potential as well as an analytic linearized perturbation around the ISD background, which to our knowledge is the first closed form analytic radial eigenfunction on the KS background.

Our results show that angular features of the brane motion are dependent on the compactification parameters more than on initial conditions: For strongly deformed throats (relatively large ϵ) the brane 'sees' the full rounded structure of the tip and has a very rich angular motion. These oscillatory trajectories however have very little cosmological expansion. Conversely, for very sharp throats ($\epsilon \ll 1$) the brane enters a strongly DBI inflating motion, which is geometry dominated and mainly radial in nature. The coordinate velocities of the brane are very small, and the brane falls to the minimum of the potential in its first sweep down the throat, only oscillating right at the exit of inflation and at the minimum of the potential. The models and initial conditions considered were deliberately multi dimensional, and the brane samples the full IR region of the throat.

In this analysis, we have deliberately considered a set-up in which there is no obvious slow-roll regime. In particular, using the correct, fully infrared consistent corrections to the potential, we see that an inflection point potential is no longer consistent. Our model explicitly follows brane inflation from the UV to the IR region of the throat, and as such is not particularly suitable for angular inflation at the tip, as the potential deep in the IR is not sufficiently steep. However, the corrections we considered have also been used in a restricted context in an angular tip inflation, [60], although in this case, the full dependence of the eigenfunction on the radial

direction was not considered.

In all cases, these DBI trajectories have large $\gamma_{\rm DBI}$-factors and hence will generically generate large non-gaussianities if used as pure inflation models in their own right [62, 63, 93–96]. In order to construct a viable inflationary model therefore, some alternative mechanism must be found to produce perturbations, or this motion must be part of a bigger inflationary picture in which CMB scale fluctuations have already been produced (see e.g. [60]). This chapter has focussed on seeking a UV/IR consistent inflationary picture, thus we have not explored the full detail of cosmological perturbation theory, however, there are several options which could, in principle be incorporated into this model.

One particularly interesting possibility is that some curvaton mechanism might arise, either from one of the additional angular degrees of freedom, [97–99] or from the vector excitations inherent in this type of model, [100]. In the curvaton picture, [101], a (possibly more natural) option is presented in which additional fields generate perturbations, rather than having the inflaton performing all roles.

Because our angular potential is explicit, it clearly does not depend on several of the other internal angles, which could therefore provide flat directions in the potential. However, since these additional scalar degrees of freedom are part of the multifield sigma model of the throat, the dynamics of perturbation theory is quite involved and only a full analysis would reveal if this is indeed possible. Perhaps a more promising and natural approach which has recently been explored in [100] is that perturbations might be generated via a vector curvaton, although in that case the authors did not explore angular motion or corrections to the supergravity potential. This would be an extremely interesting avenue to explore.

Another interesting observation is that a nonminimal gravitational coupling (depending on the non-radial degrees of freedom) tends to increase the inflationary capacity, while decreasing the $\gamma_{\rm DBI}$-factor, [102]. However, the analysis in [102] was from a more empirical point of view, more reminiscent of a k-inflation model, [103], and it would be interesting to see whether similar results are attainable in an explicit supergravity model arising from higher order corrections to the solution (e.g. coupling to the Ricci scalar) considered in this paper.

It is also possible that since the $\gamma_{\rm DBI}$-factor varies throughout the motion, for some carefully chosen parameters this problem could be circumvented. It is interesting to use the intuition gleaned here to consider the late time evolution of more conventional slow-roll brane models, and explore what might happen as the brane approaches the tip. A slow-roll model such as the delicate universe, [52–57], uses supergravity perturbations which are strictly only allowed in the pure $T^{1,1}$ throat, however, setting this aside for a moment, we can speculate on the final brane downfall to the tip. A vast scanning of parameter space for potentials is not necessary, as the angular motion and dependence is more a quantitative than qualitative factor, and our investigation has given insight into the effect of the different compactification parameters as they vary.

Typically, a slow roll model of brane inflation will be in the intermediate adS regime of the throat geometry, and thus requires a small deformation parameter. However, as the deformation parameter becomes very small, the final roll to the tip can take a long time, and be highly relativistic. The compactification data are generally expressed differently in references [52–57], [64] , in terms of D3 flux, N, the warp hierarchy between the inflating and IR region, $a_0 = e^{A(0)}$, however, knowledge of M_p, T_3 and the UV cut-off scale of the throat, r_{UV}, allows a translation between the different parametrizations. For example, to compare to the study of Agarwal et al., [64], saturating the M_p bound and taking their stated parameter values leads to deformation parameters of $\epsilon \sim 10^{-4} - 10^{-7}$ for $a_0 \sim 10^{-3} - 10^{-5}$. With such small deformation parameters, the final sweep to the throat tip could easily incorporate several to many e-foldings of DBI inflation, and raises the question of just how much impact this final sweep could have.

Finally, our analysis has focussed on motion in only one angular direction. This was primarily to allow clarity of the angular terms in the potential, but also for simplicity. We expect that including fully generic angular motion (which would significantly complicate the analysis) will have an effect subdominant to the subdominant angular motion presented here, however, it would be useful to confirm this, in particular to confirm or rule out the possibility of a curvaton arising in this sector. In addition, our analysis could be further extended by taking higher order

corrections into account, which will also have angular dependence. While we would expect that this would be sub-dominant to the linearized correction, it would be interesting to see precisely what the impact is of these detailed corrections to the inflaton action.

Chapter 5

Spinflation with backreaction

In the previous chapter based on [1], we solved the DBI brane equations of motion in the warped deformed conifold [75] with harmonic dependent corrections from linearized perturbations around the ISD solution. We showed that just as angular motion increases the number of e-foldings (spinflation) [71–74], having additional angular dependence from linearized corrections also increases the number of e-foldings. However, this line of analysis considered D-brane inflation only from linearized perturbations around the ISD supergravity solution. In this chapter based on [2], we extend our analysis of the previous chapter by including further harmonic dependent corrections from non-linear perturbations around the ISD solution, which also contribute to the inflaton action. In the noncompact limit, non-linear perturbations are dominated by imaginary anti-self-dual (IASD) fluxes sourced by moduli stabilizing wrapped D7-branes and the flux induced potential for the probe D3-brane in ten-dimensional supergravity equals the nonperturbatively-generated D3-D7 potential in four-dimensional supergravity [57].

One particular motivation of extending our previous analysis [1] by including such nonperturbative corrections is the possibility of increasing the amount of inflation and decreasing the level of non-Gaussianity due to backreaction effects [56]. The backreaction on the mobile D3-brane is sourced by itself [52]. The D3-brane in a flux compactification containing holomorphically embedded D7-branes corrects the warp factor which in turn corrects the warped volume of four-cycles wrapped by D7-branes. This then corrects the D3-D7 potential causing the backreaction

on the D3-brane. The perturbations of the warp factor are given by the Green's function and correct the $\gamma_{\rm DBI}$-factor which controls the level of non-Gaussianity. The Green's function solves the noncompact supergravity equation of motion describing the perturbations around the ISD solution sourced by IASD fluxes and may be expanded in an infinite set of eigenstates of the Laplacian containing harmonic dependent hypergeometric functions [84].

In this chapter we solve the D3-brane equations of motion from the DBI action in the warped deformed conifold [75] with harmonic dependence from the leading correction terms of the warp factor and the D3-D7 potential. To solve the brane equations of motion, we note that the D3-brane potential including nonperturbative corrections depends on the functional form of the Kähler modulus and that of the D7-brane embedding. For the Kuperstein embedding of D7-branes [105] and a simple choice of an harmonic dependent trajectory on the deformed conifold, we integrate out the Kähler modulus and reduce the multifield D3-brane potential to a simple two-field potential depending on one radial and one harmonic direction of the conical geometry. In our numerical integrations we integrate out the Kähler modulus by computing its exact functional form valid on both the IR and UV regions of the supergravity background. We find that computing the Kähler modulus within the adiabatic approximation in DBI inflation requires certain hierarchies of scales which determine the set of compactification parameters different from those in slow-roll models. Integrating the brane equations of motion for the consistent choice of parameters with the numerically computed Kähler modulus shows that the DBI inflationary solutions are quite robust against non-linear harmonic dependent corrections from perturbations of the warp factor and the D3-D7 brane potential.

5.1 Review of D3/D7-brane inflation

As before, we embed a mobile D3-brane in the supergravity background described in chapter 2 and analyse its four-dimensional effective action. Recall that in the supergravity background with metric ansatz (2.1.25) the effective action takes the form

$$
\begin{aligned}
I &= \frac{M_{Pl}}{2}\int d^4x\sqrt{-g}\mathcal{R} - g_s^{-1}\int d^4x\sqrt{-g}\Big[h^{-1}(\gamma_{\rm DBI}^{-1}-1)+V(\phi^m)\Big], \qquad (5.1.1)\\
\gamma_{\rm DBI}^{-1} &= \sqrt{1-hg^{(0)}_{mn}g^{\mu\nu}\partial_\mu\phi^m\partial_\nu\phi^n}.
\end{aligned}
$$

Here g_s is the string coupling, and $M_{\rm pl}$ is the Planck-mass, as before.

To study brane inflation, we will take the position of the D3-brane to be homogeneous, $\phi^m = \phi^m(t)$, and we will consider the four-dimensional metric to be the standard unperturbed FRW metric:

$$
ds_4^2 = g_{\mu\nu}dx^\mu dx^\nu = dt^2 - a^2(t)d\mathbf{x}^2 \qquad (5.1.2)
$$

with $a(t)$ being the scale factor, as before. Also recall that the variation of the latter part of the action (5.1.1) with respect to the metric produces the energy-momentum tensor, which has the form of a perfect fluid with its energy density and pressure given by:

$$
\begin{aligned}
E &= T_3(h^{-1}[\gamma_{\rm DBI}-1]+V], \qquad (5.1.3)\\
P &= T_3(h^{-1}[1-\gamma_{\rm DBI}^{-1}]+V]. \qquad (5.1.4)
\end{aligned}
$$

Here $T_3 = ((2\pi)^3\alpha'^2)^{-1}$ is the D3-brane tension, as before. The full equations of motion are:

$$
\begin{aligned}
H^2 &= \frac{E}{3M_{\rm pl}^2}, \qquad (5.1.5)\\
\dot{H} &= -\frac{(E+P)}{2\,M_{\rm pl}^2}, \qquad (5.1.6)\\
\frac{1}{a^3}\frac{d}{dt}\left[a^3\gamma_{\rm DBI}\,g^{(0)}_{mn}\,\dot{\phi}^n\right] &= -T_3\gamma_{\rm DBI}\,\left(\gamma_{\rm DBI}^{-1}-1\right)^2\,\frac{\partial_m h}{2h^2} + \frac{\gamma_{\rm DBI}}{2}\,\frac{\partial g^{(0)}_{ln}}{\partial\phi^m}\,\dot{\phi}^l\dot{\phi}^n - \partial_m V, \qquad (5.1.7)
\end{aligned}
$$

where $g^{(0)}_{mn}$ is the unperturbed Calabi-Yau metric, as before. Recall from the previous chapter that the Planck-mass, $M_{\rm pl}$, appearing above is bounded by the UV-scale as [1]:

$$M_{\rm pl}^2 > \frac{\epsilon^{4/3} g_s M^2 T_3}{6\pi} J(\eta_{\rm UV}), \tag{5.1.8}$$

where $J(\eta) = \int I(\eta) \sinh^2 \eta$ with $I(\eta)$ given by (2.1.97).

The D3-brane potential appearing in the above equations of motion is:

$$T_3 V = \frac{1}{2} m^2 \phi^2 + T_3 \Phi_-. \tag{5.1.9}$$

Here the first term is a mass term generated for the canonical inflaton $\phi = \sqrt{T_3} r(\eta)$, which by (5.1.10) takes the form:

$$\phi = \epsilon^{2/3} \sqrt{\frac{T_3}{6}} \int_0^\eta \frac{dx}{K(x)}. \tag{5.1.10}$$

We note that the normalization is strictly dependent on the position of the brane, which affects the volume modulus (see e.g. [52–57]), and also on the trajectory of the brane, even in the slow roll approximation, due to the inflaton, ϕ, being a sigma model field, [92–94]. The last term in (5.1.9) arises from perturbations around the noncompact (ISD) supergravity solution described by Eq. (2.2.132). The homogeneous linearized solution of Eq. (2.2.132) is given by (4.1.10). The inhomogeneous non-linear solution of Eq. (2.2.132) given in its implicit form as (2.2.137) equals the nonperturbatively generated D3-brane F-term potential in four-dimensional supergravity [57]. The F-term potential takes the following form:

$$V_F = e^{\kappa^2 \mathcal{K}} \left[D_\Sigma W \mathcal{K}^{\Sigma\bar{\Xi}} \overline{D_\Xi W} - 3\kappa^2 W \overline{W} \right], \tag{5.1.11}$$

where $\{z^\Sigma\} \equiv \{\rho, z_\alpha; \alpha = 1, 2, 3\}$ and $D_\Sigma W = \partial_\Sigma W + \kappa^2 (\partial_\Sigma \mathcal{K}) W$ with $\mathcal{K}$ and W denoting the Kähler potential and superpotential, and $\kappa^2 = M_{\rm pl}^{-2}$ with $M_{\rm pl}^2$ bounded by (5.1.8). From (5.1.8) one can see that large $\eta_{\rm UV}$ implies large $M_{\rm pl}$. In the noncompact limit ($M_{\rm pl} \to \infty$), the F-term potential (5.1.11) takes the form

$$V_F = \mathcal{K}^{\Sigma\bar{\Xi}} \partial_\Sigma W \overline{\partial_\Xi W}. \tag{5.1.12}$$

For any holomorphic function W on the conical geometry, we may turn on the flux (see Appendix A)

$$\Lambda_{\Sigma\bar{\Xi}\bar{\Gamma}} = \partial_\Sigma \partial_\Upsilon W \mathcal{K}^{\Upsilon\bar{\Theta}} \bar{\Omega}_{\bar{\Theta}\bar{\Xi}\bar{\Gamma}} = \partial\partial W \cdot \bar{\Omega}, \tag{5.1.13}$$

where Ω is the holomorphic $(3,0)$-form. Solving Eq. (2.2.132) for Eq. (5.1.13) gives [57]

$$T_3 \Phi_- = \mathcal{K}^{\Sigma\bar{\Xi}} \partial_\Sigma W \overline{\partial_\Xi W}. \tag{5.1.14}$$

The Kähler potential, $\mathcal{K}$, depends on the complex Kähler modulus $\rho = \sigma + i\chi$, and on the D3-brane position, $\{z_\alpha, \bar{z}_\alpha\}$, [104]

$$\mathcal{K}(z^\alpha, \bar{z}^\alpha, \rho, \bar{\rho}) = -3\kappa^{-2} \log[\rho + \bar{\rho} - \gamma k(z^\alpha, \bar{z}^\alpha)] \equiv -3\kappa^{-2} \log U(z, \rho). \tag{5.1.15}$$

Here $k(z^\alpha, \bar{z}^\alpha)$ is the so-called 'little' Kähler potential of the Calabi-Yau manifold, $\kappa^2 = M_{\rm pl}^{-2}$ as before, and γ is a normalization factor given by

$$\gamma = \frac{\sigma_0 T_3}{3M_{\rm pl}^2}, \tag{5.1.16}$$

where σ_0 denotes the value of σ when the D3-brane is at its stabilized configuration [47, 53]. The Kähler metric and its inverse take the form [47]

$$\mathcal{K}_{\Xi\bar{\Sigma}} = \frac{3}{\kappa^2 U^2} \left(\begin{array}{c|c} 1 & -\gamma k_{\bar{\beta}} \\ \hline -\gamma k_\alpha & U\gamma k_{\alpha\bar{\beta}} + \gamma^2 k_\alpha k_{\bar{\beta}} \end{array} \right), \tag{5.1.17}$$

$$\mathcal{K}^{\Delta\bar{\Gamma}} = \frac{\kappa^2 U}{3} \left(\begin{array}{c|c} U + \gamma k_\gamma k^{\gamma\bar{\delta}} k_{\bar{\gamma}} & k_\gamma k^{\gamma\bar{\beta}} \\ \hline k^{\alpha\bar{\delta}} k_{\bar{\delta}} & \frac{1}{\gamma} k^{\alpha\bar{\beta}} \end{array} \right), \tag{5.1.18}$$

where $k_{\alpha\bar{\beta}} \equiv \partial_\alpha \partial_{\bar{\beta}} k$ is the Calabi-Yau metric, and $k_\alpha \equiv k_{,\alpha}$. The superpotential W, also depends on the D3-brane positions, $\{z_\alpha\}$, and is given by

$$W(\rho) = W_0 + A(z^\alpha) e^{-a\rho}. \tag{5.1.19}$$

The first part of the superpotential is the Gukov-Vafa perturbative superpotential [79]. The second part in the superpotential comes from nonperturbative effects sourced by moduli stabilizing D7-branes wrapping certain four-cycles (see Appendix

A subsection A.5.4) in the compactification and $a = 2\pi/n$ is a constant with n denoting the number of wrapped branes. The inflaton dependence of the superpotential is induced by the interaction between the inflationary D3-brane and wrapped D7-branes. The displacement of the D3-brane in the compactification slightly modifies the supergravity background, perturbing the warp factor, $h = h_{\rm KS} + \delta h$, which corrects the warped volume of four-cycles (bearing the nonperturbative effects from D7-branes):

$$\delta V^w_{\Sigma_4} = \int_{\Sigma_4} d^4Y \sqrt{g^{ind}(X;Y)}\delta h(X;Y). \tag{5.1.20}$$

This change in the warped volume of four-cycles changes the nonperturbative superpotential (2.2.171) to

$$W_{\rm np} \propto \exp\Big(-\frac{T_3}{n}(V^w_{\Sigma_4} + \delta V^w_{\Sigma_4})\Big). \tag{5.1.21}$$

We can write this in the form

$$W_{\rm np} = A(X)\exp\Big(-\frac{T_3}{n}V^w_{\Sigma_4}\Big), \tag{5.1.22}$$

where

$$A(X) = A_0\exp\Big(-\frac{T_3}{n}\delta V^w_{\Sigma_4}\Big). \tag{5.1.23}$$

This superpotential correction then corrects the D3-D7 potential inducing the back-reaction on the mobile D3-brane. The prefactor in the nonperturbative part of (5.1.19) computed from corrections to the warped background takes the form [52]:

$$A(z^\alpha) = A_0\left[\frac{f(z^\alpha)}{f(0)}\right]^{1/n}, \tag{5.1.24}$$

where $f(z^\alpha)$ denotes the holomorphic embedding function of D7-branes depending on the D3-brane coordinates and A_0 is a constant.

According to this and (5.1.17) - (5.1.18), the scalar potential (5.1.11) takes the form [47, 53]

$$V_F(z^\alpha,\bar{z}^\alpha,\rho,\bar{\rho}) = \frac{\kappa^2}{3U(z,\rho)^2}\left\{\left[U(z,\rho)+\gamma k^{\gamma\bar{\delta}}k_\gamma k_{\bar{\delta}}\right]|W_{,\rho}|^2-3(\overline{W}W_{,\rho}+c.c.)\right\} + \frac{\kappa^2}{3U(z,\rho)^2}\left[\left(k^{\alpha\bar{\delta}}k_{\bar{\delta}}\overline{W}_{,\bar{\rho}}W_{,\alpha}+c.c.\right)+\frac{1}{\gamma}k^{\alpha\bar{\beta}}W_{,\alpha}\overline{W}_{,\bar{\beta}}\right]. \quad (5.1.25)$$

The first part in Eq. (5.1.25) is the standard KKLT F-term potential, and the second part arises exclusively from corrections to the nonperturbative superpotential. To derive the explicit form of this potential, we need to consider appropriate formulas for the various terms in the potential and specify an embedding for D7-branes.

We first note that the Kähler potential on the deformed conifold is given by (A.6.173) and its inverse reads as

$$k^{\bar{i}j} = \frac{r^3}{k''}\left[R^{\bar{i}j}+\coth\eta\left(\frac{k''}{k'}-\coth\eta\right)L^{\bar{i}j}\right], \quad (5.1.26)$$

where $k'=dk/d\eta$ and $k''=d^2k/d\eta^2$, and $R^{\bar{i}j}$ and $L^{\bar{i}j}$ are 3×3 matrices given by

$$R^{\bar{i}j} = \delta^{\bar{i}j}-\frac{z_i\bar{z}_j}{r^3}, \quad (5.1.27)$$

$$L^{\bar{i}j} = \left(1-\frac{\epsilon^4}{r^6}\right)\delta^{\bar{i}j}+\frac{\epsilon^2}{r^3}\frac{z_iz_j+\bar{z}_i\bar{z}_j}{r^3}-\frac{z_i\bar{z}_j+\bar{z}_iz_j}{r^3}. \quad (5.1.28)$$

By noting that $k_{\bar{i}}L^{\bar{i}j}=L^{\bar{i}j}k_j=0$, we have the norm

$$k^{\bar{i}j}k_{\bar{i}}k_j = \frac{3}{4}\frac{\epsilon^{4/3}}{2^{1/3}}\frac{[\sinh(2\eta)-2\eta]^{4/3}}{\sinh^2\eta}. \quad (5.1.29)$$

In the same way, we may compute

$$k^{\bar{i}j}k_{\bar{i}}W_j = \frac{3}{4}\frac{\cosh\eta}{\sinh^3\eta}[\sinh(2\eta)-2\eta]\sum_{j=1}^{3}\left(z_j-\bar{z}_j\frac{\epsilon^2}{r^3}\right)A_je^{-a\rho}, \quad (5.1.30)$$

$$k^{\bar{i}j}\overline{W}_{\bar{i}}W_j = \frac{3}{2\cdot 2^{2/3}}\epsilon^{2/3}\frac{\cosh\eta}{\sinh\eta}[\sinh(2\eta)-2\eta]^{2/3} \times\left\{R^{\bar{i}j}\overline{W}_{\bar{i}}W_j+\left[\frac{2}{3}\frac{\sinh(2\eta)}{\sinh(2\eta)-2\eta}-\coth^2\eta\right]\times L^{\bar{i}j}\overline{W}_{\bar{i}}W_j\right\}, \quad (5.1.31)$$

where

$$R^{\bar{i}j}\overline{W}_{\bar{i}}W_j = e^{-2a_n\sigma}\Big[\sum_{i=1}^{3}|A_i|^2 - \frac{1}{r^3}\Big(\sum_{i=1}^{3}z_i\bar{A}_i\Big)\Big(\sum_{j=1}^{3}\bar{z}_jA_j\Big)\Big], \tag{5.1.32}$$

$$\begin{aligned} L^{\bar{i}j}\overline{W}_{\bar{i}}W_j &= e^{-2a_n\sigma}\Big\{\sum_{i=1}^{3}\Big(1-\frac{\epsilon^4}{r^6}\Big)|A_i|^2 - \frac{1}{r^3}\Big(\sum_{i,j=1}^{3}\bar{A}_i\Big[z_i\bar{z}_j + z_j\bar{z}_i - \frac{\epsilon^2}{r^3} \\ &\quad \times(z_iz_j+\bar{z}_i\bar{z}_j)\Big]A_j\Big)\Big\}. \end{aligned} \tag{5.1.33}$$

Under substitution of (5.1.29), (5.1.30) and (5.1.31) the F-term potential (5.1.25) takes the functional form $V_F = V_F(z_1+\bar{z}_1, |z_1|^2, \eta, \sigma, \tau)$.

We next embed a space-filling D7-brane in the deformed conifold using the Kuperstein embedding defined by the algebraic equation [105]

$$f(z_4) = \mu - z_4 = 0. \tag{5.1.34}$$

This equation describes a surface embedded in the deformed conifold. From the definition of the deformed conifold we note that along the surface $z_4 = \mu$ the radial coordinate r satisfies

$$r^2 = \sum_{i=1}^{3}|z_i|^2+\mu^2 \geq \Big|\sum_{i=1}^{3}z_i\Big|^2+\mu^2 = |\epsilon^2-\mu^2|+\mu^2 = \begin{cases}\epsilon^2 & \text{for } \mu\leq\epsilon \\ 2\mu^2-\epsilon^2 & \text{for } \mu\geq\epsilon\end{cases}, \tag{5.1.35}$$

where $r^2 = \epsilon^2\cosh\eta$. We now consider two cases, $\mu > \epsilon$ and $\mu < \epsilon$. In the former case, the minimal value of the radial coordinate η along the surface $z_4 = \mu$ is $\eta_{\rm min} = 2\cosh^{-1}(\frac{\mu}{\epsilon})$. In this case, the D7-brane probe does not reach the bottom of the deformed conifold throat at the IR location $\eta = 0$. In the later case, $\eta_{\rm min}$ is zero. From these results we see that the D7-brane configuration has a free parameter μ and by making this parameter large enough, $\mu > \epsilon$, the probe brane ends at a finite distance at the radial coordinate η away from the IR location.

The prefactor of the nonperturbative superpotential, Eq. (5.1.24), and its derivative with respect to the independent coordinates now take the form

$$A(z_1) = A_0\Big(1-\frac{z_1}{\mu}\Big)^{1/n}, \tag{5.1.36}$$

$$A_i(z_1) = -\frac{A_0}{n\mu}\left(1-\frac{z_1}{\mu}\right)^{1/n-1}\delta_{i1}. \tag{5.1.37}$$

5.2 Multifield D-brane inflation

To obtain a simple trajectory depending only on one harmonic mode, say $\theta_1 = \theta$, we fix the rest of the angular directions of $T^{1,1}$ by imposing the following constrains

$$\begin{aligned} &\frac{\varphi_1-\varphi_2\pm\psi}{2} = \pm\frac{\pi}{2}, \qquad &&\frac{\varphi_1+\varphi_2+\psi}{2} = \pi, \\ &\frac{\psi-\varphi_1-\varphi_2}{2} = 0, \qquad &&\theta_2 = 0. \end{aligned} \tag{5.2.38}$$

Accordingly to this, the coordinates on the deformed conifold read as

$$\begin{aligned} z_1 &= -\epsilon\cosh\left(\frac{\eta}{2}\right)\cos\left(\frac{\theta}{2}\right), \qquad & z_2 &= -i\epsilon\sinh\left(\frac{\eta}{2}\right)\cos\left(\frac{\theta}{2}\right), \\ z_3 &= -i\epsilon\sinh\left(\frac{\eta}{2}\right)\sin\left(\frac{\theta}{2}\right), \qquad & z_4 &= +\epsilon\cosh\left(\frac{\eta}{2}\right)\sin\left(\frac{\theta}{2}\right). \end{aligned} \tag{5.2.39}$$

The imaginary part of the Kähler modulus can be integrated out by

$$\frac{e^{ia\chi}}{A} \to \frac{1}{|A|}. \tag{5.2.40}$$

Accordingly, the four-dimensional supergravity potential is[1](see Appendix B)

$$\begin{aligned} V_F &= \frac{2\kappa^2 a_n^2|A_0|^2 e^{-2a_n\sigma}}{U^2}|g(\eta,\theta)|^{2/n} \\ &\quad\times\left\{\frac{U}{6}+\frac{1}{a_n}\left(1-\frac{|W_0|}{|A_0|}\frac{e^{a_n\sigma}}{g(\eta,\theta)^{1/n}}\right)+F(\eta,\theta)\right\}, \end{aligned} \tag{5.2.41}$$

where

$$\begin{aligned} F(\eta,\theta) &= \frac{\gamma}{4}\epsilon^{4/3}K^4\sinh^2\eta - \frac{\epsilon K^3}{an\mu g}\cos\left(\frac{\theta}{2}\right)\cos\left(\frac{\eta}{2}\right)\sinh^2\left(\frac{\eta}{2}\right) \\ &\quad+\frac{\epsilon^{2/3}K^2}{4n^2a^2\mu^2\gamma g^2}\left[\sinh^2\left(\frac{\eta}{2}\right)\cos^2\left(\frac{\theta}{2}\right)+\frac{2}{3K^2}\sin^2\left(\frac{\theta}{2}\right)\right]. \end{aligned} \tag{5.2.42}$$

[1]It is straightforward to check that for $\theta = 0$ our two-field potential (5.2.41) coincides with the single field potential derived in [51].

Here we have defined

$$U(\eta,\theta) = 2\sigma(\eta,\theta) - \gamma k(\eta), \tag{5.2.43}$$

$$g(\eta,\theta) = 1 + \frac{\epsilon}{\mu}\cosh\left(\frac{\eta}{2}\right)\cos\left(\frac{\theta}{2}\right). \tag{5.2.44}$$

Compactifying the warped deformed conifold throat via attaching it to the compact Calabi-Yau space at some finite radius $r_{\rm UV}$ requires Kähler modulus stabilization. This involves integrating out σ by the assumption that it evolve adiabatically while remaining in its instantaneous minimum $\sigma_*(\eta,\theta)$ using the following equation:

$$\left.\frac{\partial(V_F + V_{\rm uplift})(\eta,\theta)}{\partial\sigma}\right|_{\sigma_\star(\eta,\theta)} = 0. \tag{5.2.45}$$

Here we have added a D-term potential $V(\eta,\sigma) = D_{\rm uplift}/U(\eta,\sigma)^2$ which is needed to uplift KKLT AdS minimum to a dS minimum. The uplifting can be sourced by distant anti-D3-branes or wrapped D7-branes. The instantaneous minimum of σ is denoted by σ_* including a shift due to its coordinate dependence induced by adding a mobile D3-brane to the compactification. The functional form of σ_* can be determined by the numerical solution of the transcendental equation (5.2.45), which we will solve in the next section. Before turning to numerical computation, we need to look at the minimum of the D3-D7 potential which specifies σ_F and $D_{\rm uplift}$ and constrains the rest of parameters on which these depend.

The critical value σ_F of the Kähler modulus before uplifting is determined by the condition $D_\sigma W|_{\eta=0,\,\theta=0,\,\sigma_F} = 0$, or equivalently [30],

$$e^{a\sigma_F} = \frac{|A_0|}{|W_0|}\left(1 + \frac{2}{3}a\sigma_F\right)g(0,0)^{1/n} \quad \Rightarrow \quad \left.\frac{\partial V_F}{\partial\sigma}\right|_{\sigma_F} = 0, \tag{5.2.46}$$

where g is given by (5.2.44). We may write this in the form:

$$\sigma_F \;=\; \frac{1}{a}\log\left[\frac{|A_0|}{|W_0|}\left(1 + \frac{2}{3}a\sigma_F\right)\left(1 + \frac{\epsilon}{\mu}\right)^{1/n}\right]. \tag{5.2.47}$$

From Eq. (5.2.41) and Eq. (5.2.46) we note that

$$V_F(0,\sigma_F) = -\frac{3a^2\kappa^2 W_0^2}{2\sigma_F(3+2a\sigma_F)^2}. \tag{5.2.48}$$

The uplifting parameter is given by

$$s = \frac{V_{\rm uplift}(0,\sigma_F)}{|V_F(0,\sigma_F)|} \quad \text{with} \quad V_{\rm uplift}(0,\sigma_F) = \frac{D_{\rm uplift}}{4\sigma_F^2}. \tag{5.2.49}$$

From this we obtain

$$D_{\rm uplift} = \frac{6s\,a^2\kappa^2 W_0^2\sigma_F}{(3+2a\sigma_F)^2}. \tag{5.2.50}$$

Here $1 \leq s \leq 3$ to avoid decompactification, a is determined by the choice of n, κ depends on the UV cut-off, and the value of σ_F can be derived from Eq. (5.2.47) once the set of parameters $\{\epsilon,\, \mu,\, n,\, s,\, |A_0|,\, |W_0|\,\}$ are specified. We also note that uplifting the KKLT AdS minimum to a dS minimum introduces a small shift in the stabilized volume, $\sigma_0 \equiv \sigma_F + \delta\sigma$. At the tip, we have [54]:

$$a\sigma_0 \approx a\sigma_F + \frac{s}{a\sigma_F}. \tag{5.2.51}$$

Here we note that both Eq. (5.2.47) and Eq. (5.2.51) which give σ_F and $\delta\sigma$, respectively, are derived from the local minimum of the F-term potential (5.2.41) at the tip. The critical value σ_m of the Kähler modulus away from the tip and its shift $\delta\sigma_m$ can be derived from the global minimum of the F-term potential (5.2.41). We note that:

$$\frac{\partial V_F}{\partial\sigma} = \frac{2a_n^2\kappa^2 A_0^2}{U^2} g^{2/n} e^{-2a_n\sigma}\left[\left(\frac{|W_0|}{|A_0|}\frac{e^{a_n\sigma}}{g^{1/n}} - 1 - \frac{a_n U}{3} - 2F\left(a_n + \frac{2}{U}\right)\right)\right], \tag{5.2.52}$$

$$\begin{aligned}\frac{\partial^2 V_F}{\partial\sigma^2} = \frac{2a_n^2\kappa^2 A_0^2}{U^2} g^{2/n} e^{-2a_n\sigma}\Bigg[&2\left(\frac{a_n^2 U}{3} + \frac{26}{3U} + \frac{12}{a_n U^2} + \frac{8a_n}{3}\right) \\ &- \frac{|W_0|}{|A_0|}\frac{e^{a_n\sigma}}{g^{1/n}}\left(a_n + \frac{8}{U} + \frac{24}{a_n U^2}\right) + 4F\left(a_n^2 + \frac{4a_n}{U} + \frac{6}{U^2}\right)\Bigg].\end{aligned} \tag{5.2.53}$$

Thus the global minimum of V_F requires

$$\frac{|W_0|}{|A_0|}\frac{e^{a_n\sigma}}{g^{1/n}} = 1 + \frac{a_n U}{3} + 2aF\frac{a_n U + 2}{a_n U + 4}, \tag{5.2.54}$$

or

$$\sigma_m = \frac{1}{a_n}\left[g(\eta,\theta)^{1/n}\frac{|A_0|}{|W_0|}\left(1+\frac{a_nU}{3}+2a_nF\frac{a_nU+2}{a_nU+4}\right)\right]. \tag{5.2.55}$$

Stability of this minimum under the addition of V_D requires that σ is not too small (e.g. $\sigma \simeq 10$) which in turn tells us that $|A_0|/|W_0|$ has to be very small. A reasonable approximation in which F has a less impact gives

$$\sigma_m \simeq -\log\frac{|W_0|}{|A_0|}+\log\left|\frac{2}{3}\log\frac{|W_0|}{|A_0|}\right|, \tag{5.2.56}$$

At this minimum we have:

$$\begin{aligned} V(\sigma_m) &= -\frac{6a_n^2\kappa^2W_0^2}{2U_m}\frac{(aU_m+4)[(a_nU_m+4)+6aF]}{(a_nU_m+4)(a_nU_m+3)+6aF(a_nU_m+2)^2}, \\ V''(\sigma_m) &= \frac{6a_n^2\kappa^2W_0^2}{U_m^3}\left\{\frac{(a_nU_m+4)[(a_nU_m+4)(a_n^2U_m^2+5a_nU_m-12)}{[(a_nU_m+4)(a_nU_m+3)+6a_nF(a_nU_m+2)]^2}\right. \\ &\quad \left.+\frac{+6a_nF(a_n^2U_m^2+6a_nU_m+4)]}{[(a_nU_m+4)(a_nU_m+3)+6a_nF(a_nU_m+2)]^2}\right\}. \end{aligned} \tag{5.2.57}$$

Thus we have

$$\begin{aligned} \frac{V''(\sigma_m)}{V(\sigma_m)} &= -2\frac{[(a_nU_m+4)(a_n^2U_m^2+5a_nU_m-12)+6aF(a_n^2U_m^2+6a_nU_m+4)]}{U_m^2[(a_nU_m+4)+6a_nF]} \\ &= -2a_n^2\left(1+\frac{5}{a_nU_m}-\frac{12}{a_n^2U_m^2}\right)-\frac{12a_nF(a_nU_m+16)}{U_m^2[(a_nU_m+4)+6a_nF]}. \end{aligned} \tag{5.2.58}$$

We also note that

$$V_D(\sigma_m)=\frac{D_{\text{uplift}}}{U_m^2}, \qquad V_D'(\sigma_m)=-\frac{4V_D(\sigma_m)}{U_m}, \qquad V_D''(\sigma_m)=\frac{24V_D(\sigma_m)}{U_m^2}. \tag{5.2.59}$$

Under the assumption that V_D only shifts the minimum by a small amount gives:

$$V'(\sigma_m+\delta\sigma) = V_D'(\sigma_m+\delta\sigma)+V_F'(\sigma_m+\delta\sigma) \simeq V_D'(\sigma_m)+\delta\sigma V_F''(\sigma_m)=0 \tag{5.2.60}$$

$$\Rightarrow \qquad \delta\sigma = -\frac{V_D'(\sigma_m)}{V_F''(\sigma_m)}=\frac{4V_D(\sigma_m)}{U_mV_F(\sigma_m)}\frac{V(\sigma_m)}{V''(\sigma_m)}. \tag{5.2.61}$$

The degree to which these run with η depends on $k(\eta)$ and F. First look at k, which is an increasing function of η:

$$\gamma k(\eta_{\rm UV}) \sim \frac{\sigma_0 T_3}{3M_{\rm pl}^2}\epsilon^{4/3}e^{2\eta_{\rm UV}/3} \tag{5.2.62}$$

Now we note that the Planck-mass is given by [1]:

$$M_{\rm pl}^2 = \frac{\beta(g_sM)^2}{6\pi g_s}\epsilon^{4/3}T_3 J_{\rm UV}, \tag{5.2.63}$$

where $J_{\rm UV}$ is the integral computed in the previous chapter (see Fig. 4.1), $J_{\rm UV} \sim \eta_{\rm UV}e^{2\eta_{\rm UV}/3}$, and β is the ratio of the actual volume of the Calabi-Yau space to the warped deformed conifold throat volume, usually taken to be order unity. Hence

$$\gamma k(\eta_{\rm UV}) \sim \frac{\sigma_0}{\beta}\frac{2\pi g_s}{\eta_{\rm UV}(g_sM)^2}, \tag{5.2.64}$$

which we can see is still pretty small as we take g_sM big.

$F(\eta,\theta)$ on the other hand is maximal at $\theta = \pi$, where

$$F(\eta) = \frac{\gamma}{4}\epsilon^{4/3}K^4\sinh^2\eta + \frac{(\epsilon/\mu)^2}{6a^2n^2\gamma\epsilon^{4/3}}, \tag{5.2.65}$$

the first of which is similar to γk, and hence small. The second term is

$$\frac{(\epsilon/\mu)}{6a_n^2n^2\gamma\epsilon^{4/3}} \sim \mathcal{O}(\eta_{\rm UV}e^{\eta_{\rm UV}}(g_sM)^2), \tag{5.2.66}$$

which is not at all small. This therefore provides a strong steer to the value of μ. We would like to remark here that in most of the brane inflation models in the literature (e.g. see [51, 54]) the perturbative expansion of the potential is analysed in either the UV or the IR region. In these models ϵ and μ are considered to have similar order magnitude. However, we note that a consistent expansion along the entire throat including both the UV and IR regions requires a large hierarchy between ϵ and μ. In particular, the final piece of our potential term $F(\eta,\theta)$ given by Eq. (5.2.42) scales as $\epsilon^{-4/3}(\epsilon/\mu)^2$. Unless the hierarchy between ϵ and μ is large this term will dominate the potential and destabilize the vacuum expansion. Moreover, the key point here is that in our DBI brane inflation set up the full potential contains a large leading order mass term for the radial coordinate and in order to keep the adiabatic

approximation (5.2.45) valid the hierarchy between ϵ and μ has to be large, so that the mass generated for the Kähler modulus is much larger than the Hubble rate (see Section 4).

As mentioned above, apart from the shift induced by uplifting, $\delta\sigma$, the addition of a mobile D3-brane in the compactification induces a further shift in the Kähler modulus that depends on the coordinates of the brane, $\sigma_*(\eta,\theta)$. Thus the nonperturbatively generated D3-D7 potential about a dS minimum takes the form:

$$\begin{aligned} V_F + V_D &= \frac{2\kappa^2 a_n^2 |A_0|^2 e^{-2a_n\sigma_*(\eta,\theta)}}{U[\eta,\sigma_*(\eta,\theta)]^2}|g(\eta,\theta)|^{2/n} \\ &\quad \times\left\{\frac{U[\eta,\sigma_*(\eta,\theta)]}{6}+\frac{1}{a_n}\left(1-\frac{|W_0|}{|A_0|}\frac{e^{a_n\sigma_*(\eta,\theta)}}{g(\eta,\theta)^{1/n}}\right)+F(\eta,\theta)\right\} \\ &\quad +\frac{D_{\rm uplift}}{U[\eta,\sigma_*(\eta,\theta)]^2}. \end{aligned} \tag{5.2.67}$$

Hence the total potential takes the form:

$$\begin{aligned} T_3 V &= T_3\left(\frac{1}{2}m_0^2\left[r(\eta)^2+c_2K(\eta)\sinh\eta\cos\vartheta\right]+V_0\right) \\ &\quad +V_F+V_D. \end{aligned} \tag{5.2.68}$$

Here $D_{\rm uplift}$ is given by (5.2.50), the constant V_0 is chosen so that the global minimum of V is $V=0$, and c_2 is an arbitrary constant. Because c_2 multiplies a solution to a free Laplace equation, it is not fixed. For a self-consistent expansion, we expect c_2 to be smaller, or of a magnitude comparable with other terms in the potential.

Finally, to derive the explicit form of the D3-brane equations of motion on the deformed conifold for the simplest case including only one angular direction for the potential (5.2.68) first note that a simple S^3 round metric on the deformed conifold can be obtained from (2.1.66) as:

$$ds^2 = A(\eta)d\eta^2 + B(\eta)d\theta^2, \tag{5.2.69}$$

where

$$A(\eta)=\frac{\epsilon^{4/3}}{6K(\eta)^2}, \qquad B(\eta)=\frac{\epsilon^{4/3}K(\eta)}{4}\big[\cosh(\eta/2)+\sinh(\eta/2)\big]. \tag{5.2.70}$$

The brane equations of motion can then be derived upon cross elimination from (5.1.7) in the following form (see Appendix C):

$$\begin{aligned}\ddot{\eta} &= -\frac{3H}{\gamma_{\rm DBI}^2}\dot{\eta}+\frac{h'}{\gamma_{\rm DBI}h}\dot{\eta}^2(1-\gamma_{\rm DBI})+\frac{h'}{2h^2A}(\gamma_{\rm DBI}^{-1}-1)^2\\ &\quad -\frac{1}{2A}(A'\dot{\eta}^2-B'\dot{\theta}^2)+h\dot{\theta}\dot{\eta}\frac{V_\theta}{\gamma_{\rm DBI}T_3}-(1-hA\dot{\eta}^2)\frac{V_\eta}{\gamma_{\rm DBI}AT_3}\\ &\quad -\dot{\eta}\dot{\theta}(1-\gamma_{\rm DBI}^{-1})\frac{h_\theta}{h},\end{aligned} \tag{5.2.71}$$

$$\begin{aligned}\ddot{\theta} &= -\frac{3H\dot{\theta}}{\gamma_{\rm DBI}^2}+(1-\gamma_{\rm DBI})\dot{\theta}\dot{\eta}\frac{h'}{\gamma_{\rm DBI}h}-\dot{\theta}\dot{\eta}\frac{B'}{B}+h\dot{\theta}\dot{\eta}\frac{V_\eta}{\gamma_{\rm DBI}T_3}\\ &\quad -(1-hB\dot{\theta}^2)\frac{V_\theta}{\gamma_{\rm DBI}BT_3}-(1-\gamma_{\rm DBI}^{-1})\left[\dot{\theta}^2-\frac{(1-\gamma_{\rm DBI}^{-1})}{2hB}\right]\frac{h_\theta}{h}.\end{aligned} \tag{5.2.72}$$

Here we note that in the absence of non-linear corrections including the contribution of the D3-D7 potential and perturbations of the warp factor, the potential (5.2.68) and Eqs. (5.2.71) - (5.2.72) reduce to the D3-brane potential and equations of motion including only linearized corrections studied in the previous chapter [1]. We also note that in the slow-roll regime $\gamma_{\rm DBI}\simeq 1$ and the perturbations of the warp factor have no effect. However, since we are neither slow-rolling nor restricting ourselves to the linearized case, we need to take into account the perturbations of the warp factor which amount superpotential corrections in the D3-D7 potential. For the warped deformed conifold, the perturbations of the warp factor in the tip region can be expressed as [84]

$$\begin{aligned}\delta h &= -(2\pi)^4 g_s p(\alpha')^2\mathcal{G}(\eta,y_4)\\ &= \frac{16\pi\cdot 3^{2/3}g_s p(\alpha')^2}{(2\epsilon)^{8/3}\cdot\eta}\left[1+2\sqrt{2}y_4+6y_4^2+8\sqrt{2}y_4^3-\cdots\right] \quad \text{with}\end{aligned} \tag{5.2.73}$$

$$y_4 = \left[\cos\left(\frac{\theta_1}{2}\right)\sin\left(\frac{\theta_2}{2}\right)e^{\frac{i(\varphi_1-\varphi_2+\psi)}{2}}-\sin\left(\frac{\theta_1}{2}\right)\cos\left(\frac{\theta_2}{2}\right)e^{\frac{-i(\varphi_1-\phi_2-\psi)}{2}}\right]. \tag{5.2.74}$$

Here $\mathcal{G}(\eta,y_4)$ is the Green's function (expanded in the eigenfunctions of the Laplacian) on the deformed conifold given by (2.2.140), y_4 comes from (2.1.62) and p specifies the number of mobile D3-branes, which we take to be $p=1$. By the first

angular condition in (5.2.38) along an S^3 ($\theta_1 = 0$) for relations (5.2.73) and (5.2.74) we have

$$\delta h = \frac{16\pi \cdot 3^{2/3} g_s p (\alpha')^2}{(2\epsilon)^{8/3} \cdot \eta} \left[1 + 2\sqrt{2} y_4 + 6 y_4^2 + 8\sqrt{2} y_4^3 - \cdots\right] \quad \text{with} \tag{5.2.75}$$

$$y_4 = -\frac{1}{\sqrt{2}} \sin\left(\frac{\theta}{2}\right). \tag{5.2.76}$$

In the off-tip region, where r is large, we may use the very first line in (5.2.73) together with relations (2.2.142) - (2.2.146) for the quantum numbers $j_1 = j_2 = R/2 = 1/2$ and $m_1 = m_2 = 1/2$, and obtain δh in the form

$$\delta h \simeq -\frac{10 g_s p \alpha'^2}{\pi^2} \cos^4\frac{\theta}{2} \left(\frac{1}{r^4}\right) + \cdots \quad \text{with} \tag{5.2.77}$$

$$r^3 = \epsilon^2 e^{\eta}. \tag{5.2.78}$$

5.3 Inflationary solutions

In order to integrate the full brane equations of motion, we first need to specify a suitable choice of parameters and then compute the real part of the Kähler modulus that appears in the brane equations of motion. To choose a reasonable set of compactification parameters, we note the following points. Firstly, we require a large hierarchy between A_0 and W_0 to guarantee large σ_F which ensures suppressed α'-corrections. Secondly, we also need a large hierarchy between ϵ and μ in addition to the A_0/W_0 hierarchy to guarantee a valid perturbative expansion, $\delta\sigma \ll 1$. When both these hierarchies are turned on, σ_* can be computed within the adiabatic approximation from Eq. (5.2.45). We also remark from the literature that choosing a large value of the UV-scale, $\eta_{\rm UV}$, sets a large value for the Planck-mass (e.g. see previous chapter [1]) in which case curvature corrections may be omitted and non-linear corrections are dominated by IASD fluxes sourced by moduli stabilizing wrapped D7-branes whose number is given by $n > 1$. Furthermore, we remark that the supergravity solution requires large $g_s M$ and the value of s has to be chosen within the range $1 \leq s \leq 3$ to ensure a small positive cosmological constant and to avoid runaway decompactification.

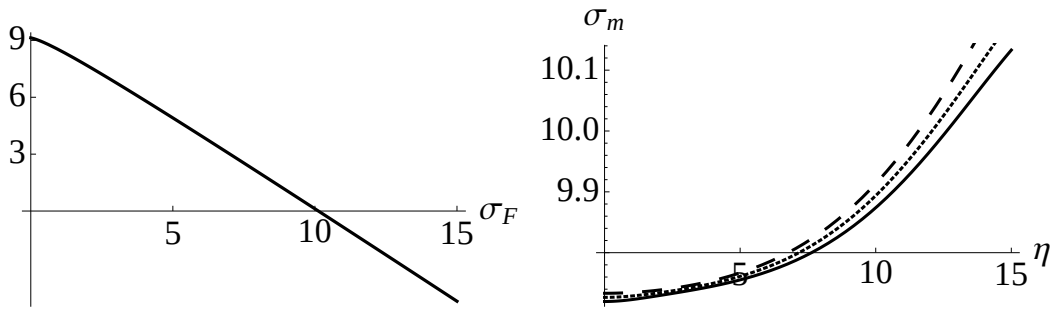

Figure 5.1: The behaviour of σ_F obtained from the root of Eq. (5.2.47) for choice of compactification parameters (4.1), and the behaviour of σ_m for choice of parameters (4.1) with $\theta = 0\,(\text{solid}), \pi/2\,(\text{tiny-dashed})$ and $\pi\,(\text{large-dashed})$.

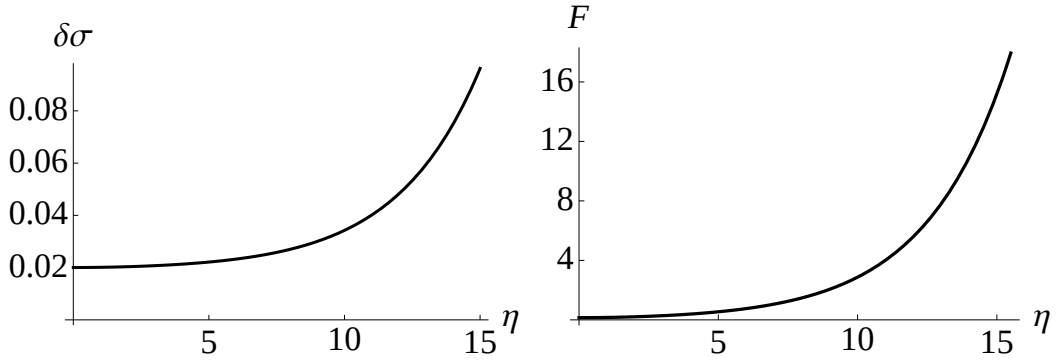

Figure 5.2: The behaviour of the function F and $\delta\sigma$ for the choice of parameters (4.1) and $\theta = \pi$.

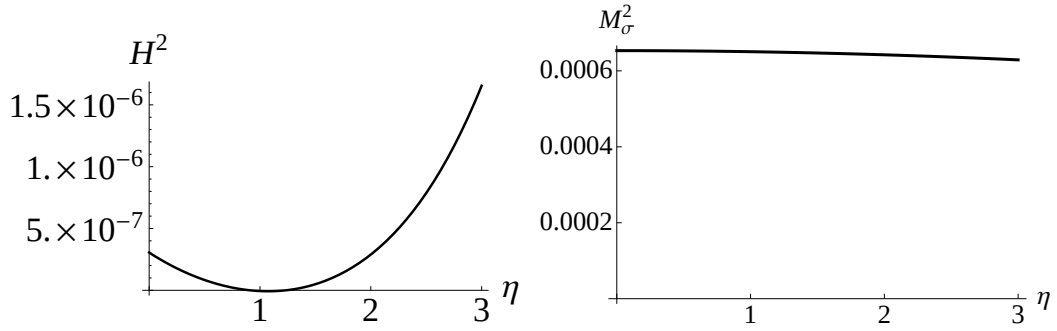

Figure 5.3: The Hubble rate, $H^2 \simeq V/3M_{\rm pl}^2$, and the σ mass squared, M_σ^2 for the choice of parameters (4.1) and $\theta = \pi$.

In line with the above requirements we choose in our numerical analysis the following specific set of compactification parameters:

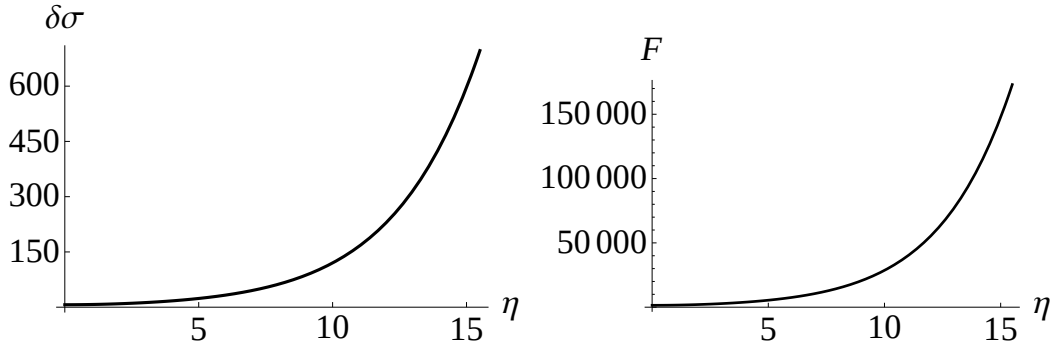

Figure 5.4: The behaviour of the function F and $\delta\sigma$ with $\mu = 0.005$ and the rest of parameters as (4.1) and $\theta = \pi$.

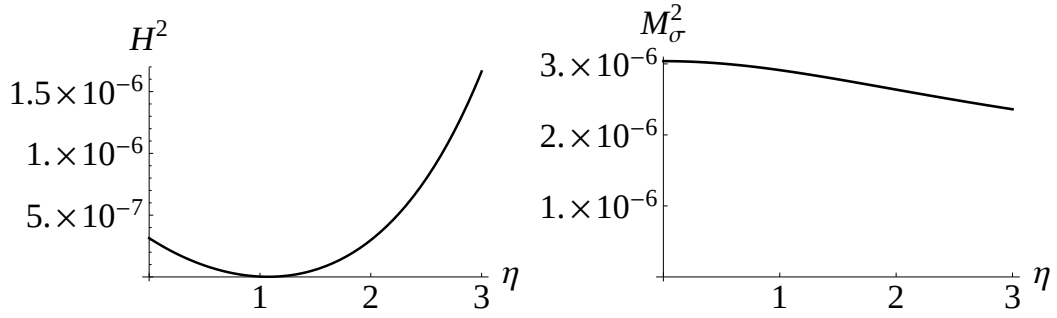

Figure 5.5: The Hubble rate, $H^2 \simeq V/3M_{\rm pl}^2$, and the σ mass squared, M_σ^2 with $\mu = 0.005$ and the rest of parameters as (4.1) and $\theta = \pi$.

$$\eta_{\rm UV} = 15, \quad n = 2, \quad s = 2, \quad \epsilon = 0.001$$
$$g_s M = 100, \ \mu = 5, \ W_0 = 29, \ A_0 = 25 \times 10^{12}. \tag{5.3.79}$$

Inspection of Eq. (5.2.47) and Eq. (5.2.55) shows that for the choice of parameters (5.3.79) σ_F and σ_m scale to large values (see Fig. 5.1); inspection of Eq. (5.2.42) and Eq. (5.2.61) shows that for the choice of parameters (5.3.79) and $\theta = \pi$ the functions $\delta\sigma$ and F scale to reasonably small values on the entire warped deformed conifold (see Fig. 5.2); for the choice of parameters (5.3.79) the mass squared of the Kähler modulus, $M_\sigma^2 \equiv V_{,\sigma\sigma}$, is much larger than the approximate squared Hubble rate, $H^2 \simeq V/3M_{\rm pl}^2$ (see Fig. 5.3), which guarantees an adiabatic expansion [54, 106]. We note here that by decreasing these hierarchies much below their values (5.3.79) makes M_σ^2 and H^2 scale similarly which invalidates the adiabatic approximation, in

addition $\delta\sigma$ and F become large which invalidates the perturbative expansion; for instance, for $\mu = 0.005$ and the rest of parameters as in (5.3.79) we show $\delta\sigma$ and F in Fig. 5.4 - Fig. 5.5.

In the literature of brane inflation, the most common way of computing the Kähler modulus, σ, is to adopt a semi - analytic approach with the assumption that σ evolves adiabatically (e.g. see [53]). In this approach, σ in $U(\eta, \sigma)$ is set to its large fixed value σ_0, and (5.2.45) is treated as an equation in the variable $\exp[-a\sigma_*(\eta)]$. The value of σ_* is then obtained from Eq. (5.2.45) by expanding in specific conical regions including either the IR or the UV regions where the canonical inflaton (5.1.10) is given by its small or large η limit, respectively. This may be a good approximation but it gives only a qualitative understanding. Here we compute σ_* by solving the transcendental equation (5.2.45) numerically to obtain the exact value of σ_* on the entire supergravity background. For the choice of parameters (5.3.79) we show σ_* in Fig. 5.6 and its derivatives in Fig. 5.7.

In order to compute σ_*, we consider the range of variables $0 \leq \eta \leq 15$ and $0 \leq \theta \leq \pi$ for the choice of parameters (5.3.79) and generate the table of values for the solution of Eq. (5.2.45). This is done numerically via grid size of 0.1 which means that about 18000 data points are calculated. These data points are interpolated by Mathematica to get the approximate function σ_* (see Fig. 5.6). To get an approximate derivative of σ_* with respect to η, and with respect to θ, which are denoted $\partial_\eta\sigma_\star$ and $\partial_\theta\sigma_*$, respectively, the above generated grid points are used to calculate the quotion of differences. These are approximate values for the differential quotient. Then, the table of values of the approximate derivative is again interpolated by Mathematica to obtain $\partial_\eta\sigma_*$ and $\partial_\theta\sigma_*$ (see Fig. 5.7).

For the choice of parameters (5.3.79) and the numerically computed Kähler modulus, we integrated the full D3-brane equations of motion, Eqs. (5.1.5) - (5.1.7) with Eq. (5.1.7) given by Eqs. (5.2.71) - (5.2.72), and our inflationary solution is displayed in Fig. 5.8. The solution describes spiral brane motion at high speed in the warped throat region of the compact Calabi-Yau space containing holomorphically embedded wrapped D7-branes involved in (Kähler) moduli stabilization. The conserved angular momentum is lifted by harmonic dependent corrections from linearized as

well as non-linear perturbations including contributions from the D3-D7 potential and corrections of the warp factor. The brane accelerates along the radial and angular directions as it falls down the throat from the UV end where it is attached to the compact Calabi-Yau space. Inflation ends when the brane reaches the IR location where the throat smoothly closes off. For the choice of parameters and the numerically computed Kähler modulus, we integrated the brane equations of motion and found that the inflationary solution is quite robust against harmonic dependent corrections from the D3-D7 potential and corrections of the warp factor. In particular, we found (as displayed in Fig. 5.8) that harmonic dependent corrections induced by the D3-D7 potential and perturbations of the warp factor do not have the effect of increasing the number of e-foldings and decreasing the $\gamma_{\rm DBI}$-factor. This result differs from our previous results [1] in which harmonic dependent correction to brane motion from linearized perturbations of the supergravity solution increased the number of e-foldings compared to the number of e-foldings produced by brane motion with conserved angular momentum (spinflation) where no supergravity corrections and hence no harmonic dependence in brane motion is present.

We repeated the above computation for various choices of initial conditions and compactification parameters and our findings are summarized as follows.

• Decreasing ϵ below its considered value while keeping other parameters fixed tends to flatten the functional form of σ_* and changes its overall scale insignificantly. Also, the decrease in ϵ leaves σ_F unchanged.

• Decreasing the value of μ while keeping other parameters fixed slightly decreases the value of σ_F and changes the scale of σ_* by a minimal amount. Note that here we decrease μ by an amount, so that the hierarchy between ϵ and μ still remains large.

• Increasing/decreasing n while keeping other parameters fixed strongly impacts the σ_F and the scale of σ_*. Also, increasing n induces fluctuations in σ_* at large η.

• Increasing/decreasing the hierarchy between A_0 and W_0 while keeping other parameters fixed increases/decreases the value of σ_F and slightly changes the scale of σ_* but leaves its overall shape unchanged. Here again we do not decrease the hierarchy between A_0 and W_0 too much. Also, increasing the hierarchy between

A_0 and W_0 by taking W_0 much smaller than its considered value increases σ_F and suppresses the uplifting contribution. This slightly changes the form of σ_* near the origin.

• Changing the set of compactification parameters and initial conditions indicates that the number of e-foldings produced by spinflation including non-linear harmonic dependent corrections depends more on the subset of compactification parameters $\{\epsilon, g_s M, \eta_{\rm UV}\}$ than on the initial conditions and is insensitive to the choice of the remaining subset of compactification parameters $\{n, s, \mu, A_0, W_0\}$. Comparing with the number of e-foldings generated by spinflation including only linearized harmonic dependent corrections each time when varying the set of parameters and initial conditions shows no difference in the number of e-foldings (as Fig. 5.8).

• The $\gamma_{\rm DBI}$-factor produced by spinflation including non-linear harmonic dependent corrections is insensitive to the choice of compactification parameters and initial conditions. Comparing with the $\gamma_{\rm DBI}$-factor produced by spinflation with only linearized harmonic dependent corrections each time when varying the set of parameters and initial conditions shows no difference in the $\gamma_{\rm DBI}$-factors (as Fig. 5.8).

The above findings show that the inflationary solution is quite robust against harmonic dependent corrections from the D3-D7 potential and perturbations of the warp factor not just for the specific choice of compactification parameters (5.3.79) but for a very large set of consistent parameters.

5.4 Summary and conclusions

In this chapter we studied brane inflation in a warped string compactification incorporating the effects of moduli stabilization and backreaction from UV-deformations of the warped throat geometry. The focus of our paper was on DBI brane inflation in the warped deformed conifold with a UV/IR consistent perturbative expansion around the noncompact ISD solution. The perturbations were dominated by IASD fluxes sourced by moduli stabilizing wrapped D7-branes.

We computed the D3-brane potential on the entire deformed conifold including non-linear corrections from the flux induced potential in ten-dimensional su-

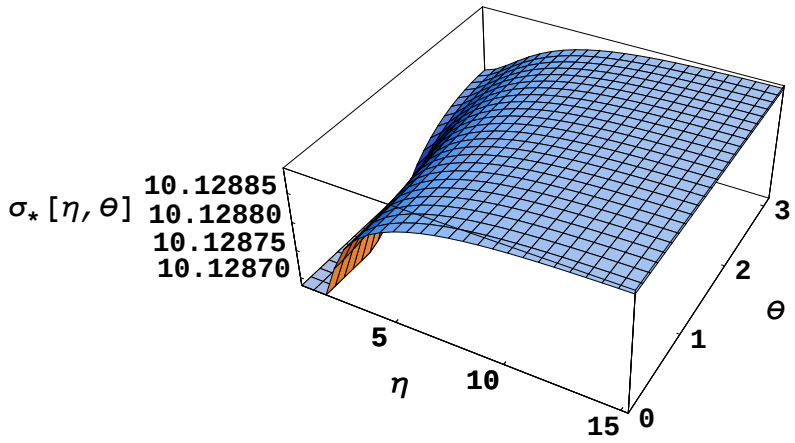

Figure 5.6: The Kähler modulus, σ_*, on the entire supergravity background with the choice of compactification parameters (4.1).

pergravity which equals the nonperturbatively generated D3-D7 brane potential in four-dimensional supergravity. For a simple choice of a trajectory on the deformed conifold, we integrated out the Kähler modulus and reduced the D3-brane potential to a simple two-field potential depending on radial and harmonic directions of the deformed conifold. We integrated out the Kähler modulus by full numerical computation determining its exact functional form on the entire supergravity background including both the IR and UV regions. We found that a UV/IR consistent perturbative expansion in the supergravity potential with the Kähler modulus integrated out within the adiabatic approach in DBI inflation requires certain hierarchies of scales that determine the set of compactification parameters different from those in slow-roll models.

For the consistent choice of parameters and the numerically computed Kähler modulus, we integrated the D3-brane equations of motion in the warped deformed conifold with harmonic dependence from the D3-brane potential and perturbations of the warp factor. We found that our numerical solutions are quite robust against non-linear perturbations including harmonic dependent corrections from perturba-

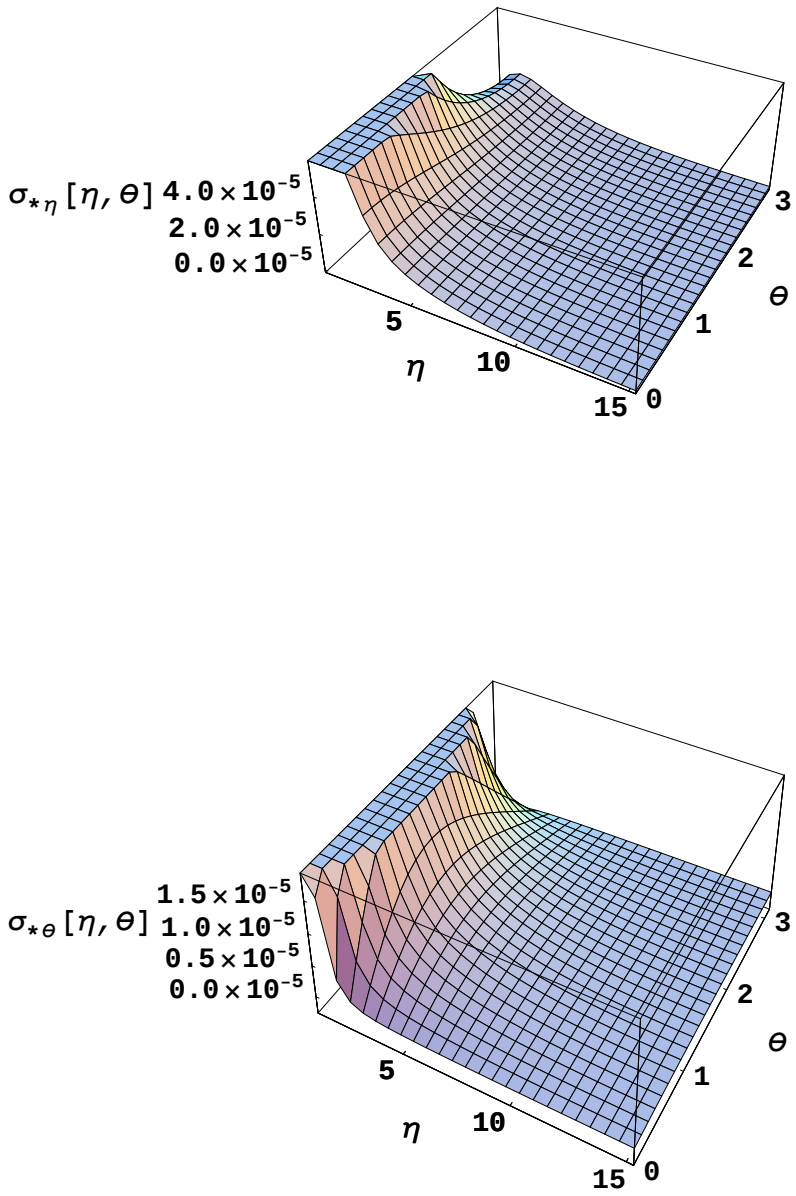

Figure 5.7: The derivatives of the Kähler modulus, $\partial_\eta\sigma_*$ and $\partial_\theta\sigma_*$, on the entire supergravity background with the choice of compactification parameters (4.1).

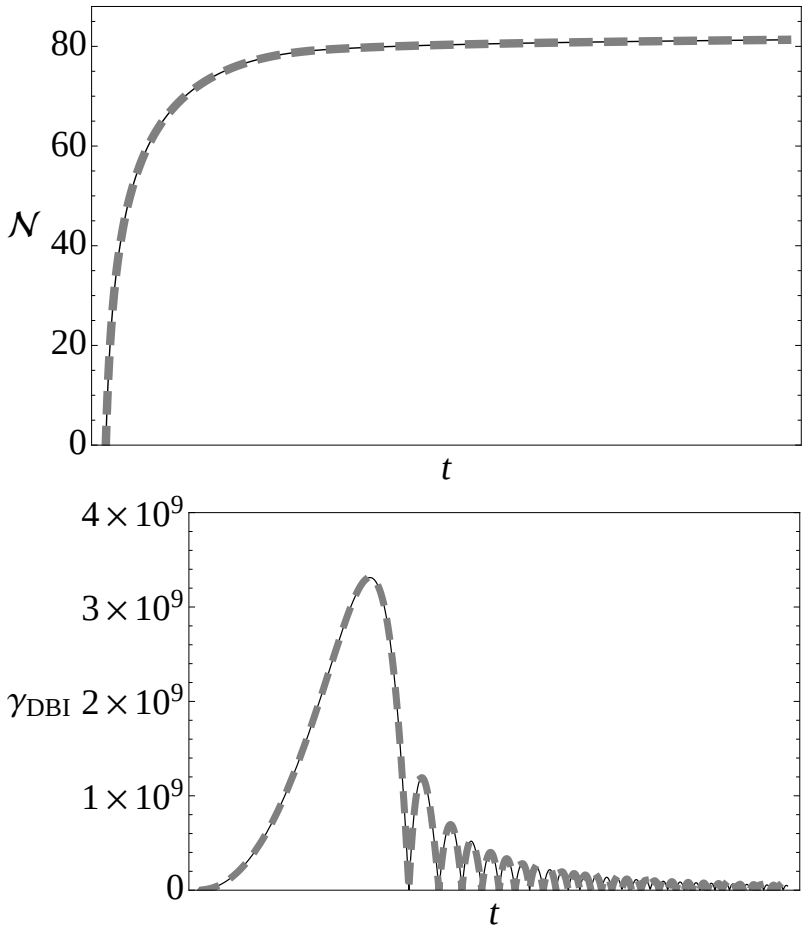

Figure 5.8: The number of e-foldings, $\mathcal{N}$, and the γ-factor, $\gamma_{\rm DBI}$, with (gray-dashed) and without (black-solid) non-linear harmonic dependent corrections for the choice of compactification parameters (4.1).

tions of the warp factor and the D3-D7 brane potential. In particular, we found that harmonic dependent corrections from the D3-D7 potential and perturbations of the warp factor do not have the effect of increasing the number of e-foldings and decreasing the $\gamma_{\rm DBI}$-factor. We therefore conclude that the most leading order harmonic dependent correction to brane (spin)inflation comes from the linearized corrections analysed in [1] with the level of non-Gaussianity remaining large.

Our analysis can be extended in several ways. One direction would be to consider different embedding functions for D7-branes with different trajectories on the deformed conifold and see how this may affect the inflationary solutions. Despite the fact that different embedding functions for D7-branes and different trajectories on the deformed conifold modify the functional form of the supergravity potential, the Kähler modulus and perturbations of the warp factor, we expect this to have a subdominant effect on the number of e-foldings and the $\gamma_{\rm DBI}$-factor. It would also be interesting to consider the possibility of a dynamical Kähler modulus (instead of stabilized) [106], and integrate the brane equations of motion for a less restricted choice of parameters. Since taking the Kähler modulus field dynamical adds to the number of brane equations of motion, we expect this to have a less trivial impact on the inflationary solutions, though we do not expect this to decrease the $\gamma_{\rm DBI}$-factor by an appreciable amount.

The other, perhaps more interesting way of extending our analysis is to consider further corrections to the inflaton action and analyse in detail the effects of cosmological perturbation theory. One particular correction comes from the contribution of the flux induced potential of harmonic type [57]. The flux induced D3-D7 potential that we considered in our inflationary analysis came from the holomorphic solution of the noncompact supergravity equation of motion which described non-linear perturbations around the ISD solution. Since the general solution should be harmonic rather than just holomorphic it would be necessary to include such harmonic contributions which have not been computed for the deformed conifold to date.

Another correction to the inflaton action arises from departures of the noncompact limit [57] considered in this paper. Despite the fact that our Planck-mass was

set large by the UV-scale we considered, it would be interesting to consider possible departures from the noncompact limit and compute further contributions to the D3-brane potential from coupling to curvature corrections which also induce harmonic dependence in brane motion [57]. In particular, coupling to the Ricci-scalar introduces a non-minimal coupling in the DBI action which corrects the $\gamma_{\rm DBI}$-factor and may have the capacity of decreasing the level of non-Gaussianity significantly [102]. It would be interesting to confirm this result in the concrete supergravity set up considered in this paper and investigate its implications for cosmological perturbations in more detail [107] in our framework.

Finally, it would be important to confirm whether in our supergravity set up multifield effects (e.g. from phase transition) induced by an instability along harmonic directions [108] do have the capacity to evade stringent constraints in cosmological perturbations for single field inflationary models. Moreover, it would be very interesting, though formidable, to consider our DBI brane inflation model along a trajectory on the deformed conifold depending on all six directions and extract the full multifield effects for cosmological perturbations in a UV/IR consistent expansion and make contact with some of the results obtained in [109] by taking the singular conifold limit. We shall leave the investigation of these for the future.

Chapter 6

Summary and conclusions

On contrary to the D-brane inflationary models constructed to realise slow-roll inflation in string theory, in string theory inflation can occur by the DBI effect with high speed and steep potentials. In this thesis we have investigated the embedding of inflation into string theory in the framework of DBI brane inflation scenario. We started with the simplest and most famous multifield DBI brane inflation scenario in IIB supergravity known as spinflation. We proceeded by including the effects of moduli stabilization in this brane inflation scenario. These effects were introduced by perturbations around the ISD solution described by the noncompact ten-dimensional supergravity equation of motion. We considered the action of the D3-brane on the warped deformed conifold subject to perturbations around the ISD solution. We derived the simplest D3-brane potential and equations of motion including beside the usual radial direction only one harmonic direction from perturbations around the ISD solution. The main focus of our analysis was on a UV/IR consistent perturbative expansion around the noncompact ISD solution. For a UV/IR consistent perturbative expansion, we determined the set of compactification parameters and solved the D3-brane equations of motion with harmonic dependence from perturbations around the noncompact ISD supergravity solution.

We first studied spinflation subject to linearized perturbations around the ISD solution described by the homogeneous solution of the noncompact supergravity equation of motion (i.e. the Laplace equation). We obtained the leading order harmonic dependent correction to the D3-brane potential from the simplest solution of

the Laplace equation on the warped deformed conifold. We analysed the parameter space and found that multifield brane motion is more sensitive to the choice of compactification parameters than to initial conditions.

We derived and solved the D3-brane equations of motion with harmonic dependence from linearized perturbations around the ISD solution. For a UV/IR consistent choice of parameters, our numerical solutions showed that linearized harmonic dependent corrections to multifield brane motion increases the inflationary capacity, compared to multifield brane motion without such corrections. However, our numerical solutions revealed in each case a very large level of non-Gaussianity rendering these multifield brane inflationary models unsatisfactory.

We then extended our analysis by studying spinflation subject to higher order non-linear perturbations around the ISD solution described by the inhomogeneous holomorphic solution of the ten-dimensional noncompact supergravity equation of motion the flux induced potential of which equals the nonperturbatively generated D3-D7 brane potential in four-dimensional supergravity. This extension was partly motivated by the fact that such non-linear corrections could potentially increase the inflationary capacity and decrease the level of non-Gaussianity. We derived the D3-D7 brane potential on the warped deformed conifold depending on the functional form of the Kähler modulus and that of D7-branes including harmonic dependence from perturbations of the warp factor. For the Kuperstein embedding of D7-branes we computed the Kähler modulus numerically and determined its exact functional form valid in both of the UV and IR regions of the warped deformed conifold. We found that integrating out the Kähler modulus within the adiabatic approximation in DBI inflation requires certain hierarchies of scales that determine the compactification parameters different from those in slow-roll models.

We derived and solved the D3-brane equations of motion with harmonic dependence from perturbations of the warp factor and the D3-D7 brane potential. For the UV/IR consistent choice of parameters and the numerically computed Kähler modulus, our numerical solutions showed that non-linear harmonic dependent corrections to brane motion do not have the effect of increasing the inflationary capacity and decreasing the level of non-Gaussianity, compared to brane motion with only

linearized harmonic dependent corrections. Therefore, we conclude that the leading order harmonic dependent corrections to multifield brane motion comes from linearized corrrections with the level of non-Gaussianity remaining large.

The main issue that we have not discussed in this thesis is cosmological perturbation theory. In particular, throughout this thesis we considered the observable noncompact four-dimensional universe to be perfectly homogeneous with the metric having the exact FRW form. In addition to that, we took the metric on the internal compact manifold to be the leading order Calabi-Yau metric. Clearly, the next step for extending our analysis would be to consider departures from such backgrounds including curvature corrections and fluctuations about the noncompact limit.

Appendix A

Rudiments of Calabi-Yau spaces

In this appendix we discuss some of relevant aspects of Calabi-Yau manifolds used in the thesis, following closely [110, 111] and [26, 27]. We first outline the nonlinear sigma-model leading to Ricci-flat Kähler manifolds known as Calabi-Yau manifolds. We then discuss the cohomology of Calabi-Yau three-folds and complete intersection Calabi-Yau three-folds which will be needed for our main discussion including the moduli space of Calabi-Yau manifolds and their conifold points.

A.1 The nonlinear sigma-model

The most popular approach to superstrings is to consider $1+1$-dimensional superconformally invariant quantum field theories over the world-sheet. The world-sheet denoted Σ is embedded in ten-dimensional spacetime denoted M_{9+1} and our four-dimensional spacetime denoted M_{3+1} emerges upon compactification by which M_{9+1} is replaced by $M_{3+1} \times \mathcal{M}$, where $\mathcal{M}$ is an internal manifold. In this approach it is natural to consider the space of mappings $X^\mu(\sigma)$ from the world-sheet Σ into the internal manifold $\mathcal{M}$, equipped with the action functional describing the propagation of superstrings

$$\begin{aligned} S_{\mathcal{M}} &= \frac{1}{\pi\alpha'}\int \{(B_{\mu\bar{\nu}} + iG_{\mu\bar{\nu}})(\bar{\partial}X^\mu \partial X^{\bar{\nu}}) - \big(B_{\mu\bar{\nu}} - iG_{\mu\bar{\nu}}\big)(\partial X^\mu \bar{\partial} X^{\bar{\nu}})\} \\ &\qquad + \text{SUSY completion} \cdots \end{aligned} \tag{A.1.1}$$

which is the integrated total 'energy' of Σ immersed in $\mathcal{M}$. Here, $G_{\mu\bar{\nu}}(X)$ is a general Hermitian metric on $\mathcal{M}$, $B_{\mu\bar{\nu}}(X)$ is the antisymmetric tensor, the dilaton Φ[1] involves the diagonal part of $G_{\mu\bar{\nu}}$ and $\int_\Sigma$ is the reparametrization invariant integration over the world-sheet Σ. A field theory such as (A.1.1), in which the kinetic term is field-dependent and so field space is effectively a curved manifold, is known as a non-linear sigma-model. The sigma-model is chosen to have full $(2,2)$-supersymmetry on the world-sheet, the background (vacuum) metric is Kähler and the background value of $B_{\mu\bar{\nu}}$ vanishes:

$$\begin{aligned} S_{\mathcal{M}} &= \int_\Sigma d^2\sigma d^2\xi d^2\bar{\xi}\mathcal{K}(\mathbf{X},\bar{\mathbf{X}}) \\ G_{\mu\bar{\nu}}(\mathbf{X},\bar{\mathbf{X}}) &= \partial_\mu\partial_{\bar{\nu}}\mathcal{K}(\mathbf{X},\bar{\mathbf{X}})\big|_{\xi=\bar{\xi}=0}, \end{aligned} \tag{A.1.2}$$

where $(\sigma^0,\sigma^1;\xi^\pm,\bar{\xi}^\pm)$ denote the coordinates of the $(2,2)$-super Riemann surface of genus g_Σ, $\mathbf{X}^\mu$ are the coordinate chiral superfields and $\partial_\mu = \partial/\partial\mathbf{X}^\mu$. The required conformal invariance of the sigma-model implies that $G_{\mu\bar{\nu}}$ is Ricci-flat, to lowest order. Thus the internal manifold is a Ricci-flat Kähler manifold known as Calabi-Yau manifold, which we turn to discuss now.

A.2 Kähler manifolds

A complex manifold X is a real, even-dimensional manifold equipped with a geometric structure called a complex structure. To see how the complex structure comes about, let X be a real, even-dimensional manifold. We define an almost complex structure J on X to be a smooth tensor J^b_a on X satisfying $J^b_a J^b_c = -\delta^c_a$. Let v be a smooth vector field on X, written v^a in index notation, and define a new vector field Jv by $(Jv)^b = J^b_a v^a$. Therefore J operates linearly on vector fields. The equation $J^b_a J^b_c = -\delta^c_a$ implies that $J(Jv) = -1$, so that $J^2 = -1$. It is indicative that J gives each tangent space T_pX the structure of a complex vector space. By gluing these spaces together we obtain a tangent bundle denoted TX and the almost complex structure is associated with endomorphism J of the tangent bundle satisfying:

[1] As briefly discussed chapter 2, these form the bosonic content of string spectrum.

$$J : TX \to TX \quad \text{with} \quad J^2 = -\text{id}. \tag{A.2.3}$$

For all smooth vector fields v and w on X, we may define a vector field $N_J(v, w)$ by:

$$N_J(v, w) = [v, w] + J([Jv, w] + [v, Jw]) - [Jv, Jw], \tag{A.2.4}$$

where $[\,,]$ is the Lie bracket of vector fields. The vector field N_J is a tensor, meaning that $N_J(v, w)$ is pointwise bilinear in v and w. N_J is often called the Nijenhuis tensor of J. If $N_J \equiv 0$ we then call J a complex structure and X a complex manifold. Clearly the eigenvalues of J are $\pm i$ associated with are the eigenspaces $T^{1,0}$ and $T^{0,1}$, called the holomorphic and antiholomorphic tangent bundle, respectively. The tangent bundle of X can be written as the direct sum of these subspaces

$$T_{\mathbb{C}}X = T^{1,0}X \oplus T^{0,1}X. \tag{A.2.5}$$

On a complex manifold X, we may also denote the holomorphic cotangent bundle $T^*_{\mathbb{C}}X$ for holomorphic complex dual of $T_{\mathbb{C}}X$ on X and have

$$T^*_{\mathbb{C}}X = (T^*X)^{1,0} \oplus (T^*X)^{0,1}. \tag{A.2.6}$$

The cotangent bundle T^*X is also identified with the bundle of holomorphic one-forms denoted Ω^1_X. The bundle of holomorphic n-forms (also called holomorphic volume forms) is the determinant bundle of T^*X

$$\Omega = \wedge^n \Omega^1_X = \det T^*X \stackrel{\text{def}}{=} \mathcal{K}_X \tag{A.2.7}$$

On an almost complex manifold X one has the complex vector bundles

$$\bigwedge\nolimits^k_{\mathbb{C}} X \stackrel{\text{def}}{=} \bigwedge\nolimits^k (T_{\mathbb{C}}X)^* \quad \text{and} \quad \bigwedge\nolimits^{p,q} X \stackrel{\text{def}}{=} \bigwedge\nolimits^p (T^{1,0}X)^* \otimes \bigwedge\nolimits^q (T^{0,1}X)^*. \tag{A.2.8}$$

Their (sheaves of) sections are denoted by A^k_X and $A^{p,q}_X$, respectively. Elements in $A^{p,q}(X)$, i.e. sections of $A^{p,q}_X$, are called (p, q)-forms. There exists a natural direct sum decomposition in terms of these (p, q)-forms

$$\bigwedge\nolimits^k_{\mathbb{C}} X = \bigoplus_{p+q=k} \bigwedge\nolimits^{p,q}_{\mathbb{C}} X \qquad \text{and} \qquad A^k_{X,\mathbb{C}} = \bigoplus_{p+q=k} A^{p,q}_X, \tag{A.2.9}$$

the complex conjugation of which is given by

$$\overline{\bigwedge\nolimits^{p,q} X} = \bigwedge\nolimits^{q,p} X \qquad \overline{A^{p,q}_X} = A^{q,p}_X. \tag{A.2.10}$$

If $d : A^k_{X,\mathbb{C}} \to A^{k+1}_{X,\mathbb{C}}$ is the $\mathbb{C}$-linear extension of the exterior differential, then we may write $d = \partial + \bar{\partial}$ and define the nilpotent operators

$$\partial : A^{p,q}_X \longrightarrow A^{p+1,q}_X \qquad \partial \cdot \partial = 0, \tag{A.2.11}$$

$$\bar{\partial} : A^{p,q}_X \longrightarrow A^{p,q+1}_X \qquad \bar{\partial} \cdot \bar{\partial} = 0. \tag{A.2.12}$$

Using this, we may define the (p, q)-Dolbeault cohomology as

$$H^{p,q}(X) \stackrel{\text{def}}{=} \frac{\mathrm{Ker}(\bar{\partial} : A^{p,q}(X) \longrightarrow A^{p,q+1}(X))}{\mathrm{Im}(\bar{\partial} : A^{p,q-1}(X) \longrightarrow A^{p,q+1}(X))}. \tag{A.2.13}$$

The topological invariants are the Hodge numbers defined by:

$$h^{p,q} \stackrel{\text{def}}{=} \dim H^{p,q}_{\bar{\partial}}(X) \tag{A.2.14}$$

Every complex manifold X underlies a real manifold which is Riemanian if endowed with a Riemanian metric g. If the for any point $x \in X$ the scalar product g_x on T_xX is compatible with the almost complex structure (A.2.3) J_x, then the metric g is called Hermitian and the complex manifold is called an Hermitian manifold. Associated with an Hermitian metric g on X is the fundamental $(1, 1)$-form $\omega \stackrel{\text{def}}{=} g(JX, Y)$, which in terms of local coordinates reads as

$$\omega \stackrel{\text{def}}{=} i g_{\mu\bar{\nu}} dz^\mu \wedge dz^{\bar{\nu}}. \tag{A.2.15}$$

This fundamental form is called Kähler form if it is closed,

$$d\omega = 0. \tag{A.2.16}$$

In this case the Hermitian metric $g_{\mu\bar{\nu}}$ is Kähler and the complex Hermitian manifold $\mathcal{M}$ is a Kähler manifold. The cohomology class of ω is called the Kähler class and

the space of choices of the Kähler class forms the Kähler cone (for more detail see below). Locally, the Kähler metric can be expressed in terms of the the Kähler potential $\mathcal{K}(z,\bar{z})$ as

$$g_{\mu\bar{\nu}} = \frac{\partial}{\partial z^{\mu}} \frac{\partial}{\partial \bar{z}^{\bar{\nu}}} \mathcal{K}(z,\bar{z}). \tag{A.2.17}$$

The Kähler potential need not to be globally defined. The potential

$$\mathcal{K}'(z,\bar{z}) = \mathcal{K}(z,\bar{z}) + f(z) + f(z)^* \tag{A.2.18}$$

gives the same metric. This transformation is called Kähler transformation.

Equipped with an Hermitian metric on X we may consider the Hermitian scalar product $\langle \alpha, \beta \rangle$ for any $\alpha, \beta \in A^{p,q}$ and define the adjoint operators $\bar{\partial}^{\dagger}$ and $\partial^{\dagger}$ with respect to this Hermitian product

$$\langle \bar{\partial}^{\dagger}\alpha, \beta \rangle \stackrel{\text{def}}{=} \langle \alpha, \bar{\partial}\beta \rangle, \qquad \langle \partial^{\dagger}\alpha, \beta \rangle \stackrel{\text{def}}{=} \langle \alpha, \partial\beta \rangle. \tag{A.2.19}$$

In more detail, according to the Hodge $*$-operator

$$* : A^{p,q} \longrightarrow A^{n-q,n-p}, \tag{A.2.20}$$

we may define the adjoint operators as

$$\bar{\partial}^{\dagger} \stackrel{\text{def}}{=} - * \bar{\partial} * \qquad \partial^{\dagger} \stackrel{\text{def}}{=} - * \partial * . \tag{A.2.21}$$

Given these adjoint operators, we may define the Laplacian on X as

$$\Delta_{\bar{\partial}} \stackrel{\text{def}}{=} \bar{\partial}^{\dagger}\bar{\partial} + \bar{\partial}\bar{\partial}^{\dagger}, \qquad \Delta_{\partial} \stackrel{\text{def}}{=} \partial^{\dagger}\partial + \partial\partial^{\dagger}. \tag{A.2.22}$$

Clearly, the Laplace operators respect the bidegree,

$$\Delta_{\bar{\partial}},\, \Delta_{\partial} : A^{p,q}(X) \longrightarrow A^{p,q}(X). \tag{A.2.23}$$

A form $\alpha \in \mathcal{A}^k(X)$ annihilated by the Laplacian, i.e. $\Delta_{\bar{\partial}}(\alpha) = 0$, is called "$\bar{\partial}$-harmonic". The space of harmonic forms are denoted by

$$\mathcal{H}^k_{\bar{\partial}}(X) \stackrel{\text{def}}{=} \{\alpha \in A^k_{\mathbb{C}}(X) \mid \Delta_{\bar{\partial}}(\alpha) = 0\}, \tag{A.2.24}$$

$$\mathcal{H}^{p,q}_{\bar\partial}(X) \stackrel{\text{def}}{=} \{\alpha \in A^{p,q}_{\mathbb{C}}(X) \mid \Delta_{\bar\partial}(\alpha) = 0\}. \tag{A.2.25}$$

In a similar way, one defines ∂-harmonic forms and the spaces $\mathcal{H}^k_\partial(X)$ and $\mathcal{H}^{p,q}_\partial(X)$. The spaces $\mathcal{H}^k_\partial(X)$ and $\mathcal{H}^k_{\bar\partial}(X)$ respect the bidegree decompositions

$$\mathcal{H}^k_{\bar\partial}(X) = \bigoplus_{p+q=k} \mathcal{H}^{p,q}_{\bar\partial}(X), \quad \mathcal{H}^k_\partial(X) = \bigoplus_{p+q=k} \mathcal{H}^{p,q}_\partial(X). \tag{A.2.26}$$

The Hodge $*$-operator induces $\mathbb{C}$ linear isomorphisms

$$* : \mathcal{H}^{p,q}_{\bar\partial}(X) \simeq \mathcal{H}^{n-q,n-p}_\partial(X). \tag{A.2.27}$$

If the Hermitian manifold is compact, then we have a non-degenerate pairing

$$\mathcal{H}^{p,q}_{\bar\partial}(X) \times \mathcal{H}^{n-q,n-p}_\partial(X) \longrightarrow \mathbb{C}, \quad (\alpha, \beta) \longrightarrow \int_X \alpha \wedge \beta. \tag{A.2.28}$$

This give the Serre duality on the level of harmonic forms

$$\mathcal{H}^{p,q}_{\bar\partial}(X) \simeq \mathcal{H}^{n-q,n-p}_\partial(X)^*. \tag{A.2.29}$$

On a Kähler manifold both decompositions (A.2.26) coincide the and for Laplace operators (A.2.22) we have

$$\Delta_\partial = \Delta_{\bar\partial}. \tag{A.2.30}$$

Furthermore, on a Kähler manifold there exists the decomposition

$$H^k(X, \mathbb{C}) = \bigoplus_{p+q=k} H^{p,q}(X). \tag{A.2.31}$$

There are also the following relations:

• Hodge star duality

$$* : H^{p,q}(X) \simeq H^{n-q,n-p}(X) \tag{A.2.32}$$

• Complex conjugation

$$\overline{H^{p,q}}(X) = H^{q,p}(X), \tag{A.2.33}$$

• The Serre duality (A.2.29) yields

$$H^{p,q}(X) = H^{n-p,n-q}(X)^*. \tag{A.2.34}$$

According to these relations, we can write down the Hodge numbers of a compact Kähler manifold X as

$$b^k = \sum_{j=0}^{k} h^{j,k-j}, \quad h^{p,q} = h^{q,p} = h^{m-p,m-q} = h^{m-q,m-p}. \tag{A.2.35}$$

Apart from cohomology groups which describe important properties of X, there are holonomy groups which classify such manifolds. On a manifold X, we may consider parallelly transporting a vector $\vec{v}_p$ tangent to X at $p \in X$, along a closed path back to p. The transformation required to bring the parallelly transported vector $\vec{v}'_p$ back to the original $\vec{v}_p$ is called holonomy. The set of such transformations, parameterized by closed paths in X containing p forms a group called holonomy group, which is independent of the choice of $p \in X$. In the case contractible paths, the resulting group is called the restricted holonomy group, which is isomorphic to the holonomy algebra. On a n-dimensional Kähler manifold the holonomy algebra must be contained in $\mathfrak{u}(n)$. The Riemann tensor simplifies to

$$R_{\mu\bar{\nu}\rho}{}^{\bar{\sigma}} = \partial_\mu \Gamma_{\bar{\nu}\rho}{}^{\bar{\sigma}} = R_{\mu\bar{\rho}\nu}{}^{\bar{\sigma}}, \qquad \Gamma_{\bar{\nu}\rho}{}^{\bar{\sigma}} = g^{\tau\bar{\sigma}} \partial_{\bar{n}u} g_{\tau\bar{\rho}}, \tag{A.2.36}$$

and the Ricci-tensor takes the form

$$R_{\mu\bar{\nu}} \overset{\text{def}}{=} R_{\mu\bar{\sigma}\bar{\nu}}{}^{\bar{\sigma}} = R_{\mu\bar{\nu}\bar{\sigma}}{}^{\bar{\sigma}}. \tag{A.2.37}$$

On a Kähler manifold the Ricci-tensor can be written in the form

$$R_{\mu\bar{\nu}} = \partial_\mu \partial_{\bar{\nu}} \ln\, g^{1/2}, \quad g^{1/2} = \mathrm{Det}[g_{\mu\bar{\nu}}]. \tag{A.2.38}$$

An important example of a Kähler manifold is the complex projective space $\mathbb{P}^n$, where $\ln\, g^{1/2}$ is the Fubini-Study metric. Associated with the Riemann tensor is the $\mathfrak{u}(n)$-valued Riemann $(1,1)$-form

$$\Theta_{\bar{\rho}}^{\bar{\sigma}} \stackrel{\text{def}}{=} dz^{\mu} \wedge dz^{\bar{\nu}} R_{\mu\bar{\nu}\bar{\rho}}{}^{\bar{\sigma}}, \tag{A.2.39}$$

and the corresponding Ricci $(1,1)$-form is given by

$$\Theta \stackrel{\text{def}}{=} \Theta_{\bar{\rho}}^{\bar{\rho}}, \tag{A.2.40}$$

which is the $\mathfrak{u}(1)$-valued trace of the Riemann $(1,1)$-form. As we shall briefly discuss in the next section, in superstring compactifications only manifolds of special holonomy for which the Ricci $(1,1)$-form and hence the Ricci tensor vanishes, guarantee the resulting $3+1$-dimensional model to be physically consistent.

A.3 Calabi-Yau manifolds

In string theory it is well known that strings propagate in 9+1-dimensional Minkowski spacetime (denoted M_{9+1}). In order to obtain the usual 3+1-dimensional Minkowski spacetime (denoted M_{3+1}) one has to compactify M_{9+1} by replacing it with $M_{3+1} \times \mathcal{M}$. As we shall discuss below, the phenomenologically motivated $N = 1$ local supersymmetry and other consistency requirements imply that $\mathcal{M}$ is a Calabi-Yau space. This ansatz was originally introduced in [25] by taking the 'point-field limit' restricting in the outset to the massless modes of the $9+1$-dimensional string theory with the assumption that $\mathcal{M}$ is smooth.

A.3.1 Motivation

The first attempt in superstring compactifications was to make the heterotic string physically realistic. This involves restricting to the massless modes and replacing the $9+1$-dimensional Minkowski spacetime, M_{9+1}, with a product of a $3+1$-dimensional maximally symmetric spacetime and some 'internal' compact manifold $\mathcal{M}$. For the $3+1$-dimensional model to have $N = 1$ supersymmetry, consistency will require the $3+1$-dimensional spacetime to be Minkowskian, M_{3+1}, and $\mathcal{M}$ to be Ricci-flat and Kähler if Riemannian.

The supersymmetry parameter in the original heterotic string model is a spinor transforming as the $\mathbf{8}_S$ representation of the $SO(8)$ helicity subgroup of the Lorentz

group $SO(1,9)$. By compactifying M_{9+1} to $M_{3+1} \times \mathcal{M}$, the helicity subgroup gets broken to $SO(2) \times SO(6)$ and the 8-component spinor yields four 2-component spinors of $SO(2)$, which correspond to four independent supersymmetries in the 3+1-dimensional sense. For parametrizing the $N = 1$ supersymmetry of the effective 3+1-dimensional model, one and only one linear combination of these is needed. To have no prefered spinor in the $3+1$-dimensional effective model, the background values of fermionic fields are chosen to vanish. Consistency then requires the supersymmetry transformations to preserve this ansatz along one of the component supersymmetries. The supersymmetry transformations take the form:

$$\delta_\varepsilon \langle \mathbf{B} \rangle = \varepsilon \cdot \langle \mathbf{F} \rangle, \qquad \delta_\varepsilon \langle \mathbf{F} \rangle = \varepsilon \cdot \langle \mathbf{B}' \rangle. \tag{A.3.41}$$

Here ε parametrizes the supersymmetry transformations, $\langle \mathbf{B} \rangle$ and $\langle \mathbf{F} \rangle$ depend on the background fields and transform as tensorial (spinorial) representations of the Lorentz group. The condition $\langle \mathbf{F} \rangle = 0$ requires $\langle \mathbf{B}' \rangle = 0$, which constrains the various background fields relating to $\mathcal{M}$ and by that determines its geometry, the vacuum configuration. Furthermore, it is assumed that M_{3+1} has maximal symmetry making it Minkowskian order by order in the string tension α', and the connection on $\mathcal{M}$ is chosen to be torsion-free leaving only Riemannian candidates for $\mathcal{M}$. The (later) manifolds are in part classified by their holonomy groups (see previous section). Now note that spinors in odd-dimensional spaces are pseudoreal, so if the $\mathcal{M}$ contains an odd-dimensional factor the emerging $3 + 1$-dimensional model will have to have particles of both helicities. This would accompany the left handed neutrino with a right handed neutrino, in gross contradiction with experiment. This contradiction can be avoided only if, $\mathcal{M}$ has $\mathfrak{su}(3)$ holonomy for which one spinor together with its conjugate is invariant under holonomy and taken to be covariantly constant on $\mathcal{M}$ and will guarantee $N = 1$ supersymmetry in M_{3+1}. Recall from the previous section that on a n-dimensional Kähler manifold the holonomy algebra must be contained in $\mathfrak{u}(n) \approx \mathfrak{su}(n) \times \mathfrak{u}(1)$, where $\mathfrak{u}(1)$ is generated by the trace of the $\mathfrak{u}(n)$ generators. Being interested in the (complex) three-dimensional case and wanting the holonomy to be $\mathfrak{su}(3)$ instead of the full $\mathfrak{u}(3)$, there must exist a metric for which the Ricci $(1,1)$-form (A.2.40) and hence the Ricci-tensor (A.2.37)

vanishes. Kähler manifolds of this special type are known as Calabi-Yau manifolds, the existence of which was first conjectured by Calabi and then proven by Yau.

A.3.2 Calabi-Yau three-folds

Now given a complex manifold X over which l is a holomorphic line bundle with a nontrivial global holomorphic section f, we can define a subspace $\mathcal{M} \subset X$ to consist of all points $x \in X$ for which $f(x) = 0$. Considering f as a mapping that takes all points $x \in \mathcal{M} \subset X$ to 0, we write $\mathcal{M} = f^{-1}(0)$ and call $\mathcal{M}$ a hypersurface in X. The hypersurface $\mathcal{M}$ fails to be a complex submanifold if f is singular, which is the case when there is at least one point where both f and all its gradients $\partial_\mu f$ vanish. On the contrary, if at every point $x \in X$ at least one section if l is nonzero, the a generic section of l defines a nonsingular hypersurface $\mathcal{M} \stackrel{\text{def}}{=} f^{-1}(0)$. If $\mathcal{M}$ has three complex dimensions and is Ricci-flat Kähler with $SU(3)$ holonomy it defines a Calabi-Yau three-fold.

One way to describe a Calabi-Yau three-fold $\mathcal{M}$ is to look at its cohomology groups $H^{p,q}_{\bar\partial}(\mathcal{M})$, where $h^{p,q} \stackrel{\text{def}}{=} \dim H^{p,q}_{\bar\partial}(\mathcal{M})$. We note that any compact Kähler manifold with trivial canonical bundle is Ricci-flat. Thus by a Calabi-Yau three-fold we mean (here) a compact Kähler manifold of dimension $n = 3$ with trivial canonical bundle. The triviality of the canonical bundle means that $\mathcal{M}$ has to admit a nonsingular and nowhere vanishing holomorphic volume form Ω such that $\Omega' = \lambda\Omega$. Now given the nowhere vanishing holomorphic three-form Ω on our three-fold $\mathcal{M}$, we get the following isomorphism:

$$\Omega : T\mathcal{M} \xrightarrow{\sim} \wedge^2 T^*\mathcal{M}, \tag{A.3.42}$$

which yields

$$\Omega : H^q(\mathcal{M}, T\mathcal{M}) \xrightarrow{\sim} H^{2,q}(\mathcal{M}). \tag{A.3.43}$$

This means that to every holomorphic tangent vector v^μ, there is a projectively unique holomorphic two-form $\omega_{\nu\rho} \stackrel{\text{def}}{=} v^\mu \Omega_{\mu\nu\rho}$. Thus the three-form Ω is the (trivial) section of the of the trivial canonical bundle $\mathcal{K}_\mathcal{M} \approx \mathbb{C}_\mathcal{M}$. The triviality implies that

the Serre duality

$$H^q(\mathcal{M},\mathcal{V})^* \approx H^{3-q}(\mathcal{M},\mathcal{V}\otimes\mathcal{K}_{\mathcal{M}}) \tag{A.3.44}$$

simplifies to the following relation with $\otimes\mathcal{K}_{\mathcal{M}}$ dropped

$$H^q(\mathcal{M},T\mathcal{M})^* \approx H^{3-q}(\mathcal{M},T^*\mathcal{M}). \tag{A.3.45}$$

This together with (A.3.42) implies

$$H^{2,q}(\mathcal{M})^* \approx H^{3-q}(\mathcal{M},T^*\mathcal{M}) \equiv H^{1,3-q}(\mathcal{M}). \tag{A.3.46}$$

In addition to this, because of $H^{3,0}(\mathcal{M}) \approx \mathbb{C}$ there is a new duality giving

$$H^{p,0}(\mathcal{M})^\star \approx H^{3-p,0}(\mathcal{M}). \tag{A.3.47}$$

By using the holomorphic duality relations (A.3.45) and (A.3.47) together with with Hodge star duality (A.2.32) and complex conjugation (A.2.33) we can derive the Hodge numbers of Calabi-Yau three-folds. To derive the Hodge numbers, $h^{p,q}$, on Calabi-Yau three-fold we first note that $h^{p,q} \equiv 0$ for $p+q > 6$. The rest of the (nonvanishing) Hodge numbers on Calabi-Yau three-folds can be determined as follows. Hodge star duality (A.2.32), $h^{p,q} = h^{n-q,n-p}$, with the assumption that the manifolds that we are considering have a single connected piece which for complex three-folds $h^{3,3} = 1$ implies $h^{3,3} = h^{0,0} = 1$. The combination of Hodge star duality with complex conjugation (A.2.33), $h^{p,q} = h^{q,p}$, implies $h^{3,2} = h^{2,3} = h^{0,1} = h^{1,0}$. The combination of Hodge star duality with complex conjugation, and the holomorphic duality relations (A.3.45) and (A.3.47), $h^{0,q} = h^{0,3-q}$ and $h^{p,0} = h^{3-p,0}$, implies $h^{3,0} = h^{0,0} = 1$ and $h^{3,1} = h^{1,3} = h^{2,0} = h^{0,2} = h^{1,0}$. To determine $h^{1,0}$ we note that for any harmonic s-form ω we may write:

$$F(\omega) = R^n_m \omega_{[nr_2\cdots r_s]}\omega^{[nr_2\cdots r_s]} + \frac{s-1}{2} R^{n\ q}_{m\ p}\omega_{[nqr_3\cdots r_s]}\omega^{[mpr_3\cdots r_s]}, \tag{A.3.48}$$

where R^n_m and $R^{n\ q}_{m\ p}$ are Ricci and Riemann tensors, respectively. Then, if $F(\omega)$ is positive semi-definite, ω is covariently constant. Now choosing the Ricci-flat

metric on our Calabi-Yau three-fold, $R^n_m = 0$, implies $F(\omega) \equiv 0$ for one-forms. Thus the for ω to be harmonic it also has to be covariently constant. But on the other hand we know that ω cannot be covariently constant because it transforms as $\mathbf{3} \oplus \mathbf{3}^*$ under $SU(3)$ holonomy and therefore transforms nontrivially under parallel transport. Hence $h^1 = h^{1,0} = h^{0,1} = 0$. In total, for Calabi-Yau three-folds thw Hodge numbers are:

$$h^{3,1} = h^{1,3} = h^{2,0} = h^{0,2} = h^{1,0} = 0, \qquad h^{3,3} = h^{3,0} = h^{0,3} = h^{0,0} = 1 \tag{A.3.49}$$

Thus the only Hodge numbers that remain undetermined are:

$$h^{1,1}, \qquad h^{2,1} = h^{1,2} \tag{A.3.50}$$

The Hodge numbers $h^{1,1}$ and $h^{2,1}$ give number of possible Kähler forms and the dimension of the moduli space of complex structures, respectively (see Sec. 4 below). The question that arises here is whether one can find coordinates on moduli space and construct the explicit form of the metric. As we shall discuss below, for a special class of complete intersection Calabi-Yau three-folds, known as conifolds, the explicit form of the metric can be constructed (see Sec. 5 below).

A.3.3 Complete intersection Calabi-Yau 3-folds

One of the simplest and most popular ways of constructing Calabi-Yau manifolds is to consider hypersurface solutions in $\mathbb{P}^n$. The submanifold in $\mathbb{P}^n$ is Kähler (inheriting this property from $\mathbb{P}^n$) and vanishing of the restriction to hypersurface of the Ricci-tensor computed from the restriction of the Fubini–Study metric on $\mathbb{P}^n$ yields Calabi-Yau manifold as Polynomial solution of degree $q = n+1$. This can be generalized to a complete intersection of hypersurfaces in a product of complex projective spaces given by

$$\mathscr{M} \overset{\text{def}}{=} \mathbb{P}^n_1 \times \cdots \times \mathbb{P}^{n_m}_m. \tag{A.3.51}$$

By definition a complete intersection manifold is a manifold $\mathcal{M}$ embedded as a complete intersection of hypersurfaces

$$\mathcal{M} = X^1 \cap \cdots \cap X^K \hookrightarrow \mathscr{M}. \tag{A.3.52}$$

Here $\mathscr{M}$ is the embedding space and each hypesurface X^a is defined as the zero locus of a suitably chosen holomorphic polynomial

$$X^a : f^a(z_{(1)}, ..., z_{(m)}) = 0, \quad a = 1, ..., K, \tag{A.3.53}$$

which is homoneneous of degree q_a^r with respect to the homogeneous coordinates of $z_{(r)}$ of $\mathbb{P}^{n_r}_r$.

Each homogeneous polynomial f^a can be regarded as a holomorphic section of the line bundle

$$\mathcal{E} = \bigoplus_{n=1}^{K} \mathcal{E}_a, \quad \mathcal{E}_a \stackrel{\text{def}}{=} \bigotimes_r \mathcal{O}_r(q_a^r), \tag{A.3.54}$$

where $\mathcal{O}_r(1)$ stands for the hyperplane line bundle over $\mathbb{P}^{n_r}_r$.

Now let $\mathcal{E}$ be a vector bundle over $\mathscr{M}$ the sections of which form the defining system of constrains for the embedded three-fold $\mathcal{M}$. We may define a configuration by a pair $[\mathscr{M}||\mathcal{E}]$ being a matrix of an m-dimensional positive integer valued column vector n_r and an $m \times K$-dimensional positive valued matrix q_a^r of the form:

$$\begin{matrix} \mathbb{P}^{n_1} \\ \vdots \\ \mathbb{P}^{n_m} \end{matrix} \begin{bmatrix} q_1^1 & \dots & q_K^1 \\ \vdots & \ddots & \vdots \\ q_1^m & \dots & q_K^m \end{bmatrix}. \tag{A.3.55}$$

The configuration consists of the family of all complete intersections defined by a system of polynomial constrains which are represented by a configuration matrix and parametrized by the space of coefficients. This collection of varieties forms a deformation class. The configuration is represented by a configuration matrix and for a specific member of the configuration, i.e. a complete intersection space $\mathcal{M}$, one has:

$$\check{\mathcal{M}} \in \begin{matrix} \mathbb{P}^{n_1} \\ \vdots \\ \mathbb{P}^{n_m} \end{matrix} \begin{bmatrix} q_1^1 & \dots & q_K^1 \\ \vdots & \ddots & \vdots \\ q_1^m & \dots & q_K^m \end{bmatrix}. \tag{A.3.56}$$

We also note that

$$\dim\mathcal{M} = \dim\mathscr{M} - K, \quad \dim\mathscr{M} = \sum_{r=1}^{m} n_r. \tag{A.3.57}$$

The condition that each member of the configuration $[\mathscr{M}||\mathcal{E}]$ admits a Ricci-flat Kähler metric is:

$$\sum_{n=1}^{K} q_r^a = n + 1 \tag{A.3.58}$$

We now would like to discuss a particular example of a configuration which will lead us to the conifold. Consider the configuration

$$\check{\mathcal{M}} \in \begin{matrix}\mathbb{P}^5 \\ \mathbb{P}^1\end{matrix}\begin{bmatrix}4 & 1 & 1\\ 0 & 1 & 1\end{bmatrix}. \tag{A.3.59}$$

The defining equations of this configuration are encoded by the columns of this matrix and can be written in the form

$$\begin{aligned} Q(x) &= 0, \\ x^1y^1 + x^2y^2 &= 0, \\ x^3y^1 + x^4y^2 &= 0. \end{aligned} \tag{A.3.60}$$

Alternatively, we may rewrite the above configuration as

$$\check{\mathcal{M}} \in \begin{matrix}\Upsilon \\ \mathbb{P}^1\end{matrix}\begin{bmatrix}1 & 1\\ 1 & 1\end{bmatrix} \tag{A.3.61}$$

with Υ being the quartic 4-fold in $\mathbb{P}^5$ described by choice of transverse polynomials $Q(x) = \sum_{a=1}^{6}(x^a)^4 = 0$.

By choosing any specific value for $x \in \Upsilon$, (A.9) is reduced to a linear set of equations in the variable y^1 and y^2. Regarding y^1 and y^2 as the coordinates of $\mathbb{P}^1$ means that both of them cannot vanish and therefore the determinant of the coefficients must be zero:

$$\mathcal{C}(x) \stackrel{\text{def}}{=} x^1x^4 - x^2x^3 = 0. \tag{A.3.62}$$

This equation describes a Calabi-yau hypersurface $\mathcal{M}^\sharp \subset \Upsilon$ obtained by the projection $\mathcal{M}^\sharp = \wp(\check{\mathcal{M}})$ along $\mathbb{P}^1$ in (A.9). To see that $\mathcal{M}^\sharp$ is singular at $x_1, x_2, x_3, x_4 = 0$, note that $\mathcal{M}^\sharp$ is the intersection of the quartic $Q(x) = 0$ and the quadric $\mathcal{C}(x) = 0$ in $\mathbb{P}^5$, and that $Q(x)$, $\mathcal{C}(x)$, and $d\mathcal{C}(x)$ vanish at $x_1, x_2, x_3, x_4 = 0$. The choice $Q(x) = \sum_{a=1}^{6}(x^a)^4$ requires the singular points to be at $(0:0:0:0:1:\omega)$, where $\omega = -1$. Singularities from such projections arise at points and are nodes (see next section). Finally, we note that the singularity of $\mathcal{M}^\sharp$ can be smoothed out (see next section) by considering a quadric perturbation in the defining equation (A.3.62) of $\mathcal{M}^\sharp \subset \Upsilon$, i.e. $\mathcal{C}(x) = r^2(x) = t \cdot \sum_{a=1}^{6}(x^a)^2$, which is non-zero at the nodes of $\mathcal{M}^\sharp$ and defines for small $t \neq 0$ a non-singular quadric $\mathcal{M}_t^\flat$ in Υ in $\mathbb{P}^5$.

A.4 Nodes and smoothings

In this section we discuss nodes and smoothings. This together with the discussion of the previous subsection enables us to discuss the conifold and moduli space of Calabi-Yau manifolds in the next sections.

A.4.1 Smoothings in general

Given a singular complex manifold $\mathcal{M}$ containing an isolated singular point p, we smooth $\mathcal{M}$ into $\widehat{\mathcal{M}}$ by replacing $p \in \mathcal{M}$ with something bigger, called an exceptional set E. These sets are seen as formal sums of noncontractable subspaces of the resolved space $\widehat{\mathcal{M}}$. In this way, one smoothes $\mathcal{M}$ into $\widehat{\mathcal{M}}$ by stretching the singular points into bigger-than-zero dimensional exceptional sets. In a real six-dimensional space, this may be achieved by replacing the singular point p with exceptional sets of $\dim_{\mathbb{R}} E = 1, 2, 3, 4, 5$. However, The cases $\dim_{\mathbb{R}} E = 1$ and $\dim_{\mathbb{R}} E = 5$ are related by Poincare duality and are uninteresting by the following reason. The case $\dim_{\mathbb{R}} E = 1$ corresponds to exceptional sets of noncotractable circles and would imply that $H_1(\widehat{\mathcal{M}})$ - and hence $H^1(\widehat{\mathcal{M}})$ - would become nonvanishing, the holonomy of $\widehat{\mathcal{M}}$ would have to be a proper subgroup of $SU(3)$, resulting either $N = 2$ or no supersymmetry, either case of which seem to be not physically relevant. Thus the remaining relevant cases are $\dim_{\mathbb{R}} E = 2, 3 \text{ or } 4$.

• In the case $\dim_{\mathbb{R}} E = 3$, the isolated singular point $p \in \mathcal{M}$ is replaced by a 3-dimensional exceptional set E. Locally, the nocompact manifolds $\mathcal{M} - p$ and $\widehat{\mathcal{M}} - E$ are distinct as complex manifolds but in 'real' sense they are diffeomorphic. Thus something in $\dim_{\mathbb{R}} E = 3$ deforms the complex structure and one refers to this as deformation.

• The cases $\dim_{\mathbb{R}} E = 2$ and $\dim_{\mathbb{R}} E = 4$ correspond to $\dim_{\mathbb{C}} E = 1$ and $\dim_{\mathbb{C}} E = 2$, respectively. In these cases, the exceptional sets E are complex subsets of the smoothed 3-dimensional manifold $\widehat{\mathcal{M}}$, and because of this $\mathcal{M} - p$ and $\widehat{\mathcal{M}} - E$ are the same noncompact complex manifold. We say resolving in codimension 2 and 1, respectively. The case $\dim_{\mathbb{R}} E = 2$ is called blowing up whereas the case $\dim_{\mathbb{R}} E = 1$ is called small resolution, which turn to discuss now.

A.4.2 Nodes and small resolution

One of simplest cases in which small resolutions occur is called hypersurface singularity. In the case of hypersurface singularity, we describe the singularity by prescrbing its local neighbourhood as the solution of a single constraint in $\mathbb{C}^4$. Clearly, the resulting space is singular if all four gradients have a common zero–and precisely one–if we discuss isolated hypersurface singular points. The singular point can be placed at the origin through a simple coordinate transformation.

A node and the cone over $\mathbb{P}^1 \times \mathbb{P}^1$

The simplest hypersurface singular point in a three-fold is called a node. The node takes place at the tip of the cone in $\mathbb{C}^4$, and its defining equation takes the form

$$xy = zt. \tag{A.4.63}$$

The defining polynomial of the cone containing the node take the form

$$\psi \stackrel{\text{def}}{=} xy - zt. \tag{A.4.64}$$

The total Differential of this is

$$d\psi \stackrel{\text{def}}{=} dx \cdot y + x \cdot dy - dz \cdot t - z \cdot dt. \tag{A.4.65}$$

At the origin where the node is placed all four gradients have common zero and we have $d\psi = 0$. In order to find the base of this cone, we may projectivize and regard the four coordinates as $(x : y : z : t) \in \mathbb{P}^3$. For $\psi = 0$, we obtain then a non-degenerate quadric in $\mathbb{P}^3$ as the only degenerate point, $(0, 0, 0, 0, 0) \in \mathbb{C}^4$ is not in $\mathbb{P}^3$, by definition. We note that a smooth quadric in $\mathbb{P}^3$ is equal to $\mathbb{P}^1 \times \mathbb{P}^1$ and the cone has $\mathbb{C}^1$-type generators sweeping over a base $\mathbb{P}^1 \times \mathbb{P}^1$.

As discussed in the previous section, in codimension 2 the singularity can be resolved by replacing it with an exceptional set. Here, this amounts replacing the node with a copy of a $\mathbb{P}^1$. This leads to a topological ambiguity because the base of the cone is the product of two $\mathbb{P}^1$'s. In fact, with three-folds containing many nodes at each node this ambiguity occurs. Thus for a three-fold with N nodes there are 2^N distinct small resolutions. We can regard these small resolutions as halfway blow-up by which the vertex of the quadratic cone is replaced by a surface $F_0 = \mathbb{P}^1 \times \mathbb{P}^1$: by collapsing one of the two $\mathbb{P}^1$'s in F_0 we can obtain one or the other small resolution. The transition from one small resolution of the node to the blow-up and then to the other small resolution yields a bijective map called flop.

A node and the cone over $S^2 \times S^3$

The other way to describe the cone is to change the coordinates and write the defining polynomial of cone as

$$\psi = \sum_{\alpha=1}^{4} (w^\alpha)^2, \tag{A.4.66}$$

where $w^\alpha \in \mathbb{C}^4$ can be thought of as a four-vector w. $\psi = 0$ describes a surface which is smooth except at $w^\alpha = 0$. To see that this surface is a cone, note that if w^α solves $\psi = 0$ then so does $\lambda w^\alpha = 0$ for any λ, so the surface is made of complex lines through the origin and is therefore a cone. In order to obtain the base of this cone, we may write the four-vector w in terms of real and imaginary parts, $w = x + iy$, and for $\psi = 0$ we get

$$x^2 - y^2 = 0, \qquad x \cdot y = 0. \tag{A.4.67}$$

In $\mathbb{C}^4$, we also have a 7-sphere of radius r described by the equation

$$\sum_{\alpha=1}^{4} |w^\alpha|^2 = r^2. \tag{A.4.68}$$

The base manifold is the cross section of the cone, $\psi = 0$, with the 7-sphere centered at the origin of $\mathbb{C}^4$. The intersection of the space of solutions of $\psi = 0$ with Eq. (A.4.68) gives

$$x^2 = \frac{1}{2}r^2, \qquad y^2 = \frac{1}{2}r^2, \qquad x \cdot y = 0. \tag{A.4.69}$$

The first equation defines an S^3 of radius $r/\sqrt{2}$. The second equation defines an S^2 of radius $r/\sqrt{2}$ since for each point of the S^3, say $x = (r, 0, 0, 0)$, the third equation restricts y to be a 3 vector $y = (0, y^1, y^2, y^3)$. Thus, the base of the cone is a fiber bundle with base S^3 and fiber S^2. The fact that all bundles over S^3 are trivial determines the base as the product $S^2 \times S^3$, the generators of which are copies of the real semi-axis, $\mathbb{R}_{\geq 0}$.

The base topology $S^2 \times S^3$ tells us that apart from resolving the node in $\mathbb{P}^1 = S^2$ we can also replace it with an S^3. According to the previous section, this amounts to deformation because the exceptional set is (real) three-dimensional. The fact that there are two $\mathbb{P}^1$ in the base of the complex cone may give the indication that there are also two different choices of S^3's, fibering the phase of the generator of the complex cone over one or the other $\mathbb{P}^1$. Interestingly, this not the case. The argument is that the two S^3's can be rotated into each other implying that there is no topological ambiguity in the deformation of a node. To this end we note that the defining polynomial including the deformation of the node is given by (A.4.66) but with $\psi = \epsilon^2$ instead of $\psi = 0$, where ϵ is a nonzero constant called the deformation parameter which amounts replacing the node by an S^3. Now for $\psi = \epsilon^2$ and $w = x + iy$ we have

$$r^2 = x^2 + y^2, \qquad \epsilon^2 = x^2 - y^2, \tag{A.4.70}$$

from which we can see that $\epsilon \leq r < \infty$, so r is bounded below by ϵ.

A.5 Moduli spaces

In this thesis we used string compactifications to Calabi-Yau three-folds. By a Calabi-Yau three-fold, we mean a real six-dimensional manifold endowed with a complex structure and a complexified Kähler class. Thus the effective moduli space of Calabi-Yau three-folds consists of two moduli spaces: the space of complex structures, which we denote by $\mathfrak{M}$, and the complexified space of Kähler classes, which we denote by $\mathfrak{W}$. The effective moduli space $(\mathfrak{M}, \mathfrak{W})$ is smooth at its generic points but the moduli spaces of topologically distinct Calabi-Yau spaces do touch along certain special regions, which are called "boundary". These 'interface' regions correspond to certain singular limits of the respective Calabi-Yau three-folds. The inclusion of such limit points makes the moduli spaces of a huge number simply connected Calabi-Yau spaces join together to form a 'connected web'.

A.5.1 The conifold

The conifold $\mathcal{M}^\sharp$ takes place at a common boundary point where the moduli spaces of non-singular 3-folds like $\check{\mathcal{M}}$ and smooth 3-folds like $\mathcal{M}_t^\flat$ meet (see Subsec. A.3.3). In other words, the conifold can be smoothed into $\check{\mathcal{M}}$ by a resolution and into $\mathcal{M}_t^\flat$ by a deformation. This means that there are two topologically distinct ways to smooth out $\mathcal{M}^\sharp$:

$$\check{\mathcal{M}} \xleftarrow{\text{res.}} \mathcal{M}^\sharp \xrightarrow{\text{def.}} \mathcal{M}^\flat, \qquad \mathcal{M}^\flat \xrightarrow{r^2 \to 0} \mathcal{M}^\sharp \xleftarrow{\wp} \check{\mathcal{M}}. \tag{A.5.71}$$

In this process the moduli spaces of all simply connected Calabi-Yau manifolds form a connected web. In this large number of Calabi-Yau spaces conifolds arise as limit points in the two respective moduli spaces. According to Eq. (A.3.62), these conifolds have isolated nodes each of which is locally described by a constraint of the form

$$XY - UV = 0, \tag{A.5.72}$$

where X, Y, U, V serve as local coordinates. In section A.4, we saw that these local coordinates describe a cone with the tip at the origin. We also saw there that the node(s) can be smoothed out in two distinct ways. We now would like to analyse this for the conifold $\mathcal{M}^\sharp$ defined by a determinantal equation like Eq. (A.3.62) globally inside Υ.

A.5.2 The deformed and resolved conifold

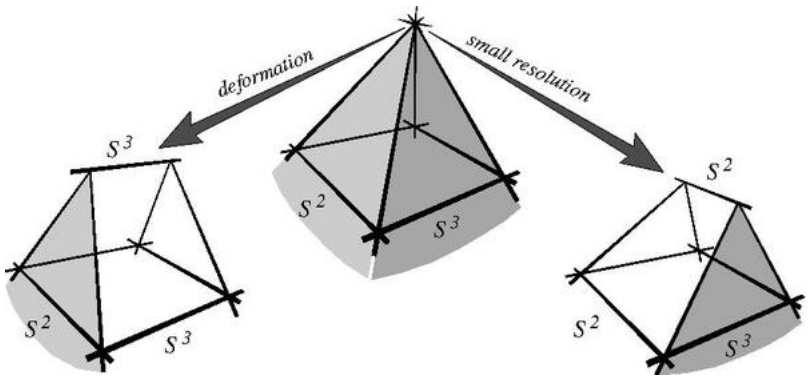

Figure A.1: The deformation and small resolution of the singular conifold near the singularity at the tip of the cone. This figure is from [111].

In section A.4 we saw that the open neighbourhood of the $p^\sharp \in \mathcal{M}^\sharp \subset \Upsilon$ around each node looks like $\mathbb{C}^4$ with X, Y, Z, V acting as local coordinates. We also saw there that this neighbourhood is a cone over the complex base $\mathbb{P}^1 \times \mathbb{P}^1$ or the real base $S^2 \times S^3$. As in section A.4, we may use the base topology and smooth out the nodes through deformation and small resolution including the processes $\mathcal{M}^\sharp \to \mathcal{M}^\flat$ and $\mathcal{M}^\sharp \to \check{\mathcal{M}}$, respectively.

The case $\mathcal{M}^\sharp \to \mathcal{M}^\flat$ is induced by perturbing the defining equation of $\mathcal{M}^\sharp \subset \Upsilon$, Eq. (A.3.62), to an equation of the form

$$\mathcal{C}(x) = r^2(x) = t \sum_{a=1}^{6} (x^a)^5, \tag{A.5.73}$$

where r^2 can be considered independent of X, Y, Z, V. To see this, we note that for (A.5.73) at four nodes $(0, e^{2\pi(2k+1)/8}, 0, 0)$ with $k = 0, 1, 2, 3$ we have $r^2 = -t(i \pm 1)$, which is clearly nonzero at $t \neq 0$ Hence, a node $p^\sharp \in \mathcal{M}^\sharp$ occurs when $r = 0$ in

$$x^2 = \frac{1}{2}r^2, \qquad y^2 = \frac{1}{2}r^2, \qquad x \cdot y = 0. \tag{A.5.74}$$

Thus each node is being inflated into an S^3 defined by

$$x^2 = \frac{1}{2}r^2, \qquad y = 0. \tag{A.5.75}$$

The case $\mathcal{M}^\sharp \to \check{\mathcal{M}}$ is induced by replacing each node $p^\sharp$ by one or the other $\mathbb{P}^1$ from the base. This is done as follows. Away from the origin, any choice of the values $(x_1, x_2, x_3, x_4) \neq 0$ fix the y_1 and y_2, and therefore specify unique a point in $\mathbb{P}^1$. At the origin $(x_1, x_2, x_3, x_4) = 0$, y_1 and y_2 remain undetermined and $\check{\mathcal{M}}$ contains a copy of $\mathbb{P}^1$ there. Projection along $\mathbb{P}^1$ replaces this copy of $\mathbb{P}^1$ by a node of $\check{\mathcal{M}}$. Hence this is the small resolution since each node $p^\sharp$ is resolved into a copy of $\mathbb{P}^1 = S^2$ described by

$$S^2 : \qquad \frac{y_1}{y_2} = \frac{x_2}{x_1} = -\frac{x_4}{x_3}. \tag{A.5.76}$$

This is not a unique choice. As discussed at the end of section A.4, there is a topological ambiguity underlying the small resolution. We can see this here explicitly by noting that a node could be rather resolved into a different exceptional $\mathbb{P}^1$ described by

$$S^2 : \qquad \frac{y_1}{y_2} = -\frac{x_3}{x_1} = -\frac{x_4}{x_2}. \tag{A.5.77}$$

The two inequivalent choices (A.5.76) and (A.5.77) are related by the following transposition

$$\begin{pmatrix} x_1 & x_2 \\ x_3 & x_4 \end{pmatrix} \to \begin{pmatrix} x_1 & x_3 \\ x_2 & x_4 \end{pmatrix},$$

which could be performed for each of the nodes independently. Recall from section A.4, that the passage from one small resolution of a node to its other small resolution is called flop. Here, we can flop all exceptional $\mathbb{P}^1$'s by interchanging $x_2 \leftrightarrow x_3$ globally. This leads to a new three-fold $\hat{\mathcal{M}}$, called the global flop of $\check{\mathcal{M}}$.

Unlike the small resolution, the desingularization of a node by the deformation $\mathcal{M}^\sharp \to \mathcal{M}^\flat$ does not lead to a topological ambiguity. In the discussion above, we

started with solving $x^2 = r^2/2$ in Eq. (A.5.74) and obtained an "S^3_x" spanned by x. In place of this, we could have started with solving $y^2 = r^2/2$ in Eq. (A.5.74) and obtain an "S^3_y" spanned by y. This may give the impression that as with the small resolution there is a topological ambiguity underlying the deformation. To see that this is not the case, we note that there is a continuous set of choices parametrized by an angle:

$$x(\theta) \stackrel{\text{def}}{=} (x\cos\theta + y\sin\theta)/2, \qquad y(\theta) \stackrel{\text{def}}{=} (-x\sin\theta + x\cos\theta)/2. \tag{A.5.78}$$

Both $x(\theta)$ and $y(\theta)$ satisfy Eq. (A.5.74), and therefore Eqs. (A.5.78) show the equivalence between all such choices, including "S^3_x" ($\theta = 0$) and "S^3_y"($\theta = \pi$).

A.5.3 L^2 and intersection cohomology

In chapter 2 we have identified the massless fields in superstring compactification with certain harmonic forms (cohomology classes) on the compactifying space $\mathcal{M}$. This was based on our discussions in section A.2 and subsection A.3.2 assuming that $\mathcal{M}$ is smooth. But from subsection A.3.2 onwards we saw that our compactifying space being the conifold can be singular and therefore we inquire if there is a cohomology which maintains the features such as (A.2.32) - (A.2.34) even when the underlying space singularizes. These requirements are satisfied by the very axioms of field theory. In particular, the $1+1$-dimensional field theory which is used to describe the propagation of superstrings in spacetime–including the compactification space–requires all physical states to be square integrable.

The cohomology theory which includes square integrability is called L^2-cohomology and denoted $H^{p,q}_{(2)}$. In this cohomology the $A^{p,q}$-forms (see sec. A.2) are required to be square–integrable with respect to a chosen norm. Moreover, $H^{p,q}_{(2)}(\mathcal{M}) = H^{p,q}(\mathcal{M})$ on any smooth manifold $\mathcal{M}$, and on a large class of singular spaces, $H^{p,q}_{(2)}$ remains well behaved respecting the properties (A.2.32) - (A.2.34).

Since the computation of $H^{p,q}_{(2)}$ could be a formidable task one has to consider the relating homology group which can be easily computed. The homology theory which pairs with $H^{p,q}_{(2)}$ (via De Rahm duality) for a class of singular spaces $X \hookrightarrow \mathbb{P}^N$

where $H^{p,q}_{(2)}$ refers to the restriction to X of the Fubini-Study metric on the $\mathbb{P}^N$ is called middle perversity intersection homology theory and denoted $\mathring{H}(X)$. This class includes manifolds with isolated conical singularities discussed in previous sections and for a n-fold X with a single isolated singularity p one has:

$$\mathring{H}(X) = \begin{cases} H_k(X) & k > n, \\ \mathrm{Im}[H_n(X-p) \to H_n(X)] & k = n, \\ H_k(X-p) & k < n. \end{cases} \tag{A.5.79}$$

Here the map in the middle dimension means as follows. First, discard all would-be n-cycles from $H_n(X)$ which contract to p. Second, discard all n-cycles which break open upon excising p. One also notes that $\mathring{H}_n(X)$ need not be computed for $k < n$ since Poincare duality relates is to $\mathring{H}_{n-k}(X)$.

A.5.4 Cycles in conifolds

We now would like to discuss the process involving the local transformation in which the deformed conifold is deformed back into the singular conifold which is then transformed into the resolved conifold,

$$\mathcal{M}^\flat \overset{r^2\to 0}{\longrightarrow} \mathcal{M}^\sharp \overset{\text{res.}}{\longrightarrow} \check{\mathcal{M}}. \tag{A.5.80}$$

The $\mathbb{R}_+$ generators of the cone $\mathcal{M}^\flat$ produce a real B^3_t-like cap by sweeping the S^2 in the base of the cone at every fixed point of the minimal $S^3_t \subset \mathcal{M}^\flat$ which is the crest of the "tent"-like neighbourhood. The B^3_t comprises the shaded region in the left hand side of Fig. A.1 and can be completed into a cycle elsewhere in $\mathcal{M}^\flat$ outside of this neighbourhood. The same process applies to the other side of the cone. Namely, by sweeping the S^3 in the base of the cone while keeping a point of the S^2 in the base fixed the $\mathbb{R}_+$ generators of the cone form "four-hoop" $S^3 \times \mathbb{R}_+$ with its boundary being the minimal S^3_t. The resulting space cannot be a cycle since it has a boundary but will be important when passing to the small resolution; it is remarkable though clear that when B^3_t becomes completed into a three-cycle, S^3_t is homotopically non-trivial and the cycle that S^3_t represents is dual to the three-cycle

completed by B^3_t. In the same way the S^2 in the boundary cannot be a cycle since it can be shrank to a point on the S^3_t at the tip of the cone.

Consider first the process $\mathcal{M}^\flat \overset{r^2\to 0}{\longrightarrow} \mathcal{M}^\sharp$ in which both the S^2 and S^3 spheres shrink to zero size at the tip of the cone implying that there are no non-trivial two- and three-cycles represented by them, respectively. However, the cycle represented by the three-space with its portion being B^3_t in Fig. A.1 remains untouched. In particular, if it represented a non-trivial cycle in $\mathcal{M}^\flat$ it will continue to do so in the nonsingular homology of $\mathcal{M}^\sharp$. But according to (A.5.79) it cannot be a non-trivial element of $\mathring{H}_3(\mathcal{M}^\sharp)$ because it turns to an open interval when the singular point is removed and is thereby contractable. On the other hand, the boundary of the "four-hoop" has shrank to zero size which lifts the local obstruction for the "four-hoop" to be a portion of a representative of a "four-cycle". In the case that there is no obstruction outside of this neighbourhood one gains a new four-cycle. According to (A.5.79), this continues to be an element of $\mathring{H}_4(\mathcal{M}^\sharp)$ since $\mathring{H}_4(\mathcal{M}^\sharp)$ and $\mathring{H}_k(\mathcal{M}^\sharp)$ are treated differently for $k \neq 3$. In addition to this, it should be noted that there is a dual element of $\mathring{H}_2(\mathcal{M}^\sharp)$ although there is no corresponding contribution to the nonsingular $H_2(\mathcal{M}^\sharp)$.

Consider then the process $\mathcal{M}^\sharp \overset{\text{res.}}{\longrightarrow} \check{\mathcal{M}}$. In this process the node is replaced by S^2_t, shown as the crest of the "tent"-like neighbourhood in the right hand side of Fig. (A.1). This produces a hole in B^3_t making it become a "three-hoop" $S^2 \times \mathbb{R}_+$, representing a trivial three-cycle. Also, here each S^3 shrinks to zero size at the tip of the cone and is homologous to a point on the S^2_t implying no non-trivial three-homology. On the contrary, each S^2 remains of finite size and is homologous to the S^2_t being locally a non-trivial element of $H_2(\mathcal{M})$. In the same way, the "four-hoop" $S^3 \times \mathbb{R}_+$ whose boundary has been shrank to a point cab be a representative of a portion of a non-trivial four-cycle dual to the non-trivial two-cycle represented by S^2_t.

A.5.5 Fluxes in conifolds

Recall from section 2 that on Calabi-Yau manifolds (including Calabi-Yau cones) we have the Kähler form J, the holomorphic $(3,0)$-form and harmonic functions f sat-

isfying $\Delta f = 0$. The Kähler form is a $(1,1)$-form and can be written componentwise in terms of the Kähler metric $g_{\alpha\bar{\beta}}$ as

$$J_{\alpha\bar{\beta}} = i g_{\alpha\bar{\beta}}, \qquad g_{\alpha\bar{\beta}} = \partial_\alpha \partial_{\bar{\beta}} \mathcal{K}. \tag{A.5.81}$$

where $\mathcal{K}$ is the Kähler potential, as before. The holomorphic $(3,0)$-form may also be expressed in components as

$$\Omega_{\alpha\beta\gamma} = q\, \varepsilon_{\alpha\beta\gamma} \quad \text{with} \quad \frac{1}{2!}\Omega_{\alpha\beta\gamma}\bar{\Omega}_{\bar{\alpha}\bar{\beta}\bar{\gamma}} g^{\bar{\beta}\beta} g^{\bar{\gamma}\gamma} = g_{\bar{\alpha}\alpha} \tag{A.5.82}$$

where q is a holomorphic function satisfying $|q|^2 = \det g$.

Using these ingredients three distinct type of closed, IASD three-form forms

$$d\Lambda = 0, \qquad \star_6 \Lambda = -i\Lambda \tag{A.5.83}$$

can be constructed on general Calabi-Yau cones, including the conifold.

The first and simplest one is of Hodge type $(1,2)$ which can be written as a contraction of the anti-holomorphic $(0,3)$-form $\bar{\Omega}$ and a holomorphic $(2,0)$-form P as

$$\Lambda^{(1,2)} = P^{(1,2)} \cdot \bar{\Omega}^{(0,3)}, \qquad \Lambda = P_{\alpha\sigma} g^{\sigma\bar{\zeta}} \bar{\Omega}_{\bar{\zeta}\bar{\beta}\bar{\gamma}}. \tag{A.5.84}$$

Here we note that only the $(0,3)$-form Ω is IASD. The two-form P can be constructed out of covariant derivatives of the holomorphic function f,

$$P_{(\alpha\sigma)} = \nabla_\alpha \nabla_\sigma f \quad \text{with} \quad \Delta f = g^{\rho\bar{\zeta}} \nabla_\rho \nabla_{\bar{\zeta}} = 0. \tag{A.5.85}$$

Thus we obtain the first three-form $\Lambda_{\mathrm{I}} = \Lambda^{(1,2)}$

$$\Lambda_{\mathrm{I}} = \nabla\nabla f \cdot \bar{\Omega}, \quad \text{or} \quad \Lambda_{\alpha\bar{\beta}\bar{\gamma}} = \nabla_\alpha \nabla_\sigma f\, g^{\sigma\bar{\zeta}} \bar{\Omega}_{\bar{\zeta}\bar{\beta}\bar{\gamma}}. \tag{A.5.86}$$

It is straightforward to show that Λ_{I} is closed, i.e., $d\Lambda_{\mathrm{I}} = \bar{\partial}\Lambda_{\mathrm{I}} + \partial\Lambda_{\mathrm{I}} = 0$. The vanishing of $\bar{\partial}\Lambda_{\mathrm{I}}$ follows from Ricci-flatness of Calabi-Yau manifolds, $R_{\alpha\bar{\beta}} = 0$, and the fact that f is harmonic, $\Delta f = 0$. The vanishing of $\partial\Lambda_{\mathrm{I}}$ follows from the commutativity of the holomorphic covariant derivatives, $[\nabla_\alpha, \nabla_\beta] = 0$.

The second closed, IASD three-form is of Hodge type $(1,2)+(2,1)_{\rm NP}$. For the two-form P, we may consider the following ansatz:

$$P_{\alpha\sigma} = \nabla_{\bar{\zeta}}\nabla_{(\alpha} f \omega_{\sigma)}^{\bar{\zeta}}, \tag{A.5.87}$$

where

$$\omega_{\sigma}^{\bar{\zeta}} \equiv \Omega_{\rho\sigma} k^{\bar{\zeta}}, \quad k^{\rho} \equiv g^{\rho\bar{\xi}}\partial_{\bar{\xi}} k. \tag{A.5.88}$$

The resulting three-form takes the form

$$\Lambda_{\rm II}^{(1,2)} = \partial\bar{\partial} f \wedge \bar{\partial} k + \frac{1}{2} J \wedge \bar{\partial}(\partial_{\rho} f\, k^{\rho}) - \frac{1}{2}\Delta f\, J \wedge \bar{\partial} k. \tag{A.5.89}$$

This three-form is not closed but adding an appropriate $(2,1)$ piece

$$\Lambda_{\rm II}^{(2,1)} = \partial\left(f + \frac{1}{2}\partial_{\rho} f\, k^{\rho}\right) \wedge J \tag{A.5.90}$$

gives the following three-form

$$\Lambda_{\rm II} = (\partial + \bar{\partial})\left(f + \frac{1}{2}\partial_{\rho} f\, k^{\rho}\right) \wedge J + \partial(\bar{\partial} f \wedge \bar{\partial} k). \tag{A.5.91}$$

In order to show that $\Lambda_{\rm II}$ is closed, i.e., $d\Lambda_{\rm II} = \bar{\partial}\Lambda_{\rm II} + \partial\Lambda_{\rm II} = 0$, one first notes that k^{σ} is holomorphic, $\partial_{\bar{\zeta}} k^{\sigma} = 0$, and that Ω is covariantly constant. This together with the antisymmetry of $\Omega_{\rho}^{\bar{\zeta}\bar{\sigma}}$ in $\bar{\zeta}$ and $\bar{\sigma}$ imply the vanishing of $\bar{\partial}\Lambda_{\rm II}$. The vanishing of $\partial\Lambda_{\rm II}$ follows from $\Delta f = 0$ and adding an extra $(2,1)$ piece.

The third closed, IASD three-form is of Hodge type $(1,2)+(2,1)_{\rm NP}+(3,0)$. For the two-form P, we may consider the following ansatz:

$$P_{\alpha\sigma} = \nabla_{\bar{\zeta}}\nabla_{\bar{\rho}}\omega_{\bar{\alpha}}^{\bar{\zeta}}\omega_{\sigma}^{\bar{\rho}}. \tag{A.5.92}$$

The resulting three-form takes the form

$$\Lambda_{\rm III}^{(1,2)} = \bar{\partial}(\bar{\partial} f \cdot \omega) \wedge \bar{\partial} k. \tag{A.5.93}$$

This three-form is not closed but adding an appropriate $(2,1)$ and $(3,0)$ pieces

$$\Lambda_{\rm III}^{(2,1)} = (\bar{\partial} h \cdot \omega) \wedge J, \qquad \Lambda_{\rm III}^{(3,0)} = (2h + k^{\xi}\partial_{\xi} h)\Omega \tag{A.5.94}$$

gives the following three-form

$$\Lambda_{\rm III} = (2h + k^\xi \partial_\xi h)\Omega + (\bar\partial h \cdot \omega) \wedge J + \bar\partial(\bar\partial f \cdot \omega) \wedge \bar\partial k. \tag{A.5.95}$$

The fact that $d\Lambda_{\rm III} = 0$ follows from Ricci-flatness, $\Delta f = 0$ and adding appropriate $(2,1)$ and $(3,0)$ pieces, as above.

A.5.6 Complex structure moduli

Recall that on every manifold $\mathcal{M}$ we can locally define a point p and approximate the local neighbourhood of p by a tangent space $T_p\mathcal{M}$. When $\mathcal{M}$ is a Calabi-Yau three-fold, i.e., (complex) even dimensional, there is a map J from every tangent space to itself given by

$$J : T_p\mathcal{M} \to T_p\mathcal{M}, \qquad \text{satisfying} \qquad J^2 = -\text{Id}. \tag{A.5.96}$$

This map defines an almost complex structure (see section A.1) on $\mathcal{M}$. The choice of J depends on the number of parameters and we can deform the space so as to become a different complex manifold though remaining in the same topological class. The space spanned by such parameters is called deformation space.

In section A.4 we saw that conical singularities can be removed by replacing them with an exceptional set. In codimension two, this amounted small resolutions of nodes. The fact that there is a finite number of nodes and small resolutions, and that the defining polynomials of $\mathcal{M}^\sharp$ depend on those defining $\check{\mathcal{M}}$ (see Eq. (A.3.62) and Eq. (A.3.60)), leads to the identification

$$\check{\mathfrak{M}} \to \mathfrak{M}^\sharp = \lim_{t\to 0} \mathfrak{M}^\flat \subset \mathfrak{M}^\flat_+. \tag{A.5.97}$$

Here, $\mathfrak{M}^\sharp$ and $\check{\mathfrak{M}}$ parameterize the complex structure of $\mathcal{M}^\sharp$ and $\check{\mathcal{M}}$, respectively, and $\mathfrak{M}^\flat_+$ parameterizes the complex structure of $\mathcal{M}^\flat$.

A.5.7 Kähler class moduli

Locally on an even dimensional manifold we can define on each tangent space a metric g and associated with it the fundamental form $\omega \stackrel{\text{def}}{=} g(JX, Y)$, where J is

the almost complex structure underlying the even dimensional manifold. Due to its dependence on the almost complex structure, the fundamental form is a $(1,1)$-form and is expressed in terms of local coordinates as

$$\omega \stackrel{\text{def}}{=} i g_{\mu\bar{\nu}} dz^{\mu} \wedge dz^{\bar{\nu}}. \tag{A.5.98}$$

In addition to being even dimensional, our Calabi-Yau three-fold is also a Kähler manifold, which means that $g_{\mu\bar{\nu}}$ is a Kähler metric and its associated $(1,1)$-form is closed, $d\omega = 0$. Furthermore, in order to be Kähler form, the $(1,1)$-form ω must also satisfy the following condition

$$\int_{\mathcal{C}} \omega > 0, \quad \int_{\mathcal{S}} \omega^2 > 0, \quad \int_{\mathcal{M}} \omega^3 > 0, \tag{A.5.99}$$

where $\mathcal{C}$ and $\mathcal{S}$ denote all curves and all surfaces in the manifold $\mathcal{M}$, respectively. Locally this means that ω is self-conjugate (real) and positive such that $g_{\mu\bar{\nu}}$ is in any local coordinate chart a Hermitian and positive matrix. On our Calabi-Yau three-fold therefore the $(1,1)$-form (A.5.98) represents the Kähler cohomology class, the space of choices of which $\{\omega^{(1,1)} | \, d\omega = 0\}$ is a cone, called the Kähler cone. To see why this is a cone, note that since ω is a $(1,1)$-form it can be determined by the linear combination of $(1,1)$-forms $\omega = v^A e_A$ from a complete set and real coefficients v^A, so if J_x and J_y are both positive, then so is $v^x J_x + v^y J_y$ for v^x, $v^y \in \mathbb{R}_+$. In string theory, we can extend and complexify this cone by noting that the action (A.1.1) describing the propagation of superstrings over the world-sheet not only contains a Kähler metric $g_{\mu\bar{\nu}}$ but also an antihermitian two-form $B_{\mu\bar{\nu}}$. We may expand this antihermitian two-form as harmonic $(1,1)$-form $B = u^A e_A$ and include it by considering the combination $(B + i\omega) = (u^A + iv^A)e_A = w^A e_A$ giving the complexified Kähler form, where $\{e_A\}$ form a basis of $H^{1,1}(\mathcal{M})$ and w^A are the $h^{1,1}$ complex parameters. The space spanned by w^A is referred to as the complexified Kähler cone $\mathfrak{W}$.

Thus the moduli space of Calabi-Yau three-folds consists of the space of complex structures, at every point of which there is Kähler cone: at every point the metric endowed with the almost complex structure and associated with is the Kähler form, the complete set of which spans the Kähler cone. By varying the complex structure

the associated Kähler cones vary into each other in a uniform way, so that the total space has a structure of a fibration. In other words, since $\mathfrak{W}$ depends on the complex structure in $\mathfrak{M}$ we expect the combined moduli space of Calabi-Yau manifolds to be a space fibered over the space of complex structures, with the Kähler cones as fibers.

A.5.8 The metric on moduli space

As briefly discussed in chapter 1, the metric has variations of mixed type, $\delta g_{\mu\bar{\nu}}$, and of pure type $\delta g_{\bar{\mu}\bar{\nu}}$, $\delta g_{\mu\nu}$. The variations of mixed type can be associated with the real $(1,1)$-form

$$i\delta g_{\mu\bar{\nu}} dx^{\mu} \wedge dx^{\bar{\nu}}. \tag{A.5.100}$$

The zero modes of this $(1,1)$-form correspond to elements of $H^{1,1}(\mathcal{M})$, which are variations of the Kähler class and give rise to $h^{1,1}$ real parameters. The variations of the pure type can be associated with complex $(2,1)$-form

$$\Omega^{\bar{\nu}}_{\kappa\lambda} \delta g_{\bar{\mu}\bar{\nu}} dx^{\kappa} \wedge dx^{\lambda} \wedge dx^{\bar{\mu}}, \tag{A.5.101}$$

where Ω is the holomorphic $(3,0)$-form. The zero modes of this $(2,1)$-form correspond to elements of $H^{2,1}(\mathcal{M})$, which are variations of the complex structure and give $h^{2,1}$ complex parameters. Recall from section A.1 that apart from the metric, $g_{\mu\bar{\nu}}$, the Calabi-Yau sigma-model also underlies an anti-hermitian two-form B (see Eq. (A.1.1)) and we saw in the previous section that including B complexifies the Kähler cone. Thus in addition to variations of the metric, we also consider variations of the anti-hermitian two-form B, $\delta B_{\mu\bar{\nu}}$. In total we have the following variations

$$\delta g_{\mu\bar{\nu}}, \qquad \delta g_{\bar{\mu}\bar{\nu}}, , \qquad \delta g_{\mu\nu}, \qquad \delta B_{\mu\bar{\nu}}. \tag{A.5.102}$$

In order to choose a metric on the space spanned by these variables, we may neglect the following: (1) derivative terms (these are systematically introduced by the sigma-model corrections) (2) a possible term $(g^{mn}\delta g_{mn})^2$, since $g^{mn}\delta B_{mn}$ vanishes, this

term would spoil the symmetry between g_{mn} and B_{mn} (3) terms from other possible sectors. Upon these restrictions, the most general metric is

$$\begin{aligned} ds^2 &= \frac{1}{V}\int_{\mathcal{M}} ||\delta g_{\mu\nu}||^2 + ||\delta g_{\mu\bar{\nu}} + \delta B_{\mu\bar{\nu}}||^2 \\ &= \frac{1}{2V}\int_{\mathcal{M}} g^{\kappa\bar{\mu}} g^{\lambda\bar{\nu}} [\delta g_{\kappa\lambda}\delta g_{\bar{\mu}\bar{\nu}} + (\delta g_{\kappa\bar{\lambda}}\delta g_{\lambda\bar{\mu}} + \delta B_{\kappa\bar{\nu}}\delta B_{\bar{\mu}\lambda})]\sqrt{g}dx^6, \end{aligned} \quad (A.5.103)$$

where V is the volume of the Calabi-Yau manifold M. This metric is block-diagonal and includes blocks that correspond to deformations of the complex structure and of the Kähler class, which we turn to discuss now.

A.5.9 The complex structure moduli space

To analyse the deformations of the complex structure, we may consider an open neighbourhood of $\mathfrak{M}$ containing local coordinates t^α with $\alpha = 1, ..., h^{2,1}$ and define the following relations

$$\varphi_{\alpha\kappa\lambda\bar{\mu}} \stackrel{\text{def}}{=} -\frac{1}{2}\Omega_{\kappa\lambda}{}^{\bar{\nu}}\frac{\partial g_{\bar{\mu}\bar{\nu}}}{\partial t^\alpha}, \qquad \varphi_\alpha \stackrel{\text{def}}{=} \frac{1}{2}\varphi_{\alpha\kappa\lambda\bar{\mu}} dx^\kappa \wedge dx^\lambda \wedge dx^{\bar{\mu}}, \quad (A.5.104)$$

where each φ_α is a harmonic $(2,1)$-form. By inverting, we obtain the variation of the metric in the form

$$\delta g_{\bar{\mu}\bar{\nu}} = -\frac{1}{||\Omega||^2}\bar{\Omega}^{\rho\sigma}_{\bar{\mu}}\varphi_{\alpha\rho\sigma\bar{\nu}}\delta t^\alpha, \qquad ||\Omega||^2 \stackrel{\text{def}}{=} \frac{1}{6}\Omega_{\mu\nu\rho}\bar{\Omega}^{\mu\nu\rho}. \quad (A.5.105)$$

Using these relations we find

$$\begin{aligned} 2G_{\alpha\bar{\beta}}\delta t^\alpha \delta t^{\bar{\beta}} &= \frac{1}{2V}\int g^{\kappa\bar{\nu}} g^{\mu\bar{\lambda}} \delta g_{\kappa\mu}\delta g_{\bar{\lambda}\bar{\nu}} g^{1/2} d^6x \\ &= -\frac{2i}{V||\Omega||^2}\delta t^\alpha \delta t^{\bar{\beta}} \int \varphi_\alpha \wedge \bar{\varphi}_{\bar{\beta}}. \end{aligned} \quad (A.5.106)$$

From this relation we obtain the Weil-Peterson metric

$$G_{\alpha\bar{\beta}}\delta t^\alpha \delta t^{\bar{\beta}} = -\left(\frac{i\int \varphi_\alpha \wedge \bar{\varphi}_{\bar{\beta}}}{i\int \Omega \wedge \bar{\Omega}}\right)\delta t^\alpha \delta \bar{t}^{\bar{\beta}}. \quad (A.5.107)$$

Under a change in the complex structure the holomorphic three-form Ω becomes a linear combination of the (3,0)-forms and (2,1)-forms

$$\frac{\partial\Omega}{\partial t^\alpha} = K_\alpha\Omega + \varphi_\alpha. \tag{A.5.108}$$

It follows then

$$\begin{aligned} G_{\alpha\bar\beta} &= -\frac{\partial}{\partial t^\alpha}\frac{\partial}{\partial t^\beta}\log\left(i\int_M \Omega\wedge\bar\Omega\right) \\ &= \frac{\partial}{\partial t^\alpha}\left[\frac{-1}{\int\Omega\wedge\bar\Omega}\int\Omega\wedge\frac{\bar\partial\bar\Omega}{\partial t^{\bar\beta}}\right] \\ &= -\frac{1}{(\int\Omega\wedge\bar\Omega)^2}\int\frac{\partial\Omega}{\partial t^\alpha}\wedge\bar\Omega\int\Omega\wedge\frac{\bar\partial\bar\Omega}{\partial t^\alpha} + \frac{1}{\int\Omega\wedge\bar\Omega}\int\frac{\partial\Omega}{\partial t^\alpha}\wedge\frac{\bar\partial\bar\Omega}{\partial t^{\bar\beta}}\bar\Omega \\ &= -\frac{i\int\varphi_\alpha\wedge\bar\varphi_{\bar\beta}}{i\int\Omega\wedge\bar\Omega}. \end{aligned} \tag{A.5.109}$$

Recall the relation between the metric and the Kähler potential

$$G_{\alpha\bar\beta} = \frac{\partial}{\partial t^\alpha}\frac{\partial\mathcal{K}}{\partial t^{\bar\beta}}. \tag{A.5.110}$$

This tells us that the space of complex structures is Kähler and by the above the Kähler potential is

$$\mathcal{K}^{2,1} = -\log\left(i\int_M\Omega\wedge\bar\Omega\right). \tag{A.5.111}$$

In order to know more about the the metric on the moduli space $\mathfrak{M}$, we need to analyse the holomorphic three-form Ω in greater detail. We recall that Ω is an element of the real degree-three cohomology and that the cohomology groups are isomorphic to the space of harmonic forms. If we can choose which of the existing harmonic three-forms is regarded as the purely holomorphic one, then we have specified the complex structure. The existing choices are then parameterized by expanding Ω over the basis o the dual three-homology.

Let (A^a, B_b) with $a, b = 0, ..., b_{2,1}$ be a canonical homology basis for $H_3(\mathcal{M};\mathbb{Z})$ and let (α_a, β^b) be the dual cohomology basis such that

$$\int_{A^b}\alpha_a = \int_{\mathcal{M}}\alpha_a\wedge\beta^b = \delta_a^b \qquad \int_{B^a}\beta^b = \int_{\mathcal{M}}\beta^b\wedge\alpha_a = -\delta_a^b. \tag{A.5.112}$$

In addition to that define periods of Ω as follows

$$z^a \stackrel{\text{def}}{=} \int_{A^a} \Omega, \qquad \mathscr{G}_a \stackrel{\text{def}}{=} \int_{B_a} \Omega. \tag{A.5.113}$$

Locally in the moduli space the complex structure of $\mathcal{M}$ is totally determined by the z^a and therefore locally one has $\mathscr{G}_a = \mathscr{G}_a(z)$. The z^a cannot vanish simultaneously since $\Omega(z) \to \lambda\Omega(z)$ implies $z^a \to \lambda z^a$ by which the z^a can be regarded as projective coordinates for the complex structure and Ω as being homogeneous of degree 1 in these coordinates

$$z^a \in \mathbb{P}^{b^{2,1}}, \qquad \Omega(\lambda z) = \lambda\Omega(z). \tag{A.5.114}$$

We then expand Ω in the form

$$\Omega = z^a\alpha_a - \mathscr{G}_a(z)\beta^a. \tag{A.5.115}$$

From Eq. (A.5.108) it follows that

$$\int_{\mathcal{M}} \left(\Omega \wedge \frac{\partial\Omega}{\partial z^a}\right) = 0, \tag{A.5.116}$$

which gives the relation

$$2\mathscr{G}_a = \frac{\partial}{\partial z^a}(z^c\mathscr{G}_c). \tag{A.5.117}$$

Therefore $\mathscr{G}_a$ is the gradient of a function that is homogeneous degree two

$$2\mathscr{G}_a = \frac{\partial}{\partial z^a}, \qquad \mathscr{G}_a(\lambda z) = \lambda^2\mathscr{G}_a(z). \tag{A.5.118}$$

It can also be shown that

$$\frac{\partial^2\Omega}{\partial z^\alpha \partial z^\beta} \in H^{(3,1)} \oplus H^{(2,1)} \oplus H^{(1,2)}, \tag{A.5.119}$$

and also that

$$\int_{\mathcal{M}} \left(\Omega \wedge \frac{\partial^2\Omega}{\partial z^\alpha \partial z^\beta}\right) = 0, \qquad \int_{\mathcal{M}} \left(\frac{\partial\Omega}{\partial z^a} \wedge \frac{\partial\Omega}{\partial z^b}\right) = 0. \tag{A.5.120}$$

The Yukawa coupling reads as

$$\kappa_{\alpha\beta\gamma} \stackrel{\text{def}}{=} -\int_{\mathcal{M}} \Omega \wedge \chi^\mu_\alpha \wedge \chi^\nu_\beta \wedge \chi^\mu_\gamma \Omega_{\mu\nu\rho} \tag{A.5.121}$$

where

$$\chi^{\mu}_{\alpha} = \frac{1}{2||\Omega||^2}\overline{\Omega}^{\mu\rho\sigma}\chi_{\alpha\rho\sigma\bar{\nu}}dx^{\bar{\nu}} = \chi^{\mu}_{\alpha\,\bar{\nu}}dx^{\bar{\nu}}. \tag{A.5.122}$$

It is not difficult to show that

$$\begin{aligned}\int_{\mathcal{M}} \Omega \wedge \chi^{\mu}_{\alpha} \wedge \chi^{\nu}_{\beta} \wedge \chi^{\mu}_{\gamma}\Omega_{\mu\nu\rho} &= \int_{\mathcal{M}} \Omega \wedge \frac{\partial^3\Omega}{\partial z^{\alpha}\partial z^{\beta}\partial z^{\gamma}} \\ &= \frac{\partial^3\mathscr{G}}{\partial z^{\alpha}\partial z^{\beta}\partial z^{\gamma}}.\end{aligned} \tag{A.5.123}$$

The Yukawa coupling and $\mathcal{G}$ do not vanish in general. It is also straightforward to show that

$$i\int \Omega \wedge \overline{\Omega} = i\left(\bar{z}^a\frac{\partial\mathscr{G}}{\partial z^a} - z^a\frac{\partial\overline{\mathscr{G}}}{\partial\bar{z}^a}\right). \tag{A.5.124}$$

Recall form that the Kähler potential takes the form

$$\mathcal{K}^{2,1} = -\log\left(i\int_M \Omega\wedge\bar{\Omega}\right). \tag{A.5.125}$$

Hece we have the relation

$$\exp(-\mathcal{K}^{2,1}) = -i\left(z^a\frac{\partial\overline{\mathscr{G}}}{\partial\bar{z}^a} - \bar{z}^a\frac{\partial\mathscr{G}}{\partial z^a}\right). \tag{A.5.126}$$

Thus the Kähler potential is completely determined in terms of a holomorphic function $\mathcal{G}$ of homogeneous degree two and the Kähler manifold is therefore of a special type; a Kähler manifold with holomorphic prepotential. To this end, we note that $\mathcal{G}$ is determined by the Yukawa coupling which receives no quantum corrections and so the metric structure on the moduli space $\mathfrak{M}$ is exact.

The vector space $H^{(3,0)} \oplus H^{(2,1)}$ is a linear subspace of $H^3(\mathcal{M})$ that has holomorphic variations with the z^a. For this vector space there is a basis of the form

$$\frac{\partial\Omega}{\partial z^a} = \alpha_a - \frac{\partial\mathscr{G}}{\partial z^a\partial z^b}\beta^b. \tag{A.5.127}$$

According to this the period matrix

$$\varpi \overset{\text{def}}{=} \left(\int_{A^b}\frac{\partial\Omega}{\partial z^a}, \int_{B_b}\frac{\partial\Omega}{\partial z^a}\right) \tag{A.5.128}$$

is of the form

$$\varpi = (1, \mathbb{G}), \qquad \mathbb{G}_{ab} = \frac{\partial^2 \mathscr{G}}{\partial z^a \partial z^b}. \tag{A.5.129}$$

From this we note now that

$$i \int_{\mathcal{M}} \left(\frac{\partial \Omega}{\partial z^a} \wedge \frac{\partial \overline{\Omega}}{\partial z^b} \right) = -2 \mathrm{Im} \mathbb{G}_{ab}. \tag{A.5.130}$$

This tells us that $\mathrm{Im}\mathbb{G}_{ab}$ has signature $(h^{2,1}, 1)$, a condition similar to lying in the Siegal upper half-plane.

A.5.10 The Kähler class moduli space

To analyse the deformations of the Kähler class, we may consider an open neighbourhood of $\mathfrak{W}$ containing local coordinates $w^A \in \mathfrak{W}$ with a basis e_A, $A = 1, ..., h^{1,1}$, so that

$$B + iJ = w^A e_A, \qquad w^A = u^A + iv^A. \tag{A.5.131}$$

By Eq. (A.5.103) the inner product on $H^{1,1}$ takes the form

$$G(\rho, \sigma) = \frac{1}{2V} \int_{\mathcal{M}} \rho_{\mu\bar{\nu}} \sigma_{\rho\bar{\sigma}} g^{\mu\bar{\sigma}} g^{\rho\bar{\nu}} g^{1/2} d^6 x = \frac{1}{2V} \int_{\mathcal{M}} \rho \wedge * \sigma, \tag{A.5.132}$$

where ρ and σ are real $(1,1)$-forms. We may also rewrite this in terms of the cubic term defined as

$$\kappa(\rho, \sigma, \tau) \stackrel{\text{def}}{=} \int \rho \wedge \sigma \wedge \tau \tag{A.5.133}$$

in the virtue of the identities

$$V = \frac{1}{3!} \kappa(J, J, J), \qquad * \sigma = -J \wedge \sigma + \frac{3}{2} \frac{\kappa(\sigma, J, J)}{\kappa(J, J, J)} J \wedge J. \tag{A.5.134}$$

From these relations we obtain

$$G(\rho, \sigma) = -3 \left[\frac{\kappa(\rho, \sigma, J)}{\kappa(J, J, J)} - \frac{3}{2} \frac{\kappa(\rho, J, J) \kappa(\sigma, J, J)}{\kappa^2(J, J, J)} \right]. \tag{A.5.135}$$

In term of local coordinates, a straightforward computation gives

$$G_{A\bar{B}} \stackrel{\text{def}}{=} \frac{1}{2}G(e_A, e_B) = -\frac{\partial}{\partial w^A}\frac{\partial}{\partial w^{\bar{B}}}\log\kappa(J,J,J). \tag{A.5.136}$$

Thus the space of w^A is also a Kähler manifold and that the Kähler potential is the logarithm of the volume of the Calabi-Yau manifold. We may also set

$$f(w) \stackrel{\text{def}}{=} \frac{1}{3!}\kappa_{ABC}w^A w^B w^C \qquad \text{with} \qquad \kappa_{ABC} = \kappa(e_A, e_B, e_C), \tag{A.5.137}$$

and obtain

$$\begin{aligned}\kappa(J,J,J) &= \kappa_{ABC}v^A v^B v^C, \\ &= -\frac{3}{4}i\big[2(f(w)-f(\bar{w})) - (w^A-\bar{w}^A)(f_{,A}(w)-f_{,A}(\bar{w}))\big].\end{aligned} \tag{A.5.138}$$

We may also define

$$\mathscr{F}(w) \stackrel{\text{def}}{=} -\frac{1}{3!}\frac{\kappa_{ABC}w^A w^B w^C}{w^0}. \tag{A.5.139}$$

Here we have introduced an extra coordinate w^0, so that $\mathscr{F}$, in analogy to $\mathscr{G}$, is homogeneous of degree two; w^0 will be set to unity after differentiation. In this way, we find

$$\exp(-\mathcal{K}_{1,1}) = \frac{4}{3}\int J^3 = -i\left(w^j\frac{\partial\overline{\mathscr{F}}}{\partial w^j} - w^{\bar{j}}\frac{\partial\mathscr{F}}{\partial w^j}\right), \tag{A.5.140}$$

where the Kähler potential is shifted and j runs over the value of zero. From this relation we can see that the parameters of the Kähler class comprise a Kähler manifold with holomorphic prepotential whose structure is very similar to the manifold of the complex structure parameters.

As before, we note that there are a number of restrictions. One restriction is that not all values of v^A are allowed

$$V = \frac{1}{3!}\kappa_{ABC}v^A v^B v^C > 0. \tag{A.5.141}$$

The other restriction follows from rewriting the metric in the form

$$G(\rho,\sigma) = -3\left\{\frac{\kappa(\rho,\sigma,J)}{\kappa(J,J,J)} - \frac{\kappa(\rho,J,J)\kappa(\sigma,J,J)}{\kappa^2(J,J,J)}\right\} + \frac{3}{2}\frac{\kappa(\rho,J,J)\kappa(\sigma,J,J)}{\kappa^2(J,J,J)}. \quad \text{(A.5.142)}$$

To see what this form of metric can tell us, we note that any $(1,1)$-form can be written in terms of 'J parallel' and 'J orthogonal' terms:

$$\rho = \rho^{\perp} + \rho^{\parallel} = (\rho - \frac{1}{6}\rho_{mn}J^{mn}J) + \frac{1}{6}\rho_{mn}J^{mn}J, \quad \text{(A.5.143)}$$

where $\rho^{\parallel}$ is covariantly constant if ρ is harmonic. The metric then decomposes into $G(\rho^{\perp},\sigma^{\perp})$ and $G(\rho^{\parallel},\sigma^{\parallel})$ each of which has to be positive definite. The part $G(\rho^{\parallel},\sigma^{\parallel})$ obviously has this property, but

$$G(\rho^{\perp},\sigma^{\perp}) = -3\frac{\kappa(\rho^{\perp},\sigma^{\perp},J)}{\kappa(J,J,J)} > 0 \quad \text{(A.5.144)}$$

imposes a restriction: $\kappa_{AB}(v) = \kappa_{ABC}v^A$ has to be negative definite on $H^2_{\perp}$ but positive definite on $H^2_{\parallel}$. Therefore it must have signature $(1, h^{1,1}-1)$, which can change only if one of the eigenvalues passes through zero. The boundary of the allowed region is therefore given by

$$\det \kappa_{AB}(v) = 0. \quad \text{(A.5.145)}$$

The fundamental restriction on the parameters is of course that the Kähler form J be positive and this implies both positive volume and positive $G_{A\bar{B}}$.

A.6 Metrics on Calabi-Yau cones

In this final section we discuss the main tool that we have used everywhere in the thesis, the explicit from of the metric on the conifold.

A.6.1 Finiteness of distances between manifolds

In our discussions above we encountered the Weil-Peterson type metric on the moduli space and now we wish to estimate distances in the process

$$\mathcal{M}^{\flat} \overset{r^2\to 0}{\longrightarrow} \mathcal{M}^{\sharp} \overset{\wp}{\longleftarrow} \check{\mathcal{M}}. \quad \text{(A.6.146)}$$

The right and left arrows in (A.6.146) trace different paths in the space of complex structures of $\mathcal{M}^\flat$ and in the space of complexified Kähler classes of $\check{\mathcal{M}}$, respectively.

In order to show that the distance to the conifold converges, one has to show that the exponentials of the Kähler potentials on $\mathfrak{M}$ and $\mathfrak{W}$ given respectively by $i\int_{\mathcal{M}}\Omega\wedge\overline{\Omega}$ and $\int_{\mathcal{M}}J^3$ may degenerate but mildly enough. Concerning $\int_{\mathcal{M}}J^3$ this is automatically satisfied since the dependence on the parameters is completely polynomial. We also note that the canonical bundle of $\check{\mathcal{M}}$ is being inherited by $\mathcal{M}^\sharp$ and hence the only uncertainty is in the bahaviour of $\int_{\mathcal{M}}J^3$. In the view of mirror map exchanging moduli spaces, one expects $\int_{\mathcal{M}}J^3$ to be as well behaved as $i\int_{\mathcal{M}}\Omega\wedge\overline{\Omega}$, which will be discussed below in terms of monodromy of cycles.

Monodromy of cycles

Recall from our discussions above that for any $t\neq 0$ the manifold $\mathcal{M}_t^\flat$ is smooth and we may choose a symplectic basis $\{A^a,B_a\}$ for $H(\mathcal{M}_t^\flat,\mathbb{Z})$ so that $A^1,\ldots,A^k$ form a subgroup of $H(\mathcal{M}_t^\flat,\mathbb{Z})$ produced by the three-spheres. There is no obstruction to this as none of the three-spheres intersects with any of the others. It follows that $B_{k+1},\ldots,B_{h^{2,1}+1}$ do not intersect with these three-spheres either and can be represented by cycles away from the nodes. On the other hand, $B_1,\ldots,B_k$ do intersect with these three-spheres and each will include some of the three-hoops discussed above.

The basis $\{A^a,B_a\}$ is an integral basis and is therefore locally a constant function of t. However, if we consider nontrivial closed paths in the t-disk around the conifold point, the basis will generally change. The integral cycles $B_a(t)$ are dual to the $A^a(t)$ cycles and because $A^a(t)\cap A^b(t)=0$, there is no obstruction for $B_a(t)$ to acquire multiplets of $A^a(t)$. For a locally single-valued quantity, the multi-valuedness around nontrivial closed paths is called monodromy. If we define the monodromy operator by M, then $M(A^a(t))$ and $M(B_b(t))$ result from transporting $A^a(t)$ and $B_b(t)$ around $t=0$ in the t-disc and one has

$$M(A^a(t))=A^a(t),\qquad M(B_b(t))=B_b(t)+\sigma_{ab}A^b, \tag{A.6.147}$$

where σ_{ab} is an integral matrix the entries of which vanish for a or $b>k$.

Finiteness in the space of complex structure

We now would like to discuss the finiteness in the space of complex structure based on the monodromy properties of $A^a(t)$ and $B_b(t)$ cycles. We may consider the following periods

$$z^a(t) = \int_{A^a} \Omega_t, \qquad \mathscr{G}_a(t) = \int_{B_a} \Omega_t. \tag{A.6.148}$$

These are holomorphic if $t \neq 0$ and if Ω_t depends holomorphically on t and has the local representation as in (A.5.3). To estimate these periods, we consider the following.

By a suitable change of coordinates, the equation $\mathcal{C}(x) = r^2(x)$ which defines $\mathcal{M}_t^\flat$ near the node of $\mathcal{M}^\sharp$ reduces to

$$x^2 + y^2 + uv = t^2, \qquad t^2 > 0. \tag{A.6.149}$$

Here the S_t^3 is given by x, y real and $v = \bar{u}$ whereas the three-cap B_t^3 is given by $x > 0$, y imaginary and $v = -\overline{u}$.

The holomorphic volume form takes the form

$$\Omega = f \frac{dx \wedge dy \wedge du}{u}, \tag{A.6.150}$$

where f is nonzero and bounded at each of the nodes. Using this volume form it is straightforward to see see that $\int_{S_t^3} \Omega$ and $\int_{B_t^3} \Omega$ remain bounded as $t \to 0$. It follows then $\lim_{t\to 0} z^a(t) = 0$ for $1 \leq a \leq k$ which upon generalizing yields that all periods are bounded. The monodromy of cycles implies that $\mathcal{G}_a(t)$ is not single valued. However, we note that

$$\widehat{\mathcal{G}}_a(t) \stackrel{\text{def.}}{=} \mathcal{G}_a(t) - \frac{1}{2\pi i} \sigma_{ab} z^b \log(t) \tag{A.6.151}$$

is single valued by the fact that the action of monodromy cancels between the two terms on the LHS. The single-valuedness and the boundedness imply that the singularity at $t = 0$ is removable so that $\widehat{\mathcal{G}}_a(t)$ is also holomorphic at the origin.

According to these, the exponential of the Kähler potential becomes

$$
\begin{aligned}
i\int_{\mathcal{M}_t}\Omega\wedge\overline{\Omega} &= -2\mathrm{Im}(\overline{z}^a(t)\mathcal{G}_a(t)) \\
&= -2\mathrm{Im}\big(\overline{z}^a(t)\widehat{\mathcal{G}}_a(t)+\frac{1}{2\pi i}\overline{z}^a(t)\sigma_{ab}\overline{z}^b(t)\log(t)\big). \quad \text{(A.6.152)}
\end{aligned}
$$

By $z^a(0)=0=z^b(0)$ for $\sigma_{ab}\neq 0$, this takes the form

$$
a(t)+b(t)|t|^2\log|t|, \tag{A.6.153}
$$

where $a(t)$ and $b(t)$ are C^∞ functions and $a(0)\neq 0$. This shows the asymptotic behavior of the Kähler potential for the Weil–Peterson metric along the disk in the moduli space parametrized by t. It reveals that the metric diverges at worst logarithmically. Hence the distance to the origin remains finite even though the metric becomes singular at $t=0$.

A.6.2 Metrics on conifolds

In order to obtain the (unique) metric on the conifold, we need to find the Ricci-flat metric compatible with the Kähler structure of the cone. For this, we first need to parameterize the base of the cone. This can be done by rewriting the Eq. (A.4.67) and Eq. (A.4.67) in terms of the following matrix

$$
W\equiv\frac{1}{\sqrt{2}}w^\alpha\sigma_\alpha=\frac{1}{\sqrt{2}}\begin{pmatrix} w^3+iw^4 & w^1-iw^2 \\ w^1+iw^2 & -w^3+iw^4 \end{pmatrix}. \tag{A.6.154}
$$

Here $\sigma_\alpha\equiv(\sigma_i,i\,\mathbb{I})$ with σ_i being the usual Pauli matrices. In terms of (A.6.154) we can rewrite Eq. (A.4.66) for $\psi=0$ and Eq. (A.4.68) in the form

$$
\mathrm{Det}W=-\frac{1}{2}\sum_{\alpha=1}^{4}(w^\alpha)^2=0, \tag{A.6.155}
$$

and

$$
\mathrm{tr}W^\dagger W=\sum_{\alpha=1}^{4}|w^\alpha|^2=r^2. \tag{A.6.156}
$$

If we define the following matrix

$$Z = W/r, \tag{A.6.157}$$

then Eq. (A.6.155) and Eq. (A.6.156) take the form

$$\mathrm{Det}Z = 0, \qquad \mathrm{tr}Z^\dagger Z = 1. \tag{A.6.158}$$

These equations have the general solution of the form

$$Z = L_1 Z_0 L_2^\dagger, \tag{A.6.159}$$

$$Z_0 = \begin{pmatrix} 0 & 1 \\ 0 & 0 \end{pmatrix} = \frac{1}{2}(\sigma_1 + i\sigma_2). \tag{A.6.160}$$

Here L_i for $i = 1, 2$ are $SU(2)$ matrices given in terms of Euler angles as

$$L_i = \begin{pmatrix} \cos\frac{\theta_i}{2} e^{i(\psi_i+\phi_i)/2} & -\sin\frac{\theta_i}{2} e^{-i(\psi_i-\phi_i)/2} \\ \sin\frac{\theta_i}{2} e^{i(\psi_i-\phi_i)/2} & \cos\frac{\theta_i}{2} e^{-i(\psi_i+\phi_i)/2} \end{pmatrix}. \tag{A.6.161}$$

This shows that $SU(2) \times SU(2)$ acts transitively on the base of the cone. A Kähler potential $\mathcal{K}$ invariant under $SU(2) \times SU(2)$ depends only on r^2 and the associated Kähler metric takes the form

$$ds^2 = |\mathrm{tr}W^\dagger dW|^2 \mathcal{K}''(r^2) + \mathrm{tr}(dW^\dagger dW)\mathcal{K}'(r^2), \tag{A.6.162}$$

where $\mathcal{K}'(r^2) = d\mathcal{K}/d(r^2)$ and $\mathcal{K}''(r^2) = d^2\mathcal{K}/d^2(r^2)$. By substituting (A.6.154) into (A.6.162) and noting that the Ricci tensor on a Kähler manifold is given by (A.2.38), we obtain the Ricci-flat metric on the conifold in the following form:

$$ds^2 = d\rho^2 + \rho^2 \left[\frac{1}{9} \left(d\psi + \sum_{i=1}^{2} \cos\theta_i d\varphi_i \right)^2 + \frac{1}{6} \sum_{i=1}^{2} (d\theta_i^2 + \sin^2\theta_i d\varphi_i^2) \right], \tag{A.6.163}$$

where

$$\rho \equiv \sqrt{\frac{3}{2}} r^{2/3}. \tag{A.6.164}$$

To obtain the metric on the deformed conifold, note that in terms of (A.6.154) we can rewrite Eq. (A.4.66) for $\psi = \epsilon^2$ and Eq. (A.4.68) in the form

$$\mathrm{Det}W = -\frac{\epsilon^2}{2}, \tag{A.6.165}$$

and

$$\mathrm{tr}W^\dagger W = \sum_{A=1}^{4} |w^\alpha|^2 = r^2. \tag{A.6.166}$$

The general solution is

$$W_\epsilon = rZ_\epsilon, \quad Z_\epsilon = L_1 Z_\epsilon^{(0)} L_2^\dagger, \tag{A.6.167}$$

where the L_is are the same as before and

$$Z_\epsilon = \begin{pmatrix} 0 & a \\ b & 0 \end{pmatrix}. \tag{A.6.168}$$

We note that for $\rho \neq \epsilon$ there is again a transitive $SU(2)\times SU(2)$ action. By (A.6.168) into (A.6.162), it is straightforward to obtain the Ricci-flat Kählar metric on the deformed conifold as:

$$\begin{aligned} ds^2 &= (r^2\zeta' - \zeta)\left(1 - \frac{\epsilon^4}{r^4}\right)\left[\frac{(dr)^2}{r^2(1-\frac{\epsilon^4}{r^4})} + \frac{1}{4}(d\psi + \cos\theta_1 d\varphi_1 + \cos\theta_2 d\varphi_2)^2\right] \\ &+ \frac{\zeta}{4}(\sin^2\theta_1 d\phi_1^2 + d\theta_1^2 + \sin^2\theta_2 d\phi_2^2 + d\theta_2^2) \\ &+ \zeta\frac{\epsilon^2}{2r^2}[\cos\psi(d\theta_1 d\theta_2 - d\varphi_1 d\varphi_2 \sin\theta_1 \sin\theta_2) \\ &+ \sin\psi(\sin\theta_1 d\varphi_1 d\theta_2 - \sin\theta_2 d\varphi_2 d\theta_1)], \end{aligned} \tag{A.6.169}$$

where $\zeta \stackrel{\mathrm{def}}{=} r^2\mathcal{K}'(r^2)$, $\zeta \stackrel{\mathrm{def}}{=} \zeta'(r^2)$ and by Ricci-flatness

$$\zeta = \frac{\epsilon^4}{2}\frac{(\sinh 2\eta - 2\eta)^{1/3}}{\tanh\eta}. \tag{A.6.170}$$

By adopting the basis of 1-forms

$$g^{1,3} = \frac{e^1 \mp e^3}{\sqrt{2}}, \quad g^{2,4} = \frac{e^2 \mp e^4}{\sqrt{2}}, \quad g^5 = e^5 \tag{A.6.171}$$

with

$$e^1 = -\sin\theta_1 d\varphi_1, \qquad e^2 = d\theta_1, \qquad e^3 = \cos\psi \sin\theta_2 d\varphi_2 - \sin\psi d\theta_2,$$
$$e^4 = \sin\psi \sin\theta_2 d\varphi_2 + \cos\psi d\theta_2, \qquad e^5 = d\psi + \cos\theta_1 d\varphi_1 + \cos\theta_2 d\varphi_2, \quad \text{(A.6.172)}$$

it is straightforward to see that the Kähler potential and meteric on the deformed conifold take the form

$$\mathcal{K}(\eta) = \frac{\epsilon^{4/3}}{2^{1/3}} \int_0^\eta d\eta' [\sinh(2\eta') - 2\eta']^{1/3}. \quad \text{(A.6.173)}$$

$$ds_6^2 = g_{mn}^{(0)} dy^m dy^n = \frac{1}{2}\epsilon^{4/3} K(\eta) \Bigg[\frac{1}{3K(\eta)^3} \{d\eta^2 + (g^5)^2\} + \cosh^2\frac{\eta}{2}\{(g^3)^2 + (g^4)^2\} + \sinh^2\frac{\eta}{2}\{(g^1)^2 + (g^2)^2\} \Bigg], \quad \text{(A.6.174)}$$

where

$$K(\eta) = \frac{(\sinh(2\eta) - 2\eta)^{1/3}}{2^{1/3}\sinh\eta}, \quad r^3 = \sum_{\alpha=1}^{4} |z_\alpha|^2 = \epsilon^2 \cosh\eta. \quad \text{(A.6.175)}$$

Appendix B

The supergravity F-term potential

B.1 Coordinates and trajectories

For the deformed conifold we have

$$\sum_{\alpha=1}^{4}(z_\alpha)^2 = \epsilon^2, \tag{B.1.1}$$

$$z_1 = \epsilon\Big[\cosh\left(\frac{\Xi}{2}\right)\cos\left(\frac{\theta_+}{2}\right)\cos\left(\frac{\phi_+}{2}\right)+i\sinh\left(\frac{\Xi}{2}\right)\cos\left(\frac{\theta_-}{2}\right)\sin\left(\frac{\phi_+}{2}\right)\Big], \tag{B.1.2}$$

$$z_2 = \epsilon\Big[-\cosh\left(\frac{\Xi}{2}\right)\cos\left(\frac{\theta_+}{2}\right)\sin\left(\frac{\phi_+}{2}\right)+i\sinh\left(\frac{\Xi}{2}\right)\cos\left(\frac{\theta_-}{2}\right)\cos\left(\frac{\phi_+}{2}\right)\Big], \tag{B.1.3}$$

$$z_3 = \epsilon\Big[-\cosh\left(\frac{\Xi}{2}\right)\sin\left(\frac{\theta_+}{2}\right)\cos\left(\frac{\phi_-}{2}\right)+i\sinh\left(\frac{\Xi}{2}\right)\sin\left(\frac{\theta_-}{2}\right)\sin\left(\frac{\phi_-}{2}\right)\Big], \tag{B.1.4}$$

$$z_4 = \epsilon\Big[-\cosh\left(\frac{\Xi}{2}\right)\sin\left(\frac{\theta_+}{2}\right)\sin\left(\frac{\phi_-}{2}\right)-i\sinh\left(\frac{\Xi}{2}\right)\sin\left(\frac{\theta_-}{2}\right)\cos\left(\frac{\phi_-}{2}\right)\Big]. \tag{B.1.5}$$

Here we have used $\Xi = \eta + i\psi$, $\phi_+ = \phi_1 + \phi_2$, $\phi_- = \phi_1 - \phi_2$, $\theta_+ = \theta_1 + \theta_2$ and $\theta_- = \theta_1 - \theta_2$. The angular constraints are:

$$\frac{\phi_1 - \phi_2 \pm \psi}{2} = \pm\frac{\pi}{2}, \qquad \frac{\phi_1 + \phi_2 + \psi}{2} = \pi,$$
$$\frac{\psi - \phi_1 - \phi_2}{2} = 0, \qquad \theta_2 = 0. \tag{B.1.6}$$

To fix z_1 and z_2 take the following conditions from (6)

$$\frac{\phi_1 + \phi_2 + \psi}{2} = \pi, \qquad \frac{\psi - (\phi_1 + \phi_2)}{2} = 0 \qquad \theta_2 = 0. \tag{B.1.7}$$

Setting $\theta_1 = \theta$, $\psi = \pi$ and $\phi_1 + \phi_2 = \pi$, for z_1 and z_2 we obtain

$$\begin{aligned} z_1 &= \epsilon\left[\cosh\left(\frac{\eta + i\pi}{2}\right)\cos\left(\frac{\theta}{2}\right)\cos\left(\frac{\pi}{2}\right) + i\sinh\left(\frac{\eta + i\pi}{2}\right)\cos\left(\frac{\theta}{2}\right)\sin\left(\frac{\pi}{2}\right)\right] \\ &= -\epsilon\cosh\left(\frac{\eta}{2}\right)\cos\left(\frac{\theta}{2}\right), \end{aligned} \tag{B.1.8}$$

$$\begin{aligned} z_2 &= \epsilon\left[-\cosh\left(\frac{\eta + i\pi}{2}\right)\cos\left(\frac{\theta}{2}\right)\sin\left(\frac{\pi}{2}\right) + i\sinh\left(\frac{\eta + i\pi}{2}\right)\cos\left(\frac{\theta}{2}\right)\cos\left(\frac{\pi}{2}\right)\right] \\ &= -i\epsilon\sinh\left(\frac{\eta}{2}\right)\cos\left(\frac{\theta}{2}\right). \end{aligned} \tag{B.1.9}$$

To fix z_3 and z_4 take the following conditions from (6)

$$\frac{\phi_1 - \phi_2 + \psi}{2} = +\frac{\pi}{2}, \qquad \frac{\phi_1 - \phi_2 - \psi}{2} = -\frac{\pi}{2} \qquad \theta_2 = 0. \tag{B.1.10}$$

Setting $\theta_1 = \theta$, $\psi = \pi$ and $\phi_1 - \phi_2 = 0$, for z_3 and z_4 we obtain

$$z_3 = \epsilon\left[-\cosh\left(\frac{\eta + i\pi}{2}\right)\sin\left(\frac{\theta}{2}\right)\right] = -i\epsilon\sinh\left(\frac{\eta}{2}\right)\sin\left(\frac{\theta}{2}\right), \tag{B.1.11}$$

$$z_4 = \epsilon\left[-i\sinh\left(\frac{\eta + i\pi}{2}\right)\sin\left(\frac{\theta}{2}\right)\right] = \epsilon\cosh\left(\frac{\eta}{2}\right)\sin\left(\frac{\theta}{2}\right). \tag{B.1.12}$$

In summary we have then the following coordinates:

$$z_1 = -\epsilon\cosh\left(\frac{\eta}{2}\right)\cos\left(\frac{\theta}{2}\right), \qquad z_2 = -i\epsilon\sinh\left(\frac{\eta}{2}\right)\cos\left(\frac{\theta}{2}\right),$$
$$z_3 = -i\epsilon\sinh\left(\frac{\eta}{2}\right)\sin\left(\frac{\theta}{2}\right), \qquad z_4 = +\epsilon\cosh\left(\frac{\eta}{2}\right)\sin\left(\frac{\theta}{2}\right). \tag{B.1.13}$$

In order to obtain an angular stable trajectory, we may impose a further condition $\theta_1 = 0$, so that (B.1.13) becomes

$$\begin{aligned} z_1 &= -\epsilon \cosh\left(\frac{\eta}{2}\right), \qquad & z_2 &= -i\epsilon \sinh\left(\frac{\eta}{2}\right), \\ z_3 &= 0, & z_4 &= 0. \end{aligned} \tag{B.1.14}$$

It is straightforward to check that both of coordinates choices (B.1.13) and (B.1.14) satisfy the condition (B.1.1).

B.2 The F-tem potential

We now derive the D3-brane F-term potential on the entire deformed conifold along the trajectories (B.1.13) and (B.1.14). Recall from Chapter 5 that the F-term potential takes the form

$$\begin{aligned} V_F(z^\alpha, \bar{z}^\alpha, \rho, \bar{\rho}) &= \frac{\kappa^2}{3U(z,\rho)^2}\left\{\left[U(z,\rho) + \gamma k^{\gamma\bar{\delta}} k_\gamma k_{\bar{\delta}}\right]|W_{,\rho}|^2 - 3(\overline{W}W_{,\rho} + c.c.)\right\} \\ &\quad + \frac{\kappa^2}{3U(z,\rho)^2}\left[\left(k^{\alpha\bar{\delta}} k_{\bar{\delta}} \overline{W}_{,\bar{\rho}} W_{,\alpha} + c.c.\right) + \frac{1}{\gamma} k^{\alpha\bar{\beta}} W_{,\alpha} \overline{W}_{,\bar{\beta}}\right]. \end{aligned} \tag{B.2.15}$$

Here $\kappa^2 = M_{Pl}^{-2}$, $U = 2\sigma - \gamma k$, $\gamma = \sigma_0 T_3 / 3M_{Pl}^2$, $k^{\gamma\bar{\delta}}$ is the inverse (5.1.26) of the Calabi-Yau metric resulting from the Kähler potential k (A.6.173) whose derivative with respect to coordinates is denoted by k_γ, and $W_{,\alpha}$ and $W_{,\rho}$ denote the derivatives of the superpotential W (5.1.19) with respect to the coordinates z^α and the Kähler modulus $\rho = \sigma + i\chi$, respectively. We also have the standard formula

$$r^3 = \sum_{\alpha=1}^{4} |z_\alpha|^2 = \epsilon^2 \cosh\eta. \tag{B.2.16}$$

In what follows, we derive the explicit form of the potential (B.2.15) by computing each of its terms for the angular stable trajectory

$$z_1 = -\epsilon \cosh\left(\frac{\eta}{2}\right). \tag{B.2.17}$$

• The computation of $k^{\gamma\bar{\delta}}k_\gamma k_{\bar{\delta}}|W_{,\rho}|^2$. According to the value of $A(z^\alpha)$ given by (5.1.36), we get

$$\begin{aligned} |W_{,\rho}|^2 &= \overline{W_{,\rho}}W_{,\rho} = (-a_n\overline{A(z^\alpha)}e^{-a_n\bar{\rho}})(-aA(z^\alpha)e^{-a_n\rho}) \\ &= a_n^2|A_0|^2|g(\eta)|^{2/n}e^{-a_n(\rho+\bar{\rho})}, \end{aligned} \tag{B.2.18}$$

where

$$g(\eta) = 1 - \frac{z_1}{\mu} = 1 + \frac{\epsilon}{\mu}\cosh\left(\frac{\eta}{2}\right). \tag{B.2.19}$$

Thus by (B.2.18), (5.1.29) and (A.6.175) we obtain

$$\begin{aligned} k^{\gamma\,\bar{\delta}}k_\gamma k_{\bar{\delta}}|W_{,\rho}|^2 &= \frac{3}{4}\frac{\epsilon^{4/3}}{2^{1/3}}\frac{[\sinh(2\eta)-2\eta]^{4/3}}{\sinh^2\eta}a_n^2|A_0|^2|g(\eta)|^{2/n}e^{-2a_n\sigma} \\ &= \frac{3}{2}\epsilon^{4/3}a_n^2|A_0|^2K(\eta)^4\sinh^2\eta|g(\eta)|^{2/n}e^{-2a_n\sigma}. \end{aligned} \tag{B.2.20}$$

• The computation of $\overline{W}W_{,\rho} + c.c.$. we have

$$\begin{aligned} W\overline{W_{,\rho}} + c.c. &= -aW_0(A(z^\alpha)e^{-a_n\rho} + \overline{A(z^\alpha)}e^{-a_n\bar{\rho}}) \\ &\quad -2a_n|A(z^\alpha)|^2e^{-a_n(\rho+\bar{\rho})} \end{aligned} \tag{B.2.21}$$

By substituting the Kähler modulus with its value $\rho = \sigma + i\chi$ and integrating out the imaginary part by $e^{ia\chi}/A \to 1/|A|$, we obtain

$$\begin{aligned} \overline{W}W_{,\rho} + c.c. &= -aW_0(A(z^\alpha)e^{-a(\sigma+i\chi)} + \overline{A(z^\alpha)}e^{-a(\sigma-i\chi)}) \\ &\quad -2a_n|A(z^\alpha)|^2e^{-2a_n\sigma} \\ &= -2a_n|g(\eta)|^{2/n}|A_0|^2e^{-2a_n\sigma}\left(1 - \frac{|W_0|}{|A_0|}\frac{e^{a_n\sigma}}{g(\eta)^{1/n}}\right). \end{aligned} \tag{B.2.22}$$

• The computation of $k^{\alpha\bar{\delta}}k_{\bar{\delta}}\overline{W}_{,\bar{\rho}}W_{,\alpha}+c.c.$. In order to compute this term, we first note that according to (5.1.37), (5.1.31) and (A.6.175) we have

$$\begin{aligned} k^{\alpha\bar{\delta}}k_{\bar{\delta}}W_{,\alpha} &= \frac{3}{4}\frac{\cosh\eta}{\sinh^3\eta}[\sinh(2\eta)-2\eta]\sum_{j=1}^{3}\left(z_\alpha-\bar{z_\alpha}\frac{\epsilon^2}{r^3}\right)A_\alpha e^{-a_n\rho} \\ &= \frac{-3A_0}{2n\mu}\cosh\eta K(\eta)^3 z_1\left(1-\frac{\epsilon^2}{r^3}\right)\left(1-\frac{z_1}{\mu}\right)^{1/n-1}e^{-a_n\rho} \end{aligned} \tag{B.2.23}$$

Thus by using (B.2.23) and we obtain

$$\begin{aligned} k^{\alpha\bar{\delta}}k_{\bar{\delta}}W_{,\alpha}\overline{W}_{,\bar{\rho}} &= -\frac{3A_0}{2n\mu}\cosh\eta K(\eta)^3 z_1\left(1-\frac{\epsilon^2}{r^3}\right)\left(1-\frac{z_1}{\mu}\right)^{1/n-1}e^{-a_n\rho} \\ &\quad\times -e^{-a_n\bar{\rho}}a_n\overline{A(z^\alpha)} \\ &= -\frac{3a_n|A_0|^2\epsilon K(\eta)^3}{n\mu g(\eta)}\cosh\left(\frac{\eta}{2}\right)\sinh^2\left(\frac{\eta}{2}\right)|g(\eta)|^{2/n}\times e^{-2\sigma a_n}. \end{aligned} \tag{B.2.24}$$

We also note that

$$k^{\alpha\bar{\delta}}k_{\bar{\delta}}\overline{W}_{,\bar{\rho}}W_{,\alpha}+c.c.=2k^{\alpha\bar{\delta}}k_{\bar{\delta}}\overline{W}_{,\bar{\rho}}W_{,\alpha}. \tag{B.2.25}$$

• The computation of $k^{\alpha\bar{\beta}}W_{,\alpha}\overline{W}_{,\bar{\beta}}$. To compute this term according to (5.1.31), we first need to compute $R^{\bar{\alpha}\beta}\overline{W}_{,\bar{\alpha}}W_{,\beta}$ and $L^{\bar{\alpha}\beta}\overline{W}_{,\bar{\alpha}}W_{,\beta}$ according to (5.1.32) and (5.1.33), respectively:

$$R^{\bar{\alpha}\beta}\overline{W}_{,\bar{\alpha}}W_{,\beta} = e^{-2a_n\sigma}\frac{|A_0|^2}{n^2\mu^2}|g(\eta)|^{2/n-1}\left(\frac{\sinh^2(\eta/2)}{\cosh\eta}\right), \tag{B.2.26}$$

$$\begin{aligned} L^{\bar{\alpha}\beta}\overline{W}_{,\bar{\alpha}}W_{,\beta} &= e^{-2a_n\sigma}\left\{\sum_{\alpha=1}^{3}\left(1-\frac{\epsilon^4}{r^6}\right)|A_\alpha|^2-\frac{1}{r^3}\left(\sum_{\alpha,\beta=1}^{3}\bar{A}_\alpha\right.\right. \\ &\quad\left.\left.\left[z_\alpha\bar{z_\beta}+z_\beta\bar{z_\alpha}-\frac{\epsilon^4}{r^3}(z_\alpha z_\beta+\bar{z_\alpha}\bar{z_\beta})\right]A_\beta\right)\right\} \\ &= e^{-2a_n\sigma}|A_1|^2\left(1-\frac{\epsilon^2}{r^3}\right)\left\{\left(1+\frac{\epsilon^2}{r^3}\right)-\frac{2z_1^2}{r^3}\right\}. \end{aligned} \tag{B.2.27}$$

By using the (B.2.16), we also note that

$$1+\frac{\epsilon^2}{r^3}-\frac{2z_1^2}{r^3} = 0 \tag{B.2.28}$$

$$\Rightarrow L^{\bar{\alpha}\beta}\overline{W}_{,\bar{\alpha}}W_{,\beta}=0. \tag{B.2.29}$$

Thus by (B.2.29), (B.2.26) and (A.6.175) we obtain

$$\begin{aligned} k^{\bar{\alpha}\,\beta}\overline{W}_{,\bar{\alpha}}W_{,\beta} &= \frac{3}{2\cdot 2^{2/3}}\epsilon^{2/3}\frac{\cosh\eta}{\sinh^2\eta}[\sinh(2\eta)-2\eta]^{2/3}\{R^{\bar{\alpha}\,\beta}\overline{W}_{\bar{\alpha}}W_{\beta}+0\} \\ &= \frac{3\epsilon^{2/3}|A_0|^2e^{-2a_n\sigma}}{2n^2\mu^2}K(\eta)^2|g(\eta)|^{2/n-2}\sinh^2\left(\frac{\eta}{2}\right). \end{aligned} \tag{B.2.30}$$

Putting the above computed expressions into the potential (B.2.15) and factorizing yields

$$V_F = \frac{\kappa^2}{U^2}2a_n^2|A_0|^2|g(\eta)|^{2/n}e^{-2a_n\sigma}\left\{\frac{U}{6}+\frac{1}{a}\left(1-\frac{|W_0|}{|A_0|}\frac{e^{a_n\sigma}}{g(\eta)^{1/n}}\right)+F(\eta)\right\}, \tag{B.2.31}$$

where

$$F(\eta) = \epsilon^{4/3}\gamma\left[K(\eta)\sinh\left(\frac{\eta}{2}\right)\right]^2\left[K(\eta)\cosh\left(\frac{\eta}{2}\right)-\frac{\epsilon/\mu}{4\pi\epsilon^{4/3}\gamma g(\eta)}\right]^2. \tag{B.2.32}$$

Now we derive the potential (B.2.15) for the trajectory

$$z_1=-\epsilon\cosh\left(\frac{\eta}{2}\right)\cos\left(\frac{\theta}{2}\right). \tag{B.2.33}$$

• The computation of $k^{\alpha\bar{\delta}}k_{\bar{\delta}}W_{,\alpha}\overline{W}_{,\bar{\rho}}$. For the trajectory (B.2.33), we can immediately see that the final three lines in (B.2.24) become

$$
\begin{aligned}
k^{\alpha\bar{\delta}}k_{\bar{\delta}}W_{,\alpha}\overline{W}_{,\bar{\rho}} &= \frac{3a_n|A_0|^2}{2n\mu}\cosh\eta K(\eta)^3\bigg(-\epsilon\cosh\left(\frac{\eta}{2}\right)\cos\left(\frac{\theta}{2}\right)\bigg)\\
&\quad\times\bigg(\frac{\cosh\eta-1}{\cosh\eta}\bigg)\bigg[\bigg|1+\frac{\epsilon}{\mu}\cosh\left(\frac{\eta}{2}\right)\cos\left(\frac{\theta}{2}\right)\bigg|^2\bigg]^{1/n}\\
&\quad\times\bigg(1+\frac{\epsilon}{\mu}\cosh\left(\frac{\eta}{2}\right)\cos\left(\frac{\theta}{2}\right)\bigg)^{-1}e^{-a_n(\rho+\bar{\rho})}\\
&= -\frac{3a_n|A_0|^2}{n\mu g(\eta,\theta)}\epsilon K(\eta)^3\cosh\left(\frac{\eta}{2}\right)\cos\left(\frac{\theta}{2}\right)\sinh^2\left(\frac{\eta}{2}\right)\\
&\quad\times|g(\eta,\theta)|^{2/n}e^{-2a_n\sigma},
\end{aligned}
\tag{B.2.34}
$$

where

$$
g(\eta,\theta)=1+\frac{\epsilon}{\mu}\cosh\left(\frac{\eta}{2}\right)\cos\left(\frac{\theta}{2}\right). \tag{B.2.35}
$$

As before, we also have

$$
k^{\alpha\bar{\delta}}k_{\bar{\delta}}\overline{W}_{,\bar{\rho}}W_{,\alpha}+c.c.=2k^{\alpha\bar{\delta}}k_{\bar{\delta}}\overline{W}_{,\bar{\rho}}W_{,\alpha}. \tag{B.2.36}
$$

• The computation of $k^{\alpha\bar{\beta}}W_{,\alpha}\overline{W}_{,\bar{\beta}}$. To compute this term according to (5.1.31) for the trajectory (B.2.33), we first need to compute $R^{\bar{\alpha}\beta}\overline{W}_{,\bar{\alpha}}W_{,\beta}$ and $L^{\bar{\alpha}\beta}\overline{W}_{,\bar{\alpha}}W_{,\beta}$ according to (5.1.32) and (5.1.33) for (B.2.33), respectively:

$$
\begin{aligned}
R^{\bar{\alpha}\beta}\overline{W}_{\bar{\alpha}}W_{\beta} &= e^{-2a_n\sigma}\frac{|A_0|^2}{n^2\mu^2}\bigg|1-\frac{z_1}{\mu}\bigg|^{2/n-2}\bigg(1-\frac{|z_1|^2}{r^3}\bigg)\\
&= e^{-2a_n\sigma}\frac{|A_0|^2}{n^2\mu^2}|g(\eta,\theta)|^{2/n-2}\\
&\quad\times\frac{1}{\cosh\eta}\bigg(\cosh\eta-\cosh^2(\eta/2)\cos^2(\theta/2)\bigg).
\end{aligned}
\tag{B.2.37}
$$

$$
\begin{aligned}
L^{\bar{\alpha}\beta}\overline{W}_{,\bar{\alpha}}W_{,\beta} &= e^{-2a_n\sigma}|A_1|^2\bigg(1-\frac{\epsilon^2}{r^3}\bigg)\bigg\{\bigg(1+\frac{\epsilon^2}{r^3}\bigg)-\frac{2z_1^2}{r^3}\bigg\}\\
&= e^{-2a_n\sigma}\frac{|A_0|^2}{n^2\mu^2}\bigg|1-\frac{z_1}{\mu}\bigg|^{2/n-2}\bigg(1-\frac{\epsilon^2}{r^3}\bigg)\bigg\{\bigg(1+\frac{\epsilon^2}{r^3}\bigg)-\frac{2z_1^2}{r^3}\bigg\}.
\end{aligned}
\tag{B.2.38}
$$

It is straightforward to see that

$$\left(1-\frac{\epsilon^2}{r^3}\right)\left\{\left(1+\frac{\epsilon^2}{r^3}\right)-\frac{2z_1^2}{r^3}\right\} \;=\; \tanh^2\eta\sin^2\left(\frac{\theta}{2}\right), \tag{B.2.39}$$

which coincides with (B.2.29) for $\theta = 0$. Putting this into (B.2.38) we obtain this time a nonvanishing result

$$L^{\bar{\alpha}\beta}\overline{W}_{,\bar{\alpha}}W_{,\beta} \;=\; e^{-2a_n\sigma}\frac{|A_0|^2}{n^2\mu^2}|g(\eta,\theta)|^{2/n-2}\tanh^2\eta\sin^2\left(\frac{\theta}{2}\right). \tag{B.2.40}$$

We now put (B.2.40) and (B.2.37) in the formula (5.1.31)

$$\begin{aligned} k^{\bar{\alpha}\,\beta}\overline{W}_{,\bar{\alpha}}W_{,\beta} \;=\; & \frac{3}{2\cdot 2^{2/3}}\epsilon^{2/3}\frac{\cosh\eta}{\sinh^2\eta}[\sinh(2\eta)-2\eta]^{2/3}\Big\{R^{\bar{\alpha}\beta}\overline{W}_{,\bar{\alpha}}W_{,\beta} \\ & +\left[\frac{2}{3}\frac{\sinh(2\eta)}{\sinh(2\eta)-2\eta}-\coth^2\eta\right]\times L^{\bar{\alpha}\beta}\overline{W}_{,\bar{\alpha}}W_{,\beta}\Big\}. \end{aligned} \tag{B.2.41}$$

Simplifying gives

$$\begin{aligned} k^{\bar{\alpha}\beta}\overline{W}_{,\bar{\alpha}}W_{,\beta} \;=\; & \frac{3}{2}\epsilon^{2/3}K(\eta)^2e^{-2a_n\sigma}\frac{|A_0|^2}{n^2\mu^2}|g(\eta,\theta)|^{2/n-2} \\ & \times\left\{\sinh^2\left(\frac{\eta}{2}\right)+\sin^2\left(\frac{\theta}{2}\right)\left(\frac{2}{3K(\eta)^3}-\sinh^2\left(\frac{\eta}{2}\right)\right)\right\}. \end{aligned} \tag{B.2.42}$$

Putting the above computed expressions together we obtain the angular dependent F-term potential as

$$V_F \;=\; \frac{2\kappa^2a_n^2|A_0|^2|g(\eta,\theta)|^{2/n}e^{-2a_n\sigma}}{U^2}\left\{\frac{U}{6}+\frac{1}{a_n}\left(1-\frac{|W_0|}{|A_0|}\frac{e^{a_n\sigma}}{g(\eta,\theta)^{1/n}}\right)+F(\eta,\theta)\right\}, \tag{B.2.43}$$

where

$$\begin{aligned} F(\eta,\theta) \;=\; & \epsilon^{4/3}\frac{\gamma}{4}K(\eta)^4\sinh^2\eta-\frac{\epsilon K(\eta)^3}{2\pi\mu g(\eta)}\cosh\left(\frac{\eta}{2}\right)\sinh^2\left(\frac{\eta}{2}\right)\cos\left(\frac{\theta}{2}\right) \\ & +\frac{\epsilon^{2/3}K(\eta)^2}{4\gamma(2\pi)^2\mu^2}|g(\eta)|^{-2} \\ & \times\sin^2\left(\frac{\eta}{2}\right)\left[1-\sin^2\left(\frac{\theta}{2}\right)\left(1-\frac{2}{3K(\eta)^3\sinh^2(\eta/2)}\right)\right]. \end{aligned} \tag{B.2.44}$$

The new potential (B.2.43) yields the old potential (B.2.31) when we set $\theta = 0$. To see this, it is straightforward to check that the term $F(\eta, \theta)$ in (B.2.43) given as (B.2.44) becomes equal to the term $F(\eta)$ in (B.2.31) when $\theta = 0$; the other terms are exactly the same when $\theta = 0$.

Appendix C

DBI equations of motion

In this appendix, we derive the equations of motion (4.1.19) - (4.1.20). To find the brane equations of motion, we consider the Euler-Lagrange equations

$$\frac{\partial}{\partial x^\mu}\frac{\partial \mathscr{L}}{\partial(\partial\phi^m/\partial x^\mu)} = \frac{\partial \mathscr{L}}{\partial \phi^m} \tag{C.0.1}$$

for the Lagrangian

$$\mathscr{L} = \sqrt{-g}\left[f^{-1}\sqrt{1 + f g^{(0)}_{mn} g^{\mu\nu}\partial_\mu\phi^m\partial_\nu\phi^n} - f^{-1} + V\right]. \tag{C.0.2}$$

We also recall that the fields only depend on time, $\phi^m = \phi^m(t)$, so that

$$\gamma = \frac{1}{\sqrt{1 + f g^{(0)}_{mn} g^{\mu\nu}\partial_\mu\phi^m\partial_\nu\phi^n}} = \frac{1}{\sqrt{1 - f g^{(0)}_{mn}\dot{\phi}^m\dot{\phi}^n}}. \tag{C.0.3}$$

This gives

$$\begin{aligned}\frac{\partial \mathscr{L}}{\partial(\partial\phi^m/\partial x^\mu)} &= \sqrt{-g} f^{-1}\frac{f g^{(0)}_{mn} g^{\mu\nu}\partial_\nu\phi^n}{\sqrt{1 + f g^{(0)}_{mn} g^{\mu\nu}\partial_\mu\phi^m\partial_\nu\phi^n}} \\ &= -a^3 g^{(0)}_{mn}\gamma\dot{\phi}^n.\end{aligned} \tag{C.0.4}$$

Thus the LHS of (C.0.1) becomes

$$\frac{\partial}{\partial x^\mu}\frac{\partial \mathscr{L}}{\partial(\partial\phi^m/\partial x^\mu)} = \frac{\partial}{\partial x^\mu}[-a^3 g^{(0)}_{mn}\gamma\dot{\phi}^n] \tag{C.0.5}$$

$$= -\frac{d}{dt}[a^3 g^{(0)}_{mn}\gamma\dot{\phi}^n]. \tag{C.0.6}$$

For the RHS of (C.0.1), we have

$$\frac{\partial \mathscr{L}}{\partial \phi^m} = \sqrt{-g}\left[\frac{\partial}{\partial \phi^m} f^{-1}\sqrt{1 + f g^{(0)}_{mn} g^{\mu\nu}\partial_\mu \phi^m \partial_\nu \phi^n} + f^{-2}\partial_m f + \partial_m V\right], \tag{C.0.7}$$

where

$$\begin{aligned}
\frac{\partial}{\partial \phi^m} f^{-1}\sqrt{1 + f g^{(0)}_{mn} g^{\mu\nu}\partial_\mu \phi^m \partial_\nu \phi^n} &= \sqrt{1 + f g^{(0)}_{mn} g^{\mu\nu}\partial_\mu \phi^m \partial_\nu \phi^n}\frac{\partial}{\partial \phi^m} f^{-1} \\
&\quad + f^{-1}\frac{\partial}{\partial \phi^m}\sqrt{1 + f g^{(0)}_{mn} g^{\mu\nu}\partial_\mu \phi^m \partial_\nu \phi^n} \\
&= -\sqrt{1 + f g^{(0)}_{mn} g^{\mu\nu}\partial_\mu \phi^m \partial_\nu \phi^n}\frac{\partial_m f}{f^2} \\
&\quad + f^{-1}\frac{(\partial/\partial\phi^m)(f g^{(0)}_{mn} g^{\mu\nu}\partial_\mu \phi^m \partial_\nu \phi^n)}{2\sqrt{1 + f g^{(0)}_{mn} g^{\mu\nu}\partial_\mu \phi^m \partial_\nu \phi^n}},
\end{aligned} \tag{C.0.8}$$

$$\begin{aligned}
\frac{\partial}{\partial \phi^m}(f g^{(0)}_{mn} g^{\mu\nu}\partial_\mu \phi^m \partial_\nu \phi^n) &= g^{(0)}_{mn} g^{\mu\nu}\partial_\mu \phi^m \partial_\nu \phi^n \frac{\partial f}{\partial \phi^m} \\
&\quad + f g^{\mu\nu}\partial_\mu \phi^m \partial_\nu \phi^n \frac{\partial g^{(0)}_{mn}}{\partial \phi^m} \\
&= -f\frac{\partial g^{(0)}_{mn}}{\partial \phi^m}\dot{\phi}^m\dot{\phi}^n + f^{-1}(\gamma^{-2} - 1)\partial_m f.
\end{aligned} \tag{C.0.9}$$

This gives

$$\begin{aligned}
\frac{\partial \mathscr{L}}{\partial \phi^m} &= a^3\Big[-\gamma^{-1}\frac{\partial_m f}{f^2} - \frac{\gamma}{2}\frac{\partial g^{(0)}_{mn}}{\partial \phi^m}\dot{\phi}^m\dot{\phi}^n + \frac{\gamma}{2}f^{-2}(\gamma^{-2} - 1)\partial_m f \\
&\quad + \frac{\partial_m f}{f^2} + \partial_m V\Big] \\
&= a^3\Big[-\frac{\gamma}{2}\frac{\partial g^{(0)}_{mn}}{\partial \phi^m}\dot{\phi}^m\dot{\phi}^n + \partial_m V + \frac{\partial_m f}{f^2}(-\gamma^{-1} + \frac{\gamma}{2}(\gamma^{-2} - 1) + 1)\Big].
\end{aligned} \tag{C.0.10}$$

By rearranging the last term we get

$$\begin{aligned}
-\gamma^{-1} + \frac{\gamma}{2}(\gamma^{-2} - 1) + 1 &= \gamma(-\gamma^{-2} + \frac{1}{2}(\gamma^{-2} - 1) + 1\gamma^{-1}) \\
&= -\frac{\gamma}{2}(2\gamma^{-2} - \gamma^{-2} + 1 - 2\gamma^{-1}) \\
&= -\frac{\gamma\partial_m f}{2f^2}(\gamma^{-1} - 1)^2.
\end{aligned} \tag{C.0.11}$$

Thus the RHS of (C.0.1) becomes

$$\frac{\partial \mathscr{L}}{\partial \phi^m} = a^3\Big[-\frac{\gamma}{2}\frac{\partial g^{(0)}_{mn}}{\partial \phi^m}\dot{\phi}^m\dot{\phi}^n + \partial_m V - \frac{\gamma\partial_m f}{2f^2}(\gamma^{-1}-1)^2\Big]. \quad \text{(C.0.12)}$$

Equating the LHS and the RHS of (C.0.1) gives

$$-\frac{d}{dt}[a^3 g^{(0)}_{mn}\gamma\dot{\phi}^n] = a^3\Big[-\frac{\gamma}{2}\frac{\partial g^{(0)}_{mn}}{\partial \phi^m}\dot{\phi}^m\dot{\phi}^n + \partial_m V - \frac{\gamma\partial_m f}{2f^2}(\gamma^{-1}-1)^2\Big], \quad \text{(C.0.13)}$$

or

$$\frac{1}{a^3}\frac{d}{dt}[a^3 g^{(0)}_{mn}\gamma\dot{\phi}^n] = \Big[\frac{\gamma\partial_m f}{2f^2}(\gamma^{-1}-1)^2 + \frac{\gamma}{2}\frac{\partial g^{(0)}_{mn}}{\partial \phi^m}\dot{\phi}^m\dot{\phi}^n - \partial_m V\Big]. \quad \text{(C.0.14)}$$

From Eq. (C.0.14), the radial equation of motion along the proper distance ($g_{rr}=1$) takes the form

$$\gamma\ddot{\phi} + \dot{\gamma}\dot{\phi} + 3H\gamma\dot{\phi} = \gamma(\gamma^{-1}-1)\frac{\partial_\phi f}{2f^2} + \frac{\gamma}{2}\partial_\phi g_{\alpha\beta}\dot{\theta}^\alpha\dot{\theta}^\beta - \partial_\phi V. \quad \text{(C.0.15)}$$

Recall that on the deformed conifold the metric takes the form

$$ds^2 = \mathcal{A}(\eta)d\eta^2 + \mathcal{B}(\eta)d\theta^2 = \frac{\epsilon^{4/3}}{6K^2}d\eta^2 + \epsilon^{4/3}B(\eta)d\theta^2. \quad \text{(C.0.16)}$$

Hence we obtain

$$\phi = \epsilon^{2/3}\sqrt{\frac{T_3}{6}}\int_0^\eta \frac{dx}{K(x)} \quad \Rightarrow \quad \dot{\phi} = \sqrt{T_3\mathcal{A}}\dot{\eta}. \quad \text{(C.0.17)}$$

By putting $\dot{\phi} = \sqrt{T_3\mathcal{A}}\dot{\eta}$ in (A.21), the equations of motion become

$$\begin{aligned}
\gamma\ddot{\eta} &= -\frac{\gamma\mathcal{A}'\dot{\eta}^2}{2\mathcal{A}} - 3H\gamma\dot{\eta} - \frac{1}{2}\gamma^3\dot{\eta}[(h'\dot{\eta}+h_\theta\dot{\theta})(\mathcal{A}\dot{\eta}^2+\mathcal{B}\dot{\theta}^2) \\
&\quad + h\dot{\eta}(\mathcal{A}'\dot{\eta}^2+\mathcal{B}'\dot{\theta}^2) + 2h(\mathcal{A}\dot{\eta}\ddot{\eta}+B\dot{\theta}\ddot{\theta})] + \gamma(\gamma^{-1}-1)^2\frac{h'}{2h^2\mathcal{A}} \\
&\quad + \frac{\gamma}{2}\dot{\theta}^2\frac{\mathcal{B}'}{\mathcal{A}} - \frac{V_\eta}{\mathcal{A}T_3}, \quad \text{(C.0.18)} \\
\gamma\ddot{\theta} &= -\gamma\frac{\mathcal{B}'}{\mathcal{B}}\dot{\eta}\dot{\theta} - 3H\gamma\dot{\theta} - \frac{1}{2}\gamma^3\dot{\theta}[(h'\dot{\eta}+h_\theta\dot{\theta})(\mathcal{A}\dot{\eta}^2+\mathcal{B}\dot{\theta}^2) + h\dot{\eta}(\mathcal{A}'\dot{\eta}^2+\mathcal{B}'\dot{\theta}^2) \\
&\quad + 2h(\mathcal{A}\dot{\eta}\ddot{\eta}+\mathcal{B}\dot{\theta}\ddot{\theta})] + \gamma(\gamma^{-1}-1)\frac{h_\theta}{2h^2\mathcal{B}} - \frac{V_\theta}{\mathcal{B}T_3}. \quad \text{(C.0.19)}
\end{aligned}$$

$$\begin{aligned}\gamma^3\ddot{\eta}(1-h\mathcal{B}\dot{\theta}^2)+h\gamma^3\dot{\theta}\dot{\eta}\mathcal{B}\ddot{\theta} &= -\frac{\mathcal{A}'}{2\mathcal{A}}\gamma\dot{\eta}^2-3H\gamma\dot{\eta}-\frac{1}{2}\gamma^3h'\dot{\eta}^2(\mathcal{A}\dot{\eta}^2+\mathcal{B}\dot{\theta}^2)\\ &\quad -\frac{1}{2}\gamma^3h_\theta\dot{\eta}\dot{\theta}(\mathcal{A}\dot{\eta}^2+\mathcal{B}\dot{\theta}^2)-\frac{1}{2}\gamma^3h\dot{\eta}^2(\mathcal{A}'\dot{\eta}^2+\mathcal{B}'\dot{\theta}^2)\\ &\quad +\frac{\gamma(\gamma^{-1}-1)^2h'}{2h^2\mathcal{A}}+\frac{\gamma}{2}\dot{\theta}^2\frac{\mathcal{B}'}{\mathcal{A}}-\frac{V_\eta}{\mathcal{A}T_3},\end{aligned} \tag{C.0.20}$$

$$\begin{aligned}\gamma^3\ddot{\theta}(1-h\mathcal{A}\dot{\eta}^2)+h\gamma^3\dot{\theta}\dot{\eta}\mathcal{A}\ddot{\eta} &= -\frac{\mathcal{B}'}{\mathcal{B}}\gamma\dot{\eta}\dot{\theta}-3H\gamma\dot{\theta}-\frac{1}{2}\gamma^3\dot{\theta}\dot{\eta}h'(\mathcal{A}\dot{\eta}^2+\mathcal{B}\dot{\theta}^2)\\ &\quad -\frac{1}{2}\gamma^3\dot{\theta}^2h_\theta(\mathcal{A}\dot{\eta}^2+\mathcal{B}\dot{\theta}^2)-\frac{1}{2}\gamma^3h\dot{\theta}\dot{\eta}(\mathcal{A}'\dot{\eta}^2+\mathcal{B}'\dot{\theta}^2)\\ &\quad -\frac{V_\theta}{\mathcal{B}T_3}+\gamma(\gamma^{-1}-1)^2\frac{h_\theta}{2h^2\mathcal{B}}.\end{aligned} \tag{C.0.21}$$

By cross elimination and noting that γ is given by (C.0.3), we obtain

$$\begin{aligned}\ddot{\eta} &= -\frac{3H}{\gamma^2}\dot{\eta}+\frac{h'}{\gamma h}\dot{\eta}^2(1-\gamma)+\frac{h'}{2h^2\mathcal{A}}(\gamma^{-1}-1)^2\\ &\quad -\frac{1}{2\mathcal{A}}(\mathcal{A}'\dot{\eta}^2-\mathcal{B}'\dot{\theta}^2)+h\dot{\theta}\dot{\eta}\frac{V_\theta}{\gamma T_3}-(1-h\mathcal{A}\dot{\eta}^2)\frac{V_\eta}{\gamma AT_3}\\ &\quad -\dot{\eta}\dot{\theta}(1-\gamma^{-1})\frac{h''}{h},\end{aligned} \tag{C.0.22}$$

$$\begin{aligned}\ddot{\theta} &= -\frac{3H\dot{\theta}}{\gamma^2}+(1-\gamma)\dot{\theta}\dot{\eta}\frac{h'}{\gamma h}-\dot{\theta}\dot{\eta}\frac{\mathcal{B}'}{\mathcal{B}}+h\dot{\theta}\dot{\eta}\frac{V_\eta}{\gamma T_3}\\ &\quad -(1-h\mathcal{B}\dot{\theta}^2)\frac{V_\theta}{\gamma\mathcal{B}T_3}-(1-\gamma^{-1})\left[\dot{\theta}^2-\frac{(1-\gamma^{-1})}{2h\mathcal{B}}\right]\frac{h_\theta}{h}.\end{aligned} \tag{C.0.23}$$

By substituting the values of $\mathcal{A}$ and $\mathcal{B}$ according to the RHS of Eq. (C.0.16), and noting that $h=e^{-4A}$, we obtain the equations of motion in the form

$$\begin{aligned}\ddot{\eta} &= -\frac{3H}{\gamma^2}\dot{\eta}-4A'(\gamma^{-1}-1)\dot{\eta}^2-12\epsilon^{-4/3}K^2A'e^{4A}(\gamma^{-1}-1)^2\\ &\quad +\frac{K'}{K}\dot{\eta}^2+3K^2B'\dot{\vartheta}^2+e^{-4A}\dot{\vartheta}\dot{\eta}\frac{V_\vartheta}{\gamma}-(6K^2\epsilon^{-4/3}-e^{-4A}\dot{\eta}^2)\frac{V_\eta}{\gamma}\\ &\quad +4\dot{\eta}\dot{\theta}(1-\gamma^{-1})A''\end{aligned} \tag{C.0.24}$$

$$\begin{aligned}\ddot{\vartheta} &= -\frac{3H}{\gamma^2}\dot{\vartheta}-4A'(\gamma^{-1}-1)\dot{\eta}\dot{\vartheta}-\frac{B'}{B}\dot{\eta}\dot{\vartheta}+e^{-4A}\dot{\eta}\dot{\vartheta}\frac{V_\eta}{\gamma}-\left(\frac{\epsilon^{-4/3}}{B}-e^{-4A}\dot{\vartheta}^2\right)\frac{V_\vartheta}{\gamma}\\ &\quad +4\gamma(1-\gamma^{-1})\left[\dot{\theta}^2-\frac{(1-\gamma^{-1})\epsilon^{4/3}e^{4A}}{2B}\right]A''.\end{aligned} \tag{C.0.25}$$

Here ϑ stands for either θ_i with $i = 1, 2$. If the warp factor depends only on the radial coordinate, then all the terms involving A'' vanish and Eqs. (C.0.24) - (C.0.25) reduce to Eqs. (4.1.19) - (4.1.20).

Bibliography

[1] R. Gregory and D. Kaviani, "Spinflation with Angular Potentials," JHEP **1201**, 037 (2012) [arXiv:1107.5522 [hep-th]].

[2] D. Kaviani, "Spinflation with backreaction," submitted to IJMPD, (2013) arXiv:1212.5831 [hep-th].

[3] S. Weinberg, "Cosmology," *Oxford, UK: Oxford Univ. Pr. (2008) 593 p*

[4] S. Weinberg, "Gravitation and Cosmology: Principles and Applications of the General Theory of Relativity", John-Wiley and Sons, (1972).

[5] S. Weinberg, "The quantum theory of fields. Vol. 2: Modern applications," *Cambridge, UK: Univ. Pr. (1996) 489 p*

[6] V. Mukhanov, "Physical foundations of cosmology," *Cambridge, UK: Univ. Pr. (2005) 421 p*

[7] A. Friedmann, *Z. Phys.* **10**, 377 (1922); *ibid.* **21**, 326 (1924).

[8] H. P. Robertson, *Astrophys. J.* **82**, 284 (1935); *ibid*, **83**, 187, 257 (1936).

[9] A. G. Walker, *Proc. Lon. Math. Sco.* (2) **42**, 90 (1936).

[10] A. A. Penzias and R. W. Wilson, "A Measurement of excess antenna temperature at 4080-Mc/s," Astrophys. J. **142**, 419 (1965).

[11] G.F. Smooth *et al.,* Astrophys. J. **396**, L1 (1992).

[12] G. Hinshaw *et al.*, "2-Point Correlations in the COBE DMR 4-Year Anisotropy Maps," Astrophys. J. **464**, L25 (1996) [arXiv:astro-ph/9601061].

[13] A. Kogut *et al.*, "Calibration and Systematic Error Analysis For the COBE-DMR Four-Year Sky Maps," Astrophys. J. **470**, 653 (1996) [arXiv:astro-ph/9601066].

[14] K. M. Gorski, A. J. Banday, C. L. Bennett, G. Hinshaw, A. Kogut, G. F. Smoot and E. L. Wright, "Power Spectrum of Primordial Inhomogeneity Determined from the 4-Year COBE DMR Sky Maps," Astrophys. J. **464**, L11 (1996) [arXiv:astro-ph/9601063].

[15] G. Hinshaw, A. J. Banday, C. L. Bennett, K. M. Gorski, A. Kogut, G. F. Smoot and E. L. Wright, "Band power spectra in the COBE DMR 4-year anisotropy maps," Astrophys. J. **464**, L17 (1996) [astro-ph/9601058].

[16] E. L. Wright, C. L. Bennett, K. Gorski, G. Hinshaw and G. F. Smoot, "Angular power spectrum of the microwave background anisotropy seen by the COBE differential microwave radiometer," Astrophys. J. **464**, L21 (1996) [astro-ph/9601059].

[17] D. N. Spergel *et al.,* Astrophys. J. suppl. **148**, 175 (2003).

[18] A. H. Guth, "The Inflationary Universe: A Possible Solution To The Horizon And Flatness Problems," Phys. Rev. D **23**, 347 (1981).

[19] A. D. Linde, "A New Inflationary Universe Scenario: A Possible Solution Of The Horizon, Flatness, Homogeneity, Isotropy And Primordial Monopole Problems," Phys. Lett. B **108**, 389 (1982).

[20] A. D. Linde, "Coleman-Weinberg Theory And A New Inflationary Universe Scenario," Phys. Lett. B **114**, 431 (1982).

[21] A. Albrecht and P. J. Steinhardt, "Cosmology For Grand Unified Theories With Radiatively Induced Symmetry Breaking," Phys. Rev. Lett. **48**, 1220 (1982).

[22] S. R. Coleman and E. J. Weinberg, "Radiative Corrections As The Origin Of Spontaneous Symmetry Breaking," Phys. Rev. D **7**, 1888 (1973).

[23] S. Perlmutter *et al.* [Supernova Cosmology Project Collaboration], "Measurements of Omega and Lambda from 42 high redshift supernovae," Astrophys. J. **517**, 565 (1999) [astro-ph/9812133].

[24] A. G. Riess *et al.* [Supernova Search Team Collaboration], "Observational evidence from supernovae for an accelerating universe and a cosmological constant," Astron. J. **116**, 1009 (1998) [astro-ph/9805201].

[25] P. Candelas, G. T. Horowitz, A. Strominger and E. Witten, "Vacuum Configurations for Superstrings," Nucl. Phys. B **258**, 46 (1985).

[26] P. Candelas and X. de la Ossa, "Moduli Space Of Calabi-Yau Manifolds," Nucl. Phys. B **355**, 455 (1991).

[27] P. Candelas and X. C. de la Ossa, "Comments on Conifolds," Nucl. Phys. B **342**, 246 (1990).

[28] P. Candelas, P. S. Green and T. Hubsch, "Finite Distances Between Distinct Calabi-yau Vacua: (other Worlds Are Just Around The Corner)," Phys. Rev. Lett. **62**, 1956 (1989).

[29] S. B. Giddings, S. Kachru and J. Polchinski, "Hierarchies from fluxes in string compactifications," Phys. Rev. D **66**, 106006 (2002) [hep-th/0105097].

[30] S. Kachru, R. Kallosh, A. D. Linde and S. P. Trivedi, "De Sitter vacua in string theory," Phys. Rev. D **68**, 046005 (2003) [hep-th/0301240].

[31] R. Hofmann and D. Kaviani, "The quantum of action and finiteness of radiative corrections: Deconfining SU(2) Yang-Mills thermodynamics," Quant. Matt. **1**, 41 (2012) [arXiv:1204.4112 [physics.gen-ph]].

[32] D. Kaviani, "Radiative corrections in Yang-Mills thermodynamics," AIP Conf. Proc. 1389 (2011) 646-650.

[33] D. Kaviani and R. Hofmann, "Irreducible three-loop contributions to the pressure in Yang-Mills thermodynamics," Mod. Phys. Lett. A **22**, 2343 (2007) [arXiv:0704.3326 [hep-th]].

[34] S. H. Henry Tye, "Brane inflation: String theory viewed from the cosmos," Lect. Notes Phys. **737**, 949 (2008) [arXiv:hep-th/0610221].

[35] J. M. Cline, "String cosmology," arXiv:hep-th/0612129.

[36] R. Kallosh, "On Inflation in String Theory," Lect. Notes Phys. **738**, 119 (2008) [arXiv:hep-th/0702059].

[37] C. P. Burgess, "Lectures on Cosmic Inflation and its Potential Stringy Realizations," Class. Quant. Grav. **24**, S795 (2007) [PoS **P2GC**, 008 (2006)] [PoS C **ARGESE2007**, 003 (2007)] [arXiv:0708.2865 [hep-th]].

[38] L. McAllister and E. Silverstein, "String Cosmology: A Review," Gen. Rel. Grav. **40**, 565 (2008) [arXiv:0710.2951 [hep-th]].

[39] D. Baumann, "TASI Lectures on Inflation," arXiv:0907.5424 [hep-th].

[40] D. Baumann and L. McAllister, "Advances in Inflation in String Theory," Ann. Rev. Nucl. Part. Sci. **59**, 67 (2009) [arXiv:0901.0265 [hep-th]].

[41] J. Polchinski, "Dirichlet Branes and Ramond-Ramond charges," Phys. Rev. Lett. **75**, 4724 (1995) [hep-th/9510017].

[42] G. R. Dvali and S. H. H. Tye, "Brane inflation," Phys. Lett. B **450**, 72 (1999) [arXiv:hep-ph/9812483].

[43] S. H. S. Alexander, "Inflation from D - anti-D-brane annihilation," Phys. Rev. D **65**, 023507 (2002) [arXiv:hep-th/0105032].

[44] C. P. Burgess, M. Majumdar, D. Nolte, F. Quevedo, G. Rajesh and R. J. Zhang, "The Inflationary brane anti-brane universe," JHEP **0107**, 047 (2001) [arXiv:hep-th/0105204].

[45] G. Shiu and S. H. H. Tye, "Some aspects of brane inflation," Phys. Lett. B **516**, 421 (2001) [arXiv:hep-th/0106274].

[46] S. Kachru, R. Kallosh, A. D. Linde, J. M. Maldacena, L. P. McAllister and S. P. Trivedi, "Towards inflation in string theory," JCAP **0310**, 013 (2003) [arXiv:hep-th/0308055].

[47] H. Firouzjahi and S. H. H. Tye, "Closer towards inflation in string theory," Phys. Lett. B **584**, 147 (2004) [arXiv:hep-th/0312020].

[48] C. P. Burgess, J. M. Cline, K. Dasgupta and H. Firouzjahi, "Uplifting and inflation with D3 branes," JHEP **0703**, 027 (2007) [arXiv:hep-th/0610320].

[49] F. Chen and H. Firouzjahi, "Dynamics of D3-D7 Brane Inflation in Throats," JHEP **0811**, 017 (2008) [arXiv:0807.2817 [hep-th]].

[50] H. Y. Chen, J. O. Gong and G. Shiu, "Systematics of multi-field effects at the end of warped brane inflation," JHEP **0809**, 011 (2008) [arXiv:0807.1927 [hep-th]].

[51] H. Y. Chen and J. O. Gong, "Towards a warped inflationary brane scanning," Phys. Rev. D **80**, 063507 (2009) [arXiv:0812.4649 [hep-th]].

[52] D. Baumann, A. Dymarsky, I. R. Klebanov, J. M. Maldacena, L. P. McAllister and A. Murugan, "On D3-brane potentials in compactifications with fluxes and wrapped D-branes," JHEP **0611**, 031 (2006) [arXiv:hep-th/0607050].

[53] D. Baumann, A. Dymarsky, I. R. Klebanov, L. McAllister and P. J. Steinhardt, "A Delicate Universe," Phys. Rev. Lett. **99**, 141601 (2007) [arXiv:0705.3837 [hep-th]].

[54] D. Baumann, A. Dymarsky, I. R. Klebanov and L. McAllister, "Towards an Explicit Model of D-brane Inflation," JCAP **0801**, 024 (2008) [arXiv:0706.0360 [hep-th]].

[55] D. Baumann, A. Dymarsky, S. Kachru, I. R. Klebanov and L. McAllister, "Holographic Systematics of D-brane Inflation," JHEP **0903**, 093 (2009) [arXiv:0808.2811 [hep-th]].

[56] D. Baumann, A. Dymarsky, S. Kachru, I. R. Klebanov and L. McAllister, "Compactification Effects in D-brane Inflation," Phys. Rev. Lett. **104**, 251602 (2010) [arXiv:0912.4268 [hep-th]].

[57] D. Baumann, A. Dymarsky, S. Kachru, I. R. Klebanov and L. McAllister, "D3-brane Potentials from Fluxes in AdS/CFT," JHEP **1006**, 072 (2010) [arXiv:1001.5028 [hep-th]].

[58] S. Kecskemeti, J. Maiden, G. Shiu and B. Underwood, "DBI Inflation in the Tip Region of a Warped Throat," JHEP **0609**, 076 (2006) [arXiv:hep-th/0605189].

[59] O. DeWolfe, L. McAllister, G. Shiu and B. Underwood, "D3-brane Vacua in Stabilized Compactifications," JHEP **0709**, 121 (2007) [arXiv:hep-th/0703088].

[60] E. Pajer, "Inflation at the Tip," JCAP **0804**, 031 (2008) [arXiv:0802.2916 [hep-th]].

[61] H. Y. Chen, J. O. Gong, K. Koyama and G. Tasinato, "Towards multi-field D-brane inflation in a warped throat," JCAP **1011**, 034 (2010) [arXiv:1007.2068 [hep-th]].

[62] E. Silverstein and D. Tong, "Scalar Speed Limits and Cosmology: Acceleration from D-cceleration," Phys. Rev. D **70**, 103505 (2004) [arXiv:hep-th/0310221].

[63] M. Alishahiha, E. Silverstein and D. Tong, "DBI in the sky," Phys. Rev. D **70**, 123505 (2004) [arXiv:hep-th/0404084].

[64] N. Agarwal, R. Bean, L. McAllister and G. Xu, "Universality in D-brane Inflation," arXiv:1103.2775 [astro-ph.CO].

[65] S. Kachru and L. McAllister, "Bouncing brane cosmologies from warped string compactifications," JHEP **0303**, 018 (2003) [hep-th/0205209].

[66] C. P. Burgess, PMartineau, F. Quevedo and R. Rabadan, "Branonium," JHEP **0306**, 037 (2003) [hep-th/0303170].

[67] C. P. Burgess, F. Quevedo, R. Rabadan, G. Tasinato and I. Zavala, "On bouncing brane worlds, S-branes and branonium cosmology," JCAP **0402**, 008 (2004) [hep-th/0310122].

[68] D. A. Easson, R. Gregory, G. Tasinato and I. Zavala, "Cycling in the throat," JHEP **0704**, 026 (2007) [arXiv:hep-th/0701252].

[69] C. Germani, N. E. Grandi and A. Kehagias, "A stringy alternative to inflation: The cosmological slingshot scenario," Class. Quant. Grav. **25**, 135004 (2008) [arXiv:hep-th/0611246].

[70] A. Kehagias and E. Kiritsis, "Mirage cosmology," JHEP **9911**, 022 (1999) [hep-th/9910174].

[71] D. A. Easson, R. Gregory, D. F. Mota, G. Tasinato and I. Zavala, "Spinflation," JCAP **0802**, 010 (2008) [arXiv:0709.2666 [hep-th]].

[72] D. A. Easson and R. Gregory, "Circumventing the eta problem," Phys. Rev. D **80**, 083518 (2009) [arXiv:0902.1798 [hep-th]].

[73] D. A. Easson, S. Mukohyama and B. A. Powell, "Observational Signatures of Gravitational Couplings in DBI Inflation," Phys. Rev. D **81**, 023512 (2010) [arXiv:0910.1353 [astro-ph.CO]].

[74] Y. -F. Cai, J. B. Dent and D. A. Easson, "Warm DBI Inflation," Phys. Rev. D **83**, 101301 (2011) [arXiv:1011.4074 [hep-th]].

[75] I. R. Klebanov and M. J. Strassler, "Supergravity and a confining gauge theory: Duality cascades and chiSB-resolution of naked singularities," JHEP **0008**, 052 (2000) [arXiv:hep-th/0007191].

[76] J. Polchinski, "String theory. Vol. 1: An introduction to the bosonic string," *Cambridge, UK: Univ. Pr. (1998) 402 p*
J. Polchinski, "String theory. Vol. 2: Superstring theory and beyond," *Cambridge, UK: Univ. Pr. (1998) 531 p*

[77] C. P. Herzog, I. R. Klebanov and P. Ouyang, "Remarks on the warped deformed conifold," arXiv:hep-th/0108101.

[78] I. R. Klebanov and A. A. Tseytlin, "Gravity duals of supersymmetric SU(N) x SU(N+M) gauge theories," Nucl. Phys. B **578**, 123 (2000) [hep-th/0002159].

[79] S. Gukov, C. Vafa and E. Witten, "CFT's from Calabi-Yau four folds," Nucl. Phys. B **584**, 69 (2000) [Erratum-ibid. B **608**, 477 (2001)] [arXiv:hep-th/9906070].

[80] R. Minasian and D. Tsimpis, "On the geometry of non-trivially embedded branes," Nucl. Phys. B **572**, 499 (2000) [arXiv:hep-th/9911042].

[81] S. S. Gubser, "Einstein manifolds and conformal field theories," Phys. Rev. D **59**, 025006 (1999) [hep-th/9807164].

[82] A. Ceresole, G. Dall'Agata and R. D'Auria, "KK spectroscopy of type IIB supergravity on AdS(5) x T(11)," JHEP **9911**, 009 (1999) [arXiv:hep-th/9907216].

[83] C. Krishnan and S. Kuperstein, "The Mesonic Branch of the Deformed Conifold," JHEP **0805**, 072 (2008) [arXiv:0802.3674 [hep-th]].

[84] S. S. Pufu, I. R. Klebanov, T. Klose and J. Lin, "Green's Functions and Non-Singlet Glueballs on Deformed Conifolds," J. Phys. A **44**, 055404 (2011) [arXiv:1009.2763 [hep-th]].

[85] R. G. Leigh, "Dirac-Born-Infeld Action from Dirichlet Sigma Model," Mod. Phys. Lett. A **4**, 2767 (1989).

[86] C. P. Bachas, "Lectures on D-branes," arXiv:hep-th/9806199.

[87] M. Born and L. Infeld, "Foundations Of The New Field Theory," Proc. Roy. Soc. Lond. A **144**, 425 (1934).

[88] D. Langlois, S. Renaux-Petel and D. A. Steer, "Multi-field DBI inflation: Introducing bulk forms and revisiting the gravitational wave constraints," JCAP **0904**, 021 (2009) [arXiv:0902.2941 [hep-th]].
[62, 63, 93–96].

[89] D. Baumann and L. McAllister, "A Microscopic Limit on Gravitational Waves from D-brane Inflation," Phys. Rev. D **75**, 123508 (2007) [arXiv:hep-th/0610285].

[90] C. Gordon, D. Wands, B. A. Bassett and R. Maartens, "Adiabatic and entropy perturbations from inflation," Phys. Rev. D **63**, 023506 (2001) [astro-ph/0009131].

[91] S. Groot Nibbelink and B. J. W. van Tent, "Scalar perturbations during multiple field slow-roll inflation," Class. Quant. Grav. **19**, 613 (2002) [hep-ph/0107272].

[92] A. Achucarro, J. -O. Gong, S. Hardeman, G. A. Palma and S. P. Patil, "Features of heavy physics in the CMB power spectrum," JCAP **1101**, 030 (2011) [arXiv:1010.3693 [hep-ph]].

[93] D. Langlois and S. Renaux-Petel, "Perturbations in generalized multi-field inflation," JCAP **0804**, 017 (2008) [arXiv:0801.1085 [hep-th]].

[94] M. -x. Huang, G. Shiu and B. Underwood, "Multifield DBI Inflation and Non-Gaussianities," Phys. Rev. D **77**, 023511 (2008) [arXiv:0709.3299 [hep-th]].

[95] D. Langlois, S. Renaux-Petel, D. A. Steer and T. Tanaka, "Primordial fluctuations and non-Gaussianities in multi-field DBI inflation," Phys. Rev. Lett. **101**, 061301 (2008) [arXiv:0804.3139 [hep-th]].

[96] S. Renaux-Petel and G. Tasinato, "Nonlinear perturbations of cosmological scalar fields with non-standard kinetic terms," JCAP **0901**, 012 (2009) [arXiv:0810.2405 [hep-th]].

[97] Y. -F. Cai, S. Li and Y. -S. Piao, "DBI-Curvaton," Phys. Lett. B **671**, 423 (2009) [arXiv:0806.2363 [hep-ph]].

[98] J. Zhang, Y. -F. Cai and Y. -S. Piao, "Rotating a Curvaton Brane in a Warped Throat," JCAP **1005**, 001 (2010) [arXiv:0912.0791 [hep-th]].

[99] Y. -F. Cai and Y. Wang, "Large Nonlocal Non-Gaussianity from a Curvaton Brane," Phys. Rev. D **82**, 123501 (2010) [arXiv:1005.0127 [hep-th]].

[100] K. Dimopoulos, D. Wills and I. Zavala, "Statistical Anisotropy from Vector Curvaton in D-brane Inflation," arXiv:1108.4424 [hep-th].

[101] D. H. Lyth and D. Wands, "Generating the curvature perturbation without an inflaton," Phys. Lett. B **524**, 5 (2002) [hep-ph/0110002].

[102] C. van de Bruck, D. F. Mota and J. M. Weller, "Embedding DBI inflation in scalar-tensor theory," JCAP **1103**, 034 (2011) [arXiv:1012.1567 [astro-ph.CO]].

[103] C. Armendariz-Picon, T. Damour and V. F. Mukhanov, "k - inflation," Phys. Lett. B **458**, 209 (1999) [hep-th/9904075].

[104] O. DeWolfe and S. B. Giddings, "Scales and hierarchies in warped compactifications and brane worlds," Phys. Rev. D **67**, 066008 (2003) [arXiv:hep-th/0208123].

[105] S. Kuperstein, "Meson spectroscopy from holomorphic probes on the warped deformed conifold," JHEP **0503**, 014 (2005) [arXiv:hep-th/0411097].

[106] S. Panda, M. Sami and S. Tsujikawa, "Prospects of inflation in delicate D-brane cosmology," Phys. Rev. D **76**, 103512 (2007) [arXiv:0707.2848 [hep-th]].

[107] J. M. Weller, C. van de Bruck and D. F. Mota, "Inflationary predictions in scalar-tensor DBI inflation," JCAP **1206**, 002 (2012) [arXiv:1111.0237 [astro-ph.CO]].

[108] T. Kidani, K. Koyama and S. Mizuno, "Non-Gaussianities in multi-field DBI inflation with a waterfall phase transition," arXiv:1207.4410 [astro-ph.CO].

[109] L. McAllister, S. Renaux-Petel and G. Xu, "A Statistical Approach to Multi-field Inflation: Many-field Perturbations Beyond Slow Roll," arXiv:1207.0317 [astro-ph.CO].

[110] D. Huybrechts, "Complex Geometry," Springer-Verlag Berlin Heidelberg (2005) 321 p.

[111] T. Hubsch, "Calabi-Yau manifolds: A Bestiary for physicists," Singapore, Singapore: World Scientific (1992) 362 p, 2nd ed. (1994) 374 p.